สารออกฤทธิ์ทางชีวภาพจากราเอนโดไฟต์ที่แยกได้จากหนามพุงดอ *Azima sarmentosa* Benth. & Hook.และตะบูนขาว *Xylocarpus granatum* Koenig.

นางสาวสุพิชชา โชคไพบูลย์

วิทยานิพนธ์นี้เป็นส่วนหนึ่งของการศึกษาตามหลักสูตรปริญญาวิทยาศาสตรมหาบัณฑิต
สาขาวิชาเทคโนโลยีชีวภาพ
คณะวิทยาศาสตร์ จุฬาลงกรณ์มหาวิทยาลัย
ปีการศึกษา 2552

BIOACTIVE COMPOUNDS FROM ENDOPHYTIC FUNGI ISOLATED FROM *Azima sarmentosa* Benth. & Hook. AND *Xylocarpus granatum* Koenig.

Miss Supichar Chokpaiboon

A Thesis Submitted in Partial Fulfillment of the Requirements
for the Degree of Master of Science Program in
Biotechnology Faculty of Science
Chulalongkorn University
Academic Year 2009

Thesis Title	BIOACTIVE COMPOUNDS FROM ENDOPHYTIC FUNGI ISOLATED FROM *Azima sarmentosa* Benth. & Hook. AND *Xylocarpus granatum* Koenig.
By	Miss Supichar Chokpaiboon
Field of study	Biotechnology
Thesis Advisor	Assistant Professor Khanitha Pudhom, Ph.D.
Thesis Co-Advisor	Taridaporn Buajarean, Ph.D.

Accepted by the Faculty of Science, Chulalongkorn University in Partial Fulfillment of the Requirements for the Master Degree

S. Hannongbua

.....Dean of the Faculty of Science
(Professor Supot Hannongbua, Dr.rer.nat)

THESIS COMMITTEE

Sirirat kokpol

.....Chairman
(Associate Professor Sirirat Kokpol, Ph.D.)

Khanitha Pudhom

.....Thesis Advisor
(Assistant Professor Khanitha Pudhom, Ph.D.)

Taridaporn Buajarean

.....Thesis Co-Advisor
(Taridaporn Buajarean, Ph.D.)

N. Ngamrojanavanich

.....Examiner
(Associate Professor Nattaya Ngamrojanavanich, Ph.D.)

Suthep Wiyakrutta

.....External Examiner
(Assistant Professor Suthep Wiyakrutta, Ph. D.)

สุพิชชา โชคไพบูลย์ : สารออกฤทธิ์ทางชีวภาพจากราเอนโดไฟต์ที่แยกได้จากหนามพุงดอ และตะบูนขาว. (BIOACTIVE COMPOUNDS FROM ENDOPHYTIC FUNGI ISOLATED FROM *Azima sarmentosa* Benth. & Hook. AND *Xylocarpus granatum* Koenig. อ.ที่ปรึกษาวิทยานิพนธ์หลัก : ผศ. ดร. ขนิษฐา พุดหอม, อ.ที่ปรึกษาวิทยานิพนธ์ร่วม : ดร. ธริดาพร บัวเจริญ, 163 หน้า.

จากการนำส่วนสกัดเอธิลแอซิเทตของราเอนโดไฟต์ *Rhytidhysteron* sp. จากหนามพุงดอที่เพาะเลี้ยงใน Malt extract broth มาทำการแยกให้บริสุทธิ์ พบสารอนุพันธ์แนฟธาลีนใหม่ 1 ชนิด คือ AS21B-4 (**4**) และสารที่มีการรายงานมาก่อนอีก 4 ชนิด คือ MK3018 (**1**), palmarumycin CR1 (**2**), 4-*O*-methyl-CJ12372 (**3**) และ 4-*O*-methyl-CJ12371 (**5**) นอกจากนี้เมื่อนำราเอนโดไฟต์ Basidiomycetous จากตะบูนขาวมาเพาะเลี้ยงใน Corn steep broth medium และนำส่วนสกัดเอธิลแอซิเททมาทำการแยกให้บริสุทธิ์ พบว่า ได้สารเซสควิเทอร์พีนชนิดใหม่อีก 4 ชนิด คือ merulin A (**6**), merulin B (**7**), merulin C (**8**) และ merulin D (**9**) การพิสูจน์ทราบโครงสร้างทางเคมีของสารที่แยกได้ทำโดยอาศัยวิธีการทางสเปกโทรสโกปี

เมื่อนำสารเหล่านี้มาทดสอบฤทธิ์ยับยั้งเชื้อมาลาเรีย ฤทธิ์ยับยั้งเซลล์มะเร็ง และฤทธิ์ยับยั้งเชื้อแบคทีเรีย พบว่า สาร (**8**) และ (**9**) แสดงฤทธิ์ยับยั้งมาลาเรียดีมากโดยมีค่า IC_{50} = 0.39, และ 1.35 μM ตามลำดับ ขณะที่สาร (**1**), (**3**), (**4**), (**5**) และ (**6**) มีฤทธิ์ปานกลาง ส่วนสาร (**2**) ไม่มีฤทธิ์ยับยั้งเชื้อมาลาเรีย และพบว่า สารอนุพันธ์ของแนฟธาลีนทั้ง 5 ชนิด (**1-5**) แสดงความเป็นพิษต่อเซลล์มะเร็งทุกชนิดที่ทดสอบแบบไม่จำเพาะเจาะจง ส่วนสารเซสควิเทอร์พีน (**6**), (**8**) และ (**9**) มีฤทธิ์ยับยั้งเซลล์มะเร็งทุกชนิดที่ทดสอบยกเว้นเซลล์มะเร็งปอด (CHAGO) ขณะที่สาร (**7**) แสดงฤทธิ์ปานกลางอย่างจำเพาะเจาะจงต่อเซลล์มะเร็งตับ นอกจากนี้ยังพบว่าสารทุกชนิดมีฤทธิ์ยับยั้งเชื้อแบคทีเรียที่แตกต่างกันไปด้วยค่า MIC ที่ต่างกัน

สาขาวิชา เทคโนโลยีชีวภาพ ลายมือชื่อนิสิต.....สุพิชชา โชคไพบูลย์.....
ปีการศึกษา 2552 ลายมือชื่ออ.ที่ปรึกษาวิทยานิพนธ์หลัก.....
ลายมือชื่ออ.ที่ปรึกษาวิทยานิพนธ์ร่วม.....

5072526023 : MAJOR BIOTECHNOLOGY

KEYWORDS : Fungal metabolites/ Cytotoxicity / Anti-malaria / Anti-bacteria

SUPICHAR CHOKPAIBOON: BIOACTIVE COMPOUNDS FROM ENDOPHYTIC FUNGI ISOLATED FROM *Azima sarmentosa* Benth. & Hook. AND *Xylocarpus granatum* Koenig. THESIS ADVISOR : ASST. PROF. KHANITHA PUDHOM, Ph.D., THESIS CO-ADVISOR : TARIDAPORN BUAJAREAN, Ph.D., 163 pp.

A new naphthalene derivative, AS21B-4 (**4**), was obtained from the EtOAc extract of an endophytic fungus, *Rhytidhysteron* sp. isolated from *Azima sarmentosa* Benth. & Hook., which was cultured on Malt extract broth, along with four konwn compounds, MK3018 (**1**), palmarumycin CR1 (**2**), 4-*O*-methyl-CJ12372 (**3**) และ 4-*O*-methyl- CJ12371 (**5**). Additionally, four new sesquiterpenes, merulins A-D (**6-9**), were isolated from the extract of another fungus (Basidiomycetous) of X*ylocarpus granatum* Koenig. cultured on Corn steep broth medium. The structures of these compounds were elucidated on the basis of spectroscopic studies.

Further, all isolated compounds were evaluated for their antimalarial, cytotoxic and antibacterial activity. Compounds (**8**) and (**9**) exhibited potent antimalarial activity with IC_{50} values of 0.39 and 1.35 μM, respectively, while compounds **1** and **3-6** were moderately active. For compound **2**, it showed to be inactive in this assay. Additionally, all naphthalene derivatives (**1-5**) exhibited nonselective toxicity toward all cell lines tested. Merulins A (**6**), C (**8**) and D (**9**) also showed moderate activity against all cell lines, except for CHAGO cell lines, whereas merulin B (**7**) exhibited moderate cytotoxicity selectively against only Hep-G2 cell lines. Moreover, all compounds (**1-9**) were active toward different bacterial strains with different MIC values.

Field of Study: Biotechnology
Academic Year: 2009

Student's Signature Supichar Chokpaiboon
Advisor's Signature Khanitha Pudhom
Co-Advisor's Signature T. Buajarern

ACKNOWLEDGEMENTS

I would like to express my sincere gratitude to my mentor, Assistant Professor Dr. Khanitha Pudhom, for her excellent, her valuable guidance, which motivated me to pass through this course successfully. I also would like to express my respect and gratitude to my co-advisor, Dr. Taridaporn Buajarean, for kind supervision and kind suggestions.

Many thanks to the thesis committees, Associate Professor Sirirat Kokpol, Associate Professor Dr. Nattaya Ngamrojnavanich, Faculty of Science, Chulalongkorn University, Assistant Professor Suthep Wiyakrutta, Faculty of Science, Mahidol University, for their invaluable discussion and suggestion.

I wish to thank the Thailand Graduate Institute of Science and Technology (TGIST) of the National Science and Technology Development Agency (NSTDA) for providing scholarship thoroughly. I would like to thank all staff of Bioresource Research Laboratory; especially, Mrs.Rachada Haritakun. I would like to thank Mr.Nattawut Boonyuen, Phylogenetics and Mycology Laboratories for fungal identification. I am also grateful to the National Center for Genetic Engineering and Biotechnology (BIOTEC) for supporting all technical facilities.

I wish to thank The 90th Anniversary of Chulalongkorn University Fund (Ratchadaphiseksomphot Endowment Fund) for granting in partial financial support to conduct this research. I would like to thank Associate Professor Dr. Amorn Petsom and Mrs. Songchan Puthong, Institute of Biotechnology and Genetic Engineering, Chulalongkorn University, for tumor cell lines and facilitating use of the cytotoxicity assays throughout the entire study. I am grateful to Associate Professor Dr. Nongnuj Muangsin and Mr. Thapong Teerawatananond, Department of Chemistry, Faculty of Science, Chulalongkorn University who kindly performed the X-ray crystallographic analysis.

I wish to thank all member of laboratory room 1528/1 and 1532 for their help and kind friendship, especially Mr. Thanesuan Nuanyai, for his valuable suggestions and for his comments in slide presentation. I would like to thank Miss. Phunlap Pompeng for anti-bacterial activity.

I would like to thank Mr. Siwadol Sateanpattanakul, for his mentorship, friendship and sincerely help.

Finally, I am deeply grateful to my family for their entirely care, love, and understanding. I dedicate to my father, my mother and all the teachers who have taught me since my childhood.

CONTENTS

Page

Page

LIST OF TABLES

LIST OF FIGURES

Figure **Page**

Figure **Page**

Figure **Page**

LIST OF SCHEMES

LIST OF ABBREVIATIONS

acetone-d_6	Deuterated acetone
$^{\circ}$C	Degree Celsius
^{13}C NMR	Carbon-13 nuclear magnetic resonance
$CDCl_3$	Deuterated chloroform
$CHCl_3$	Chloroform
CH_2Cl_2	Methylene chloride
δ	Chemical shift
d	Doublet (for NMR spectral data)
dd	Doublet of doublets (for NMR spectral data)
ddd	Doublet of doublet of doublet (for NMR spectral data)
dddd	Doublet of doublet of doublet of doublet (for NMR spectral data)
DNA	Deoxyribonucleic acid
DEPT	Distortionless enhancement by polarization transfer
ε	Molar absorptivity
et al	And other
EtOAc	Ethyl acetate
ESI-TOF MS	Electrospray Ionization Time of Flight Mass
g	Gram
μg	Microgram
h	Hour
^{1}H-^{1}H COSY	Homonuclear (proton-proton) correlation spectroscopy
^{1}H NMR	Proton nuclear magnetic resonance
HMBC	^{1}H-detected heteronuclear multiple bond correlation
HMQC	^{1}H-detected heteronuclear multiple quantum coherence
Hz	Hertz
IC_{50}	Inhibitory concentration required for 50% inhibition of growth
IR	Infrared
ITS	Internally transcribed spacers

J	Coupling constant
KBr	Potassium bromide
L	Liter (s)
λ_{max}	Maximum wavelength
μg	Microgram (s)
μL	Microliter (s)
μM	Micromolar
M	Molar
m	Multiplet (for NMR spectral data)
MEB	Malt Extract Broth
m.p.	Melting temperature
MeOH	Methanol
mg	Milligram
MIC	Minimum inhibitory concentration
min	Minute
ml	Milliliter
mm	Millimeter
mM	Millimolar
MHz	Megahertz
MS	Mass spectroscopy
m/z	Mass to charge ratio
nm	Nanometer
No.	Number
NMR	Nuclear magnetic resonance
NTP	Nucleotide triphosphate
PCR	Polymerase chain reaction
PDA	Potato Dextrose Agar
PDB	Potato Dextrose Broth
$[M+H]^+$	Protonated molecule
$[M+Na]^+$	Pseudomolecular ion
ppm	Part per million
q	Quartet (for NMR spectral data)

rDNA	Ribosomal deoxyribonucleic acid
rpm	Round per minute
rRNA	Ribosomal ribonucleic acid
s	Singlet (for NMR spectral data)
sp.	Species
t	Triplet (for NMR spectral data)
TAE	*Tris*-HCl, acetate and EDTA
TE	*Tris*-HCl and EDTA
TLC	Thin layer chromatography
U	Unit
UV	Ultraviolet
V	Volt
v	Volume
ν_{max}	Wave number at maximum absorption
w	Weight

CHAPTER I

INTRODUCTION

At present, human are being threatened by more and more coming diseases for example cancers, AIDS, SARS, bird flu, etc., accompanied with an increasing scope of environmental degradation, air pollution and water caused by excessive toxic organic insecticide, industry sewage, and poisonous gases. As a result, it is a must for isolating of novel and beneficial compounds to provide assistance and relief in all features of the human condition (Guo, *et al*., 2008). Natural products have been the source of therapeutics since the advent of traditional medicine and healing, and remain a dominant source to date (Donnelly, 2009). Frequency of use of natural products in the treatment and prevention of disease can be measured by the number and economic value of prescriptions, from which the extent of preference and effectiveness of drugs can be estimated indirectly. Since the discovery of penicillins in 1928, fungi have been playing an important role as source of drug and drug lead compounds (Chin, *et al*., 2006).

Endophytic microorganisms are to be found in virtually every plant on earth. These organisms reside in the living tissues of the host plant and do so in a variety of relationships ranging from symbiotic to pathogenic. Endophytes may contribute to their host plant by producing a plethora of substances that provide protection and ultimately survival value to the plant. Ultimately, these compounds, once isolated and characterized, may also have potential for use in modern medicine, agriculture, and industry. (Strobel, *et al*., 2003). Endophytes have been recognized as important sources of a variety of structurally novel active secondary metabolites with anticancer, antimicrobial and other biological activities. (Xu, *et al*., 2009).

The prospects of finding new drugs that may be effective candidates for treating newly developing diseases in humans, plants, and animals are great. Other applications in industry and agriculture may also be discovered among the novel products produced by endophytic microbes.(Strobel, *et al*., 2003).

The objectives of this study are as follows:

1. To isolate endophytic fungi from *Azima sarmentosa* Benth. & Hook. and *Xylocarpus granatum* Koenig.
2. To explore chemical constituents of the selected endophytic fungi.
3. To elucidate chemical structures of the bioactive compounds by spectroscopic analyses (1D- and 2D-NMR, MS, IR, and X-ray crystallography).
4. To evaluate the biological activities including anticancer, antibacterial, and antimalarial activities of the isolated compounds.

CHAPTER II

LITERATURE REVIEWS

2.1 Natural products

For thousands of years medicine and natural products have been closely linked through the use of traditional medicines and natural poisons, pharmacological and chemical studies of these traditional medicines. Although traditionally natural products have played an important role in drug discovery, in the past few years most pharmacy companies have either terminated or considerably scaled down their natural product operations, which were derived predominantly from plants, were the basis of most early medicines such as aspirin, digitoxin, morphine, quinine, and pilocarpine (Butler, 2004).

Additionally, many drug companies have developed interests in making products that have a larger potential profit base than anti infectious drugs (Strobel, *et al*., 2004). Modern organic chemistry, which was founded primarily upon the study of natural products, led to the isolation and identification of a multitude of such individual compounds and subsequently an understanding of their biological properties (Molyneux, 2002).

Among all known producers of small molecule natural products, microorganisms represent a rich source of biologically active metabolites that find wide-ranging applications as agrochemicals, antibiotics, immunosuppressants, antiparasitics, and anticancer agents. Unlike other organisms, microbes occupy all living and nonliving niches on earth including arctic, antarctic, and alpine regions, deserts, deep rock sediments, marine environments, and even thermal vents. (Gunatilaka, 2006). Endophytes, microorganisms that reside in the tissues of living plants, are relatively unstudied as potential sources of novel natural products for exploitation in medicine (Strobel, Daisy, and Castillo, 2002)

2.2 Endophytic fungi

Endophyte is a microorganism that colonizes interior organs of plants, but does not have pathogenic effects on its host. In their symbiotic association, the host plant (macrophyte) protects and feeds the endophyte, which “in return” produces bioactive metabolites to enhance the growth and competitiveness of the host and to protect it from herbivores and plant pathogens (Gunatilaka, 2005).

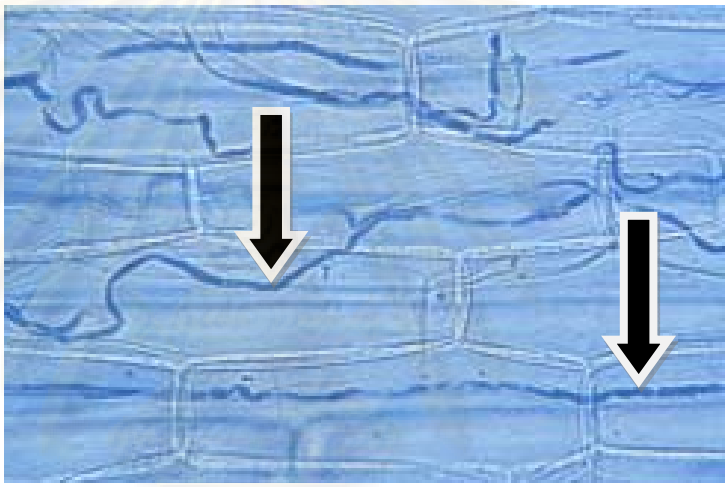

Figure 2.1 Endophytic fungal hyphae (arrows) in plant cells. (Image from: http://www.peg.ethz.ch/research/Interactions/index_EN). (Site on November 4, 2009).

2.3 Bioactive compounds from endophytic fungi

Paclitexel (Taxol®) was initially isolated from the bark of the Pacific yew, *Taxus brevifolia*, and a member of the class of taxane diterpenoids (Wani, et al., 1971). Taxol® is a cancer medication that meddle with the growth of cancer cells, slows growth and spread in the body, and used to treat breast cancer, lung cancer, and ovarian cancer (Horwitz, 2004)

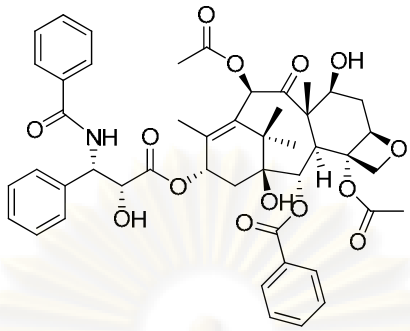

Figure 2.2 The chemical structure of Taxol®

Taxol was approved for treatment of drug resistant ovarian cancer by the Food and Drug Administrationin in 1992, and 1993. It was discovered that taxol was accidentally produced by fungus living in the yew tree, and it has since been found in a number of other endophytic fungi, together with *Nodulisporium sylviforme*, opening the occurrence of taxol production by culturing one of these species. Taxol has become the best-selling anticancer drug in history, with commercial sales of well over $1 billion in 1998 (Stierle and Strobel *et al*., 1993; Kingston, 2000).

Endophytic fungi are extensively recognized as productive sources of highly bioactive secondary metabolites that might show useful leads in the development of new pharmaceutical agents. Two new fusicoccane diterpenes, named periconicins A (**1**) and B (**2**), with antibacterial activities have been isolated by bioassay-guided fractionation from an endophytic fungus *Periconia* sp., collected from small branches of *Taxus cuspidate*. Periconicins A and B exhibited activities against the bacterial *Bacillus subtilis* (MIC 3.12 μg/mL, 25.00 μg/mL, respectively) and bacterial *Klebsiella pneumoniae* (MIC 3.12 μg/mL, 12.50 μg/mL, respectively) (Kim, *et al.*, 2004).

(**1**) (**2**)

Figure 2.3 Periconicins A and B

Two new γ-lactones, eutypellins A (**3**) and B (**4**), isolated from the endophytic fungus *Eutypella* sp. BCC 13199 showed cytotoxic activity against human small-cell lung cancer cells (NCI-H187) with an IC_{50} value of 12.0 and 206 μM respectively (Isaka, *et al.*, 2009).

(**3**) (**4**)

Figure 2.4 Eutypellins A and B

Three new esters of orsellinic acid, globosumones A-C (**5-7**) were isolated from *Chaetomium globosum* endophytic on *Ephedra fasciculata* (Mormon tea). All compounds were evaluated for inhibition of cell proliferation in a panel of four cancer cell lines, MCF-7 (breast cancer), SF-268 (CNS glioma), and MIA Pa Ca-2 (pancreatic carcinoma) and normal human fibroblast cells (WI-38). Only globosumones A (**5**) and B (**6**) were found to be moderately active (Bharat, *et al.*, 2005).

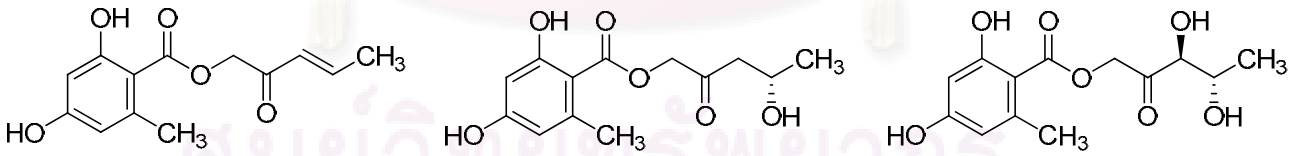

(**5**) (**6**) (**7**)

Figure 2.5 Globosumones A-C

Six new chromones, named pestalotiopsones A-F (**8-13**) were obtained from the mycelia and culture filtrate of the mangrove endophytic fungus *Pestalotiopsis* sp., which was isolated from leaves of the Chinese Mangrove plant *Rhizophora mucronata*. Compound **13** exhibited moderate cytotoxicity against the murine cancer

cell line L5178Y with an EC_{50} value of 8.93 μg/mL whereas the other investigated compounds proved to be inactive. (Wu and Proksch, *et al.*, 2009).

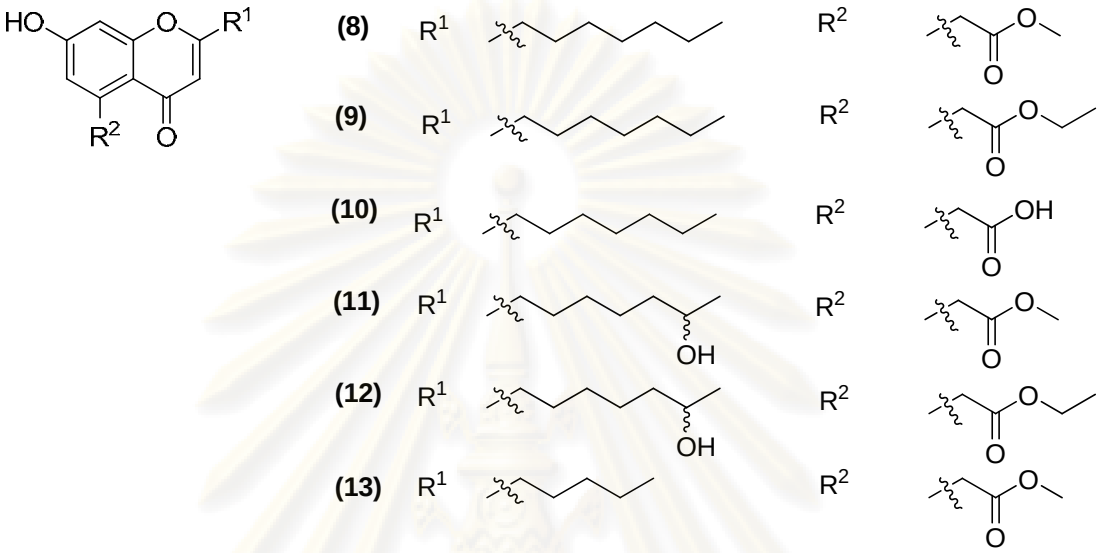

Figure 2.6 Pestalotiopsones A-F

Two new 10-oxo-10*H*-phenaleno[1,2,3-*de*]chromene-2-carboxylic acids, xanalteric acids I (**14**) and II (**15**) were obtained from extracts of the endophytic fungus *Alternaria* sp., isolated from the mangrove plant *Sonneratia alba* collected in China. The two new compounds exhibited weak antibiotic activity against multidrug-resistant *Staphylococcus aureus* (Lin and Proksch, *et al.*, 2009).

(**14**) (**15**)

Figure 2.7 Xanalteric acids I and II

2.4 Botanical Aspects, Distribution and Ethnobotanical of *Azima sarmentosa*. and *Xylocarpus granatum*.

2.4.1 *Azima sarmentosa*.

A.sarmentosa. has been used as the medicinal plant in Thailand. The roots are usually used and have a sour taste. It is utilized as an antipyretic and anti-inflammatory agent. Moreover, it can lessen the pain of wounds because of its cooling property. Also, it has been used to treat mump.(Sunintaboon, 1999)

Figure 2.8 *A.sarmentosa.*

Taxonomy of *Azima sarmentosa.*

Kingdom: Plantae

Division: Magnoliophyta

Class: Magnoliopsida

Order: Brassicales

Family: Salvadoraceae

Genus: *Azima*

Species: *A.sarmentosa*.

*A. sarmentosa.***,** is broadly distributed in the tropical regions all over the world (Pongboonrod, 1979). In Thailand, this plant is distributed in many areas such as, northern, north eastern, and south central regions of the country. *A. sarmentosa*. is rambling shrub, with axilliary. It grows to a height of 2-4 m with oval leaves 2-6 cm, has characteristic as follow: entire flower are small, dioecious, axillary, sestile, or on little-brached panicle in cluters or umbels. There have been several common names called in Thailand: Phungdo or Naam phundo (Central), Pittoh (Chiang Mai) or Khee-haet (north eastern) (Sunintaboon, 1999 ; Larsen, 2000).

In the investigation of chemical constituents of the leaf and root extracts from *A. sarmentosa.*, the first report described two compounds, 1-methoxy-indole-3-carboxaldehyde (**16**) and 1-methoxy-indole-3-acetonitrile (**17**) were isolated and exhibiting cytotoxic lethality on brine shrimp (*Artemia salina* Linn.) with LC_{50} 0.09 and 9.24 μg/mL, respectively (Sunintaboon, 1999).

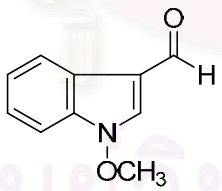

(**16**)

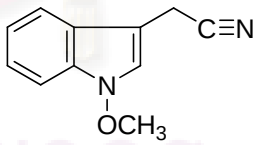

(**17**)

Figure 2.9 1-methoxy-indole-3-carboxaldehyde and 1-methoxy-indole-3-acetonitrile

2.4.2 *Xylocarpus granatum.*

X.granatum., known in the Thai vernacular as ‘‘Ta-Boon’’. The mangrove is distinguished for producing antifeedant limonoids, especially phragmalins and mexicanolides. *X.granatum.*, is a spreading tree growing up to 22 m

in height. It has red/orange-brown, irregularly cleaved and flaky bark. The trunk has large buttresses and meandering, plank-like above ground roots. The leaves up to 20 cm long, with a 2-5 cm long petiole and consist of 2-3 pairs of opposite leaflets. The leaflets are elliptic (oval) to obovate (inversely egg-shaped), 7-11 cm long and 3-6 cm wide. The fruit is a spherical, green or brown, woody capsule with four distinct sections. It is 15-23 cm in diameter and splits open after falling to reveal 8-20 cm (Wu, 2006; http : // wiki.trin.org.au / Mangroves / Xylocarpus-granatum).

Figure 2.10 *X. granatum*.

Taxonomy of *Xylocarpus granatum***.**

Kingdom: Plantae

Division: Magnoliophyta

Class: Magnoliopsida

Order: Sapindales

Family: Meliaceae

Genus: *Xylocarpus*

Species: *X.granatum***.**

X.granatum., are used as folk medicines in Southeast Asia for the treatment of diarrhea, cholera, viral diseases such as influenza, and malaria. Three new protolimonoids, protoxylocarpins F-H (**18**-**20**) were isolated from seed kernels of *X. granatum*. All compounds isolated were evaluated for cytotoxic activity against five human tumor cell lines (Pudhom, *et al.*, 2009).

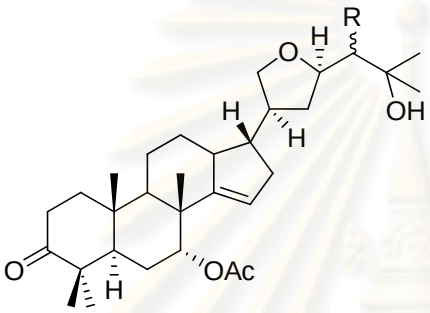

(**18**) R = β-OH

(**19**) R = α-OH

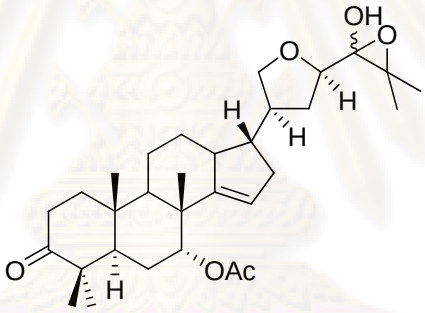

(**20**)

Figure 2.11 Protoxylocarpins F-H

Three new polyhydroxylated phragmalins, named xyloccensins Y, Z_1, and Z_2 (**21**-**23**), were isolated from the fruit of a Chinese mangrove, *X.granatum*. (Zhou, *et al.*, 2006)

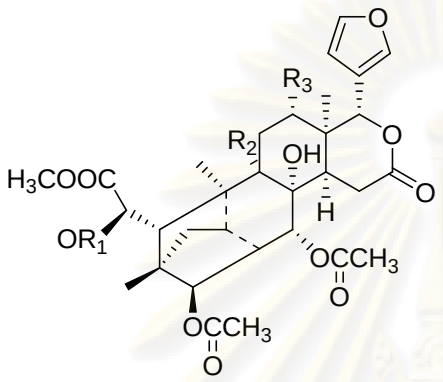

(**21**) R_1=Ac R_2=R_3=OH

(**22**) R_1=R_2=H R_3=OAc

(**23**) R_1=R_2= R_3=H

Figure 2.12 Xyloccensins Y, Z_1, and Z_2

CHAPTER III

MATERIALS AND METHODS

3.1 Plant sample Collection

Healthy leaves of *Azima sarmentosa*. and *Xylocarpus granatum*., were collected from Pan Thai Norasing, Amphoe Muang, Samutsakorn province, Thailand, in July 2008**.**

3.2 Fungal endophyte Isolation

Isolation of endophytic fungi from the leaves of plant samples was performed by Mr. Ruengrit Sappapan.

Healthy leaves were washed in tap water and air-dried. The cleaned leaf fragments were surface-sterilized as described by Schulz and co-workers (Schulz, et. al., 1995) with some modifications. These fragments were sequentially immersed in 70% EtOH for 1 min, 6% NaOCl solution for 5 min, and sterile distilled H_2O for 1 min (two times). Then, the surface-sterilized fragments were cut into small pieces (ca. 5 mm in length) using a sterile blade and placed on sterile water agar plates for further incubation at 30°C. The hyphal tip of the endophytic fungus growing out from the plant tissue was cut by a sterile pipette and transferred onto a potato dextrose agar (PDA) plate. After incubation at 30 °C for 7-14 days, culture purity was determined from colony morphology.

3.3 Selection of endophytic fungal isolate

Two endophytic fungi isolated from *A.sarmentosa*, and *X.granatum*, AS21B and XG8D, were selected for the further study based on their antimicrobial activities in previous studies by Phunmod and Phuthong, 2008. All selected fungi were cultured on appropriate medium for producing secondary metabolites, then measured crude extract by ^{1}H NMR. The crude extracts of the fungi that show characteristic interesting ^{1}H NMR signals were selected for large scale cultivation and extraction.

3.4 Large scale cultivation and extraction

The fungi of interest, AS21B and XG8D, were grown on PDA plate at 30°C for 7 days. Six pieces (6x6 mm^2) of the grown culture were cut and inoculated into 1,000 mL Erlenmeyer flasks (x25) containing 200 mL of malt extract broth (MEB) for isolate AS21B, and of corn steep broth medium for isolate XG8D, respectively, at 30°C for 3 weeks under static conditions.

The culture broth was passed through four layers of sheet cloth which were exhaustively pressed. The filtrate was extracted with an equal volume of ethyl acetate (EtOAc) for 3 times. The organic layers were combined and evaporated at 35°C to yield broth crude extract. The extraction procedure is shown in **Scheme 3.1.**

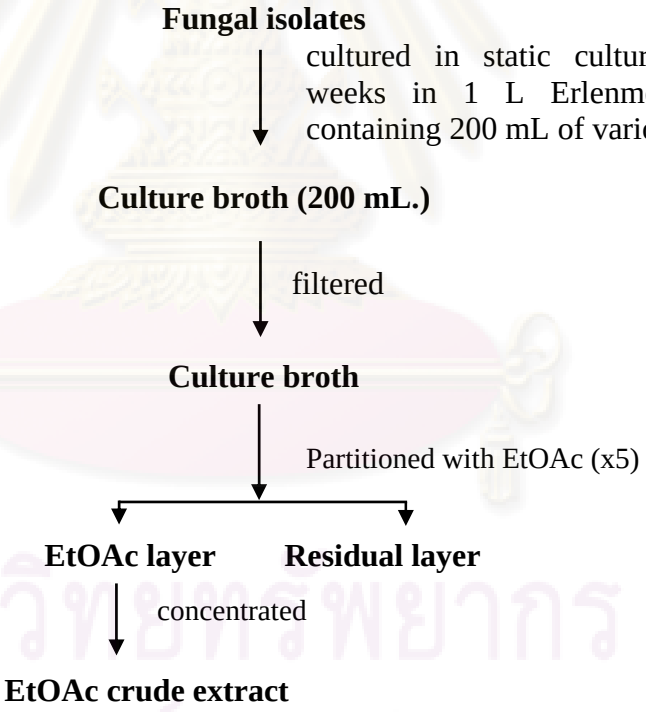

Scheme 3.1 General procedure for extraction of fungal culture broth

3.5 Isolation of bioactive compounds from crude extracts of selected endophytic fungi

3.5.1 Isolate AS21B

The 3.10 g of EtOAc crude broth extract cultured on MEB medium was pass through a Sephadex LH-20 column (3.8 × 5 cm) and eluted with MeOH to give eight fractions (A1 to A8). Fraction A2 was further subjected to SiO_2 column chromatography (CC) eluted with acetone-benzene (1:3) to afford MK3018 (compound **1**, 21.8 mg). Fraction A4 was rechromatographed over silica gel eluted with EtOAc-hexane (1:1) to give palmarumycin CR1 (compound **2**, 47.8 mg). Fraction A7 was chromatographed on a SiO_2 column (EtOAc-hexane, 1:1) to give to yield 4-*O*-methyl-CJ-12372 (compound **3**, 79.0 mg) and AS21B-4 (compound **4**, 11.5 mg), and subfraction B2 was further purified by preperative HPLC [Merck LiChroCART C_{18} (10 × 250 mm, 10 µm), MeCN:H_2O = 60:40, flow rate 5.0 mL/min], to afford 4-*O*-methyl-CJ12371 (compound **5**, 6.6 mg). The isolation of the broth crude extract of isolate AS21B is summarized in **Scheme 3.2.**

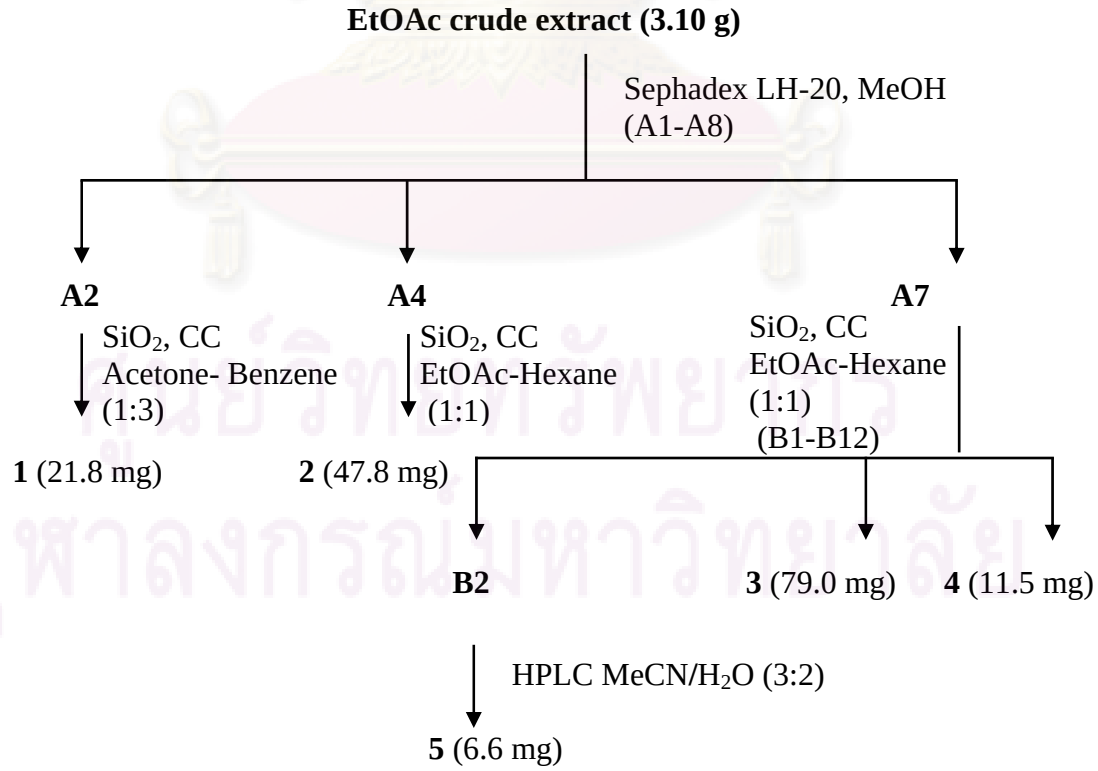

Scheme 3.2 Isolation of a broth extract of AS21B cultured on MEB medium

3.5.2 Isolate XG8D

The 4.10 g of EtOAc crude broth extract cultured on corn steep broth medium was passed through a Sephadex LH-20 column eluted with MeOH to afford six fractions (A1-A6). Fraction A5 was further purified by SiO_2 column chromatography (using 5% of MeOH in CH_2Cl_2 as eluent), and preparative HPLC [GL Science column C_{18} (20 × 250 mm, 3 µm) MeCN:H_2O = 40:60, flow rate = 8.0 mL/min] to yield merulin A (compound 6,1 42.0 mg) and merulin C (compound 8, 37.3 mg). Fraction A4 was subjected to flash column chromatography on silica gel (using 5% of MeOH in CH_2Cl_2 as eluent), and then rechromatographed on a SiO_2 column eluted with EtOAc-hexane (2:1) to afford merulin B (compound **7**, 10.0 mg). Fraction A2 was rechromatographed over silica gel eluted with EtOAc-CH_2Cl_2 (4:1) to furnish merulin D (compound **9**, 17.7 mg). The isolation of the broth crude extract of isolate XG8D is summarized as shown in **Scheme 3.3.**

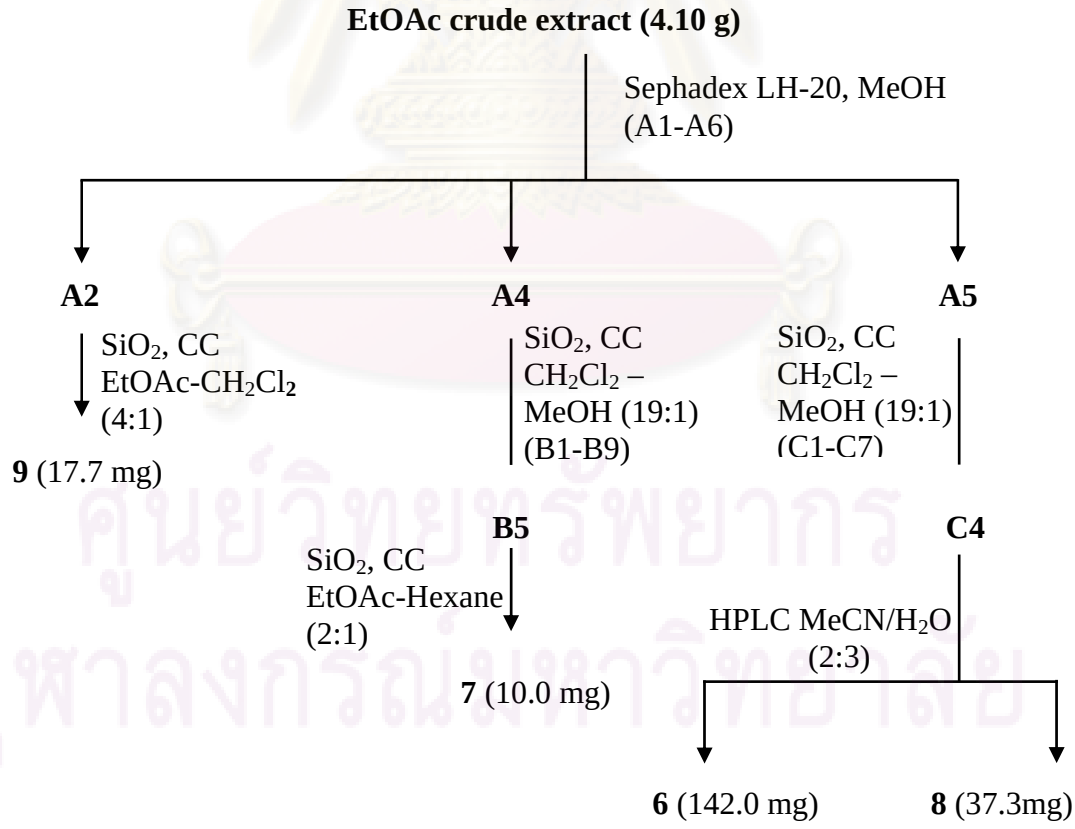

Scheme 3.3 Isolation of a broth extract of XG8D cultured on corn steep broth medium

3.6 Chromatography

3.6.1 Thin-layer chromatography (TLC)

Thin-layer chromatography (TLC) was carried out on a silica gel F254 coated on aluminium sheet (Merck). Detection was visualized under ultraviolet light at wavelengths of 254 and 356 nm and dipped with $(NH_4)_6Mo_7O_{24}$ solution in 5% H_2SO_4 /EtOH.

3.6.2 Column chromatography

Column chromatography (CC) was performed using Sephadex LH-20 (Pharmacia Code No. 17-0090-01) and Silica gel 60H (Merck code No. 7734 and No. 9385) as packing materials.

3.6.3 High performance liquid chromatography (HPLC)

High performance liquid chromatography (HPLC) was performed using a Water system (Waters 600 HPLC pump and Waters 2996 Photodiode array detector). Column Waters NovaPak C_{18} (3.9 × 150 mm, 4 µm) was used for analysis, Merck LiChroCART C_{18} (10 × 250 mm, 10 µm), Phenomenex Luna HR C_{18} (21.2 × 250 mm, 10 µm) and GL Science column C_{18} (20 × 250 mm, 3 µm) were used for separation.

3.7 Chromatography and physical property measurements

Structures of isolated compounds were elucidated by the interpretation of NMR spectra. Additional spectroscopic techniques such as MS, UV-vis, IR, and X-ray crystallography were also employed for the structural elucidation. Melting points and optical rotation properties of the compounds were also measured.

3.7.1 Nuclear magnetic resonance spectroscopy (NMR)

The NMR spectra were recorded in $CDCl_3$, DMSO-d_6, using a Varian YH400 spectrometer at 400 MHz for ^1H NMR and at 100 MHz for ^{13}C NMR using TMS (trimethylsilane) as internal standard.

The NMR spectra were recorded in $CDCl_3$, acetone-d_6, using a Bruker DRX 400 (400 MHz for ^1H, 100 MHz for ^{13}C) and a Bruker AV500D (500 MHz for ^1H, 125 MHz for ^{13}C) spectrometers.

3.7.2 Mass spectrometry (MS)

ESI-TOF mass spectra and HRESIMS were measured with a Bruker microOTOF mass spectrometer.

3.7.3 Ultraviolet-visible measurements (UV-vis)

UV-vis spectra were recorded on a Perkin Elmer Lambda 25 UV-vis spectrophotometer in $CHCl_3$ or MeOH.

3.7.4 Fourier transform infrared spectroscopy (FT-IR)

The FT-IR spectra were recorded on a Bruker VECTOR 22. Solid samples were formally examined by incorporating the sample with potassium bromide (KBr) to form a pellet.

3.7.5 Melting points

Melting points were taken on an Electrothermal IA9100 digital melting point apparatus.

3.7.6 Optical rotation

Optical rotations were measured with using a sodium D line (589 nm) JASCO DPI-370 digital polarimeter equipped with a 1 mL cell (cell length 1.00 cm).

3.7.7 X-ray crystallography

The crystal structure was solved by direct methods and using the SHELXS97 program. Crystallographic data, excluding structure factors, have been deposited at the Cambridge Crystallographic Data Centre.

3.8 Chemicals

All solvents used in this research such as hexane, dichloromethane (CH_2Cl_2), acetone, ethyl acetate (EtOAc) and methanol (MeOH) were commercial grade and purified prior to use by distillation. The reagent grade solvents were used for recrystallization.

The mobile phases for HPLC separation were HPLC grade of methanol and acetonitrile which were purchased from Scharlau and Fisher Scientific, respectively.

3.9 Culture media

Culture media used for cultivation of endophytic fungi were potato dextrose agar (PDA), water agar, malt extract broth (MEB), corn steep broth medium; the formula are shown in Appendix A.

3.10 Classification of the endophytic fungal isolates AS21B and XG8D

Isolated fungal strains AS21B and XG8D were taxonomically identified by Mr.Nattawut Boonyuen, Phylogenetics and Mycology Laboratories Central Research Unit BIOTEC, National Center for Genetic Engineering and Biotechnology, Pathum Thani, Thailand.

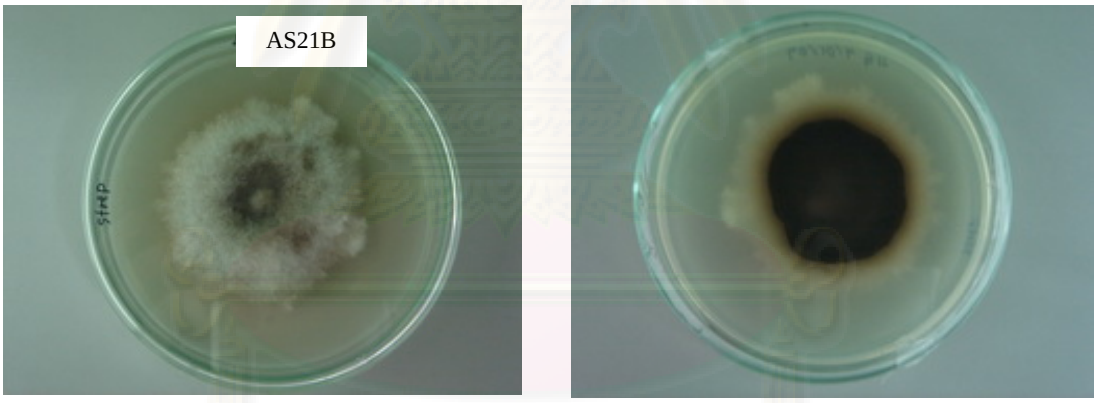

Obverse Reverse

Figure 3.1 Colony morphology of endophytic fungus isolate AS21B on PDA.

The fungus was identified based on the ITS1-5.8S-ITS2 sequence, which were amplified using universal primers ITS1, ITS4 and ITS5 (White, *et al*., 1990). A BLAST search was employed to obtain the closest-matching sequences in the GenBank database (Altschul , *et al*., 1990). This partial of the 18S sequence, complete ITS1-5.8S-ITS2 sequences, and partial of the 28S sequence of rRNA gene shown in **Figure 3.2**. It was found that DNA sequence of the ITS1-5.8S-ITS2 rRNA gene of 21B can be identified to Patellariales, Incertae sedis, Dothideomycetes, Ascomycota.

The comparisons of ITS sequence analyses showed that the DNA sequence of the strain AS21B is closely related to *Rhytidhysteron rufulum* at NCBI with 88.51% to 99.12% homology to the best matching sequences. This data suggests that AS21B fungus is *Rhytidhysteron* sp. isolate no. AS21B (Murillo , *et al*., 2009).

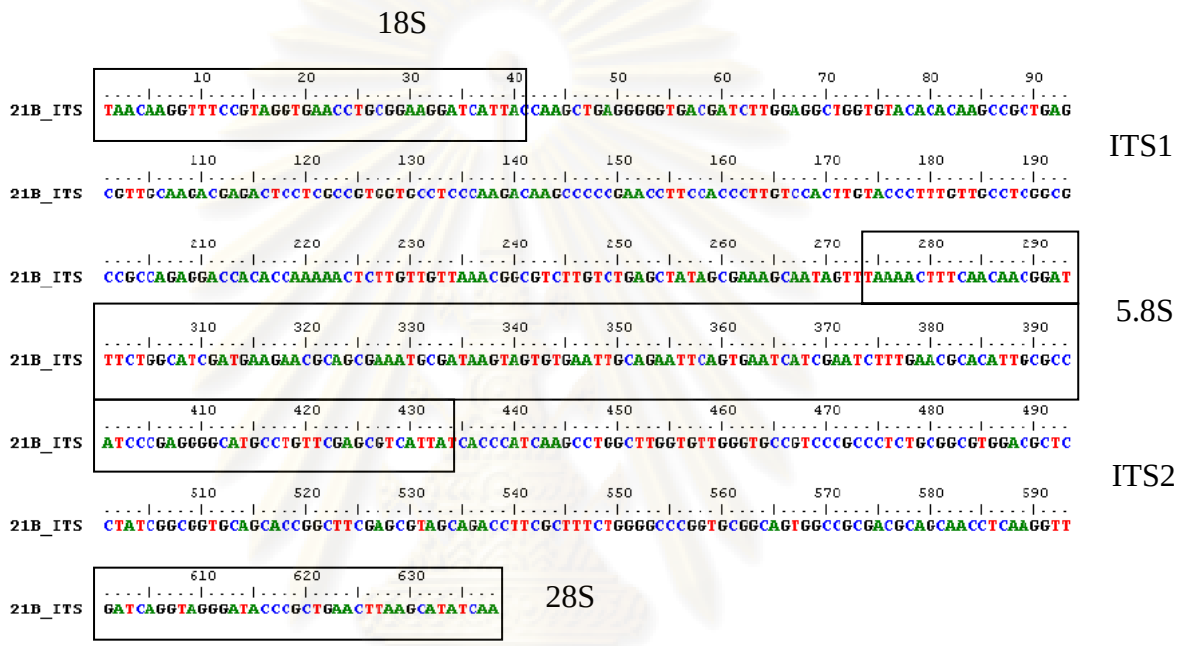

Figure 3.2 Nucleotide sequences of the partial 18S rRNA gene, complete ITS1-5.8S-ITS2, and partial 28S rRNA gene of the endophytic fungus AS21B

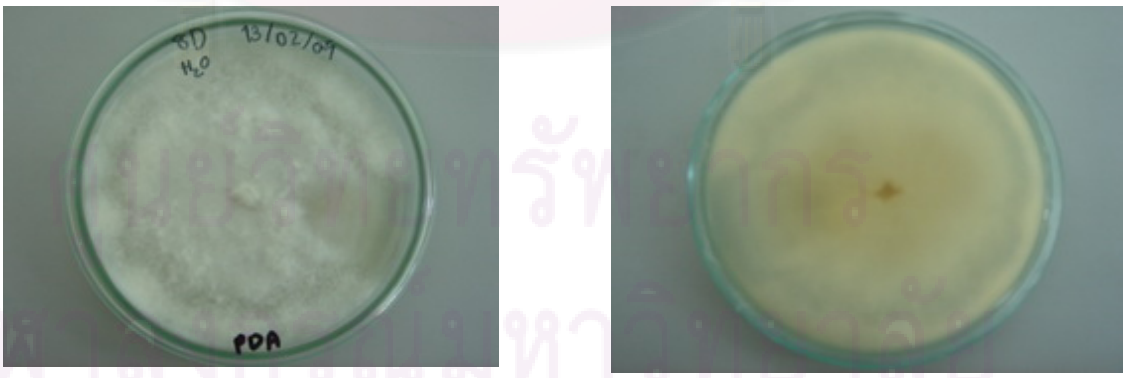

Obverse Reverse

Figure 3.3 Colony morphology of endophytic fungus isolate XG8D on PDA.

The fungus was identified based on the ITS1-5.8S-ITS2 and 28S rDNA sequences, which were amplified using universal primers JS1, JS8, ITS1, ITS4 and ITS5 (White , *et al*., 1990; Landvik, 1996). The 28S rDNA dataset including the basidiomycete endophyte coded XG8D was aligned along with representative taxa from eight major orders of Phylum Basidiomycota (Agaricales, Atheliales, Auriculariales, Boletales, Hymenochaetales, Polyporales, Russulales and Sebacinales) with their accession numbers. Within the Polyporales, five families, representing the Fomitopsidaceae, Ganodermataceae, Meruliaceae, Polyporaceae and Phanerochaetaceae, were incorporated in this analysis. Two representative taxa of the order Tremellales (*Tremella mesenteria* and *T. aurantia*) were used as the outgroup. The data were analyzed by the Clustal W (Thompson , *et al*., 1994) and PAUP phylogenetic analysis programs (Swofford, 2002). Phylogenetic data based on 28S rDNA showed that the fungus (XG8D) is well placed in the Order Polyporales. This data also demonstrated that fungus isolate number XG8D showed a close relationship with the suitable taxa from Family Meruliaceae (Order Polyporales) shown in **Figure 3.4**. In comparison of ITS sequence analyses, DNA sequence of the strain 8D was defined as 89% to 99% homology to the best matching sequence over the whole length of the sequences belonging to Order Polyporales (Subclass Incertae sedis, Class Agaricomycetes, Phylum Basidiomycota). Due to the limitation of the number taxa in Family Meruliaceae from NCBI for data comparing, the molecular data based on ITS region of this endophyte is insufficiently sensitive for genus identification (Altschul , *et al*., 1990). The DNA sequences 28SrDNA and ITS of the XG8D fungus have been submitted to GenBank with the accession number HM060640 and HM060641, respectively.

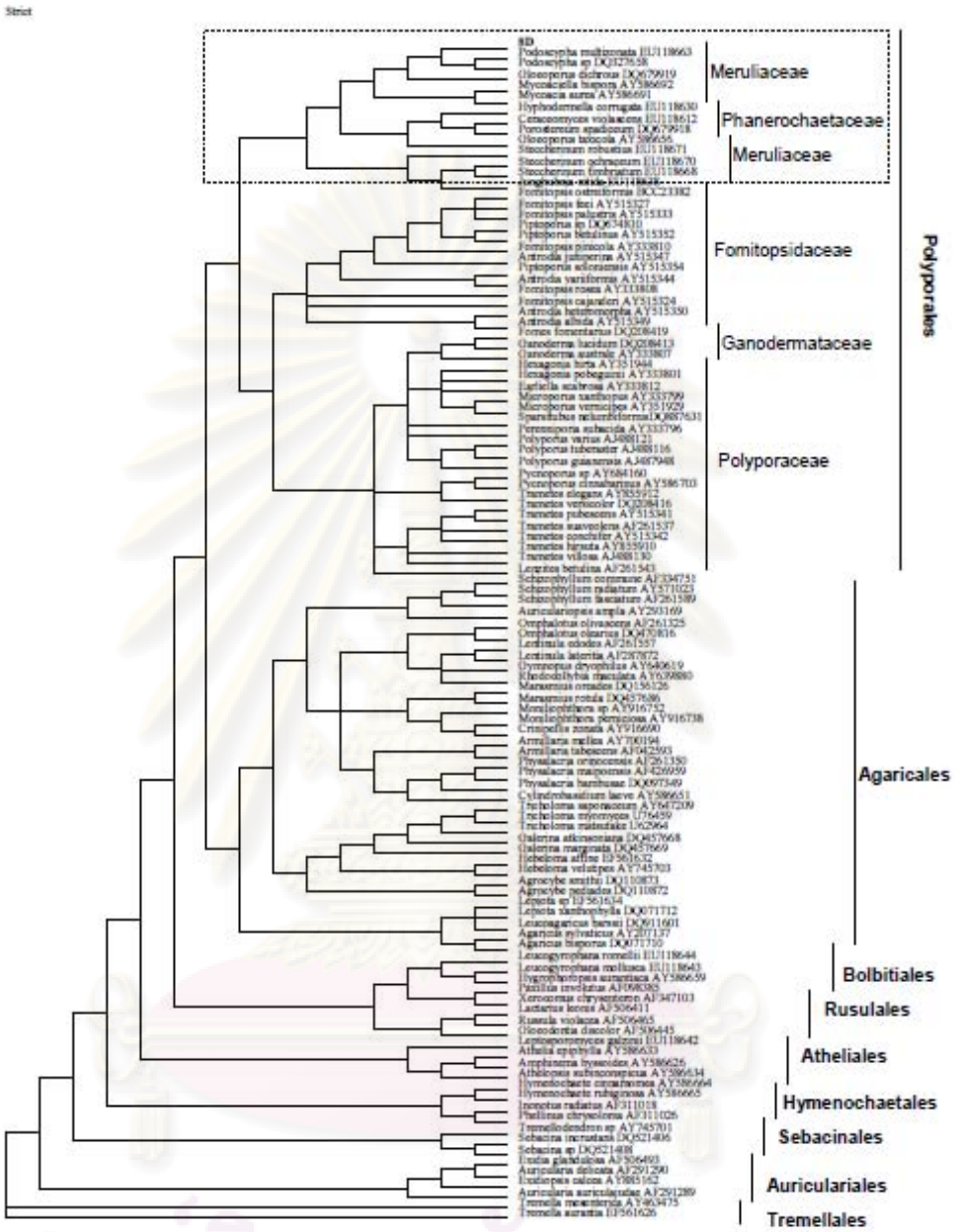

Figure 3.4 Strict consensus tree of seven equally parsimonious trees inferred from the 28S rDNA sequences.

3.11 Evaluation of biological activities

The pure compounds were evaluated for their anti-bacterial, anti-cancer and anti-malarial activities.

3.11.1 Anti-bacterial activity

A total of 12 strains of gram-positive and gram-negative bacteria (**Table 3.1**) were selected for *in vitro* antimicrobial assay. The test was performed by using microdilution assays as follows:

Table 3.1 Gram-positive and gram-negative bacteria tested

Gram-positive bacteria	Gram-negative bacteria
1. *Enterococcus faecalis* ATCC 29212	1. *Escherichia coli* ATCC 35218
2. *Enterococcus faecalis* ATCC 51299 (vancomycin resistant)	2. *Klebsiella pneumoniae* ATCC 27736
3. *Enterococcus faecium* UCLA 192	3. *Klebsiella pneumonia* (ESBL producing) ATCC 700603
4. *Salmonella typhimurium* ATCC 13311	4. *Pseudomonas aeruginosa* ATCC 27853
5. *Staphylococcus aureus* ATCC 25923	5. *Proteus vulgaris* ATCC 13315
6. *Staphylococcus epidermidis* ATCC 12228	
7. *Staphylococcus hominis* ATCC 27844	

3.11.1.1 Preparation of bacterial inocula

Bacteria were grown on Mueller Hinton agar (MHA) for 24 h at 37°C. Selected fresh single colonies were inoculated into 10 mL of Mueller Hinton broth (MHB) and incubated in shaking incubator for 2-3 h at 37°C. The turbidity of the bacterial suspension was adjusted with sterile normal saline solution to match the turbidity of 0.5 McFarland standard (OD 0.1 at 625 nm). Then the suspension was diluted 1:100 with Mueller Hinton broth (MHB) to contain $1x10^6$ CFU/mL.

3.11.1.2 Determination of minimum inhibitory concentration (MIC)

Solution of a test compound in DMSO (25.6 mg/mL) was diluted with MHB. The test compound was tested at the concentration ranges of 0.5 to 256 μg/mL. MIC is defined as the lowest concentration that inhibits growth of test microorganisms.

A 50 μL volume of MHB containing the test compound was dispensed into each well of microtiter plates (96-flat-bottom wells) for the evaluation of antibacterial activities. Sterile compound-free medium containing the corresponding amount of DMSO was dispensed in the growth control wells. The final adjusted bacterial suspensions were inoculated into each well with volume of 50 μL. Compound-free MHB in volumes of 100 µL were used as the sterility control. The experiments were done in duplicate. After incubation at 37°C for 24 h, a 20 μL of *p*-iodonitrotetrazolium (INT) solution (1mg/mL) was added into each well. The antibacterial assay plates were further incubated for 1 h. Growth in each well was indicated by a color change from colorless to violet. Compounds that inhibit microbial growth would prevent the development of a violet color. The well that shows no change in color indicates antimicrobial activity of the test compound.

3.11.2 Anticancer activity

Cytotoxic test was carried out at the institute of Biotechnology and Genetic Engineering, Chulalongkorn University. Bioassay of cytotoxicity activity was performed *in vitro* by MTT (3-(4,5-dimethylthiazol-2-yl)-2,5-diphynyltrazolium bromide) calorimetric method (Carmichael *et al*., 1987; Doyle and Griffiths, 1997; Mosmann, 1983; Tominaga et al., 1999) against hepato carcinoma (Hep-G2), colon carcinoma (SW-620), lung carcinoma (CHAGO), gastric carcinoma (KATO-3) and breast carcinoma (BT-474). In Principle, the viable cell number/well was directly proportional to the production of formazan, followed by solubilization, and could be measured spectrophotometrically.

The human cancer cell line was harvested from exponential-phase maintenance cultures (T-25 cm^2 flask), counted by trypan blue exclusion, seed cells in a 96-well culture plates at a density of $1x10^5$ cells/well in 200 μl of culture medium without compounds to be tested. Cells were cultured in a 5% CO_2 incubator at 37 ^oC, 100% relative humidity for 24 h. Culture medium containing the sample was

dispensed into the appropriate wells (control cells group, N = 3; each sample treatment group, N = 3). Peripheral wells of each plate (lacking cells) were utilized for sample blank (N = 3) and medium/DMSO blank (N = 3) “background” determination. Culture plates were then incubated for 3 days prior to the addition of tetrazolium reagent. MTT stock solution in a concentration of 5 mg/ml in PBS was sterilized by filtering through 0.45 μl filter units. MTT working solution was prepared just prior to culture application by dilution of MTT stock 1:5 (V/V) in prepared standard culture medium. The freshly prepared MTT reagent in a volume of 10 μl was added into each well and mixed gently for 1 minute on an orbital shaker. The cells were further incubated for 4 h at 37ºC in a 5% CO_2 incubator. After incubation, the formazan produced in the cells will capture as dark crystals in the bottom of the wells. All of the culture medium supernatant were removed from wells and 150 μl of DMSO was added to dissolve the resulting formazan. Samples in the culture plate were mixed for 5 minutes on an orbital shaker. Subsequently, 25 μl of 0.1 M Glycine pH 10.5 was added and the culture plate was shaken for 5 minutes. Following formazan solubilization, the absorbance was measured using a microculture plate reader at 540 nm (single wavelength, calibration factor = 1.00).

3.11.3 Antimalarial activity

Testing for anti-malarial activity was conducted by Bioassay Laboratory, National Center for Genetic Engineering and Biotechnology (BIOTEC), Thailand. The assay had been done by means of the following processes.

Plasmodium falciparum (K1, multidrug resistant strain) was cultured continuously according to the method of Tragen and Jensen. The quantitative assessment of the anti-malarial activity in vitro was performed in accordance with the microculture radioisotope technique based upon the method described by Desjardins, *et al*. A standard anti-malarial compound, dihydroartemisinin (IC_{50} values of 0.004 μM), was used as the positive control for the assay.

CHAPTER IV

RESULTS AND DISCUSSION

4.1 Chemical Constituents of the fungus *Rhytidhysteron* sp. (AS21B)

The crude extract of endophytic fungus *Rhytidhysteron* sp. (AS21B) was subjected to several step chromatographic fractionations and four naphthalene derivatives were isolated including three known compounds, MK3018 (**1**), palmarumycin CR1 (**2**), 4-*O*-methyl-CJ12372 (**3**) and 4-*O*-methyl-CJ12371 (**5**), and a new compound, AS21B-4 (**4**).

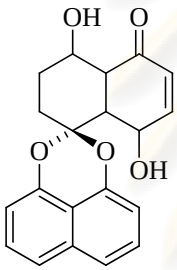

MK3018 (**1**)

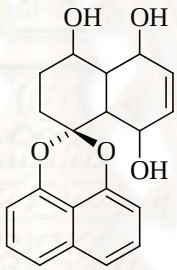

Palmarymycin CR1 (**2**)

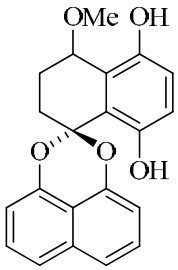

4-*O*-Methyl-CJ12372(**3**)

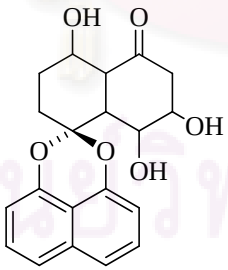

AS21B-4 (**4**)

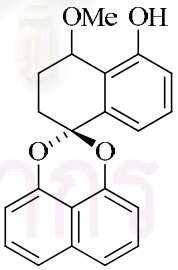

4-*O*-Methyl-CJ12371 (**5**)

Figure 4.1 The chemical structures of the compounds isolated from the fungus *Rhytidhysteron* sp. (AS21B)

4.1.1 Structure elucidation of compound 1

(**MK3018**)

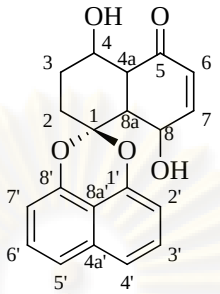

Figure 4.2 compound **1**

Molecular formula	$C_{20}H_{18}O_5$
Appearance	Yellowish pastes
m.p.	212-214 ^{o}C
$[\alpha]_D^{20}$	-71 (*c* 0.1 MeOH)
UV ($CHCl_3$) λ_{max} (log ε)	300 nm (3.62)
IR (KBr)	3397, 2962, 2945, 1926, 1124, 1112 and 1077 cm^{-1}
^1H and ^{13}C NMR ($CDCl_3$)	See Table 4.1
ESIMS *m/z*	361.10 $[M+Na]^+$ (calcd 361.11)

Compound **1** was isolated as yellowish paste and exhibited a molecular ion peak in the ESIMS at *m/z* 361.10 $[M+Na]^+$ (calcd 361.11), corresponding to a molecular formula of $C_{20}H_{18}O_5$ (12 degrees of unsaturation). The IR spectrum indicated the presence of carbonyl and olefinic/aromatic functionalities from the absorption bands at 3059 and 1660 cm^{-1}, respectively. From the ^1H and ^{13}C NMR data (Table 4.1), it was evident that seven of the 12 unsaturation units came from a ketone and six carbon-carbon double bonds (including five aromatic carbon-carbon double bonds). Therefore, the molecule was pentacyclic. The ^{13}C NMR and HSQC data revealed that **1** had one ketone carbonyl (δ_C 200.7), four sp^2 quaternary carbons (δ_C 145.7 (x2), 134.1, 113.8), eight sp^2 methines (δ_C 121.5, 127.2, 109.9, 109.8, 127.7, 120.6, 130.5, 147.2), an acetal quaternary carbon (δ_C 103.8), two oxygenated methines (δ_C 61.5, 62.9), two sp^3 methylenes (δ_C 25.4, 27.0). The ^1H NMR spectrum showed

characteristic signals for two olefinic protons at δ_H 6.12 (d, J = 10.0 Hz) and 7.11 (*dd*, J = 6.0, 10.0 Hz) and six naphthalene protons at δ_H 7.46 (m, 4H) and 6.95 (d, J = 7.5 Hz, 2H), which were assigned to H-2', H-3', H-6', H-7', H-4' and H-5', respectively. The COSY spectrum displayed an aliphatic spin system, CH_2-CH_2-CH(O)-CH-CH-CH(O)-CH=CH, which was flanked by a ketone carbonyl at C-4a and C-6 as suggested by HMBC cross-peak from H-4a to the carbonyl carbon (C-5) (Figure 4.3). On the basis of HMBC data, the acetal carbon was assigned to C-1 through the correlations of H_2-2/C-1 and H-8a/C-1. These results strongly indicated that compound **1** was MK3018, and its NMR data were identical to those previously reported as shown in Table 4.1. This compound has well documented for antibiotic activities (Ogishi *et. al.* 1989).

Table 4.1 NMR spectral data for compound **1** in $CDCl_3$

Position	**MK3018**		Compound **1**	
	^{1}H	^{13}C	^{1}H	^{13}C
1		103.8		103.8
2	1.95 (m, 2H)	25.4	1.95 (m, 2H)	25.4
3	1.76 (m, 2H)	27.0	1.78 (m, 2H)	27.0
4	4.74 (m, 1H)	63.0	4.74 (m, 1H)	62.9
4a	3.38 (dd, J = 13.2, 2.4 Hz, 1H)	46.9	3.39 (dd, J = 13.2, 2.4 Hz, 1H)	46.8
5		200.7		200.7
6	6.12 (d, J = 10.0 Hz, 1H)	130.5	6.12 (d, J = 10.0 Hz, 1H)	130.5
7	7.10 (dd, J = 10.0, 6.0 Hz, 1H)	147.2	7.11 (dd, J = 10.0, 6.0 Hz, 1H)	147.2
8	5.17 (d, J = 4.2 Hz, 1H)	61.5	5.15 (d, J = 4.2 Hz, 1H)	61.5
8a	2.90 (dd, J = 13.1, 2.1 Hz, 1H)	43.0	2.91 (dd, J = 13.2, 2.1 Hz, 1H)	42.9
1′		145.8		145.7
2′	6.94 (d, J = 7.47 Hz, 1H)	109.9	6.95 (d, J = 7.48 Hz, 1H)	109.9
3′	7.45 (m, 1H)	127.2	7.46 (m, 1H)	127.2
4′	7.45 (m, 1H)	121.5	7.46 (m, 1H)	121.5
4a′		134.2		134.1
5′	7.45 (m, 1H)	120.6	7.46 (m, 1H)	120.6
6′	7.45 (m, 1H)	127.7	7.46 (m, 1H)	127.7
7′	6.94 (d, J = 7.5 Hz, 1H)	109.8	6.95 (d, J = 7.5 Hz, 1H)	109.8
8′		145.8		145.7
8a′		113.9		113.8

*a in $CDCl_3$

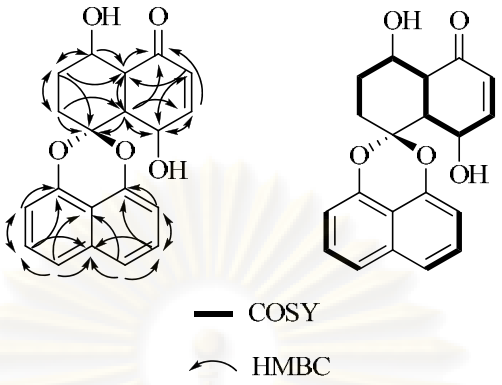

Figure 4.3 HMBC and COSY correlations of compound **1**

4.1.2 Structure elucidation of compound 2 (Palmarumycin CR1)

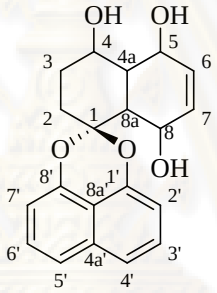

Figure 4.4 compound **2**

Molecular formula	$C_{20}H_{20}O_5$
Appearance	Yellow-brown solid
m.p.	272-274 ^{o}C
$[\alpha]_D^{20}$	-22 (*c* 0.1 MeOH)
UV ($CHCl_3$) λ_{max} (log ε)	295 nm (4.07)
IR (KBr)	3554, 3422, 3329, 2907, 1912, 1632, 1410 and 1069 cm^{-1}
^{1}H and ^{13}C NMR ($CDCl_3$)	See Table 4.2
ESIMS *m/z*	363.12 $[M+Na]^+$ (calcd 363.12)

Compound **2** was obtained as a yellow-brown solid and its molecular formula was determined as $C_{20}H_{20}O_5$ by ESIMS at *m/z* 363.12 $[M+Na]^+$ (calcd 363.12). The

^{1}H, ^{13}C (Table 4.2.) and 2D NMR (HSQC, COSY, HMBC) data revealed the presence of three oxygenated methines [δ_H 4.11 m, 4.50 m, 4.03 d (J = 4.7Hz); δ_C 65.2, 60.7, 61.8], two sp^3 methylenes [δ_H 1.88-1.48 m, 4H; δ_C 28.3, 25.7], one double bond [δ_H 5.81-5.66 m; δ_C 133.5, 128.2], one acetal quaternary carbon (δ_C 103.5) and a disubstituted naphthalene ring [δ_H 6.93 d (J = 7.4 Hz, 2H), 7.45 brs (1H), 7.50 d (J = 1.6 Hz, 1H), 7.52 d (J = 1.3 Hz, 1H), 7.47 brs (1H); δ_C 109.3 CH, 108.8 CH, 127.6 CH, 120.0 CH, 119.8 CH, 127.6 CH, 149.0 qC, 135.7 qC, 147.8 qC, 115.2 qC]. The NMR data of **2** were very similar to those of MK3018 (**1**), except for the appearance of an additional oxygenated methine and the absence of carbonyl group in **1**. These results suggested that **2** was palmarumycin CR1, 5-hydroxy-MK3018, which was confirmed by HMBC correlations of H-5/C-7, H-4/C-5 and H-6/C-5 (Figure 4.5), as well as by comparison of its NMR data (**Table 4.2**) with those reported in the literature (Wipf *et. al.* 2004).

Table 4.2 NMR spectral data for Palmarumycin CR1 and compound **2**

Position	**Palmarumycin CR1**[a]		Compound **2**[b]	
	^{1}H	^{13}C	^{1}H	^{13}C
1		105.1		103.5
2	1.90 (m, 1H) 1.76 (m, 1H)	29.6	1.88-1.48 (m, 2H)	28.3
3	1.90 (m, 2H)	26.7	1.88-1.48 (m, 2H)	25.7
4	4.31 (brs, 1H)	64.2	4.11 (m, 1H)	65.2
4a	2.38 (m, 1H)	43.3	2.41 (m, 1H)	41.6
5	4.54 (m, 1H)	67.7	4.50 (m, 1H)	60.7
6	5.92 (m, 1H)	134.8	5.81-5.66 (m, 1H)	133.5
7	5.92 (m, 1H)	129.3	5.81-5.66 (m, 1H)	128.2
8	4.76 (m, 1H)	63.2	4.03 (d, J = 4.7 Hz, 1H	61.8
8a	2.38 (m, 1H)	42.3	2.41 (m, 1H)	40.8
1′		149.0		147.5
2′	6.98 (d, J = 7.4 Hz, 1H)	110.6	6.93 (d, J = 7.4 Hz, 1H)	109.3
3′	7.46 (brs, 1H)	128.6	7.45 (brs, 1H)	127.6
4′	7.52 (d, J = 1.61 Hz, 1H)	121.7	7.50 (d, J = 1.6 Hz, 1H)	120.0
4a′		135.7		133.7
5′	7.52 (d, J = 1.3 Hz, 1H)	121.3	7.52 (d, J = 1.3 Hz, 1H)	119.8
6′	7.46 (brs, 1H)	128.4	7.47 (brs, 1H)	127.6
7′	6.95 (dd, J = 7.4 Hz, 1H)	110.2	6.93 (d, J = 7.4Hz, 1H)	108.8
8′		147.8		146.6
8a′		115.2		113.3

[a] recorded in CD_3OD , [b] recorded in DMSO-d_6

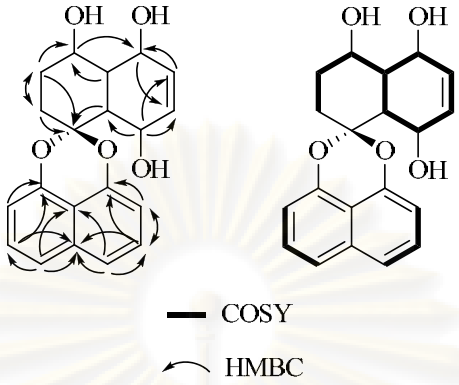

Figure 4.5 HMBC and COSY correlations of compound **2**

4.1.3 Structure elucidation of compound 3 (4-*O*-Methyl-CJ12372)

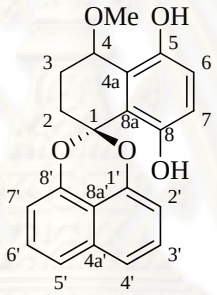

Figure 4.6 compound **3**

Molecular formula	$C_{21}H_{18}O_5$
Appearance	Colorless solid
m.p.	100-101 ^{o}C
$[\alpha]_D^{20}$	+230 (*c* 0.1 MeOH)
UV ($CHCl_3$) λ_{max} (log ε)	300 nm (3.49)
IR (KBr)	3465, 3267, 2933, 1609, 1468, 1412, 1266 and 1066 cm^{-1}
^1H and ^{13}C ($CDCl_3$)	See Table 4.3
HRESIMS *m/z*	373.10 $[M+Na]^+$ (calcd for $C_{20}H_{20}O_5Na$, 373.12)

Compound **3** was isolated as Colorless solid and the molecular formula of $C_{21}H_{18}O_5$ was established from its ESIMS (*m/z* 373.10 $[M+Na]^+$, calcd 373.12),

indicating 13 degrees of unsaturation. Its NMR data (Table 4.3) revealed the same characteristic signals as those of **2** including the signals for a disubstituted naphthalene ring and an acetal quaternary carbon with exception of the presence of a methoxy group (δ_H 3.45 s; δ_C 54.5) and a tetrasubstituted aromatic ring [δ_H 6.93 d (J = 3.1 Hz, 2H); δ_C 122.4 qC, 149.1 qC, 119.7 CH, 118.9 CH, 149.3 qC, 119.4 CH], in place of two olefinic protons and four sp^3 methines in **2**. These data strongly suggested that **3** had an additional aromatic ring relative to **2**. The methoxy group was located at C-4 due to HMBC correlation from the singlet methoxy protons at δ_H 3.45 to C-4 (δ_C 74.8). Moreover, the structure of **3** was confirmed by observed COSY and HMBC correlations as shown in Figure 4.7. Comparison of NMR data of compound **3** with those published in the literature (Sakemi *et. al.* 1995) (**Table 4.3)** indicated that compound **3** was 4-*O*-methyl-CJ-12372**.**

Table 4.3 NMR spectral data for 4-*O*-methyl-CJ12372 and compound **3**

Position	**4-*O*-Methyl-CJ12372** [a]	Compound **3** [b]	
	^{1}H	^{1}H	^{13}C
1			102.4
2	1.51 (m, 2H)	2.40 (m, 1H), 1.98 (m, 1H)	27.1
3	1.74 (m, 1H), 2.10 (m, 1H)	2.08 (m, 2H)	22.5
4	4.36(d, *J* = 8.3, 5.4 Hz, 1H)	4.81 (t, *J* = 6.3 Hz, 1H)	74.8
4a			122.4
5			149.1
6	7.58 (s, 1H)	6.93 (d, *J* = 3.1 Hz, 1H)	119.7
7	7.33 (s, 1H)	6.93 (d, *J* = 3.1 Hz, 1H)	118.9
8			149.3
8a			119.4
1′			146.9
2′	7.32 (dd, *J* = 8.3, 0.7 Hz, 1H)	7.00 (dd, *J* = 6.5, 0.65 Hz, 1H)	110.3
3′	7.14 (dd, *J* = 8.3, 7.6 Hz)	7.45 (dd, *J* = 7.6, 8.3 Hz, 1H)	127.4
4′	6.77 (dd, *J* = 7.6, 0.7 Hz, 1H)	7.56 (d, *J* = 3.0 Hz, 1H)	121.4
4a′			134.0
5′	6.78 (dd, *J* = 7.6, 0.7 Hz, 1H)	7.54 (d, *J* = 3.0 Hz, 1H)	121.2
6′	7.12 (dd, *J* = 8.3, 7.6 Hz, 1H)	7.45 (dd, *J* = 7.6, 8.3 Hz, 1H)	127.3
7′	7.30 (dd, *J* = 8.3, 0.7 Hz, 1H)	7.00 (dd, *J* = 6.5, 0.8 Hz, 1H)	110.3
8′			146.4
8a′			113.6
4-OMe		3.45 (s)	54.5

[a] $CDCl_3$: CD_3OD = 5:1, [b] $CDCl_3$

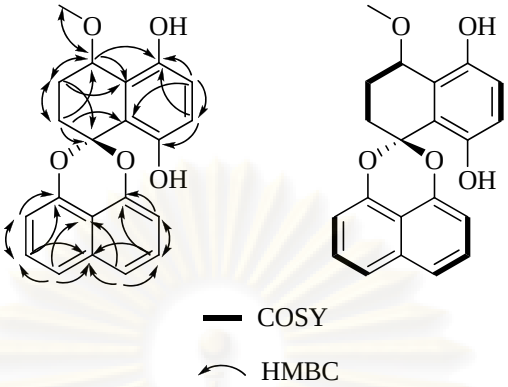

Figure 4.7 HMBC and COSY correlations of compound **3**

4.1.4 Structure elucidation of compound 4 (AS21B-4)

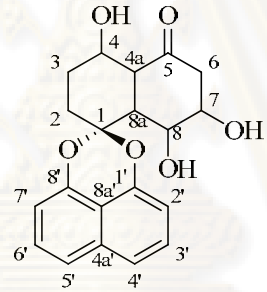

Figure 4.8 compound **4**

Molecular formula	$C_{20}H_{20}O_6$
Appearance	Yellow-brown solid
m.p.	Lack of data due to insufficient amount
$[\alpha]_D^{20}$	0 (*c* 0.1 MeOH)
UV ($CHCl_3$) λ_{max} (log ε)	300 nm (3.81)
IR (KBr)	3455, 2924, 2362, 1609, 1411, 1381, 1271 and 1055 cm^{-1}
^1H and ^{13}C ($CDCl_3$)	See Table 4.4
HRESIMS *m/z*	379.1153 $[M+Na]^+$ (calcd for $C_{20}H_{20}O_6Na$, 379.1158)

Compound **4** was isolated as a yellow-brown solid. The molecular formula was determined by HRESIMS as $C_{20}H_{20}O_6$, observing ion peak $[M+Na]^+$ at *m/z* 379.1153 (calcd 379.1158). The ^1H, ^{13}C (Table 4.2.) and 2D NMR (HSQC, COSY, HMBC) data displayed the presence of three oxygenated methines [δ_H 4.54 m, 4.77 m, 4.42 m; δ_C 62.9, 67.4, 71.3], three sp^3 methylenes [δ_H 1.74 m (1H), 1.65 m (1H), 1.94 m (2H), 3.12 m (1H), 2.47 dd (J = 2.0, 1.8 Hz, 1H); δ_C 26.1, 25.6, 44.2], an acetal quaternary carbon (δ_C 104.4), one carbonyl carbon (δ_C 212.2) and a disubstituted naphthalene ring [δ_H 6.94 d (J = 7.4 Hz, 2H), 7.40 m (2H), 7.50 m (2H), 7.52 d (J = 1.3 Hz, 1H), 7.47 brs (1H); δ_C 109.7 2xCH, 127.7 CH, 121.5 CH, 120.5 CH, 127.1 CH, 147.3 qC, 134.1 qC, 145.8 qC, 113.8 qC]. The ^1H-^1H COSY experiment led to the connection from H_2-2 to H_2-6 as show in Figure 4.9. The connectivity of ketone carbonyl (C-5) to C-4a and C-6 was confirmed by HMBC correlations of H-4a and H_2-6 to the ketone carbon (**Figure 4.9**). Actually, the NMR data of **3** indicated its structure to be closely related to that of MK3018 (**1**), with the only difference being the presence an oxygenated methine at C-7 and a methylene at C-6 replacing the $\Delta^{6,7}$ double bond in **1**. The structure assignment of **2** was further confirmed from COSY and HMBC correlations (**Figure 4.9**). Thus, the structure of 3 was elucidated as shown and given the name as **AS21B-4**.

Table 4.4 NMR spectral data for compound **4** in $CDCl_3$

Position	^1H	^{13}C	COSY	HMBC
1		104.4		
2	1.74 (m, 1H)	26.1	H-3	C-1, C-3
	1.65 (m, 1H)			
3	1.94 (m, 2H)	25.6	H-2, H-4	C-1, C-2, C-4
4	4.54 (m, 1H)	62.9	H-3, H-4a	C-3
4a	3.30 (dd, J = 1.6, 1.3 Hz, 1H)	49.0	H-4, H-8a	C-5, C-8a
5		212.2		
6	3.12 (m , 1H)	44.2	H-7	C-5
	2.47 (dd, J = 2.0, 1.7 Hz, 1H)			
7	4.77 (m, 1H)	67.4	H-6, H-8	C-6, C-8
8	4.42 (m, 1H)	71.3	H-7, H-8a	C-8a, C-7
8a	3.16 (m, 1H)	41.5	H-4a, H-8	C-1
1′		147.3		
2′	6.94 (d, J = 7.4 Hz, 1H)	109.7	H-3′, H-6′	C-1′, C-3′, C-8′, C-6′
3′	7.40 (m, 1H)	127.7	H-2′, H-	C-1′, C-2′, C-4a′, C-

			4′, H-5′, H-7′	7′, C-8′
4′	7.50 (m, 1H)	121.5	H-3′, H-6′	C-3′, C-4a′, C-8a′, C-6′
4a′		134.1		
5′	7.50 (m, 1H)	120.5	H-3′, H-6′	C-3′, C-4a′, C-8a′, C-6′
6′	7.40 (m, 1H)	127.1	H-2′, H-4′, H-5′, H-7′	C-1′, C-2′, C-4a′, C-7′, C-8′
7′	6.94 (d, *J* = 7.4 Hz, 1H)	109.7	H-3′, H-6′	C-1′, C-3′, C-8′, C-6′
8′		145.8		
8a′		113.8		

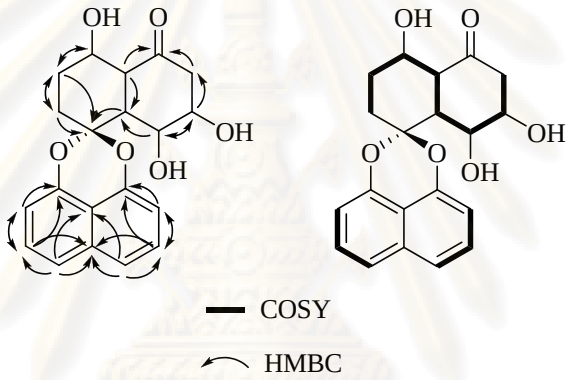

Figure 4.9 HMBC and COSY correlations of compound **4**

4.1.5 Structure elucidation of compound 5 (4-*O*-Methyl-d_3-CJ12371)

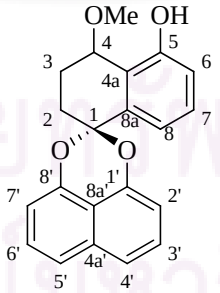

Figure 4.10 compound **5**

Molecular formula	$C_{21}H_{18}O_4$
Appearance	Colorless glass
m.p.	Lack of data due to insufficient amount
$[\alpha]_D^{20}$	0 (*c* 0.1 MeOH)
UV ($CHCl_3$) λ_{max} (log ε)	295 nm (3.96)
IR (KBr)	3450, 2925, 2361, 1610, 1460, 1274 and 1068 cm^{-1}
^1H and ^{13}C ($CDCl_3$)	See Table 4.5
HRESIMS *m/z*	357.10 $[M+Na]^+$ (calcd for $C_{21}H_{18}O_4Na$, 357.12)

Compound **5**, colorless glass, had a molecular formula of $C_{21}H_{18}O_4$, established by ESIMS (*m/z* 357.10 calcd for $[M+Na]^+$ 357.12). The NMR data of **5** and the information from its 2D NMR studies (^1H-^1H COSY, HSQC, HMBC) indicated the presence of a methoxy [δ_H 3.50 s; δ_C 54.1], a disubstituted naphthalene ring [δ_H 6.99 (dd, *J* = 7.9, 1.0 Hz, 1H), 7.36 (m, 1H), 7.41 (m, 1H), 6.93 (dd, *J* = 7.4, 3.8 Hz, 1H), 7.43 (m, 1H), 7.49 (m, 1H); δ_C 127.4 2xCH, 120.4 2xCH, 109.4 CH, 109.3 CH, 147.9 qC, 134.2 qC, 147.8 qC, 113.5 qC], an oxygenated methine [δ_H 4.92 (dd, *J* = 8.7, 6.2 Hz); δ_C 76.2], two sp^3 methylenes [δ_H 1.91 m (1H), 2.43 m (1H), 2.19 m (2H); δ_C 27.9, 23.1]. The ^1H and ^{13}C NMR data of **5** showed a close similarity to those of compound **3**, except for the presence of an additional aromatic proton (δ_H 7.41 m) instead of oxygenated aromatic quaternary carbon, the chemical shift of C-8 was upfield shifted to δ_C 118.7 when compared to **3** (δ_C 149.3). This conclusion was confirmed by the HMBC correlations of H-8/C-6, H-8/C-8a and the COSY correlation of H-8/H-7. Based on the spectroscopic data above, compound **5** was identified to be 4-*O*-methyl-CJ12371, and the comparison of its NMR data with those reported in literature is shown in **Table 4.5** (Sakemi *et. al.* 1995).

Table 4.5 NMR spectral data for 4-*O*-methyl-CJ12371 and compound **5**

Position	**4-*O*-Methyl-CJ12371**[a]		Compound **5**[b]	
	^{1}H	^{13}C	^{1}H	^{13}C
1		100.7		99.4
2	2.05 (m, 1H)	26.2	1.91 (m, 1H)	27.9
	2.20 (m, 1H)		2.43 (m, 1H)	
3	1.98 (m, 2H)	23.6	2.19 (m, 2H)	23.1
4	4.70 (br t, *J* = 3.6 Hz, 1H)	71.9	4.92 (dd, *J* = 8.66, 6.19 Hz, 1H)	76.2
4a		124.0		121.8
5		156.2		156.2
6	6.90 (dd, *J* = 7.9, 1.3 Hz, 1H)	116.9	6.99 (dd, *J* = 7.9, 1.0 Hz, 1H)	117.9
7	7.22 (dd, *J* = 8.7, 7.9 Hz, 1H)	130.1	7.36 (m, 1H)	130.0
8	7.29 (dd, *J* = 8.7, 1.3 Hz, 1H)	118.9	7.41 (m, 1H)	118.7
8a		137.2		136.5
1′		148.8		147.9
2′	6.85 (dd, *J* = 7.3, 1.1 Hz, 1H)	109.7	6.93 (dd, *J* = 7.4, 3.8 Hz, 1H)	109.4
3′	7.33 (dd, *J* = 7.9, 7.3 Hz, 1H)	127.9	7.43 (m, 1H)	127.4
4′	7.40 (br d, *J* = 7.9 Hz, 1H)	120.9	7.49 (m, 1H)	120.4
4a′		134.8		134.2
5′	7.40 (br d, *J* = 7.9 Hz, 1H)	120.9	7.49 (m, 1H)	120.4
6′	7.31 (dd, *J* = 7.9, 7.3 Hz, 1H)	127.9	7.43 (m, 1H)	127.4
7′	6.79 (dd, *J* = 7.3, 0.9 Hz, 1H)	109.7	6.93 (dd, *J* = 7.4, 3.8 Hz, 1H)	109.3
8′		148.5		147.8
8a′		114.1		113.5
4-OMe		55.7	3.50 (s, 3H)	54.1

* a $CDCl_3$: CD_3OD = 1:1, b $CDCl_3$

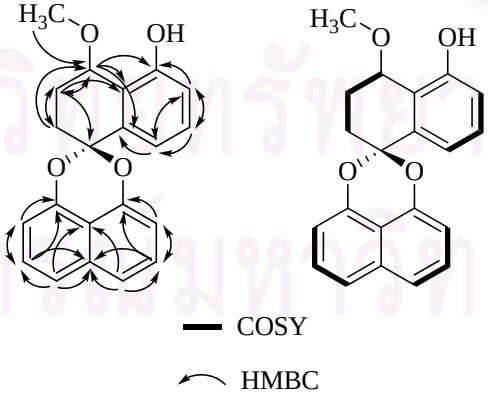

Figure 4.11 HMBC and COSY correlations of compound **5**

4.2 Chemical Constituents of Basidiomycetous fungus strain XG8D

The crude extracts from culture broth of endophytic fungus strain XG8D were subjected to fractionations using Sephadex LH-20 and silica gel column chromatography to obtain four new compounds, merulin A-D (**6**-**9**).

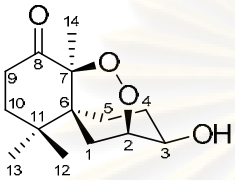

Merulin A (**6**)

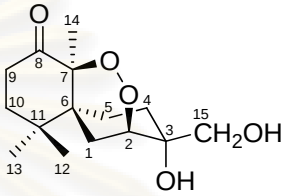

Merulin B (**7**)

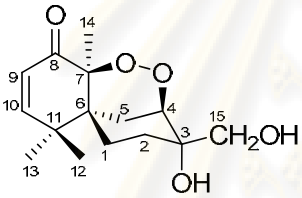

Merulin C (**8**)

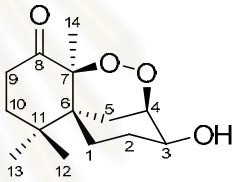

Merulin D (**9**)

Figure 4.12 The chemical structures of the compounds isolated from Basidiomycetous fungus strain XG8D

4.2.1 Structure elucidation of compound 6 (Merulin A)

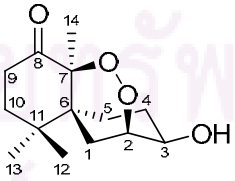

Figure 4.13 compound **6**

Melecular formula	$C_{14}H_{22}O_4$
Appearance	Colorless crystals
m.p.	214-217 ºC
$[\alpha]_D^{20}$	+230 (*c* 0.1 MeOH)
UV ($CHCl_3$) λ_{max} (log ε)	205 nm (3.38)
IR (KBr)	3515, 2970, 2928, 1719, 1454, 1294 and 1075 cm^{-1}
^1H and ^{13}C ($CDCl_3$)	See Table 4.6
HRESIMS *m/z*	277.1414 $[M+Na]^+$ (calcd for $C_{14}H_{22}O_4Na$, 277.1416)

Merulin A (**6**) was obtained as colorless crystals. Its molecular formula was established as $C_{14}H_{22}O_4$ by HRESIMS data (m/z 277.1414 $[M+Na]^+$, calcd 277.1416), indicating four degrees of unsaturation. IR absorptions implied the presence of hydroxyl (3515 cm^{-1}) and carbonyl (1719 cm^{-1}) groups. Analysis of ^{13}C and DEPT NMR spectra of **6** revealed three methyl carbons (δ_C 21.5, 24.7, and 26.2), five methylene carbons (δ_C 25.6, 30.5, 32.1, 35.6, and 35.8), two methine carbons (δ_C 69.4 and 79.1), three quaternary carbons (δ_C 37.3, 41.2, and 90.1), and one ketone carbonyl carbon (δ_C 208.4). Among them, two methines (δ_C 69.4 and 79.1) and one quaternary carbon (δ_C 90.1) were ascribed as bearing oxygen atoms. Since a carbonyl group accounted for one out of four degrees of unsaturation, the remaining three degrees of unsaturation were assumed for the presence for a tricyclic system in **1**. The ^1H-^1H COSY spectrum revealed two discrete spin systems, including $–CH_2$-CH-CH-CH_2-CH_2- (from H-1 to H-5) and $–CH_2$-CH_2- (from H-9 to H-10) as drawn with bold lines in **Figure 4.14**. Further detailed HMBC studied established the connectivity of these two fragments, methyl groups, carbonyl groups, and quaternary carbons. The correlations from a methyl singlet (Me-14) at δ_H 1.41 to C-6, C-7, and C-8 indicated the methyl (C-14) connected with the oxygenated quaternary carbon (C-7) and also confirmed the bonding of C-6, C-7, and a ketone group at C-8 which in turn correlated by methylene protons at C-9 and C-10. The cross-peaks of Me-13 and Me-14 to C-6, along with the correlations of H_2-1 and H_2-5 to C-6, completed the connectivity of the

two rings through the spiro carbon C-6 in the molecule. However, NMR data ultimately proved to be insufficient to solve the structure of **6**. The connection between C-2 and C-7 through endoperoxide linkage could not be confirmed by NMR. To clearly assign the structure, a single-crystal X-ray diffraction study was performed. The X-ray structure of **6** (**Figure 4.15**) thus revealed that **6** is an unprecedented nor-chamigrane containing endoperoxide linkage and 6/6/6 tricyclic framework and allowed the determination of its relative configuration, which was also in good accordance with its relative configuration in solution as assigned by an NOESY spectrum.

Table 4.6 NMR spectral data for compound **6**[a]

Position	**6**	
	δ_H (mult, *J* in Hz)	δ_C
1	2.05 (ddd, 13.5, 4.2, 3.9), H-1eq 1.56 (dd, 13.5, 1.8), H-1ax	30.5
2	4.14 (ddd, 4.2, 3.8, 1.8)	79.1
3	3.77 (ddd, 10.1, 7.9, 3.8)	69.4
4	2.17 (m), H-4ax and H-4eq	32.1
5	2.11 (m), H-5eq 1.59 (m), H-5ax	25.6
6	-	41.2
7	-	90.1
8	-	208.4
9	2.69 (ddd, 15.4, 14.9, 6.7), H-9α 2.45 (ddd, 15.4, 4.7, 2.4), H-9*β*	35.6
10	2.01 (ddd, 14.9, 14.8, 4.7), H-10*β* 1.58 (m), H-10α	35.8
11	-	37.3
12	0.98 (s)	26.2
13	1.26 (s)	24.7
14	1.41 (s)	21.5
15	-	

[a] Measured at 500 MHz (^{1}H) and 125 MHz (^{13}C) in $CDCl_3$

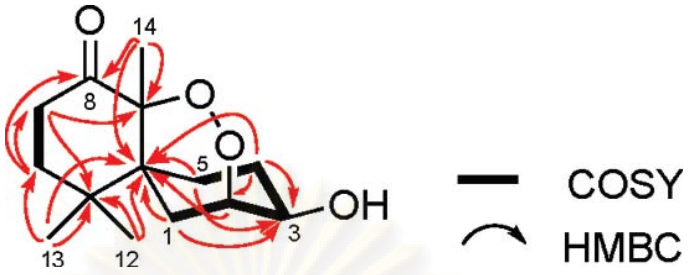

Figure 4.14 ^{1}H-^{1}H COSY and key HMBC correlations of **6**

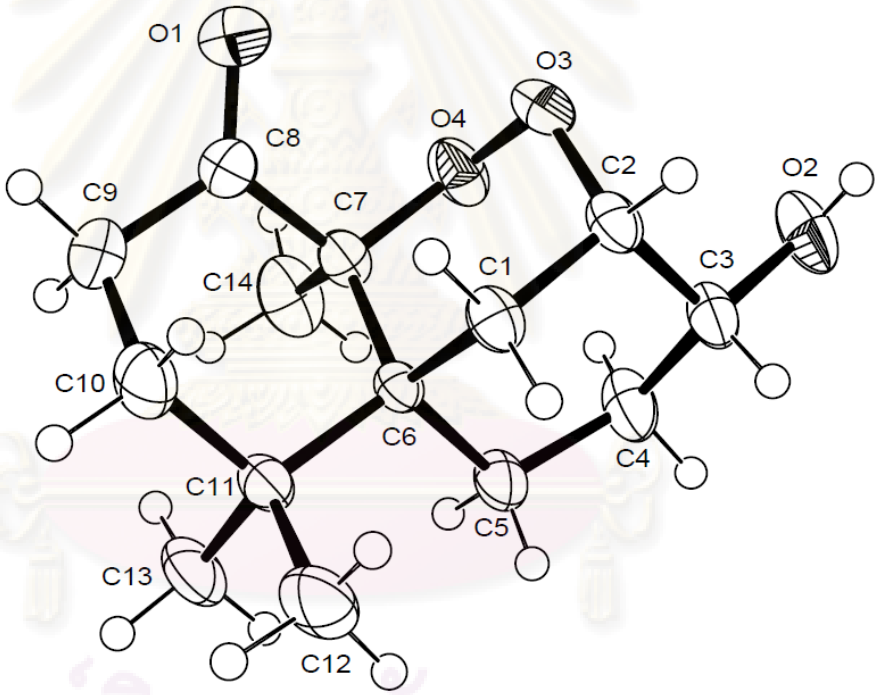

(a) top view

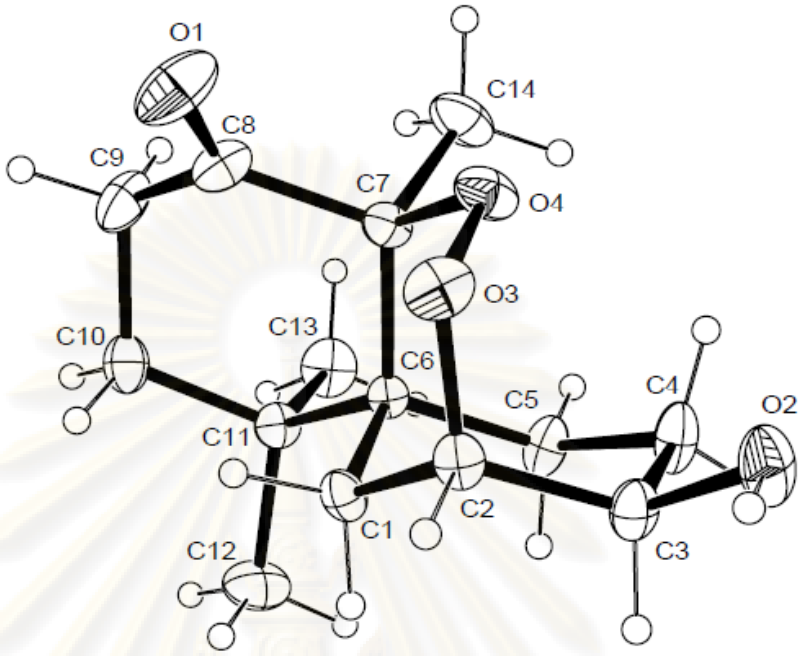

(a) side view

Figure 4.15 ORTEP diagram of **6**

X-ray Crystallographic Analysis of Merulin A (6). Crystal data:colorless crystal; $C_{14}H_{22}O_4$, M_r = 254.32, orthorhombic, $P2_12_12_1$, a = 7.3526(10) Å, b = 12.4749(3) Å, c = 13.9626(3) Å, α = β = γ = 90°, Z = 41, and V = 1280.69(4) Å^3, Mo Kα radiation, λ = 0.71073 Å. The intensity data were collected at 293 K to a maximum 2θ valueof 66.50°. Of the 15 534 reflections collected, 4861 were unique (R_{int} = 0.0282). The crystal structure was solved by direct methods and using the SHELXS97 program. Refinements were made by fullmatrix least-squares on all F^2 data using SHELXL97 to final R values [$I > 2\sigma(I)$] of R_1 = 0.0422, wR_2 = 0.1158 and goodness off it on F^2 = 1.059. All non-hydrogen atoms were anisotropic ally refined. All hydrogen atoms were added at calculated positions and refined using a rigid model. Crystallographic data for **1** have been deposited with the Cambridge Crystallographic Data Centre (deposition number CCDC 761514). Copies of the data can be obtained, free of charge, via www.ccdc.cam.ac.uk/data_request/cif, or by e-mailing data_request@ccdc.cam.ac.uk, or by contacting The Cambridge Crystallographic Data Centre, 12 Union Road, Cambridge CB2 1EZ, UK: fax:+44 1223 336033.

4.2.2 Structure elucidation of compound 7 (Merulin B)

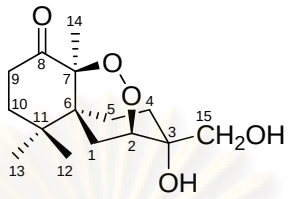

Figure 4.16 compound **7**

Melecular formula	$C_{15}H_{24}O_5$
Appearance	White powder
m.p.	94-96 ºC
$[\alpha]_D^{20}$	+170 (*c* 0.1 MeOH)
UV ($CHCl_3$) λ_{max} (log ε)	205 nm (3.14)
IR (KBr)	3406, 2966, 1728, 1444, 1374, 1354, 1126, 1055, and 1010 cm^{-1}
^1H and ^{13}C ($CDCl_3$)	See Table 4.7
HRESIMS *m/z*	285.1704 $[M+H]^+$ (calcd for $C_{15}H_{25}O_5$, 285.1702)

Merulin B (**7**) was isolated as a white powder, and the molecular formula was determined to be $C_{15}H_{24}O_5$ by HRESIMS (*m/z* 285.1704 $[M+H]^+$, calcd 285.1702) with four degrees of unsaturation. The ^1H and ^{13}C NMR data of **7** (**Table 4.7**) were strikingly similar to those of **6** with the only difference being the presence of a $–CH_2–$OH unit instead of –H at C-3. This was confirmed by the HMBC correlations from H_2-15 to C-2, C-3, and C-4. The relative configuration of **7** was similar to that of **6** as established by NOESY spectroscopic data. Key NOESY correlation between H-4ax and H_2-15 indicated the equatorial position for the $–CH_2–$OH unit at C-3 (**Figure 4.17**).

Table 4.7 NMR spectral data for compound **7**[a]

Position	**7**	
	δ_H (mult, *J* in Hz)	δ_C
1	2.05 (dd, 13.3, 1.8), H-1ax 1.78 (ddd, 13.3, 4.1, 3.4), H-1eq	27.2
2	4.03 (br s)	78.5
3	-	71.5
4	2.07 (13.9, 13.5, 6.5), H-4ax 1.65 (dd, 13.9, 6.2), H-4eq	31.4
5	1.96 (m), H-5eq 1.81 (ddd, 13.5, 13.0, 6.2), H-5ax	22.8
6	-	42.2
7	-	90.3
8	-	208.6
9	2.65 (ddd, 15.4, 14.8, 6.7), H-9α 2.41 (ddd, 15.4, 4.6, 2.3), H-9*β*	35.6
10	2.02 (ddd, 14.8, 14.4, 4.6), H-10*β* 1.55 (ddd, 14.4, 6.7, 2.3), H-10α	35.5
11	-	37.4
12	1.00 (s)	26.4
13	1.23 (s)	24.4
14	1.35 (s)	21.4
15	3.94 (d, 11.1) 3.43 (d, 11.1)	66.5

[a] Measured at 500 MHz (^{1}H) and 125 MHz (^{13}C) in $CDCl_3$

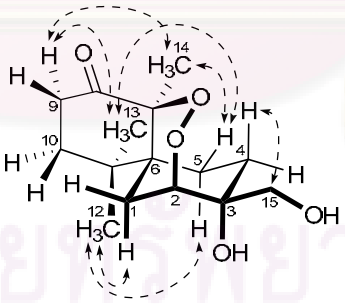

Figure 4.17 Selected NOESY correlations of **7**

4.2.3 Structure elucidation of compound 8 (Merulin C)

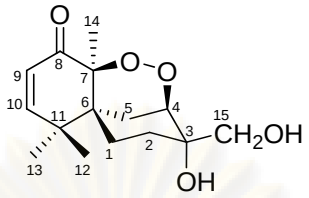

Figure 4.18 compound **8**

Melecular formula	$C_{15}H_{22}O_5$
Appearance	White powder
m.p.	142-148 ºC
$[\alpha]_D^{20}$	+203(*c* 0.1 MeOH)
UV ($CHCl_3$) λ_{max} (log ε)	205 nm (2.82)
IR (KBr)	3396, 3019, 2965, 1685, 1451, 1373, 1091, and 1029 cm^{-1}
^1H and ^{13}C ($CDCl_3$)	See Table 4.8
HRESIMS *m/z*	305.1366 $[M+Na]^+$ (calcd for $C_{15}H_{22}O_5Na$, 305.1365)

Merulin C (**8**) was isolated as a white powder. Its molecular formula was established as $C_{15}H_{22}O_5$ by HRESIMS (*m/z* 305.1366 $[M+Na]^+$, calcd 305.1365), implying five degrees of unsaturation). The ^1H and ^{13}C NMR spectra of **8** (**Table 4.8**) were closely analogous to those of **7**, except for the appearance of a new pair of doublet at δ_H 5.82 and 6.32 (J = 10.4 Hz) due to the olefinic protons, instead of two methylenes at C-9 and C-10 in **7**. All the NMR data implied that **8** is α,*β*-unsaturated ketone derivative of **7**, which was confirmed by 2D NMR (^1H-^1H COSY, HMQC, and HMBC experiments). However, analysis of NOESY spectroscopic data revealed the difference between their relative configurations. H-5eq of **7**, which has NOESY correlations with H_3-13 and H_3-14, exhibited COSY correlation with oxygenated methine (H-4) instead of the methylene protons (H_2-4). Therefore the endoperoxide linkage of **8** was proposed to attach to C-4 instead of C-2 as observed in **7**. Key

NOESY correlation between H-2ax and H_2-15 indicated the equatorial position for the $–CH_2–OH$ unit at C-3 (**Figure 4.19**).

Table 4.8 NMR spectral data for compound **8**[a]

Position	**8**	
	δ_H (mult, *J* in Hz)	δ_C
1	1.97 (ddd, 14.5, 13.1, 7.0), H-1ax 1.65 (m), H-1eq	27.0
2	2.27 (ddd, 13.3, 13.1, 6.3), H-2ax 1.54 (dd, 13.3, 7.0), H-2eq	32.5
3	-	71.9
4	4.14 (d, 4.2)	78.9
5	2.29 (ddd, 13.1, 4.2, 3.6), H-5eq 1.96 (dd, 13.1, 1.7), H-5ax	23.0
6	-	40.6
7	-	87.8
8	-	197.6
9	5.82 (d, 10.4)	123.6
10	6.32 (d, 10.4)	155.1
11	-	40.2
12	1.09	27.0
13	1.26	23.8
14	1.82	23.9
15	3.99 (d, 11.0) 3.45 (d, 11.0)	66.3

[a] Measured at 500 MHz (^1H) and 125 MHz (^{13}C) in $CDCl_3$

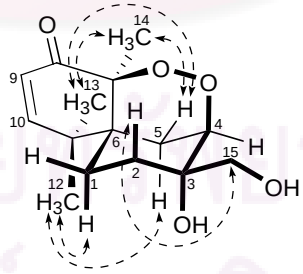

Figure 4.19 Selected NOESY correlations of **8**

4.2.4 Structure elucidation of compound 9 (Merulin D)

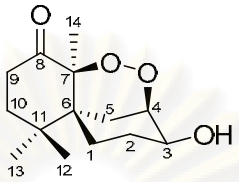

Figure 4.20 compound **9**

Melecular formula	$C_{14}H_{22}O_4$
Appearance	Yellowish paste
$[\alpha]_D^{20}$	+263(*c* 0.1 MeOH)
UV ($CHCl_3$) λ_{max} (log ε)	225 nm (3.85)
IR (KBr)	3444, 2965, 2925, 1717, 1458, 1376 and 1064 cm^{-1}
^1H and ^{13}C ($CDCl_3$)	See Table 4.9
HRESIMS *m/z*	217.1414 $[M+Na]^+$ (calcd for $C_{14}H_{22}O_4Na$, 277.1416)

Compound **9** was obtained as yellowish paste. Its molecular formula was established as $C_{14}H_{22}O_4$ by HRESIMS data (*m/z* 217.1414 $[M+Na]^+$, calcd 277.1416), indicating four degrees of unsaturation. The ^1H and ^{13}C NMR data of **9** was similar to those of **6**, except for the downfield shift of Me-14 signals [δ_H 1.91 (s), δ_C 24.0]. Analysis 2D spectra (^1H-^1H COSY, HMQC, HMBC) indicated that **9** was a stereoisomer of **6**. The large coupling constant of 10.3 Hz between H-3 and H-2ax and strong NOESY correlation between H-3 and H-5ax suggested the axial position for H-3 and implied the equatorial position for 3-OH. NOESY correlations between H_{13}-13 and H_3-14 to H-9α, H_{13}-13 and H_3-14 to H-5eq, and H_3-12 to H-1ax supported the relative configuration of **9**, whose endoperoxide linkage was suggested to attach to C-4 and C-7 positions.

Table 4.9 NMR spectral data for compound **9**[a]

Position	**9**	
	δ_H (mult, *J* in Hz)	δ_C
1	1.83 (ddd, 15.0, 12.2, 7.0), H-1ax 1.70 (m), H-1eq	28.2
2	2.28 (13.0, 12.2, 10.3), H-2ax 2.11 (13.0, 7.0), H-2eq	32.8
3	3.75 (ddd, 10.3, 7.9, 3.4)	70.3
4	4.17 (dd, 3.7, 3.4)	80.3
5	2.52 (ddd, 13.5, 5.0, 3.7), H-5eq 1.34 (dd, 13.5, 1.2), H-5ax	26.1
6	-	42.8
7	-	89.7
8	-	208.1
9	2.81 (ddd, 15.5, 12.9, 7.5), H-9α 2.31 (ddd, 15.5, 5.7, 2.6), H-9*β*	35.3
10	2.03 (ddd, 14.2, 12.9, 5.7), H-10*β* 1.67 (ddd, 14.2, 7.5, 2.6), H-10α	36.8
11	-	35.9
12	0.98 (s)	27.3
13	1.24 (s)	25.1
14	1.91 (s)	24.0
15	-	

[a] Measured at 500 MHz (^{1}H) and 125 MHz (^{13}C) in $CDCl_3$

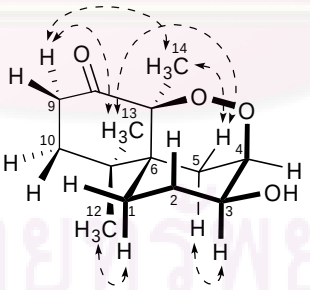

Figure 4.20 Selected NOESY correlations of **9**

4.3 Biological activities of the isolated compounds

4.3.1 Antimalarial activity

The isolated compounds were tested for antimalarial activity with the microculture radioisotope technique (Desjardins, Canfield. Haynes & Chulay, 1979) was used to determine the antimalarial activity against *Plasmodium falciparum* K1. Average IC_{50} value (n = 2) of a standard antimalarial compound, dihydroartemisinin, was 0.004 μM. Results are presented in **Table 4.10**.

Merulins C (8) and D (9) exhibited potent activity against the malarial parasite *P. falciparium* K1 tested with IC_{50} values of 0.39 and 1.35 μM, respectively, while MK3018 (**1**), 4-*O*-methyl-CJ12372 (**3**), AS21B-4 (**4**), 4-*O*-methyl-CJ12371 (**5**) merulin A (**6**) showed moderate activity with an IC_{50} range of 6.89-10.66 μM. Palmarumycin CR1 (**2**) was inactive in this assay. For merulin B (**7**), its activity was not determined due to the limitation of its quantity.

In the case of compounds from Basidiomycetous fungus, it was noticed that activity of **8** and **9**, sharing the same endoperoxide linkage at C-4, were 8- and 25-fold greater than that of **6** containing the linkage at C-2.

Table 4.10 Antimalarial activity of compounds **1- 8**

Compound	Antimalarial activity (IC_{50}, μg/mL)
MK3018 (**1**)	6.89
Palmarumycin CR1 (**2**)	I
4-*O*-Methyl-CJ-12372 (**3**)	10.56
AS21B-4 (**4**)	9.93
4-*O*-methyl-CJ12371 (**5**)	8.67
Merulin A (**6**)	10.66
Merulin B (**7**)	ND
Merulin C (**8**)	0.39
Merulin D (**9**)	1.35
Dihydroartemisinnine	0.004

I = inactive

ND = not determined

4.3.2 Cytotoxic activity

Pure isolated compounds were evaluated for cytotoxic effect against five human tumor cell lines: hepato carcinoma (HEP-G2), colon carcinoma (SW-620), lung carcinoma (CHAGO), gastric carcinoma (KATO-3) and breast carcinoma (BT-474), as well as a normal cell line, CH-Liver, by MTT colorimetric method. Results are presented in **Table 4.11**.

For the naphthalene derivatives (**1**-**5**), all compounds exhibited nonselective toxicity toward all cell lines tested. Merulins A (**6**), C (**8**) and D (**9**) gave the similar results. They showed moderate activity against four tumor cell lines, HEP-G2, SW620, KATO-3 and BT-474 and were inactive only on CHAGO cell lines. Merulin B (**7**) showed to be cytotoxic selectively against Hep-G2 cell lines with IC_{50} value of 22.72 μM, with the less toxicity on normal cell lines.

Table 4.11 Cytotoxic activity of pure compounds on Hep-G2, SW-620, CHAGO, KATO-3 and BT-474 cell lines.

Cell lines / Pure compounds	IC_{50} (μg/mL)					
	Hep-G2	SW-620	CHAGO	KATO-3	BT-474	CH-Liver
MK3018 (**1**)	17.26	11.78	18.63	22.04	8.01	18.35
Palmarumycin CR1 (**2**)	19.38	I	I	17.42	14.82	70.05
4-*O*-Methyl-CJ12372 (**3**)	24.82	12.03	21.36	19.24	9.00	19.41
AS21B-4 (**4**)	14.69	12.30	15.97	15.92	12.18	18.04
4-*O*-Methyl- CJ12371 (**5**)	18.60	13.26	15.66	17.76	3.37	15.65
Merulin A (**6**)	29.43	19.02	I	20.05	19.58	34.58
Merulin B (**7**)	22.72	I	I	I	I	136.07
Merulin C (**8**)	18.53	14.54	I	17.93	5.57	19.58
Merulin D (**9**)	22.33	13.16	I	17.61	7.37	22.71
Doxorubicin	0.14	0.16	0.81	0.98	0.91	1.28

I = inactive

4.3.3 Antibacterial activities (Determination of minimum inhibitory concentration)

A total of nine pure compounds (**1**-**9**) were determined for their minimum inhibitory concentrations (MICs) against 12 bacterial strains: *E. faecalis, E. faecalis* (vancomycin resistant), *E. faecium, S. typhimurium, S. aureus, S. epidermidis, S. hominis, E. coli, K. pneumoniae, K. pneumonia* (ESBL producing), *P. aeruginosa* and *P. vulgaris*. Their MIC values are summarized in **Table 4.12**.

MK3018 (**1**) exhibited antibacterial activity against 11 bacterial strains and it showed strongest activity toward *S. epidermidis* with MIC value of 2.00 μg/mL. Palmarumycin CR1 (**2**) was weakly active against *E. faecalis* and *S. epidermidis*. 4-*O*-Methyl-CJ12372 (**3**) and AS21B-4 (**4**) exhibited moderate activity against *S. aureus, S. epidermidis* and *S. hominis.*, whereas **3** was also active two additional strains, *E. faecalis* and *P. vulgaris*. 4-*O*-methyl-CJ12371 (**5**) showed to be inactive in this assay.

Merulins A (**6**) and D (**9**) showed weak antibacterial activity against *P. vulgaris*, while merulin C (**8**) exhibited moderate activity on this strain. Compound 8 was also active on *E. coli* and *S. typhimurium*. In addition, merulin D (**9**) also exhibited weak activity against *E. faecalis* and *E. coli*. For merulin B (**7**), its activity was not determined due to the limitation of its quantity.

Table 4.12 MIC of active compounds

Compound	EF	VEF	EFa	EC	SA	SE	SH	ST	PV
	MIC (μg/mL)	MIC (μg/mL)	MIC (μg/mL)	MIC (μg/mL)	MIC (μg/mL)	MIC (μg/mL)	MIC (μg/mL)	MIC (μg/mL)	MIC (μg/mL)
MK3018 (**1**)	8	4	16	128	I	2	8	64	32
Palmarumycin CR1 (**2**)	256	I	I	I	I	256	I	I	I
4-*O*-Methyl-CJ12372 (**3**)	I	I	I	I	16	64	64	I	I
AS21B-4 (**4**)	64	I	I	I	8	16	64	I	128
4-*O*-methyl-CJ12371 (**5**)	I	I	I	I	I	I	I	I	I

Merulin A (**6**)	I	I	I	I	I	I	I	I	256
Merulin B (**7**)	ND	ND	ND	ND	ND	ND	ND	ND	ND
Merulin C (**8**)	I	I	I	32	I	I	I	128	8
Merulin D (**9**)	256	I	I	256	I	I	I	I	128

EF : *E. faecalis*, VEF : *E. faecalis* (vancomycin resistant), EFa : *E. faecium*, EC : *E. coli*, SA : *S. aureus*, SE : *S. epidermidis*, SH : *S. hominis*, ST : *S. typhimurium*, and PV : *P. vulgaris*

I = inactive

ND = not determined

CHAPTER V

CONCLUSION

The objectives of this research are to investigate and structural elucidate bioactive compounds from endophytic fungi isolated from *A. sarmentosa* and *X. granatum*. The biological activities including anti-bacterial activities by broth microdilution assay against *E. faecalis, E. faecalis* (vancomycin resistant), *E. faecium, S. typhimurium, S. aureus, S. epidermidis, S. hominis, E. coli, K. pneumoniae, K. pneumonia* (ESBL producing), *P. aeruginosa* and *P. vulgaris*, anti-malarial activity against *P. falciparum* K1 strain and cytotoxicity against cancer cell lines: hepato carcinoma (HEP-G2), colon carcinoma (SW-620), lung carcinoma (CHAGO), gastric carcinoma (KATO-3) and breast carcinoma (BT-474), of the isolated compounds were also studied.

Two pure endophytic isolates from *A. sarmentosa* and *X. granatum*, AS21B and XG8D, were selected in this study since their crude extracts showed characteristic and interesting ^{1}H NMR profile and exhibited anti-bacterial activity. Based on molecular phylogenetic analysis, AS21B was identified as *Rhytidhysteron* sp., and isolate XG8D is Basidiomycetous fungus in the family Meruliaceae.

Fractionation of EtOAc crude extract of AS21B led to the isolation of a new naphthalene derivative, AS21B-4 (**4**), together with four know analogs including MK3018 (**1**), palmarumycin CR1 (**2**), 4-*O*-methyl-CJ12372 (**3**) and 4-*O*-methyl-CJ12371 (**5**), while that of XG8D yielded four new sesquiterpenes, merulins A-D (**6-9**). All isolated compounds were evaluated for their antimalarial, cytotoxic and antibacterial activity. Compounds (**8**) and (**9**) exhibited potent antimalarial activity with IC_{50} values of 0.39 and 1.35 μM, respectively. Compounds **1** and **3-6** showed moderate activity while compound **2** was inactive in this antimalarial assay. All naphthalene derivatives (**1-5**) exhibited nonselective toxicity toward all cell lines tested. Merulins A (**6**), C (**7**) and D (**9**) showed moderate activity against all cell lines, except for CHAGO cell lines, whereas merulin B (**7**) exhibited moderate cytotoxicity

selectively against only Hep-G2 cell lines. Compounds **1**-**6**, **8** and **9** were also evaluated for their anti-bacterial activities against different bacterial strains.

REFERENCES

Altschul, SF., Gish, W., Miller, W., Myers, EW., and Lipman DJ. (1990) Basic Local Alignment Search Tool. Journal of Molecular Biology 215: 403–410

Bharat, P., Bashyal, E. M., Wijeratne, K., Faeth, S. H., and Gunatilaka, A. A. L. (2005) Globosumones A-C, Cytotoxic Orsellinic Acid Esters from the Sonoran Desert Endophytic Fungus *Chaetomium globosum***.** Journal of Natural products 68: 724-728.

Butler, M. S. (2004). The role of natural product chemistry in drug discovery. Journal of Natural products 67: 2141-2153.

Chin, Y., Balunas , J. M., Chai, B. and Kinghorn, A. D. (2006). Drug Discovery From Natural Sources. Springer New York 2: 17-39.

Desjardins, R. E., *et al*. (1979). Quantitive assessment of antimalarial activity in vitro by a semiautomated microdilution technique. Antimicrob Agents chemother 16(6): 710-718.

Donnelly A. C. (2009). Marine Natural Products as Anticancer Agents: Therapeutic Treasures from the Deep. Journal of Marine [Online]. Available from http:// www. organicdivision. org/ Awardees/Essays/Donnelly.pdf [April 6, 2010]

Guo, B., Wang, Y., Sun, X. and Tang K. (2008). Bioactive Natural Products from Endophytes. Applied Biochemistry and Microbiology 44(2): 136–142.

Gunatilaka, A. A. L. (2006). Natural Products from Plant-Associated Microorganisms: Distribution, Structural Diversity, Bioactivity, and Implications of Their Occurrence. Journal of Natural products 69: 509-526.

Horwitz, S. B. (2004). Personal Recollections on the Early Development of Taxol. Journal of Natural products 67: 136-138.

Isaka, M., Palasarn, ., Lapanun, S., Chanthaket, R., Boonyuen, N. and Lumyong, S. (2009). *γ*-Lactones and *ent*-Eudesmane Sesquiterpenes from the Endophytic Fungus *Eutypella* sp. BCC 13199.Journal of Natural products 72: 1720-1722.

Kim, S., Dong-Sun Shin, D. S., Lee, T. and Oh, K. B. (2004). Periconicins, Two New Fusicoccane Diterpenes Produced by an Endophytic Fungus *Periconia* sp. with Antibacterial Activity. Journal of Natural products 67: 448-450.

Kingston, D. G. I. (2000). Recent Advances in the Chemistry of Taxol. Journal of Natural products 63: 726-734.

Kjer, J., Wray, V., Ebel, R. E., Ebel, R., Pretsch, A., Lin, W. and Proksch, P. (2009). Xanalteric Acids I and II and Related Phenolic Compounds from an Endophytic *Alternaria* sp. Isolated from the Mangrove Plant *Sonneratia alba*. Journal of Natural products 72: 2053-2057.

Landvik, S. (1996). *Neolecta,* a fruit-body-producing genus of the basal ascomycetes, asshown by SSU and LSU rDNA sequences. Mycological Research 100: 199–202.

Larsen, K. (2000). Salvadoraceae In Flora of Thailand. Bangkok : Forest Herbarium Press. 7 (2): 341-343.

Molyneux, R. J. (2002). Research Opportunities for Bioactive Natural Constituents in Agriculture and Food. Journal of Agricultural and Food Chemistry 50: 6939-6942

Murillo, C., Albertazzi, F.J., Carranza, J., Lumbsch, H.T. and Tamayo, G. (2009). Molecular data indicate that *Rhytidhysteron rufulum* (ascomycetes, Patellariales) in Costa Rica consists of four distinct lineages corroborated by morphological and chemical characters. Mycological Research 113: 405-416.

Ogishi, H., Chiba, N., Mikawa, T., Sakaki, T., Miyaji S.and M, Sezaki. (1988). Novel Antibiotic MK3018 Substance- Useful as Antimicrobial Agent. JP 01294686.

Pongboonrod S. (1979). Mai Thet Muang Thai. Bangkok : Kasembunnakich Press. 423-424

Phuthong, M. and Phunmod, W. (2008). Antimicrobial activity of endophytic fungi isolated from *Mammea siamensis* and mangrove forest plants. Bachelor's report, Department of Chemistry, faculty of Science, Chulalongkorn university.

Pudhom, K., Sommit, D., Nuclear, P., Ngamrojanavanich, N. and Petsom, A. (2009). Protoxylocarpins F-H, Protolimonoids from Seed Kernels of *Xylocarpus granatum*. Journal of Natural products 72: 2188-2191.

Sakemi, S., *et al* (1995). CJ-12371 and CJ 12372, Two Novel DNA Gyrase Inhibitors Fermentation, Isolation, Structural Elucidation and Biological Activities. Journal of Antibiotic 48: 134-142.

Schulz, B., *et al* (1995). Biologically active secondary metabolites of endophytic *Pezicula* sp. Mycological Research 99(8): 1007-1015.

Strobel, G.A. (2003). Endophytes as sources of bioactive products. Microbes and Infection 5: 535-544.

Strobel, G. and Daisy, B. (2003). Bioprospecting for microbial endophytes and their natural products. Microbiology and Molecular Biology Reviews 67: 491-502.

Strobel, G. and Daisy, B., Castillo, U. and Harper, J. (2004). Natural Products from Endophytic Microorganisms. Journal of Natural products 67: 257-268.

Stierle, A., Strobel, G. and Stierle, D. (1993). Taxol and taxane production by *Taxomyces andreanae*, an endophytic fungus of Pacific yew. Science 260: 214-216.

Sunintaboon, P. (1999). Chemical constitutents of leaf and root extracts from Azima sarmentosa Benth and their biological activities. Master's Thesis, Department of Chemistry, faculty of Science, Chulalongkorn university.

Swofford, D.L. (2002). Phylogenetic Analysis using Parsimony (*and other Methods). Sunderland: Sinauer Associates. 74(5): 763-766

Thompson, J.D., Higgins, D. G. and Gibson, T. J. (1994)**.** CLUSTAL W: improving the sensitivity of progressive multiple sequence alignment through sequence weighting, position-specific gap penalties and weight matrix choice. Nucleic acids research 22: 4673-4680.

Tragen, W. and Jensen, J. B. (1976). Human malaria parasites in continuous culture. Science 193: 673-675.

Wani, M. C., Taylor, H. L., Wall, M. E., Coggon, P. and McPhail, A. T. (1971). Plant antitumor agents IV. The isolation and structure of taxol, a novel antileukemic and antitumor agent from *Taxus brevifolia.* Journal of the American Chemical Society 93: 2325-2327.

White, T. J.; Bruns, T.; Lee, S.; Taylor, J. (1990) In PCR Protocols: a Guide to Methods and Applications. San Diego: Academic Press. 315-322

Wipf, P., Lynch, S. M., Birmingham, A., Tamayo, G., Jiménez, A., Campos, N. and Powis, G. (2004). Natural product based inhibitors of the thioredoxin–thioredoxin reductase system. Organic & Biomolecular Chemistry 2: 1651-1658.

Wu, J., Xiao, O. and Li, Q. (2006). Limonoids from the Mangrove *Xylocarpus granatum*. Biochemical Systematics and Ecology 34: 838-841.

Xu, J., Kjer, J., Sendker, J., Wray, V., Guan, H., Edrada, R., Lin, W., Wu, J. and Proksch, P. (2009). Chromones from the Endophytic Fungus *Pestalotiopsis* sp. Isolated from the Chinese Mangrove Plant *Rhizophora mucronata*. Journal of Natural products 72: 662-665.

Xu, L. L., Han, T., Wub, J. S., Zhang, Q. Y., Zhang, H., Huang, B. K., Rahman, K. and Qin, L. P. (2009). Comparative research of chemical constituents, antifungal and antitumor properties of ether extracts of Panax ginseng and its endophyticfungus. Phytomedicine 16: 609-616.

Zhou, Y., Cheng, F., Wu, J. and Zou, K. (2006). Polyhydroxylated Phragmalins from the Fruit of a Chinese Mangrove, *Xylocarpus granatum*. Journal of Natural products 69: 1083-1085.

APPENDICES

APPENDIX A

1. Media

1.1 Malt extract Broth (MEB)

Malt extract	20 g
Peptone	1 g
Glucose	20 g
Distilled water up to	1 L

1.2 Corn steep broth medium

Manitol	20 g
Maltose	20 g
Glucose	10 g
MSG	10 g
KH_2PO_4	0.5 g
$MgSO_4.7H_2O$	0.3 g
Yeast Extract	3.0 g
Corn steep liquor	1.0 g
Distilled water up to	1 L

1.3 Potato Dextrose Agar (PDA)

Potato dextrose burse	240 g
Agar	15g
Distilled water up to	1 L

1.5 Water Agar

Agar	15 g
Distilled water up to	1 L

2. Reagent and buffer for DNA amplification by PCR

2.1 Lysis buffer

Tris-HCl (pH 7.2)	50 mM
EDTA	50 mM
SDS	3%
2-mercaptoethanol	1%

2.2 Chlorofrom : TE-saturated phenol 1:1,v/v

2.3 TE for resuspending pellet

Tris-HCl	10 mM
EDTA	0.1 mM

2.4 Gel loading buffer

Bromophenol blue	0.25%
Sucrose in water	40% (w/v)

2.5 5-X Tris-Borate-EDTA (TBE)

Tris base	54 g
Boric acid	27.5 g
0.5 M EDTA pH 8.0	20 mL

The working solution was 1X TBE, diluted with 4 volume of distilled water.

2.6 10X Buffer

Tris HCl pH 9.0	100 mL
KCL	500 mM
Triton X-100	1%

APPENDIX B

Figure B1 ^{1}H NMR spectrum of crude (AS21B cultured on malt extract broth) in $CDCl_3$ (VarianYH400 spectrometer at 400 MHz)

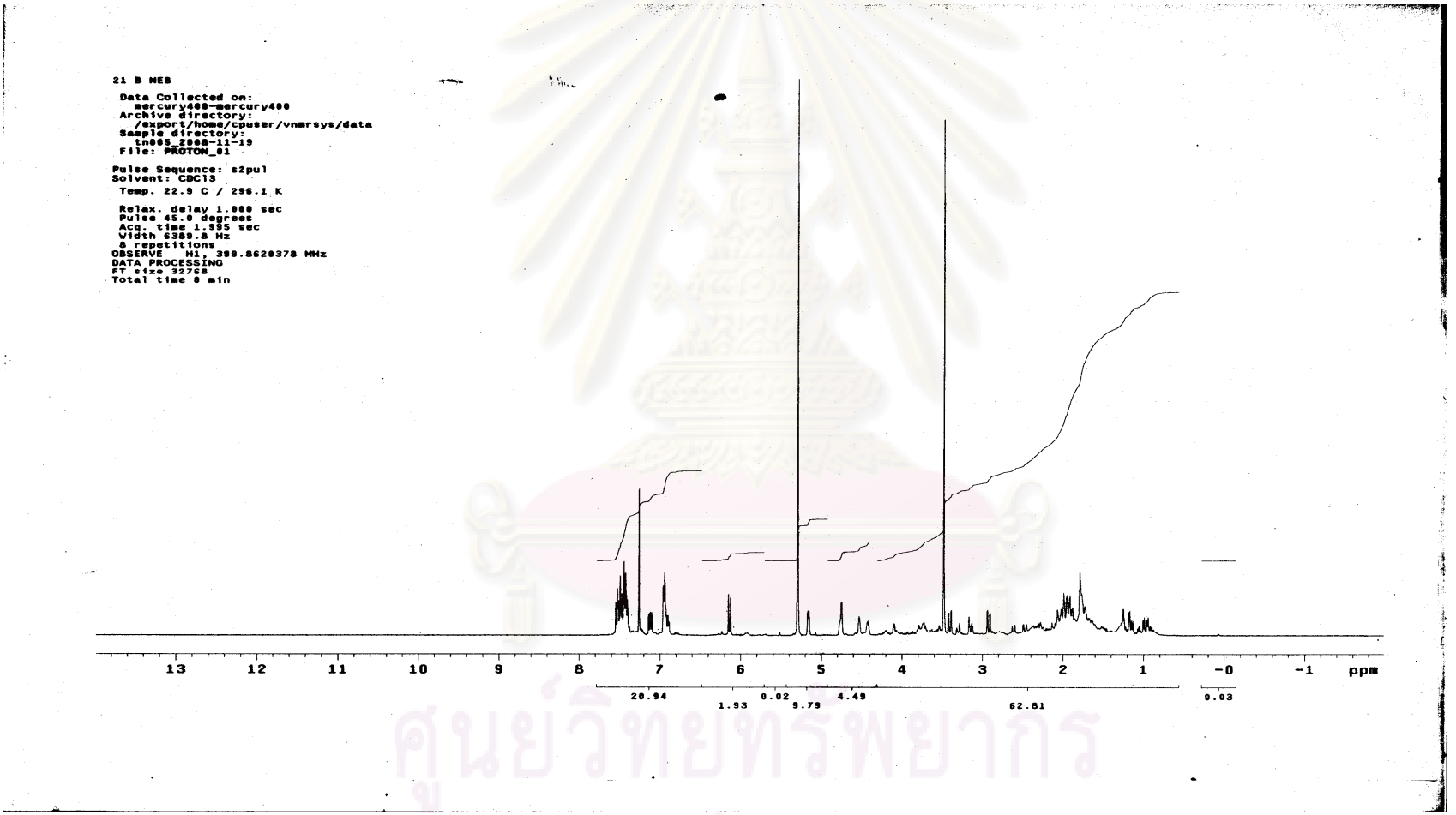

Figure B2 ^{1}H NMR spectrum of compound **1** in $CDCl_3$ (VarianYH400 spectrometer at 400 MHz

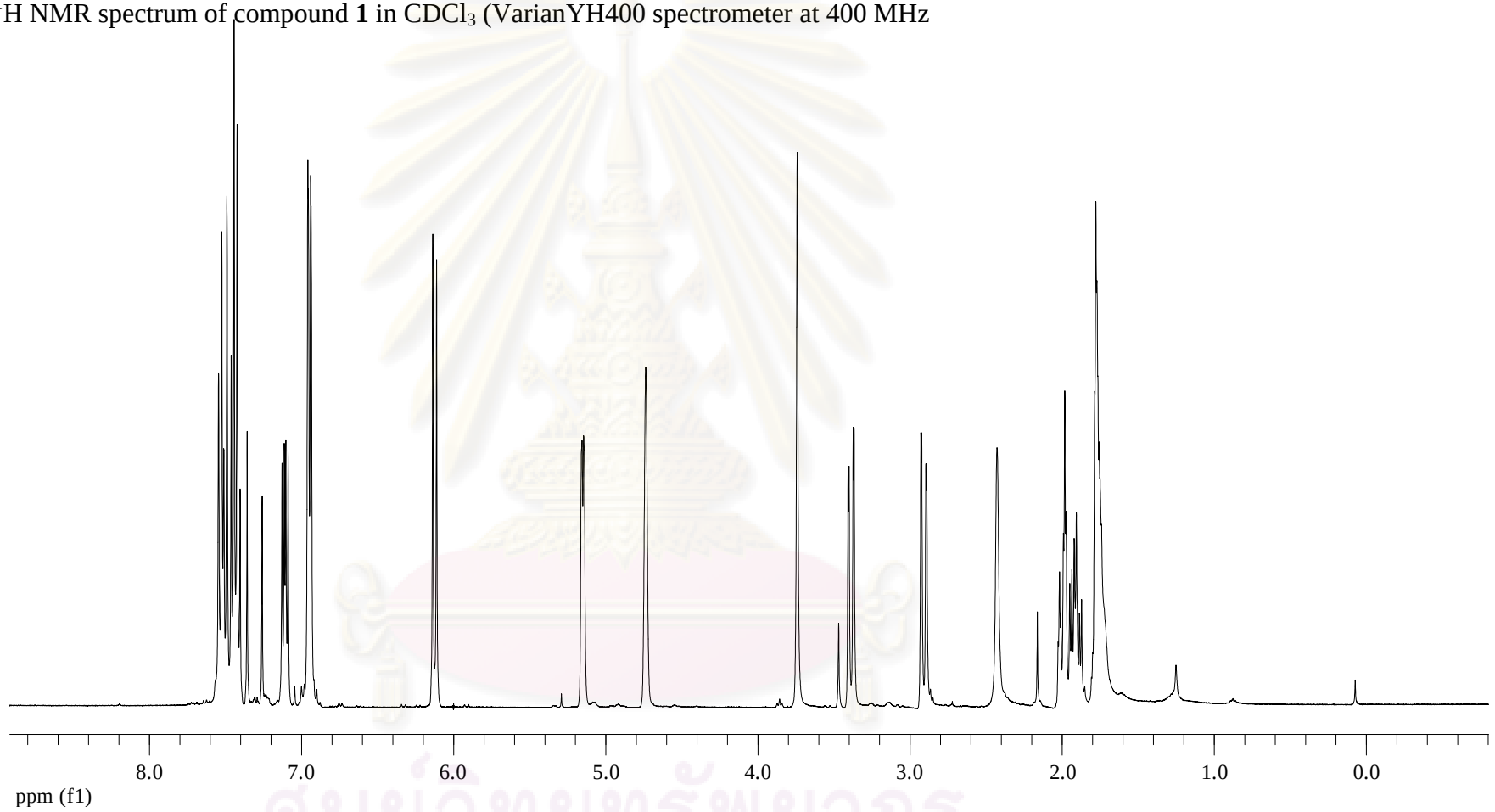

Figure B3 ^{13}C NMR spectrum of compound **1** in $CDCl_3$ (VarianYH400 spectrometer at 400 MHz)

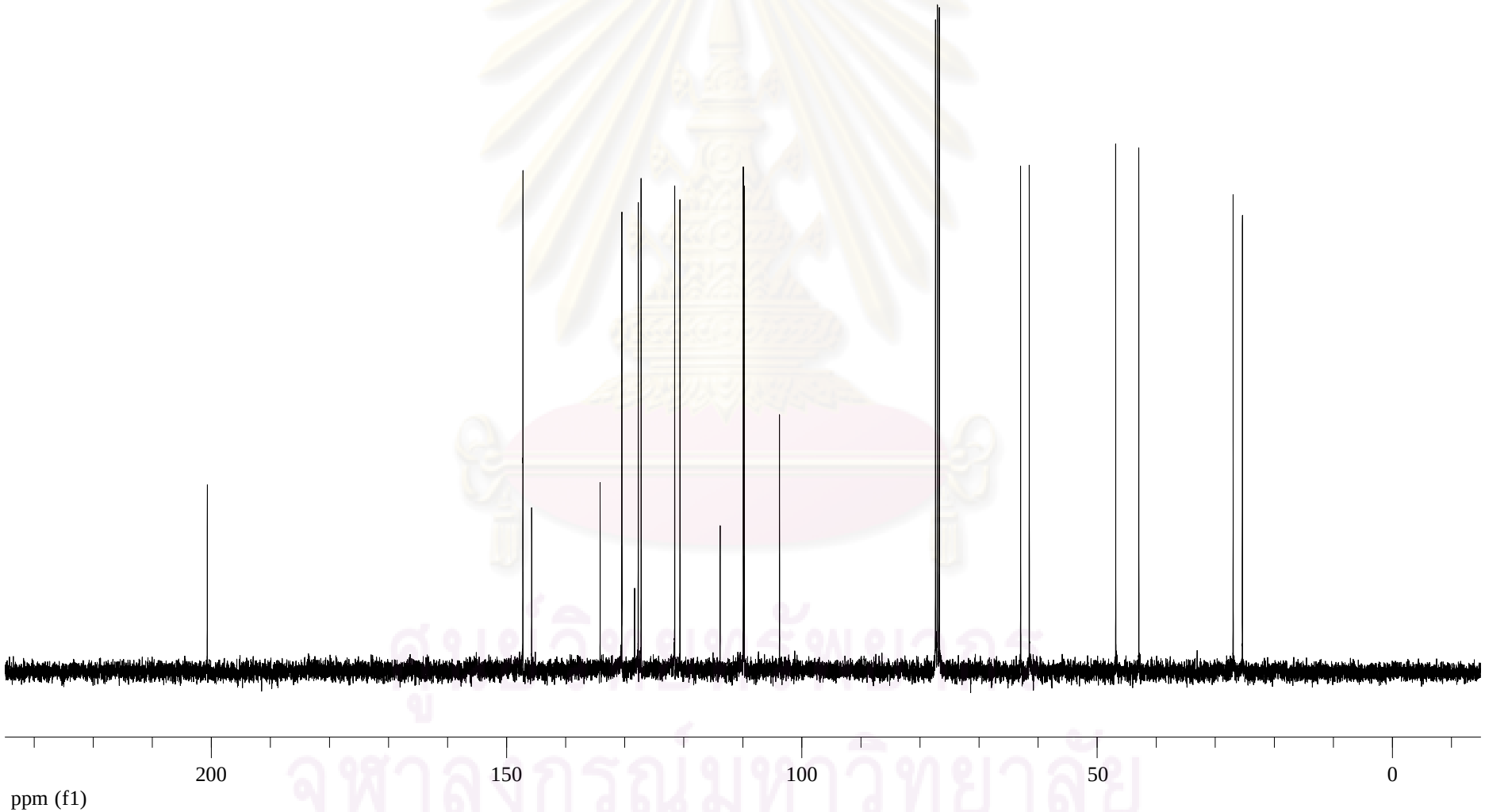

Figure B4 COSY spectrum of compound **1** in $CDCl_3$ (VarianYH400 spectrometer at 400 MHz)

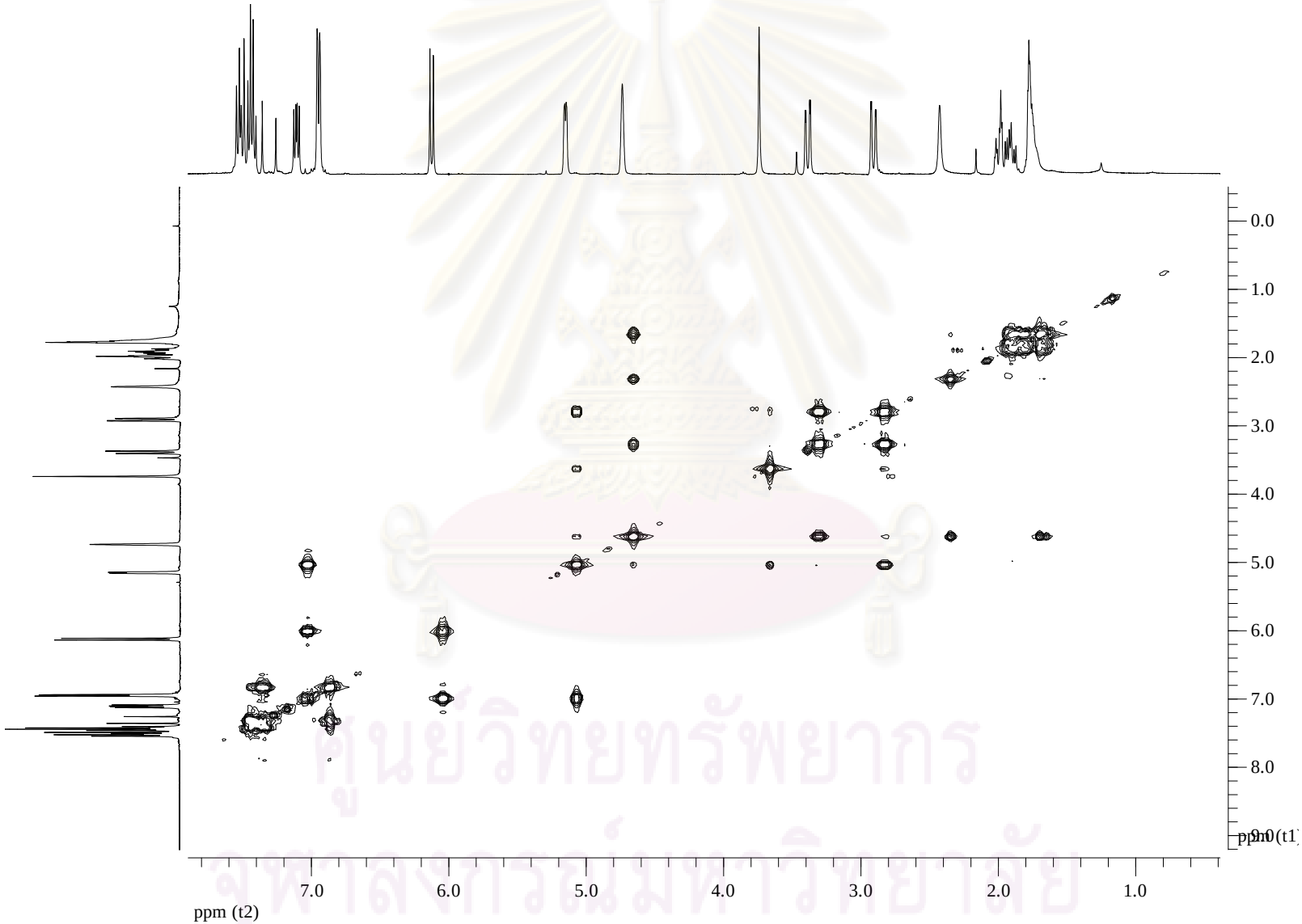

Figure B5 HSQC spectrum of compound **1** in $CDCl_3$ (VarianYH400 spectrometer at 400 MHz)

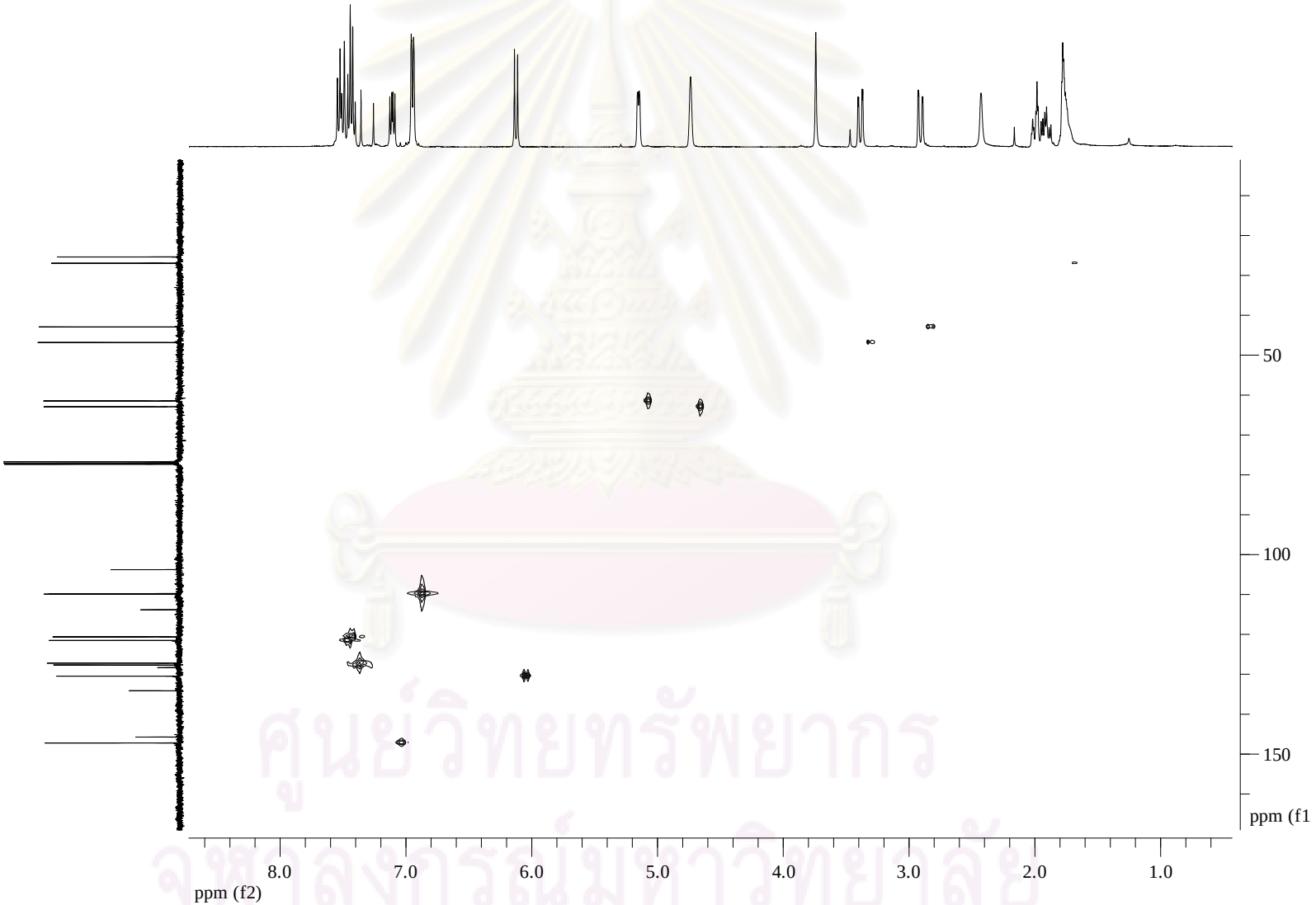

Figure B6 HMQC spectrum of compound **1** in $CDCl_3$ (VarianYH400 spectrometer at 400 MHz)

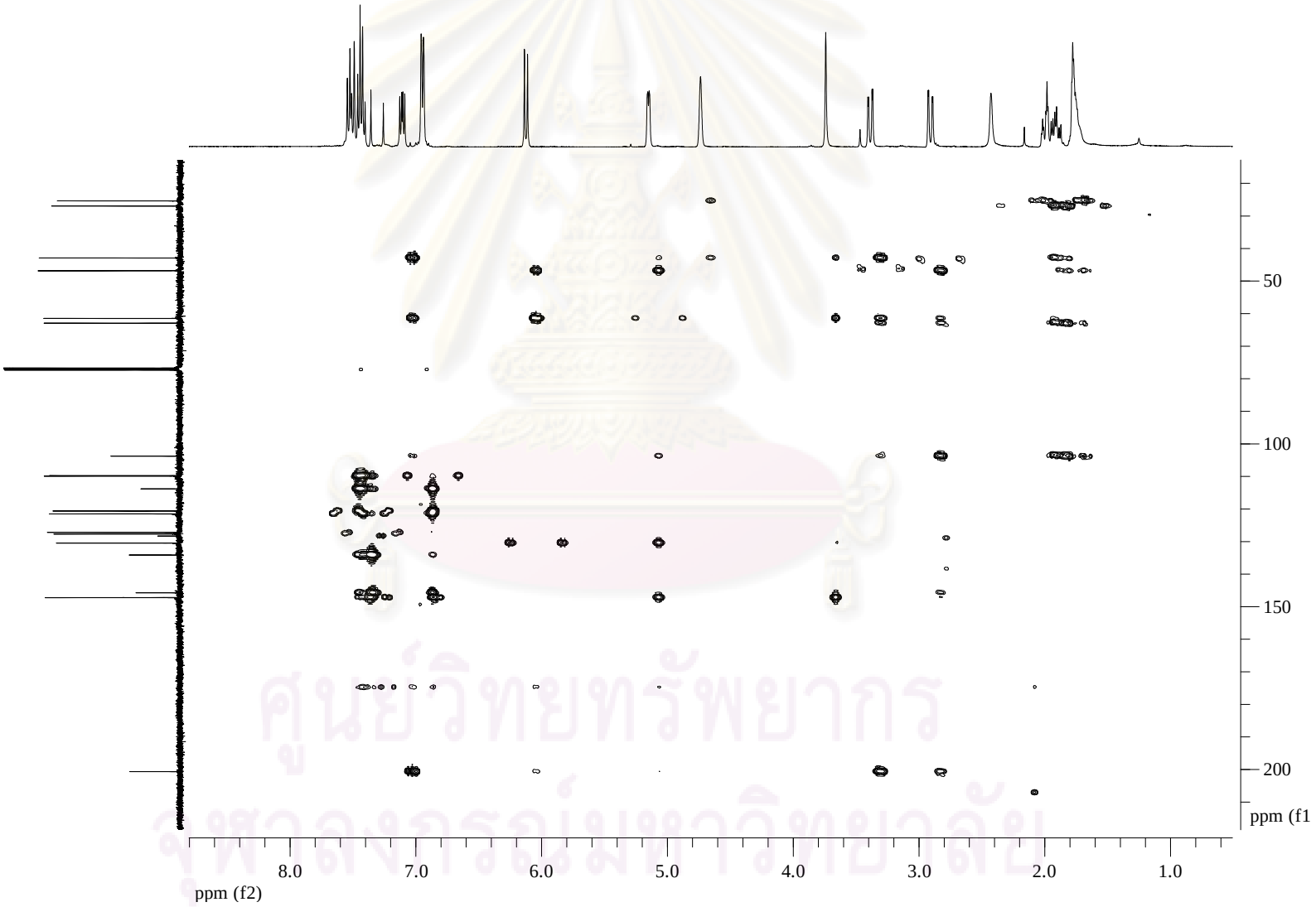

Figure B7 ^{1}H NMR spectrum of compound **2** in DMSO-d_6 (VarianYH400 spectrometer at 400 MHz)

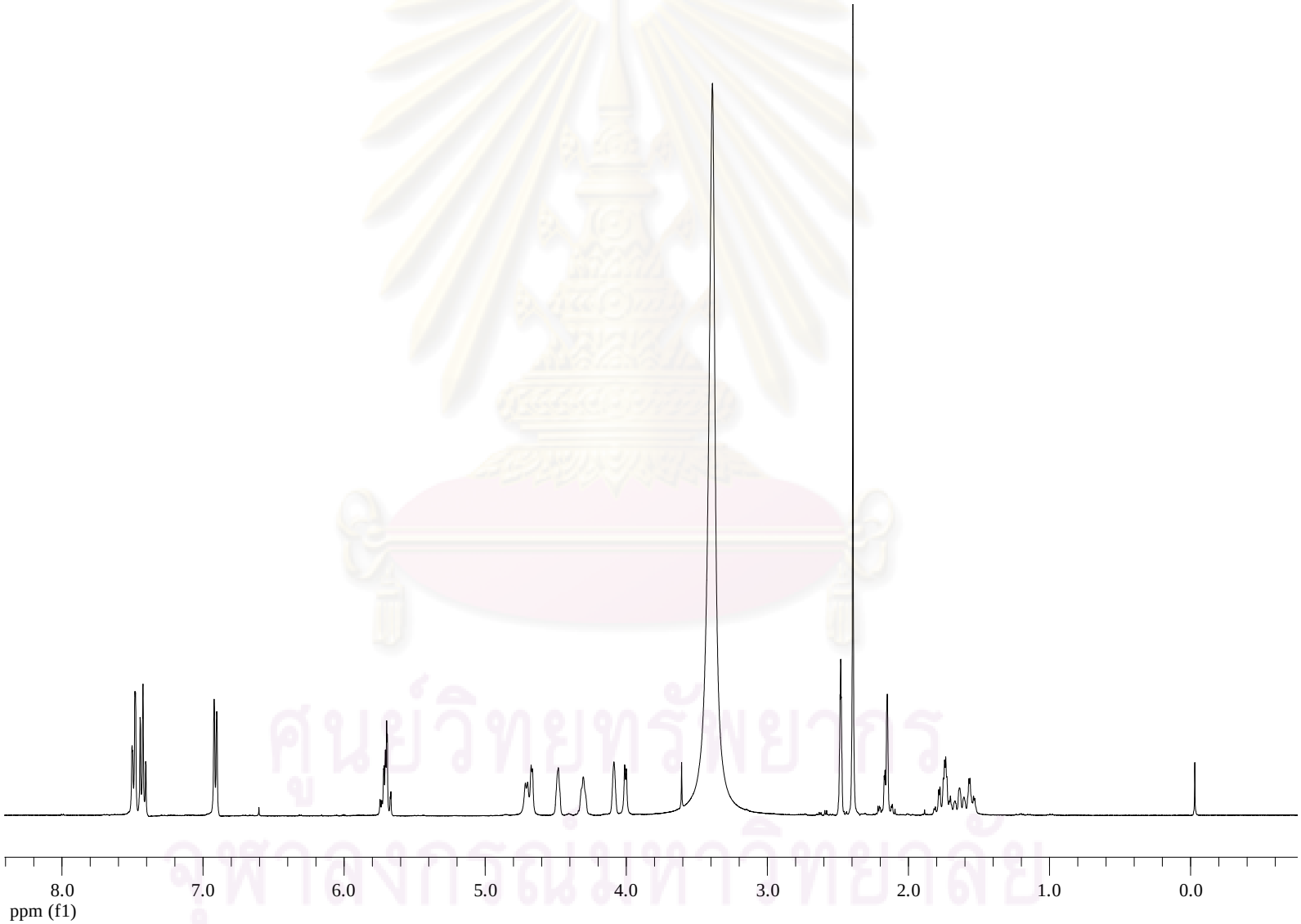

Figure B8 ^{13}C NMR spectrum of compound **2** in DMSO-d_6 (VarianYH400 spectrometer at 400 MHz)

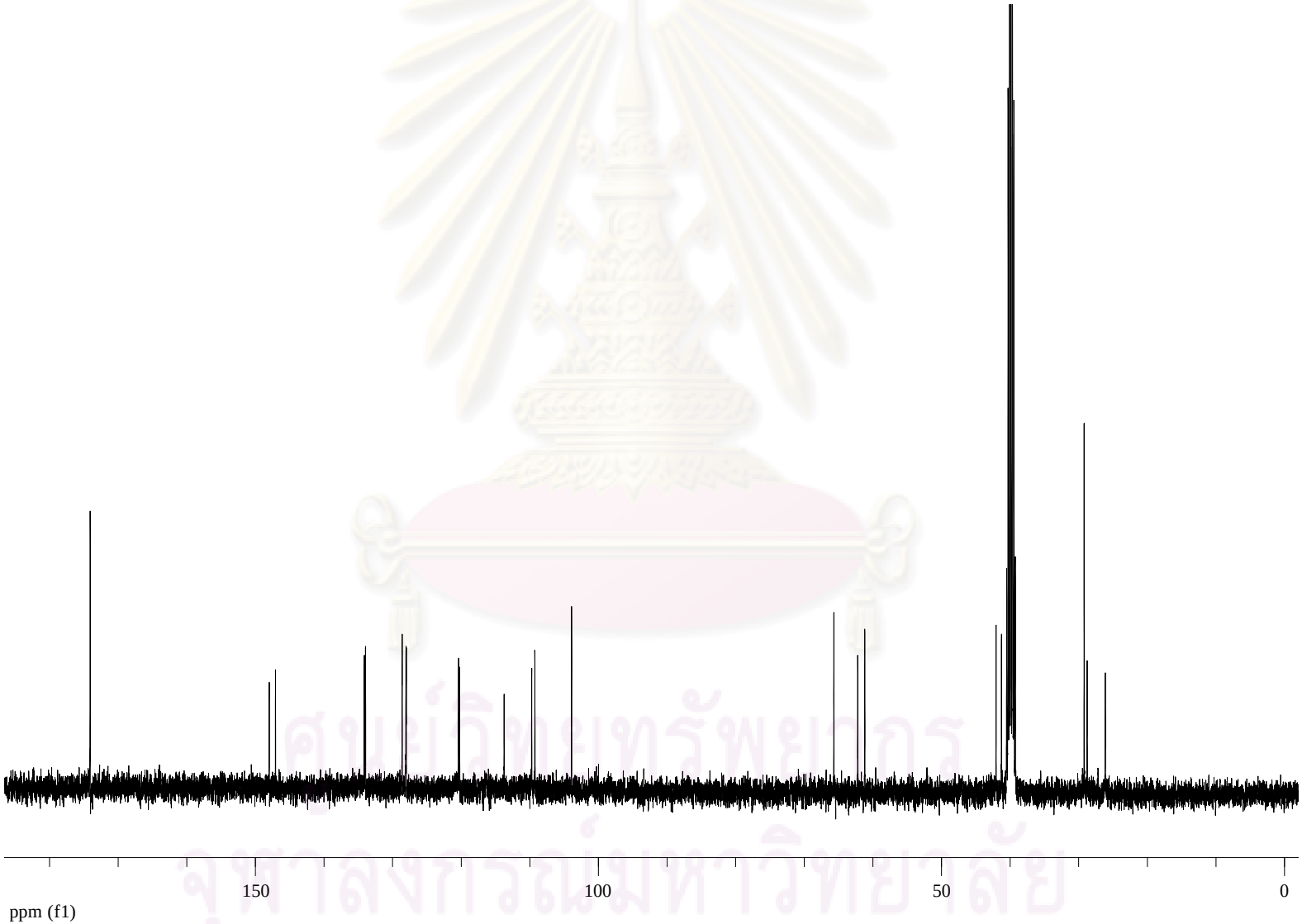

Figure B9 COSY spectrum of compound **2** in DMSO-d_6 (VarianYH400 spectrometer at 400 MHz)

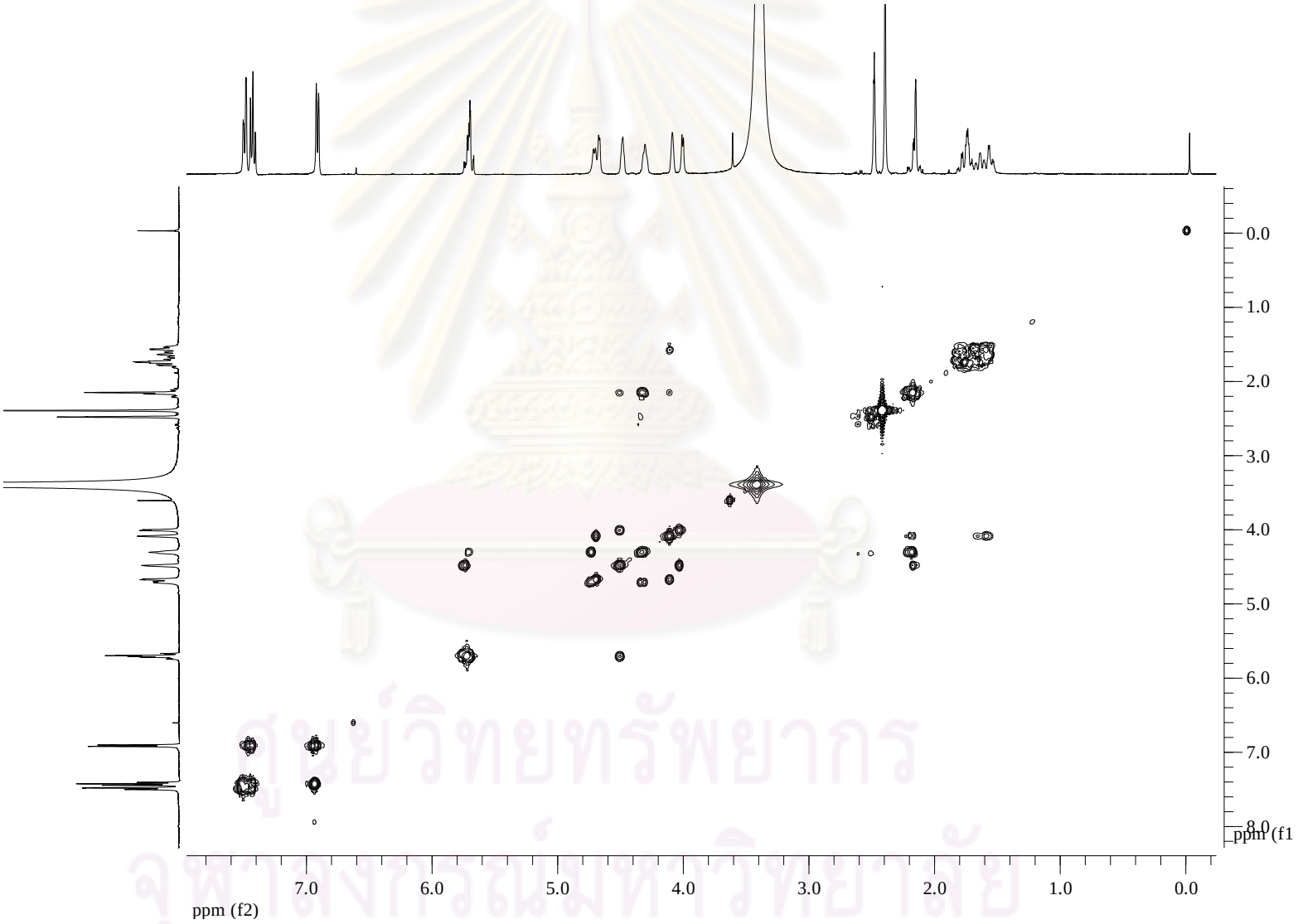

Figure B10 HSQC spectrum of compound **2** in DMSO-d_6 (VarianYH400 spectrometer at 400 MHz)

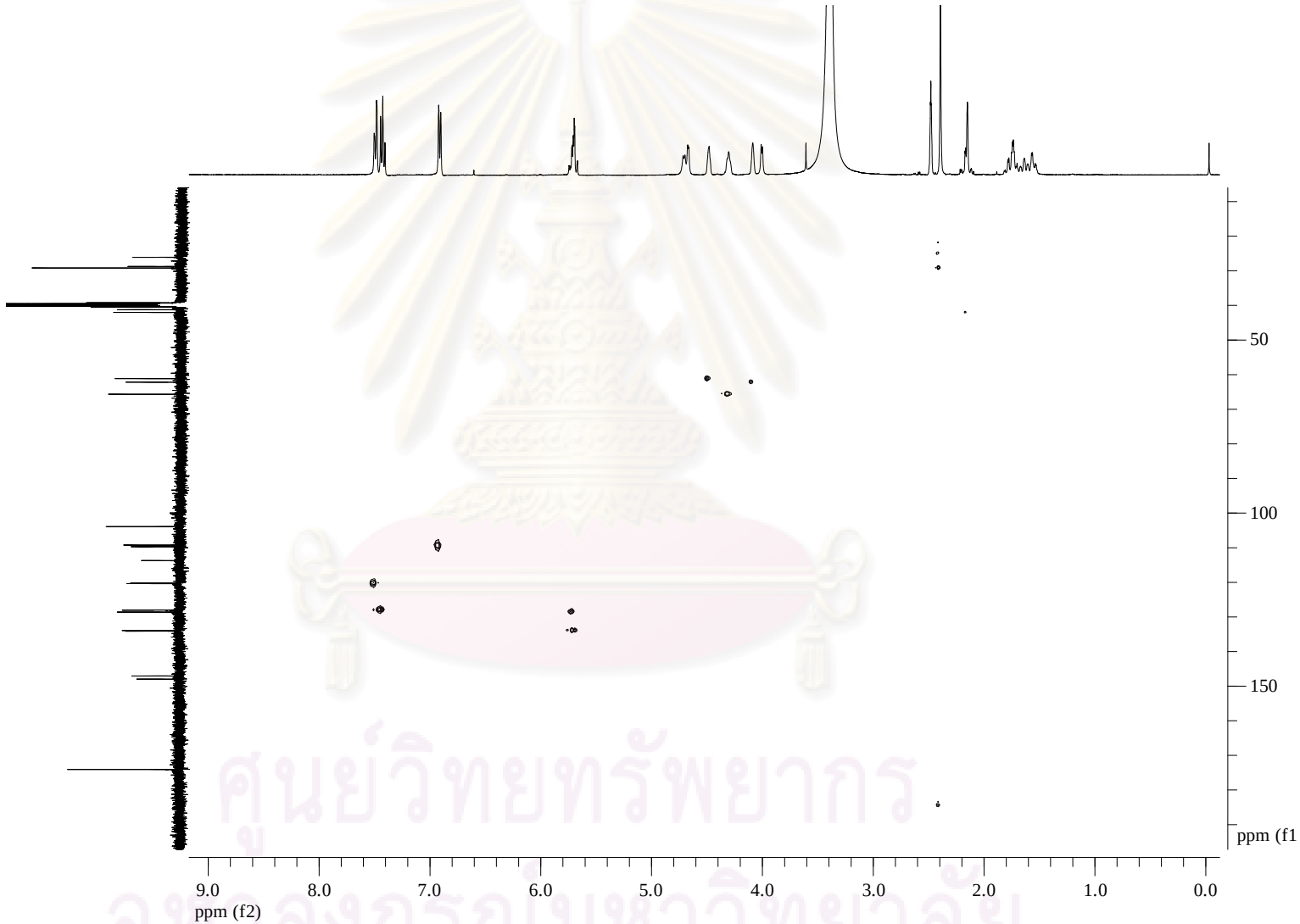

Figure B11 HMBC spectrum of compound **2** in DMSO-d_6 (VarianYH400 spectrometer at 400 MHz)

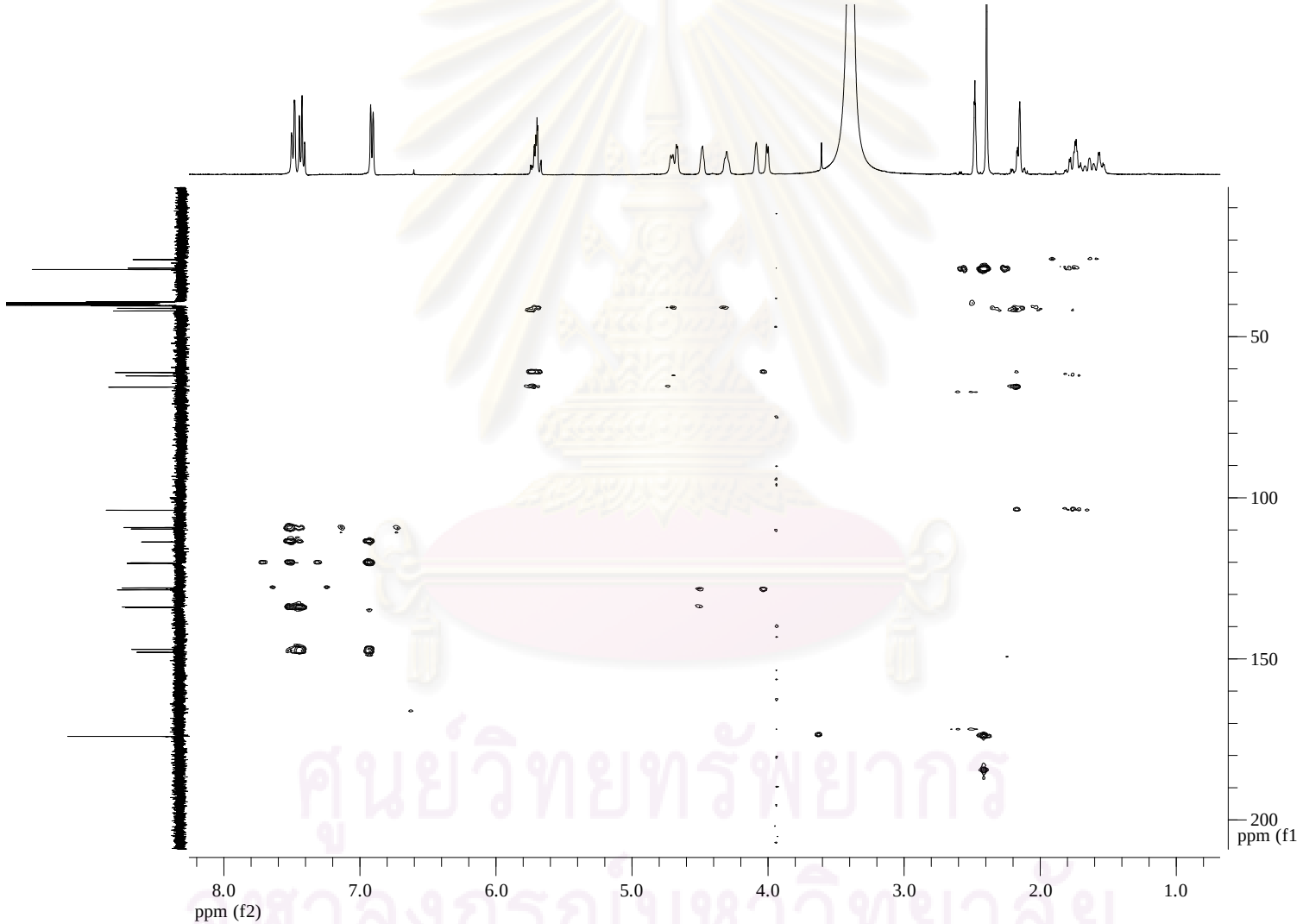

Figure B12 ^{1}H NMR spectrum of compound **3** in $CDCl_3$ (VarianYH400 spectrometer at 400 MHz)

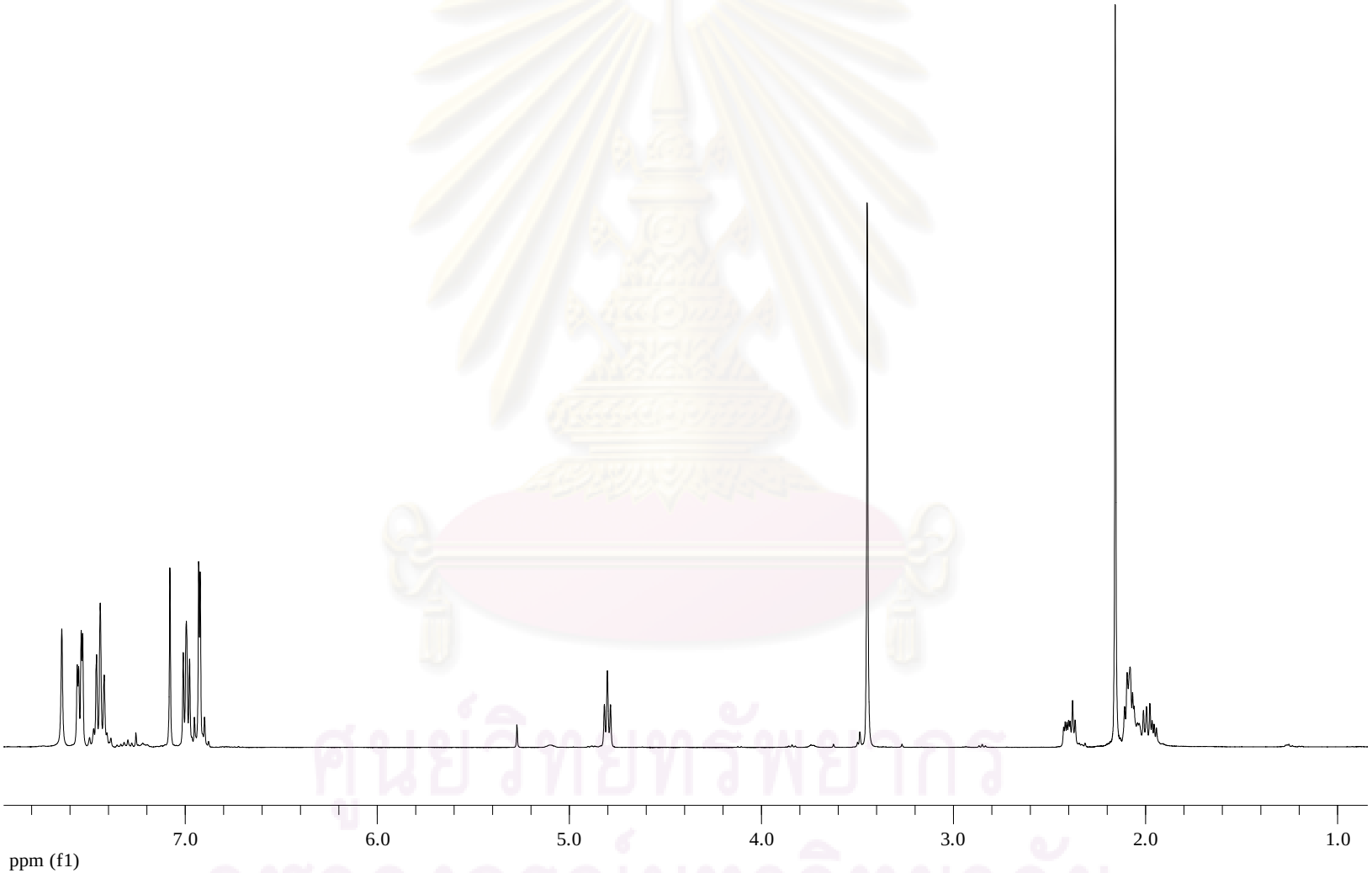

Figure B13 ^{13}C NMR spectrum of compound **3** in $CDCl_3$ (VarianYH400 spectrometer at 400 MHz)

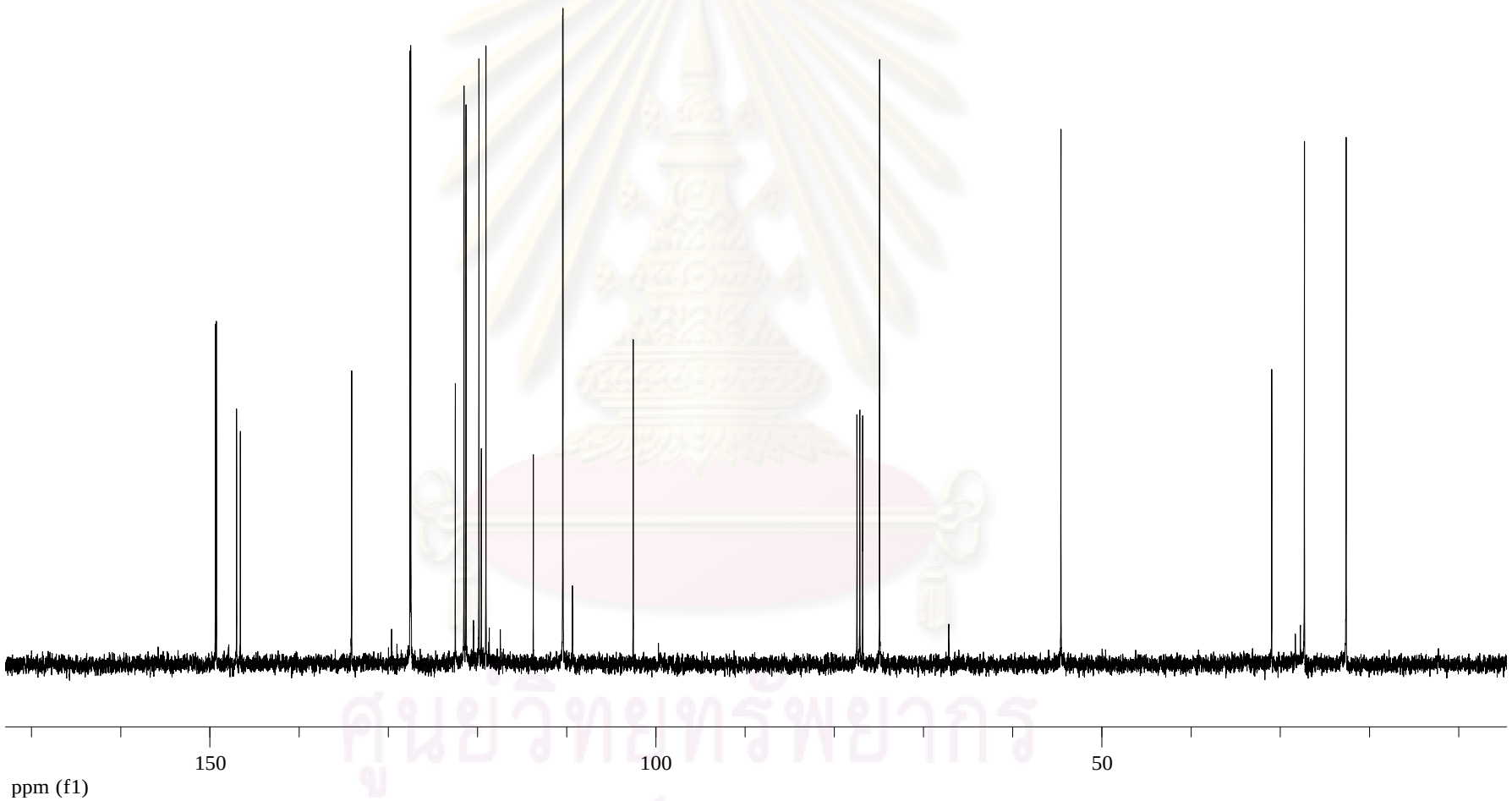

Figure B14 COSY spectrum of compound **3** in $CDCl_3$ (VarianYH400 spectrometer at 400 MHz)

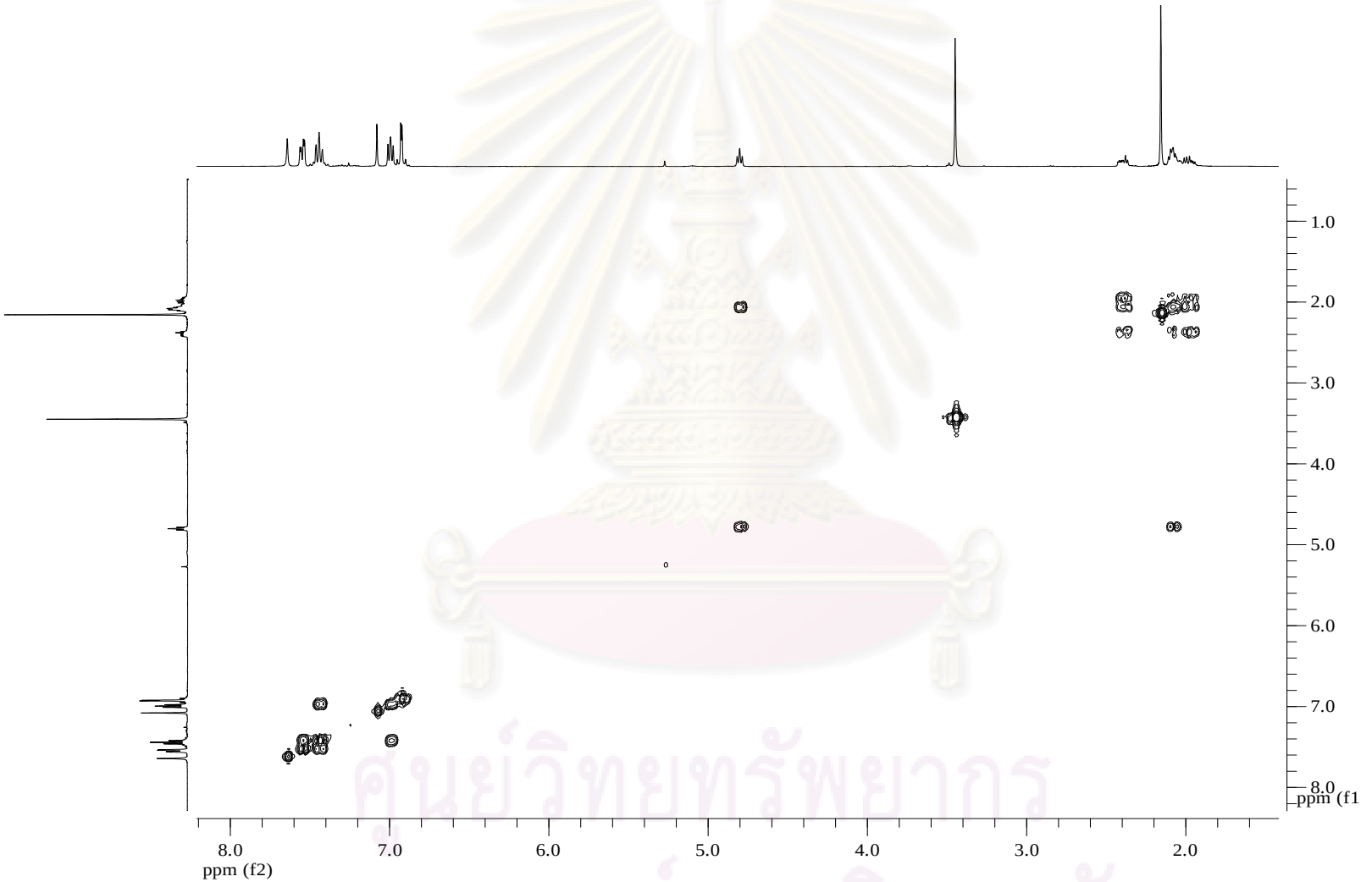

Figure B15 HSQC spectrum of compound **3** in $CDCl_3$ (VarianYH400 spectrometer at 400 MHz)

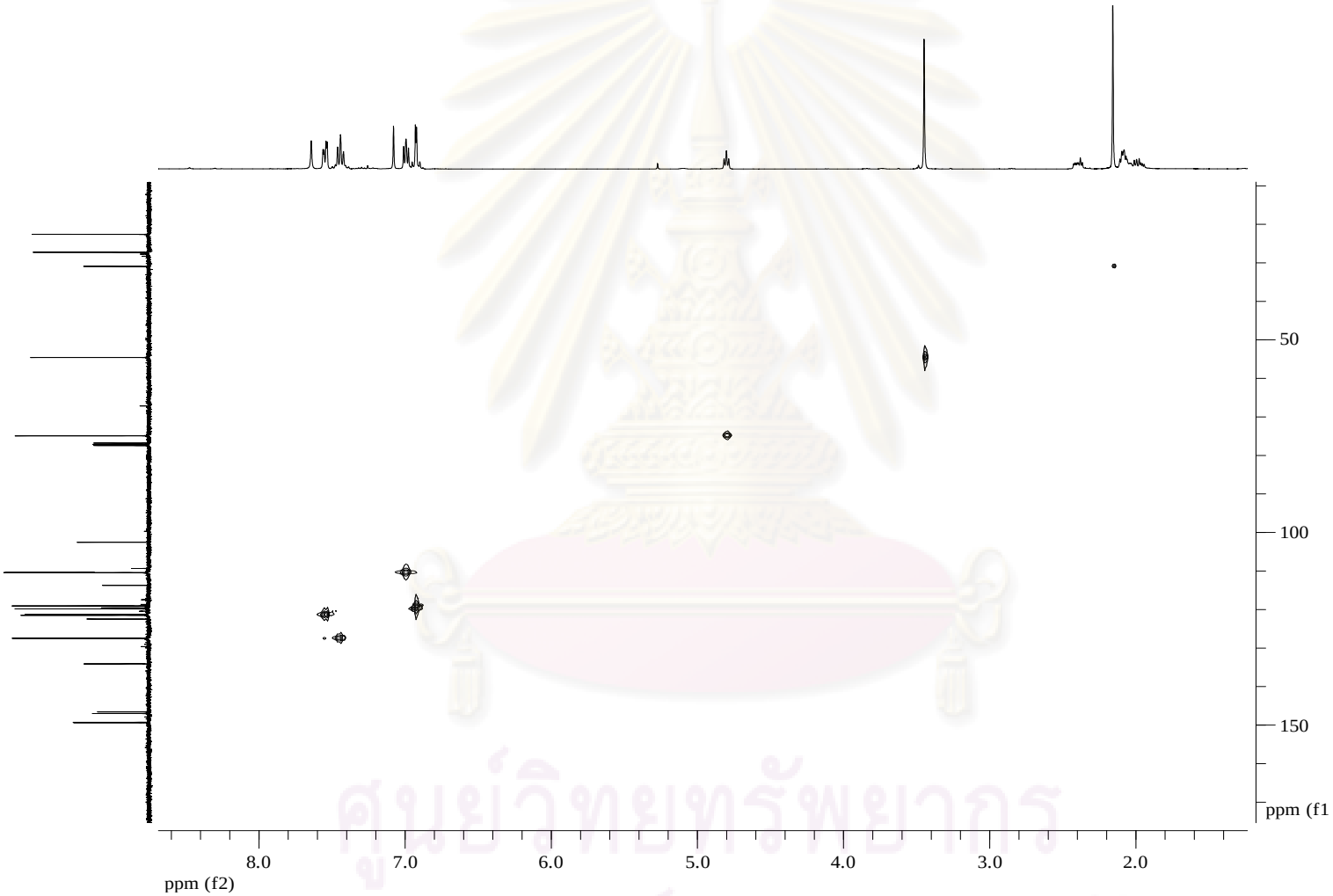

Figure B16 HMBC spectrum of compound **3** in $CDCl_3$ (VarianYH400 spectrometer at 400 MHz)

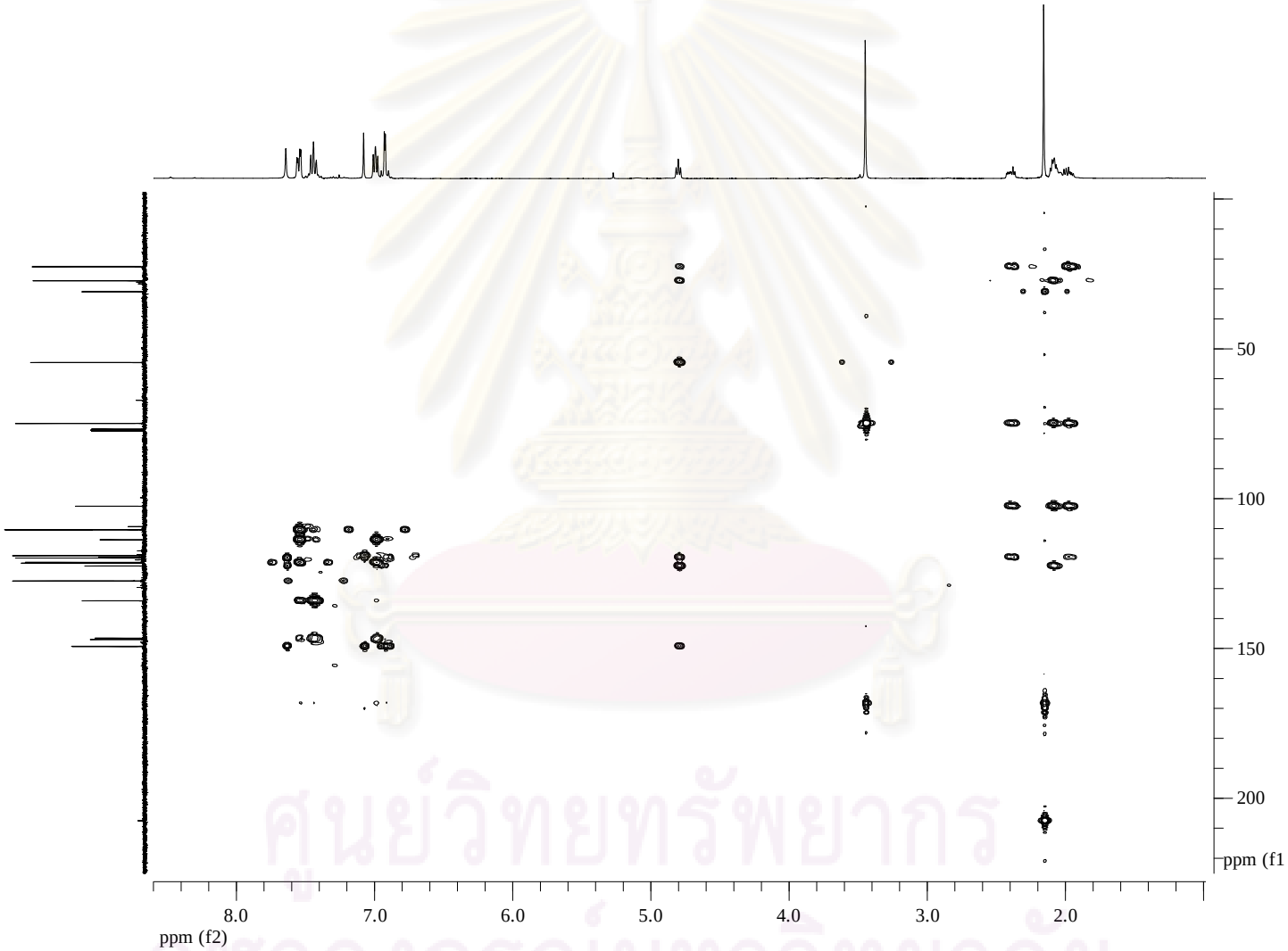

Figure B17 ^{1}H NMR spectrum of compound **4** in $CDCl_3$ (VarianYH400 spectrometer at 400 MHz)

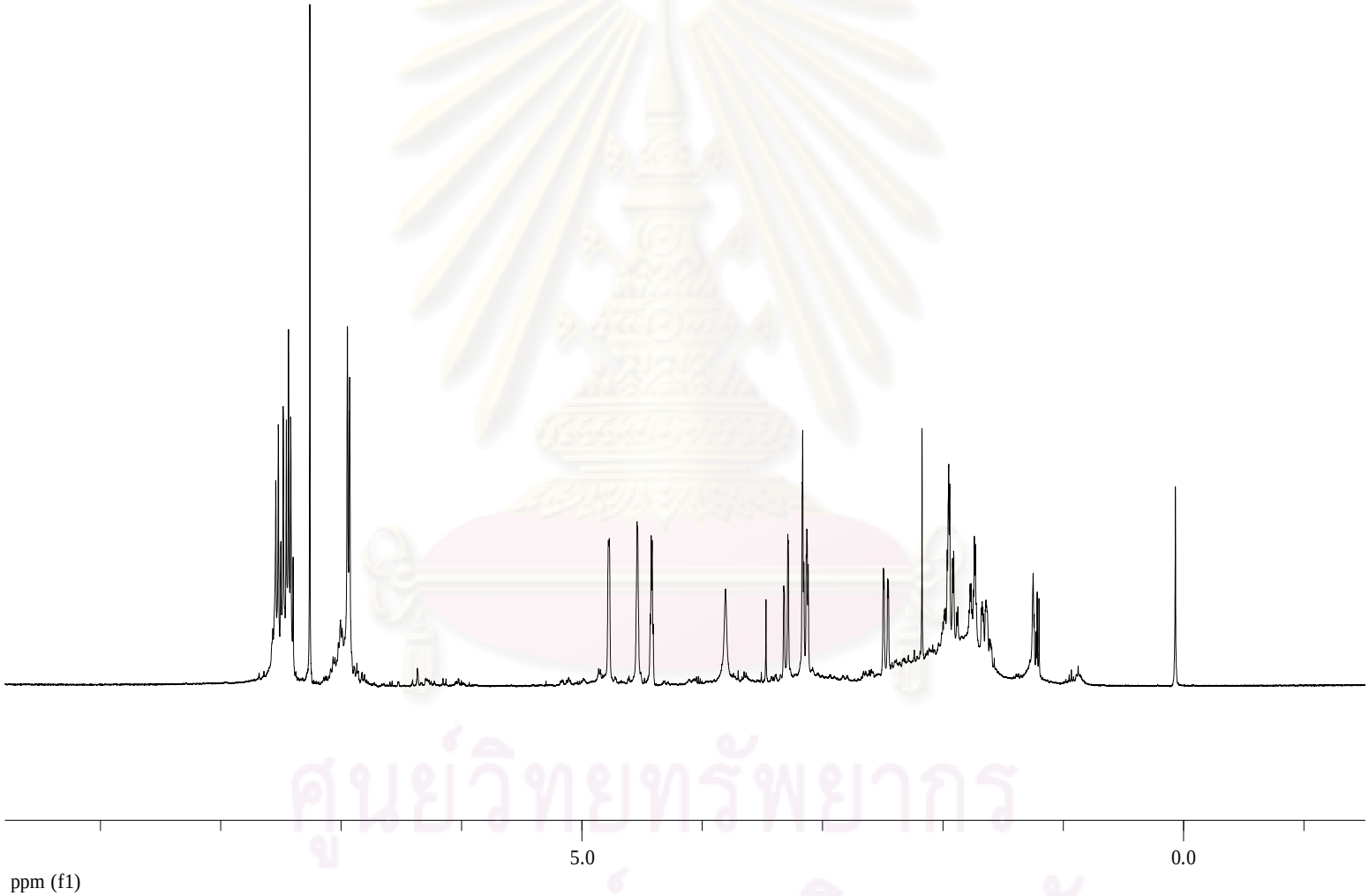

Figure B18 ^{13}C NMR spectrum of compound **4** in $CDCl_3$ (VarianYH400 spectrometer at 400 MHz)

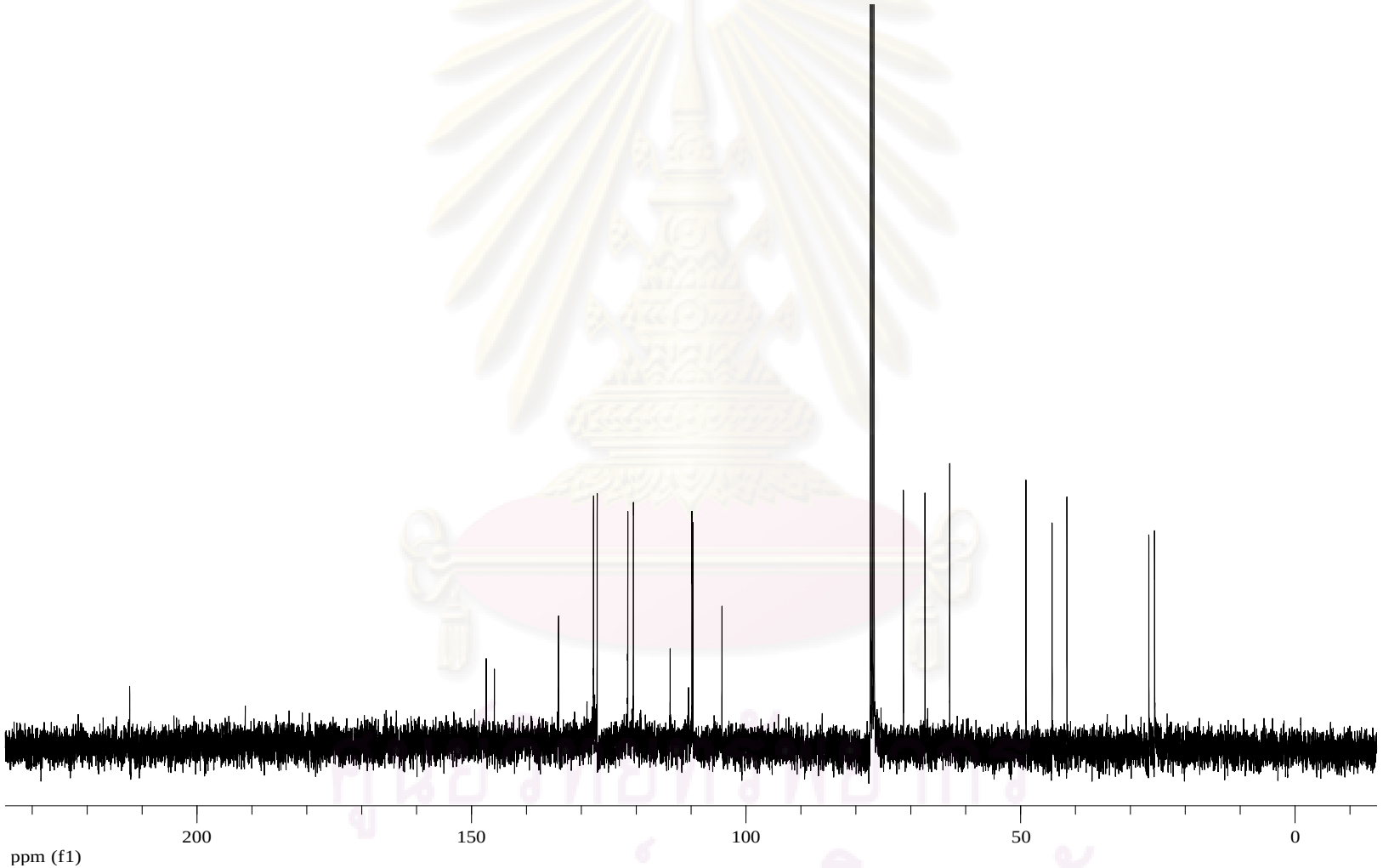

Figure B19 COSY spectrum of compound **4** in $CDCl_3$ (VarianYH400 spectrometer at 400 MHz)

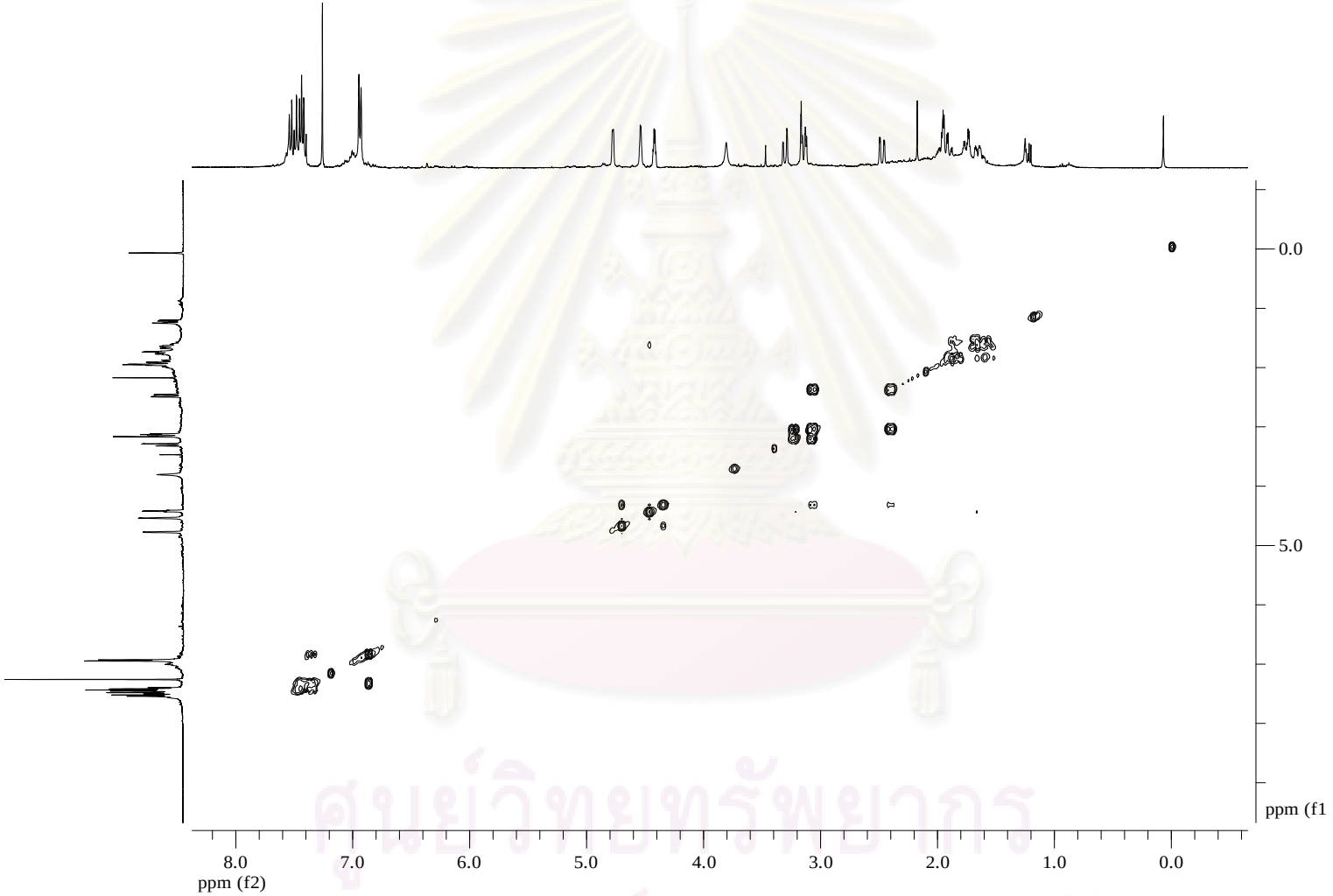

Figure B20 HSQC spectrum of compound **4** in $CDCl_3$ (VarianYH400 spectrometer at 400 MHz)

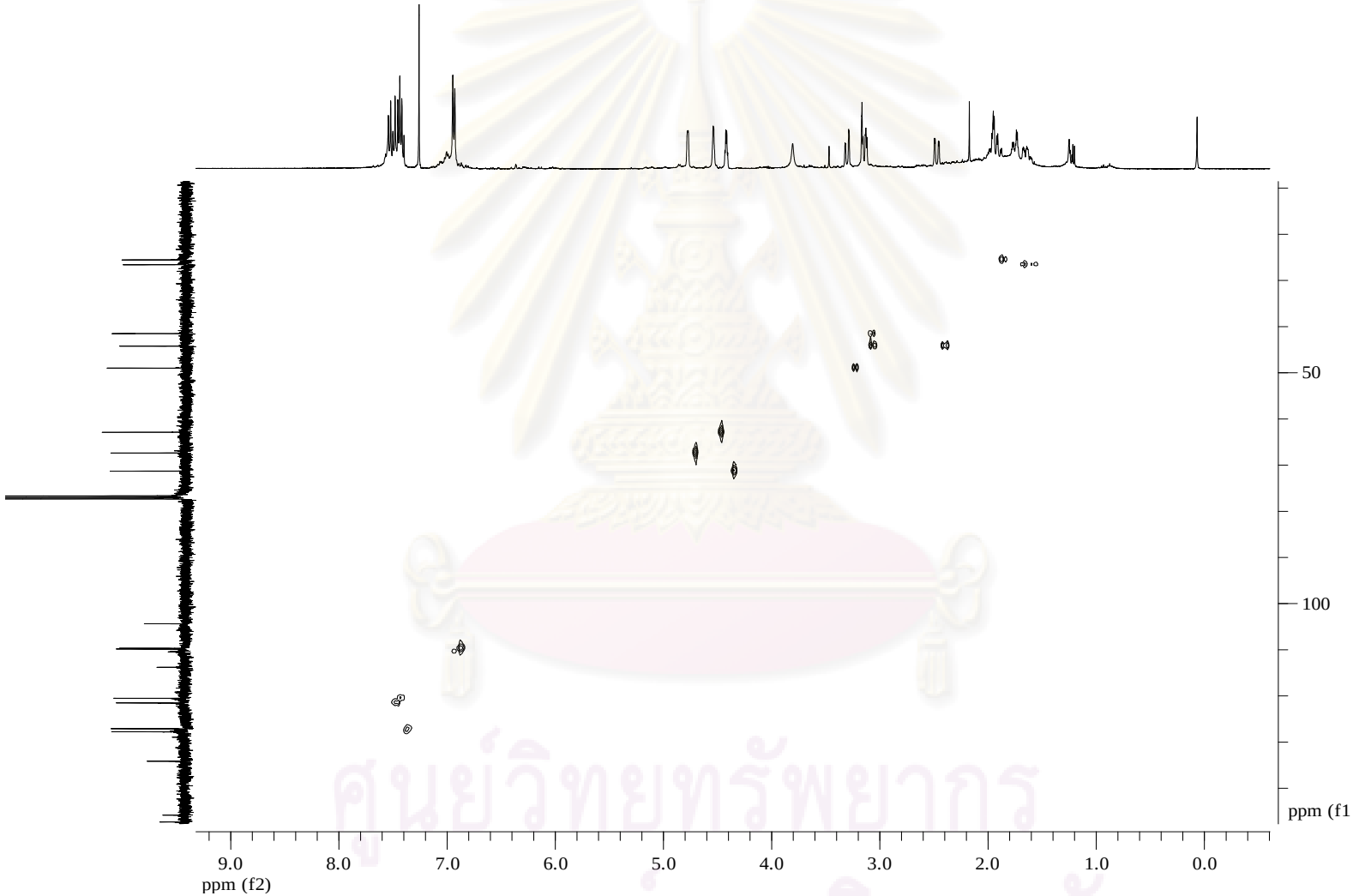

Figure B21 HMBC spectrum of compound **4** in $CDCl_3$ (VarianYH400 spectrometer at 400 MHz)

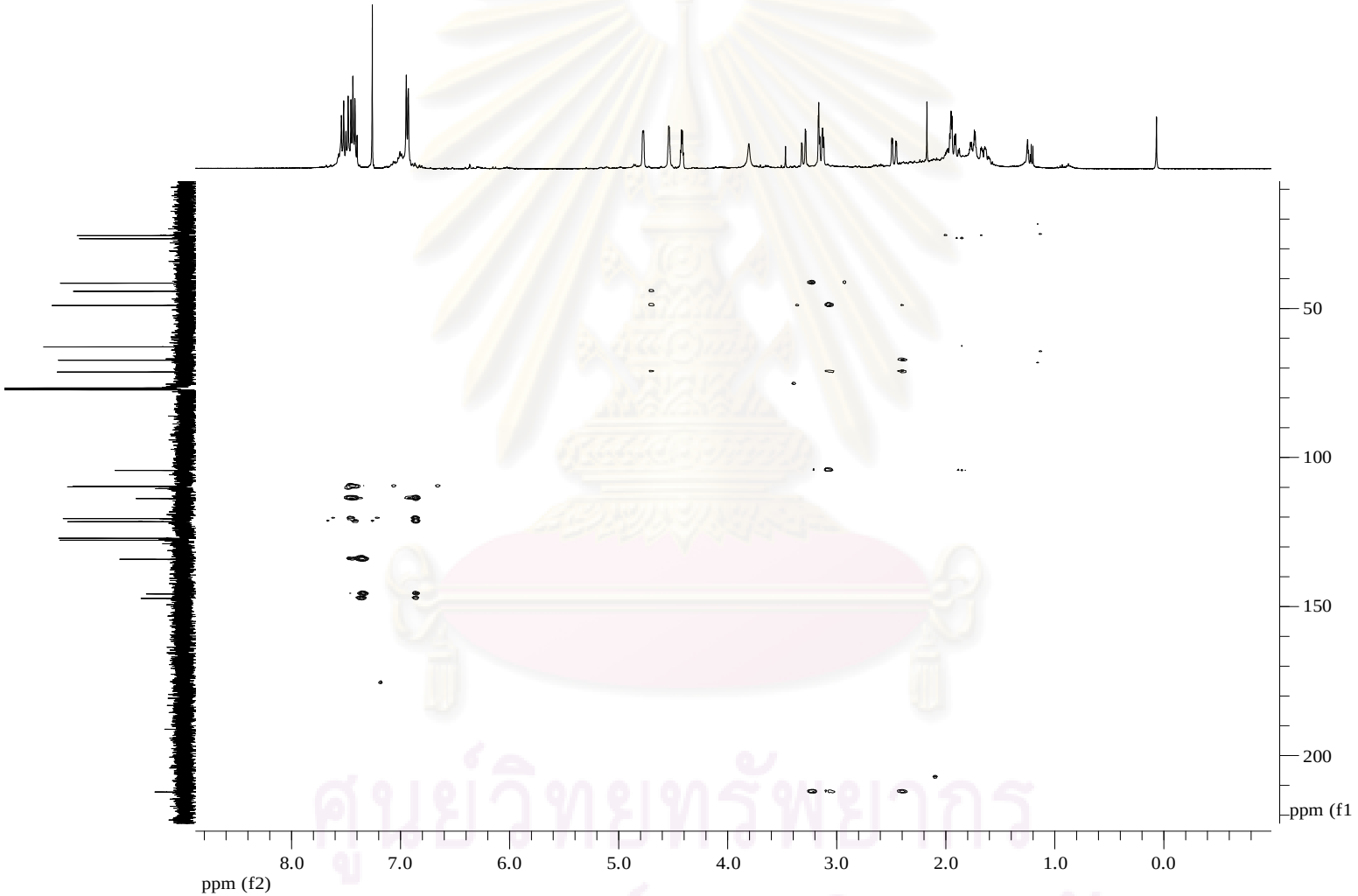

Figure B22 ^{1}H NMR spectrum of compound **5** in $CDCl_3$ (VarianYH400 spectrometer at 400 MHz)

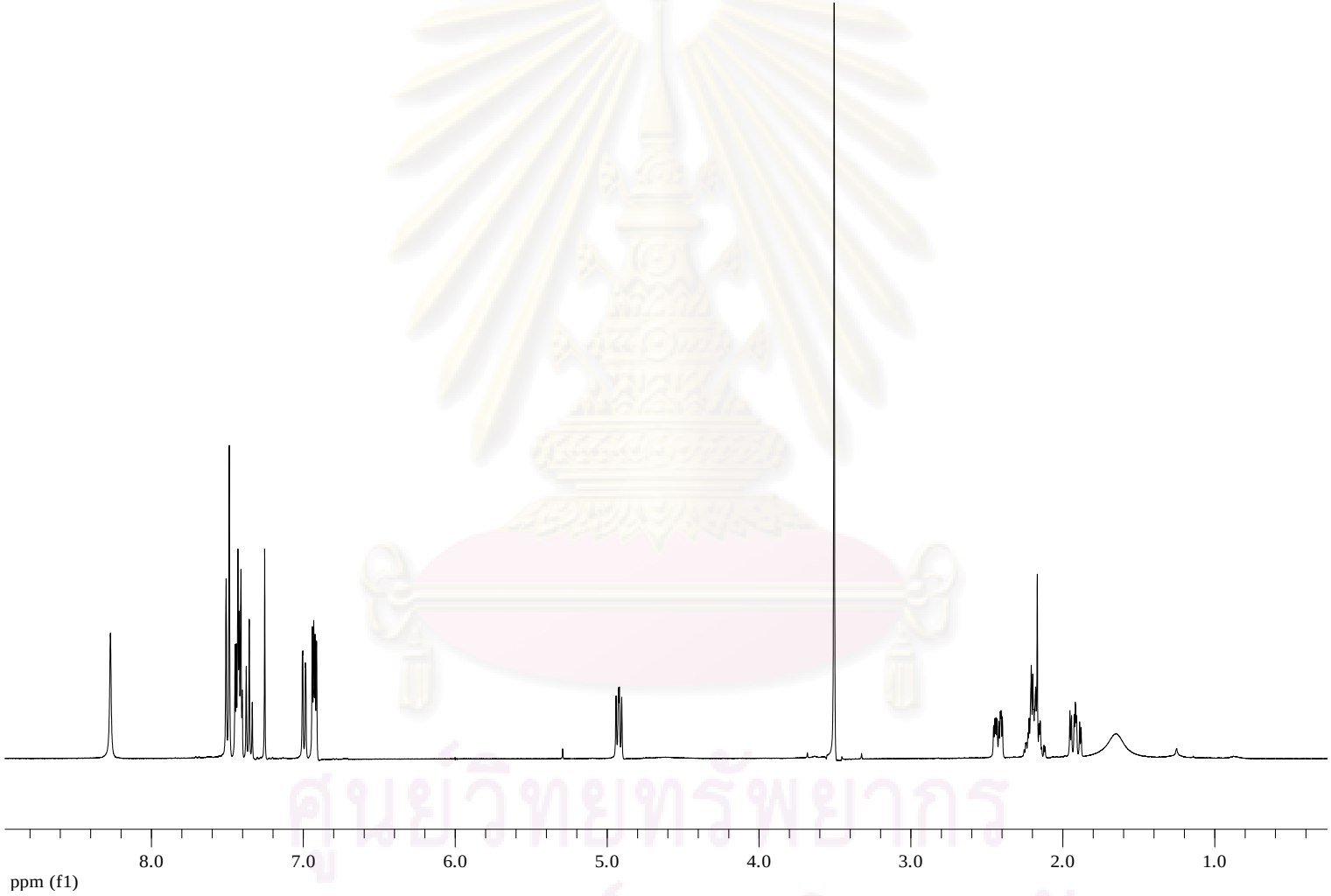

Figure B23 ^{13}C NMR spectrum of compound **5** in $CDCl_3$ (VarianYH400 spectrometer at 400 MHz)

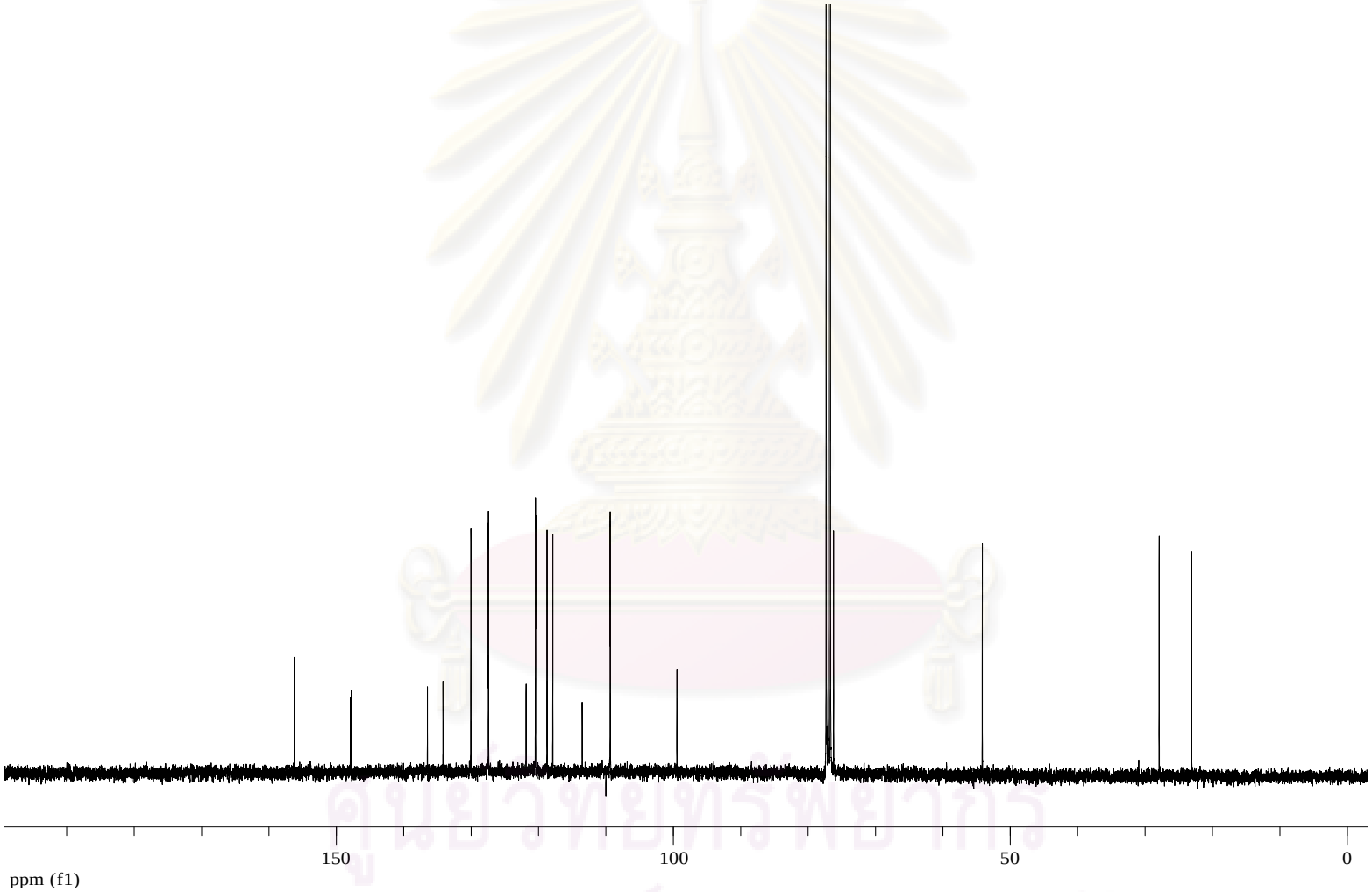

Figure B24 COSY spectrum of compound **5** in $CDCl_3$ (VarianYH400 spectrometer at 400 MHz)

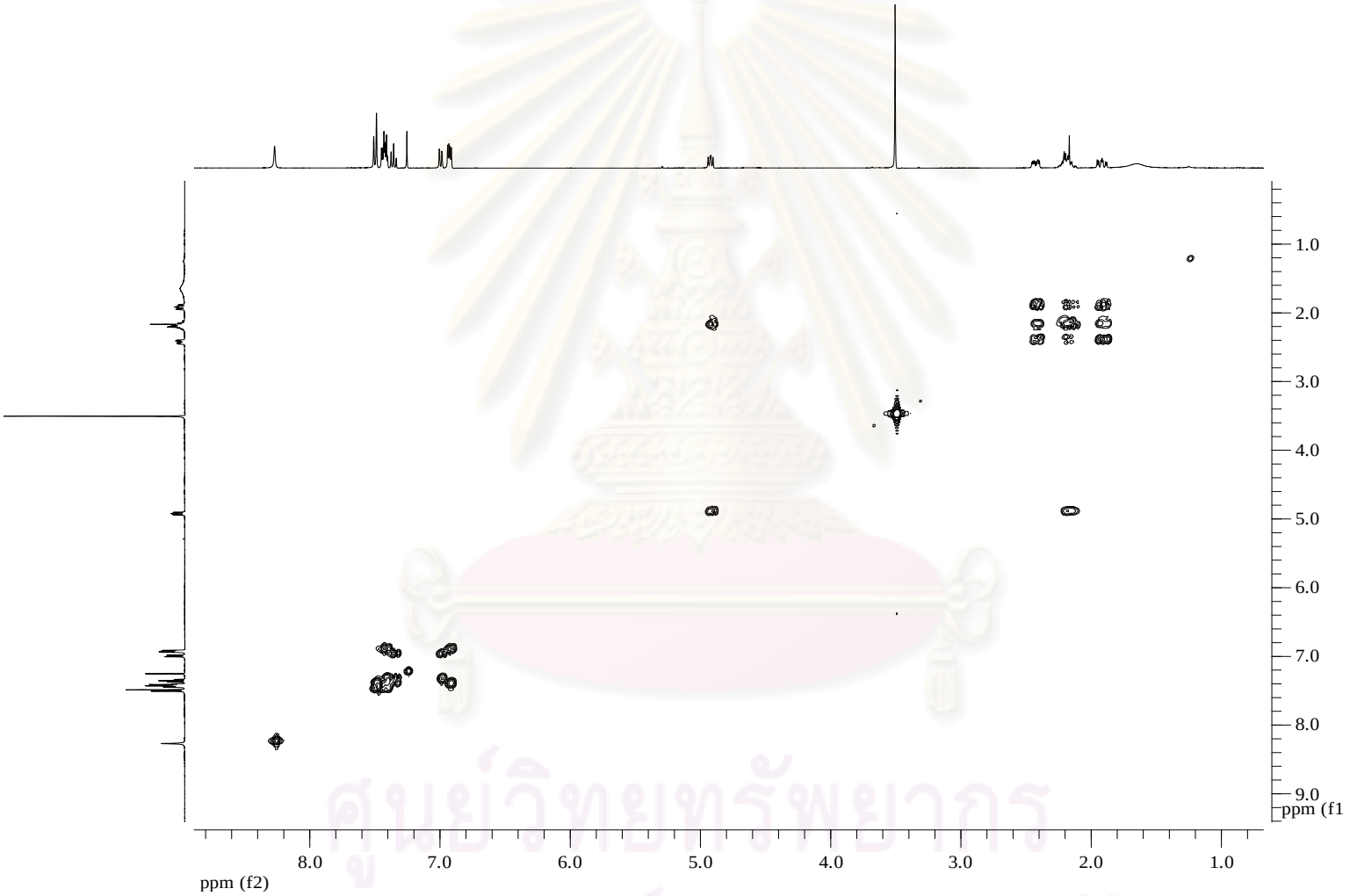

Figure B25 HSQC spectrum of compound **5** in $CDCl_3$ (VarianYH400 spectrometer at 400 MHz)

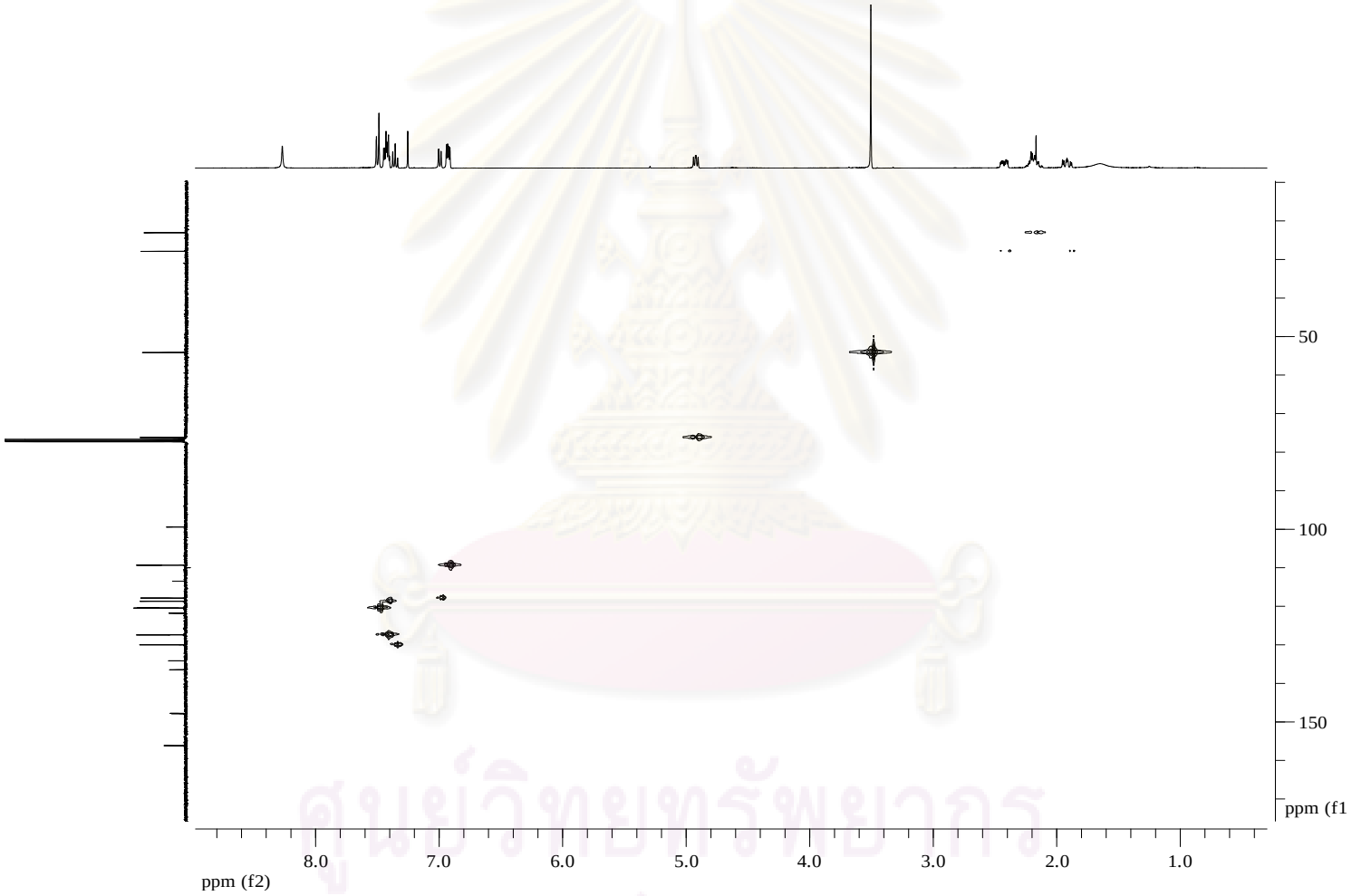

Figure B26 HMBC spectrum of compound **5** in $CDCl_3$ (VarianYH400 spectrometer at 400 MHz)

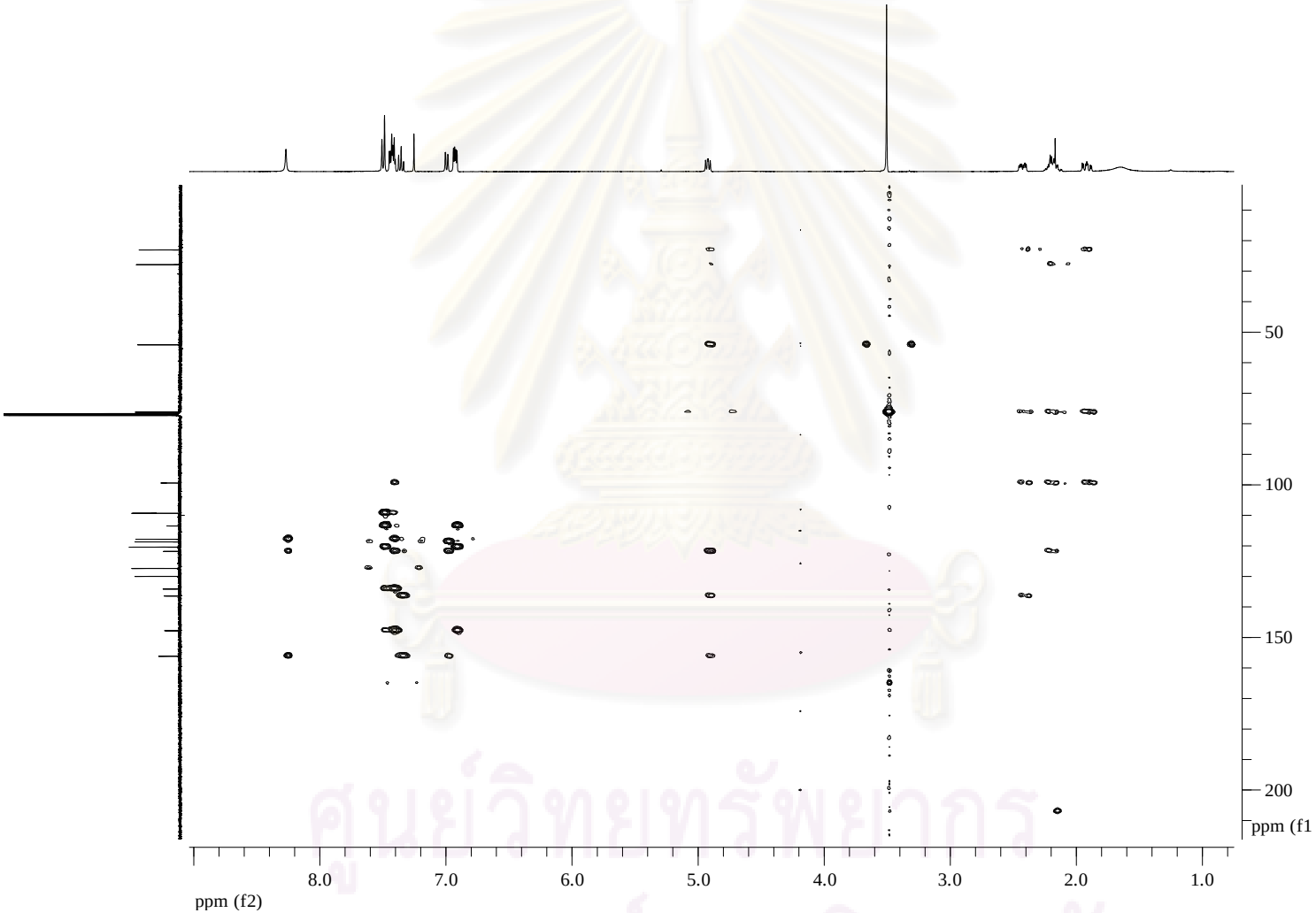

Figure B27 ^{1}H NMR spectrum of crude (XG8D cultured on corn steep broth medium) in $CDCl_3$ (VarianYH400 spectrometer at 400 MHz)

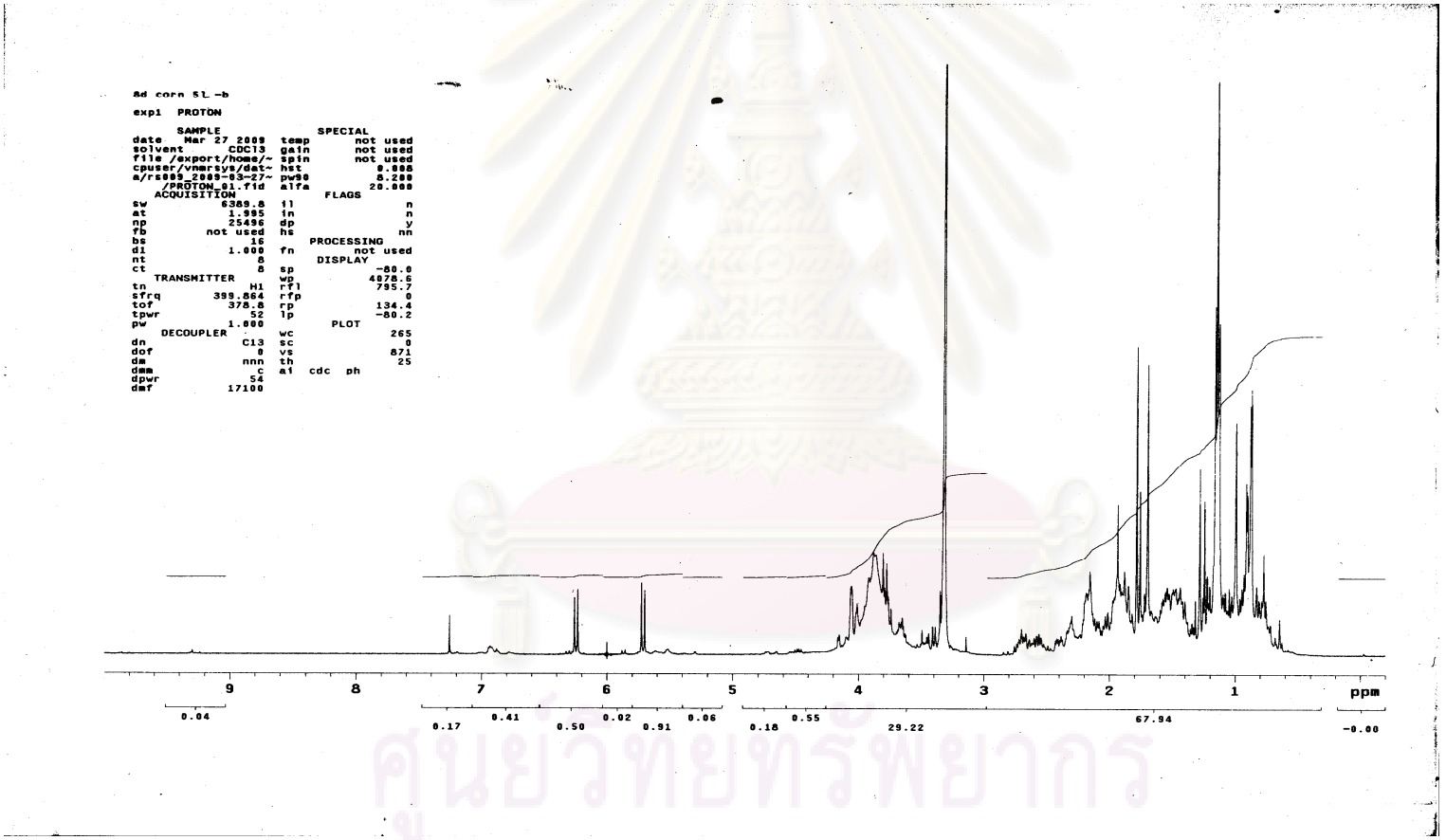

Figure B28 ^{1}H NMR spectrum of compound **6** in $CDCl_3$ (Bruker AV500D spectrometer at 500 MHz)

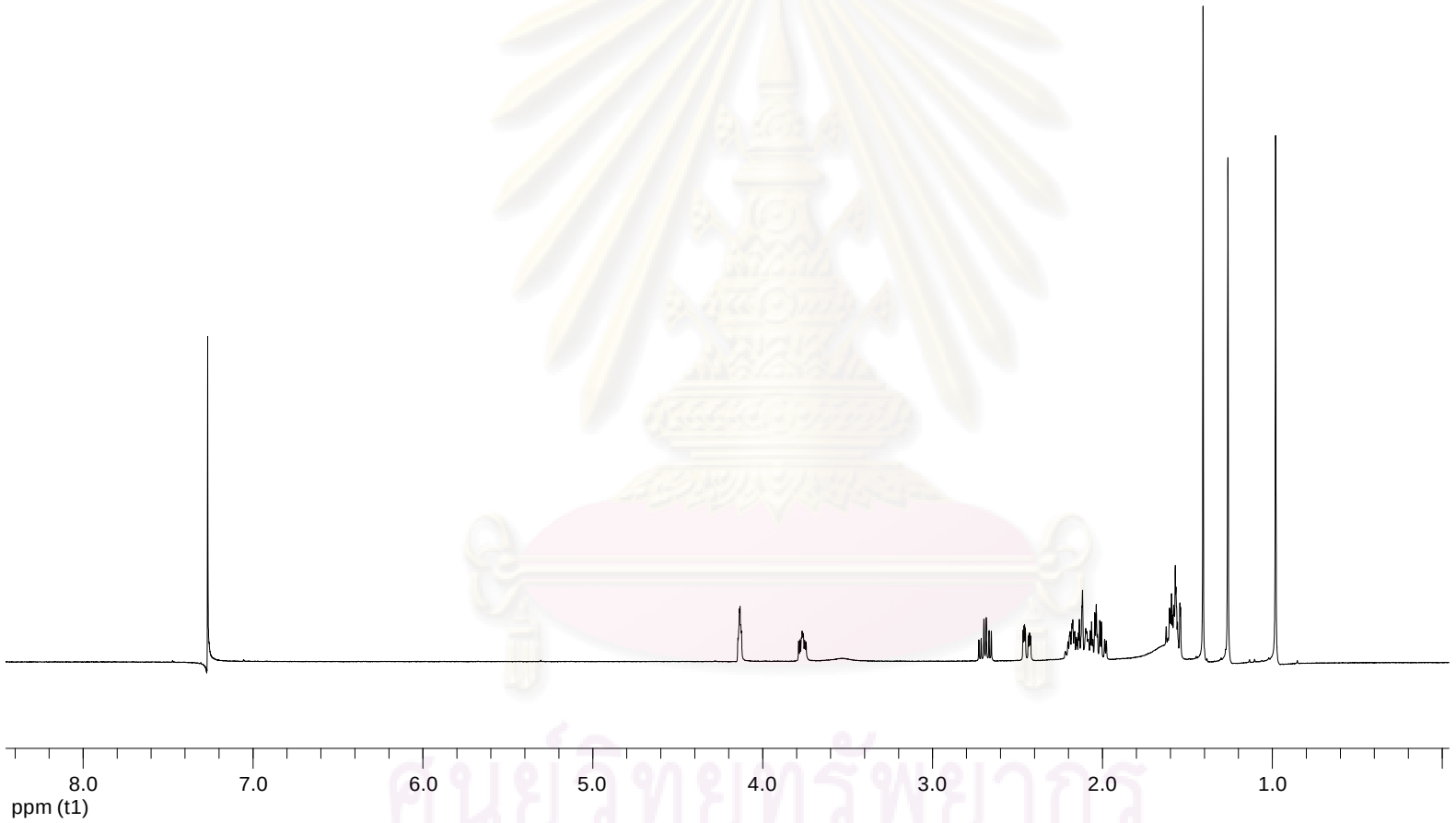

Figure B29 ^{13}C NMR spectrum of compound **6** in $CDCl_3$ (Bruker AV500D spectrometer at 500 MHz)

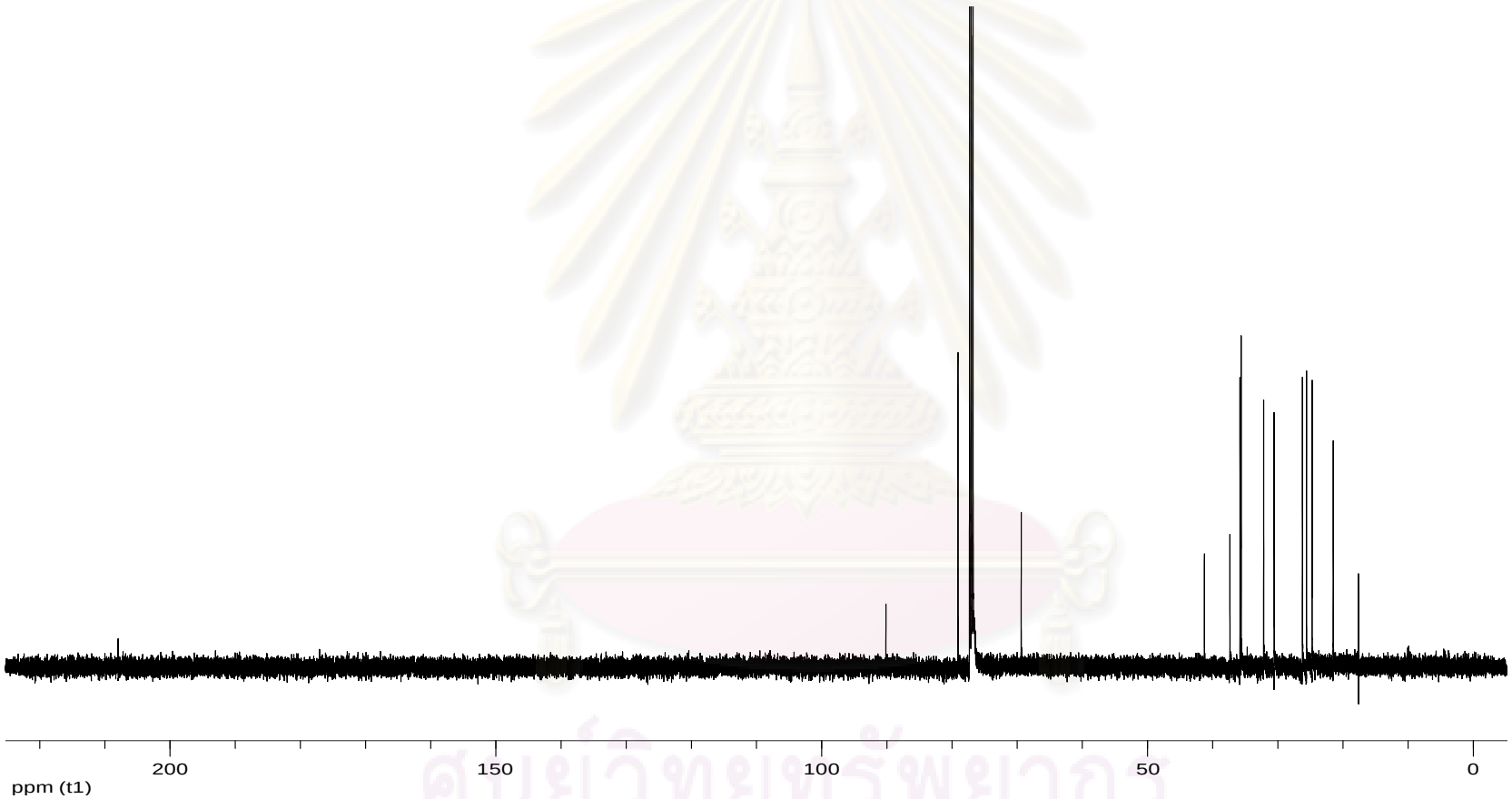

Figure B30 DEPT spectrum of compound **6** in $CDCl_3$ (Bruker AV500D spectrometer at 500 MHz)

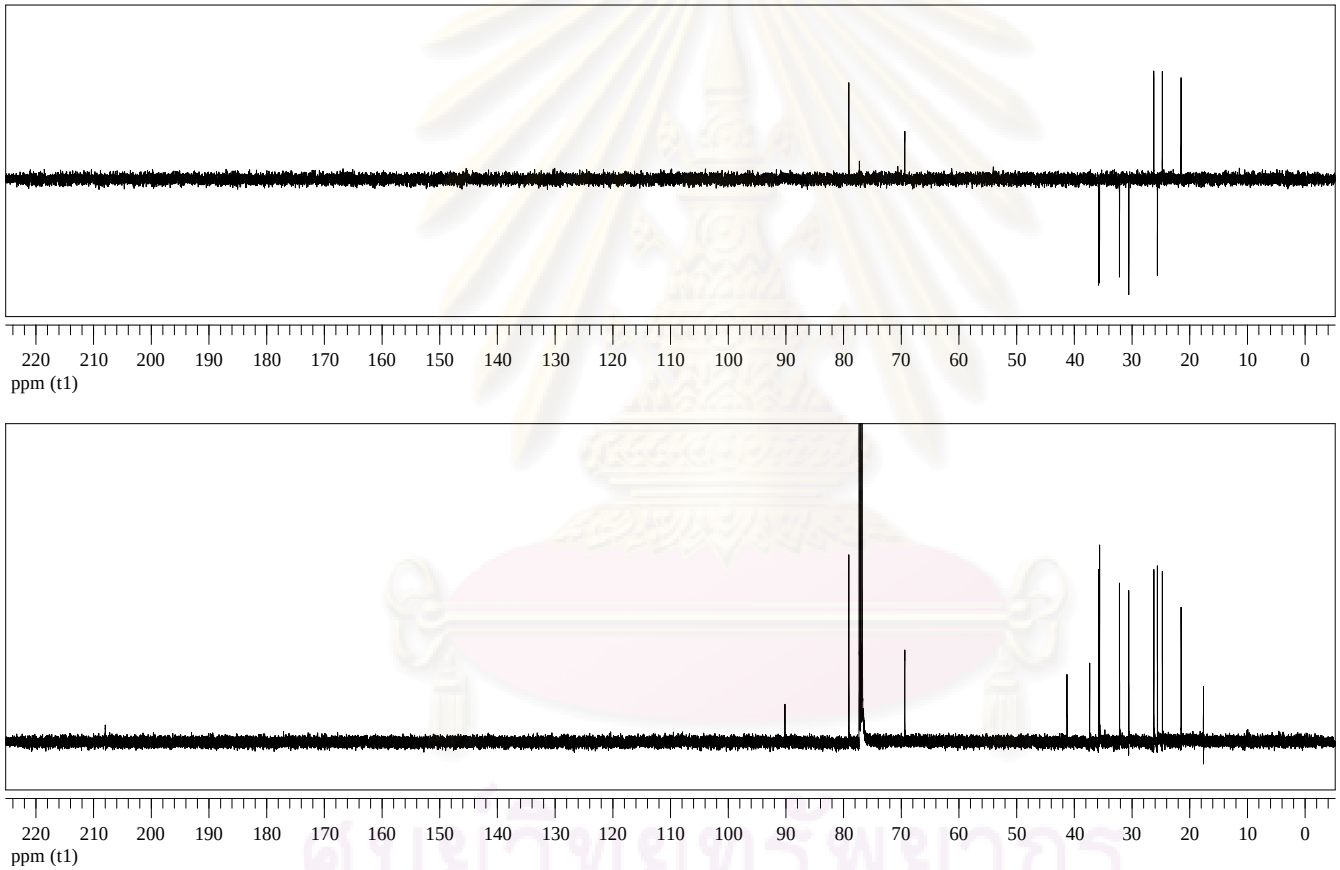

Figure B31 COSY spectrum of compound **6** in $CDCl_3$ (Bruker AV500D spectrometer at 500 MHz)

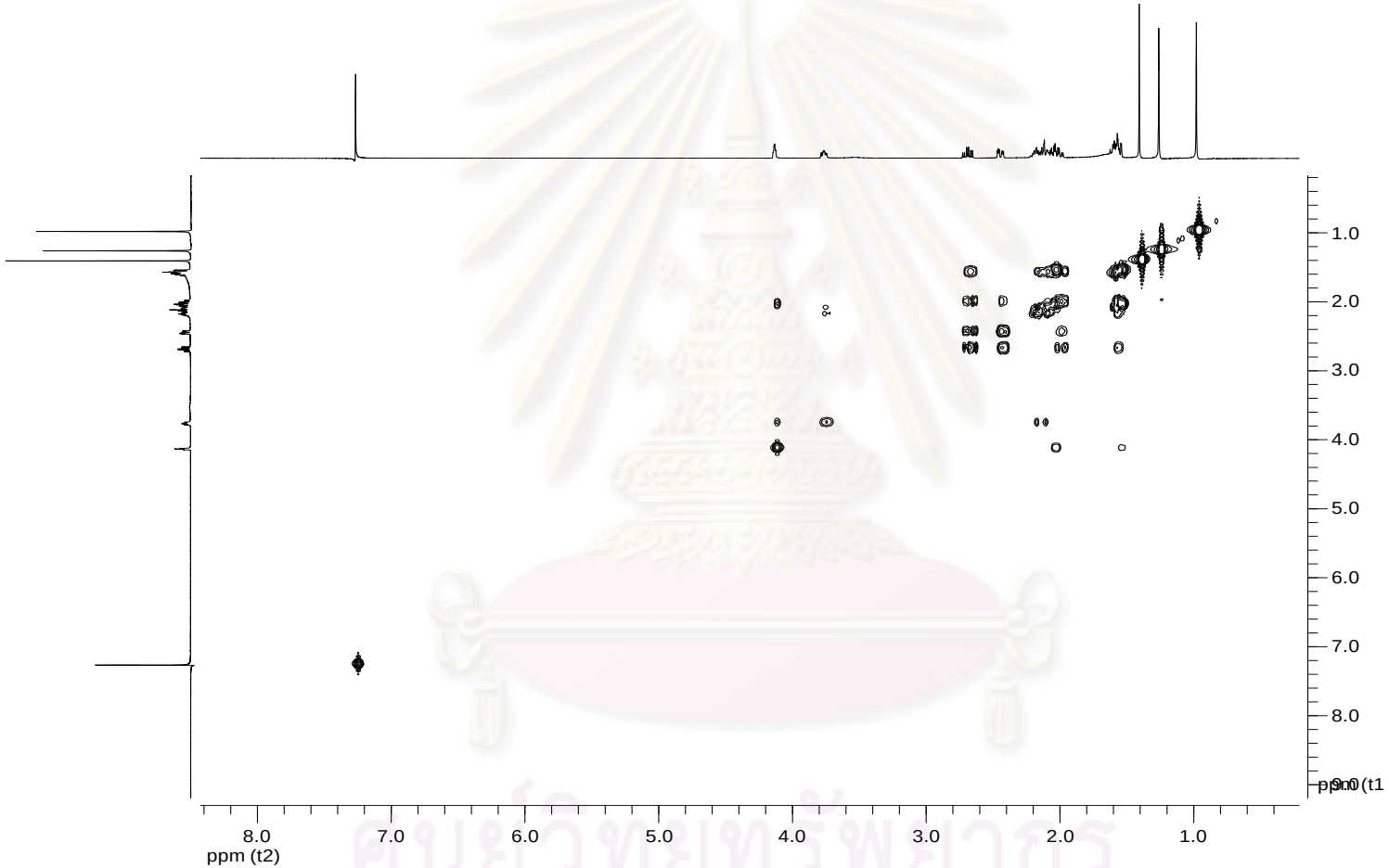

Figure B32 HMQC spectrum of compound **6** in $CDCl_3$ (Bruker AV500D spectrometer at 500 MHz)

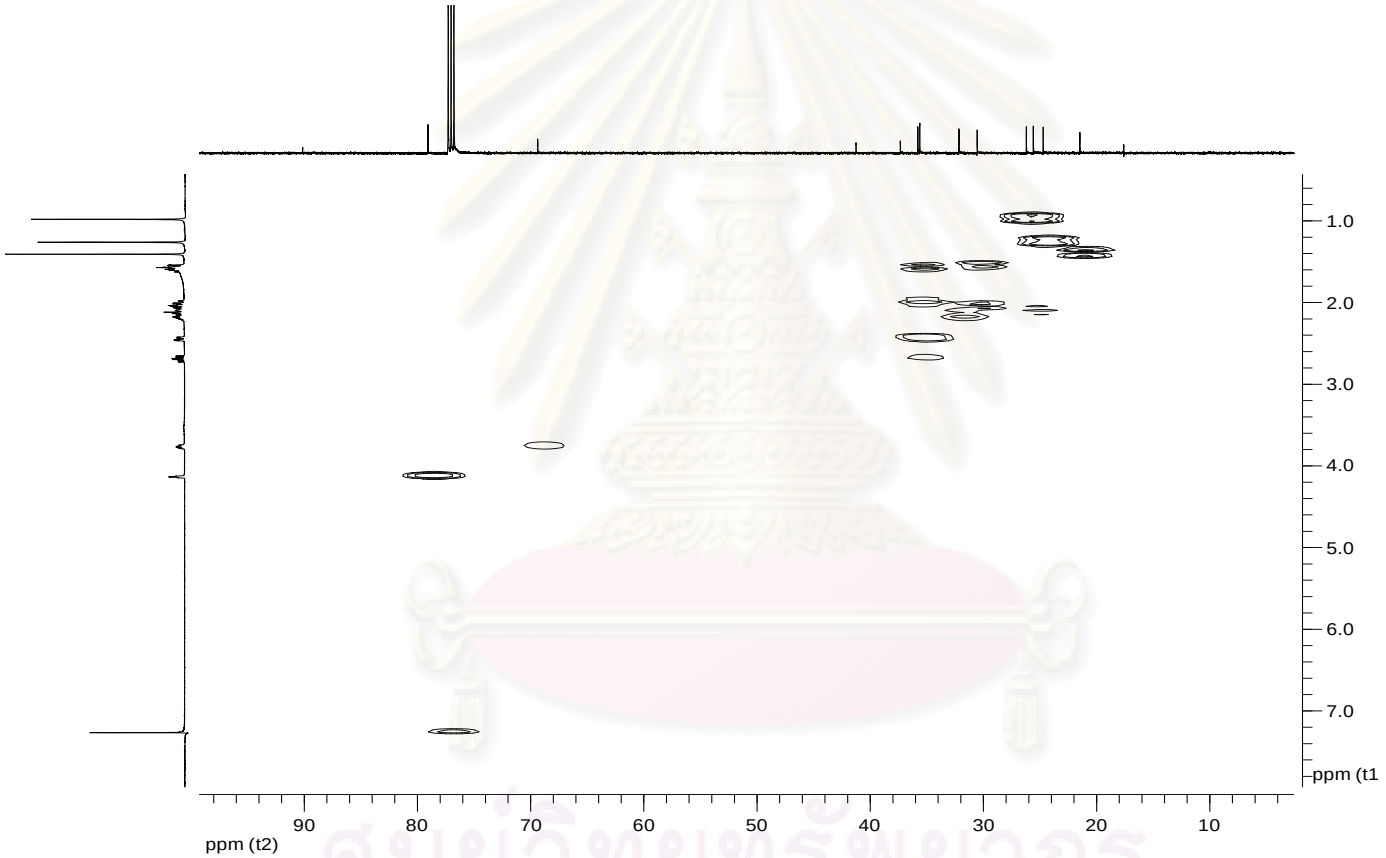

Figure B33 HMBC spectrum of compound **6** in $CDCl_3$ (Bruker AV500D spectrometer at 500 MHz)

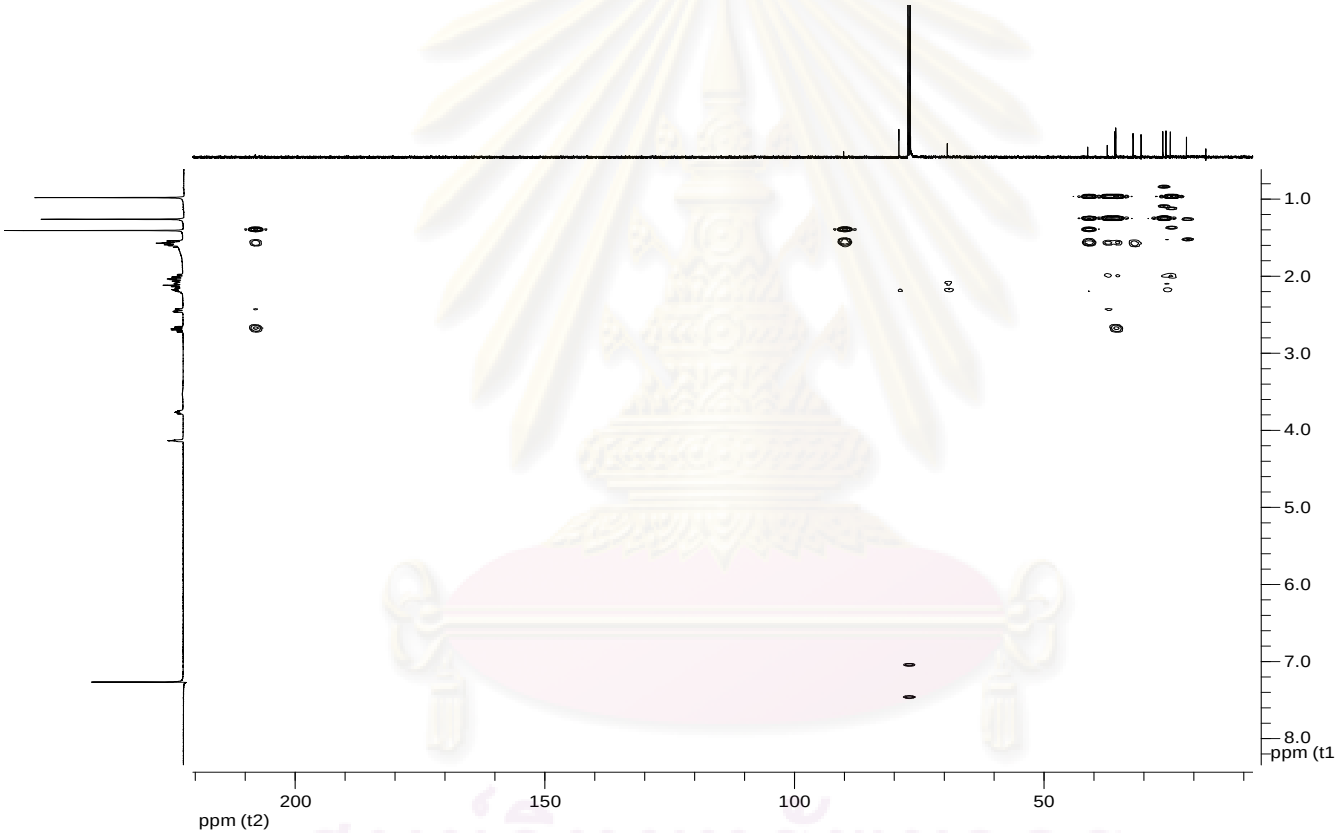

Figure B34 NOESY spectrum of compound **6** in $CDCl_3$ (Bruker AV500D spectrometer at 500 MHz)

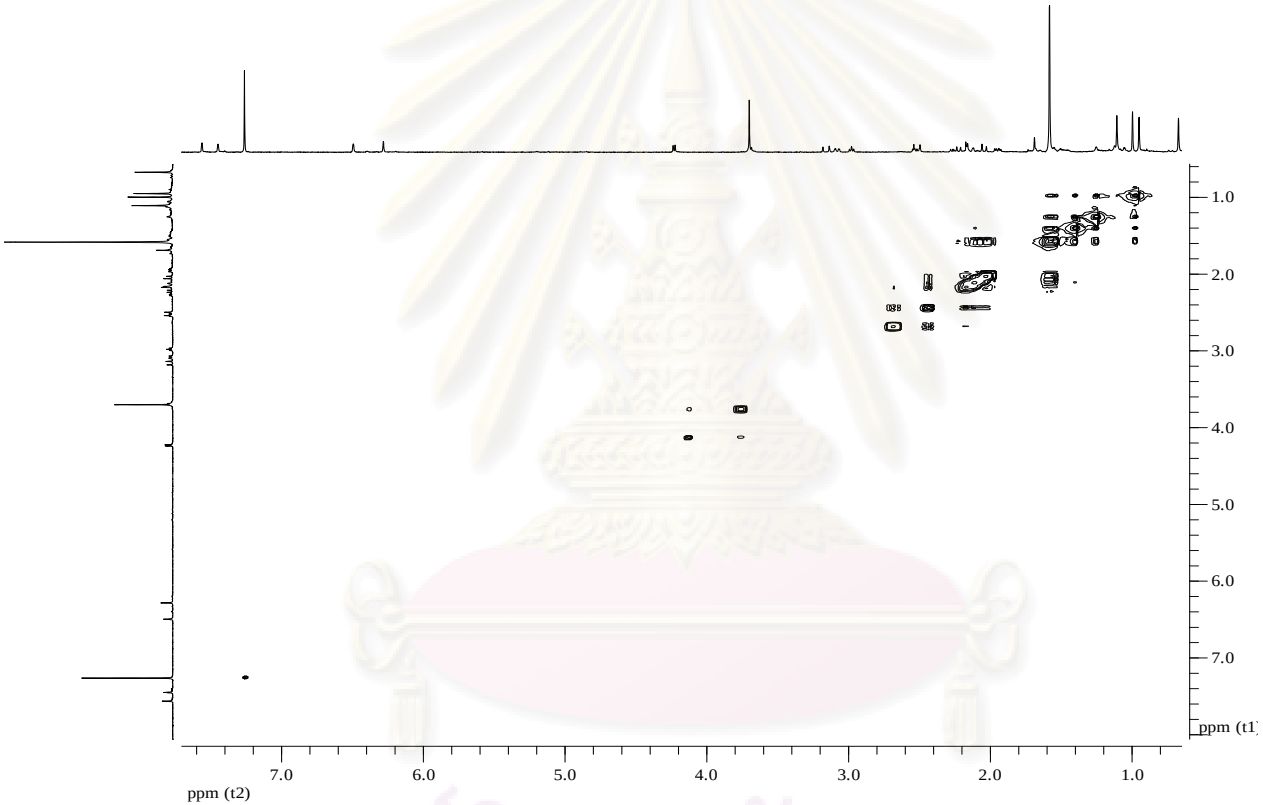

Figure B35 ^{1}H spectrum of compound **7** in $CDCl_3$ (Bruker AV500D spectrometer at 500 MHz)

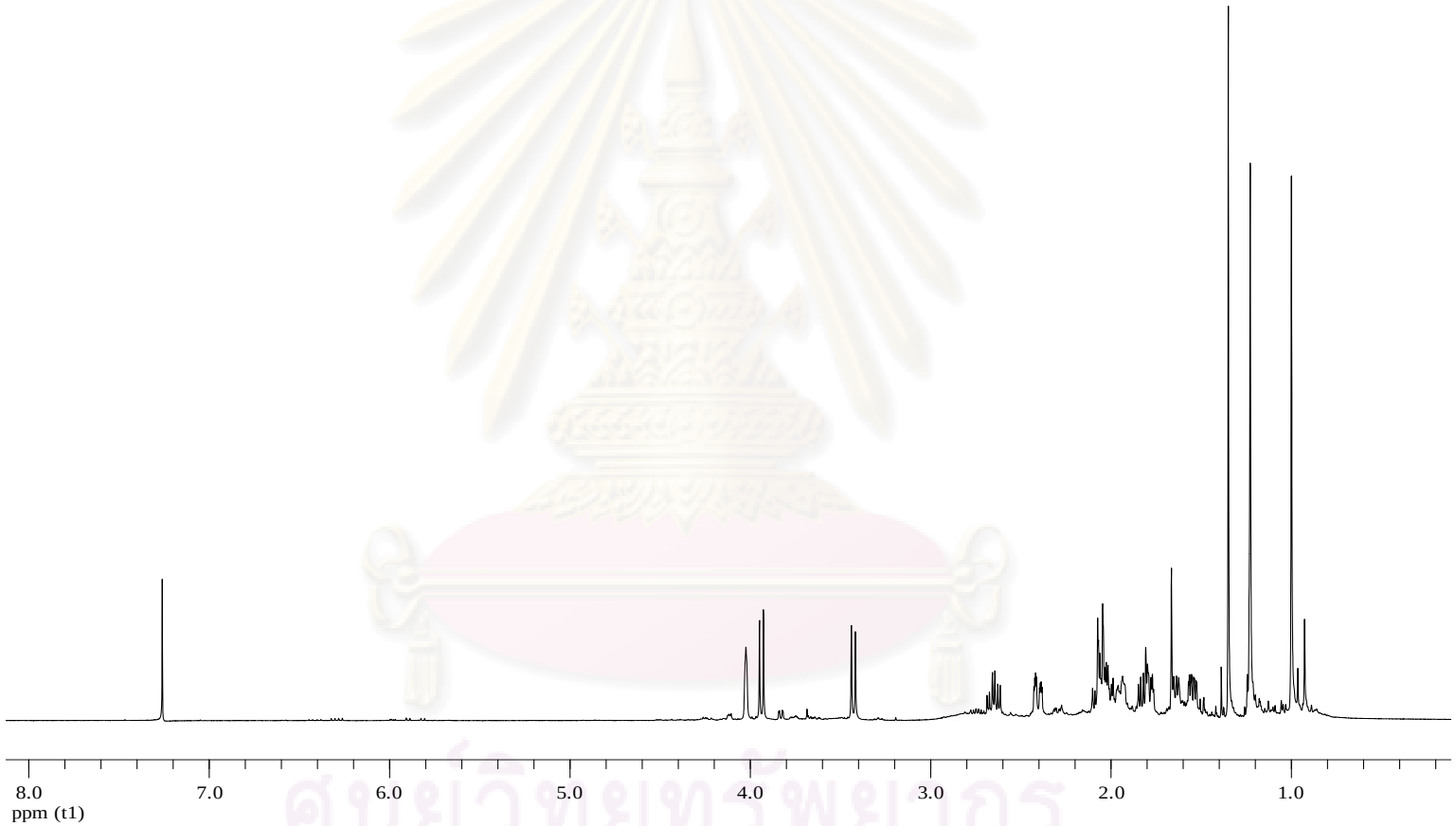

Figure B36 ^{13}C spectrum of compound **7** in $CDCl_3$ (Bruker AV500D spectrometer at 500 MHz)

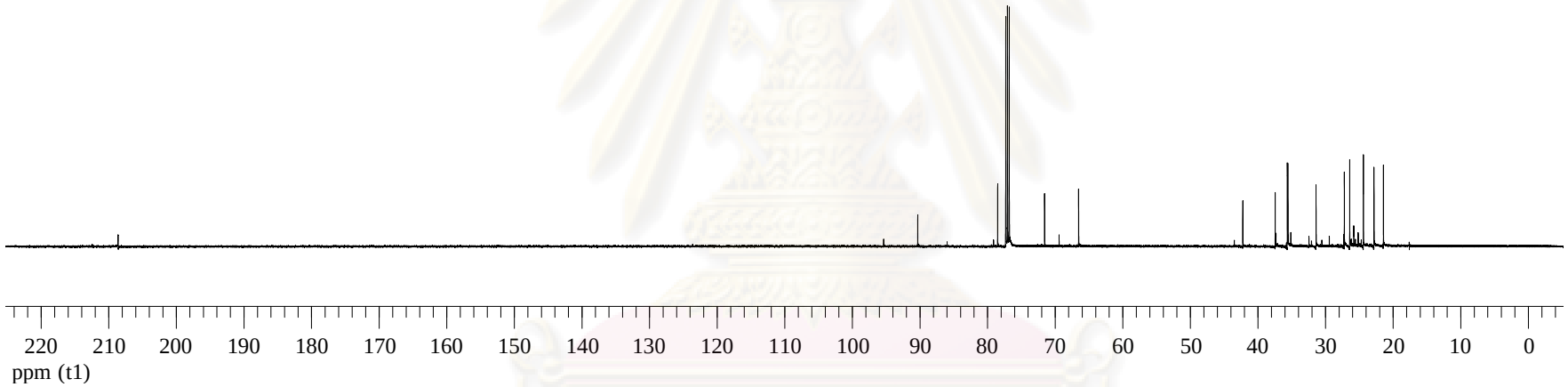

Figure B37 DEPT spectrum of compound **7** in $CDCl_3$ (Bruker AV500D spectrometer at 500 MHz)

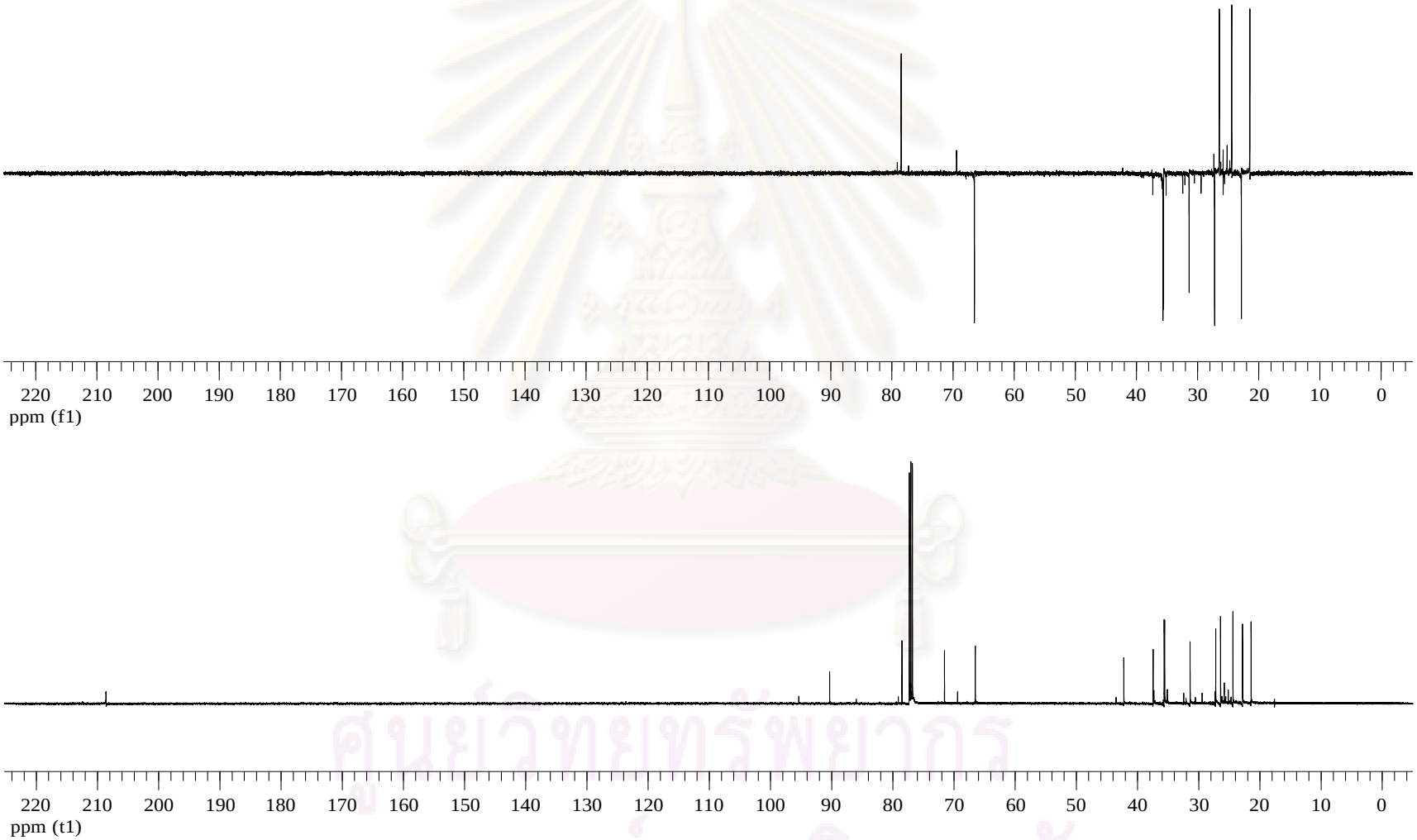

Figure B38 COSY spectrum of compound **7** in $CDCl_3$ (Bruker AV500D spectrometer at 500 MHz)

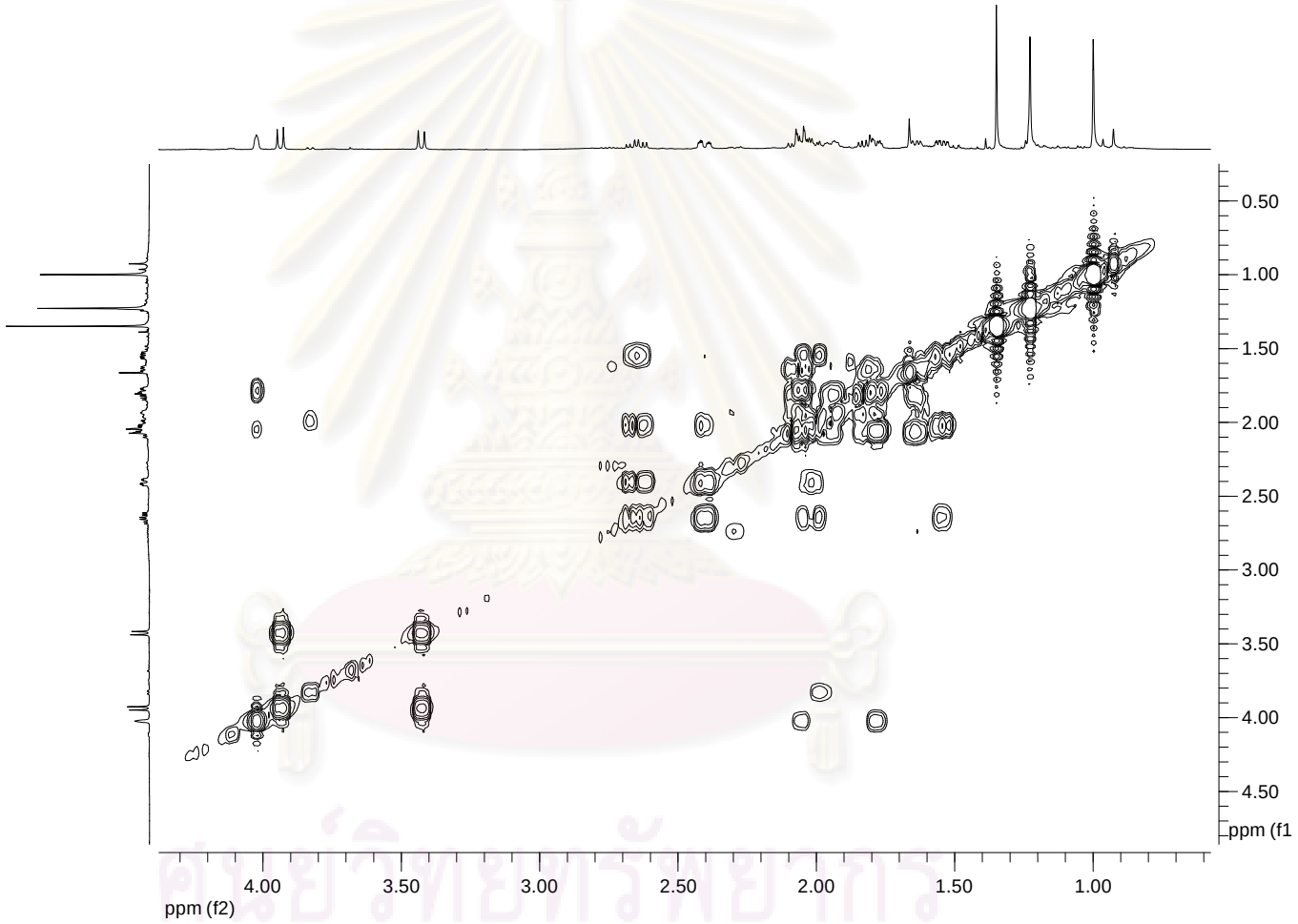

Figure B39 HMQC spectrum of compound **7** in $CDCl_3$ (Bruker AV500D spectrometer at 500 MHz)

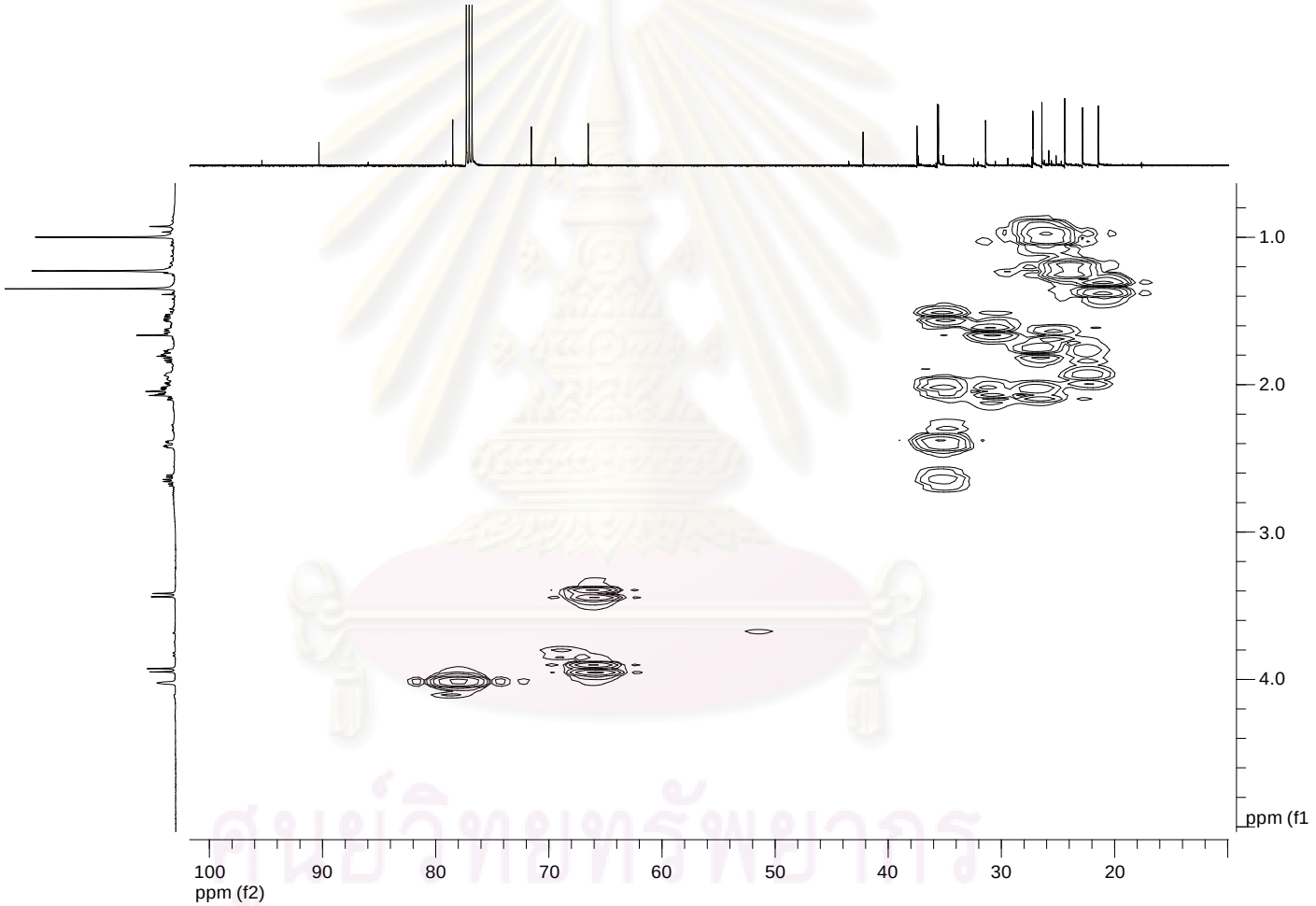

Figure B40 HMBC spectrum of compound **7** in $CDCl_3$ (Bruker AV500D spectrometer at 500 MHz)

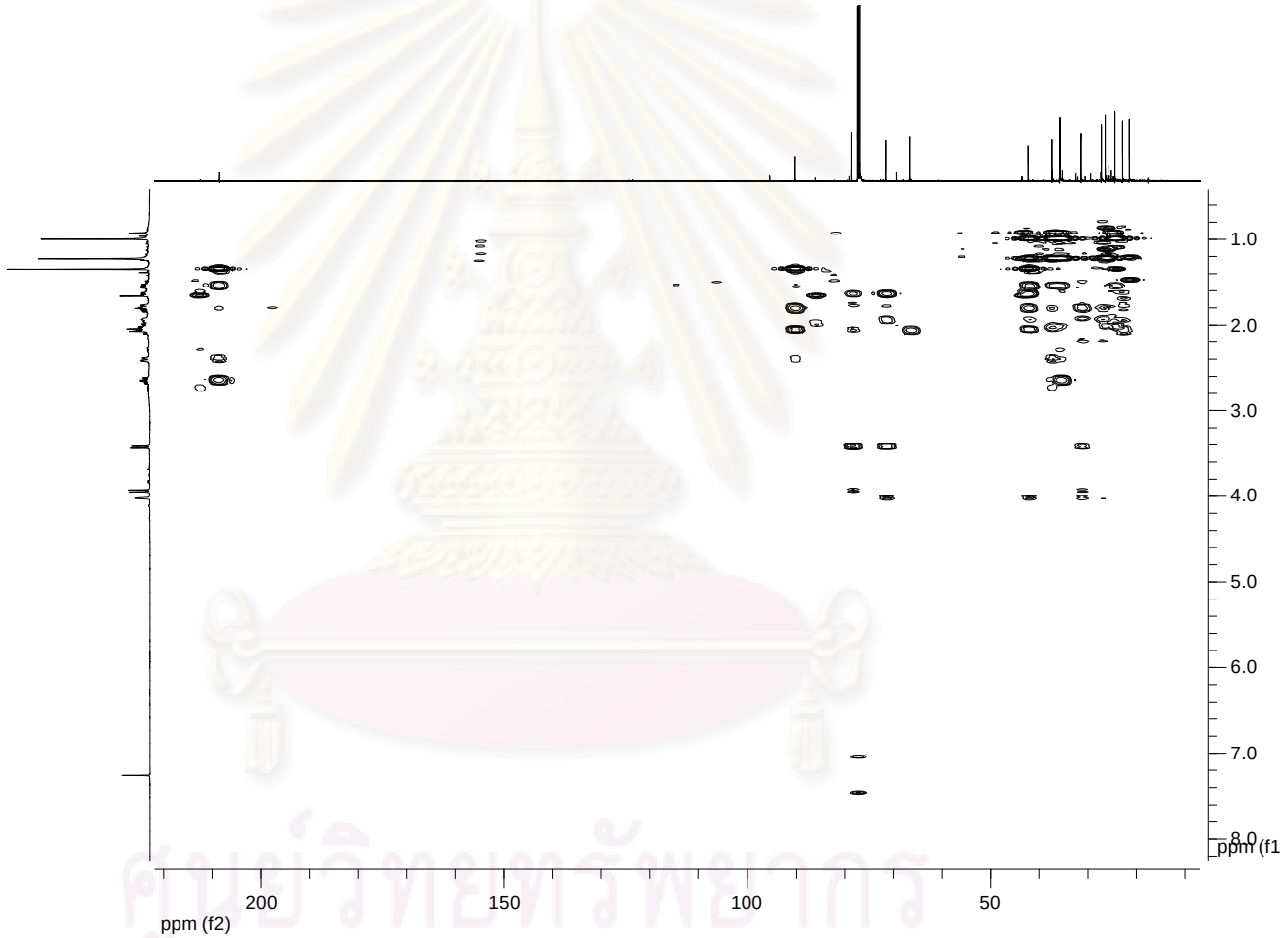

Figure B41 NOESY spectrum of compound **7** in $CDCl_3$ (Bruker AV500D spectrometer at 500 MHz)

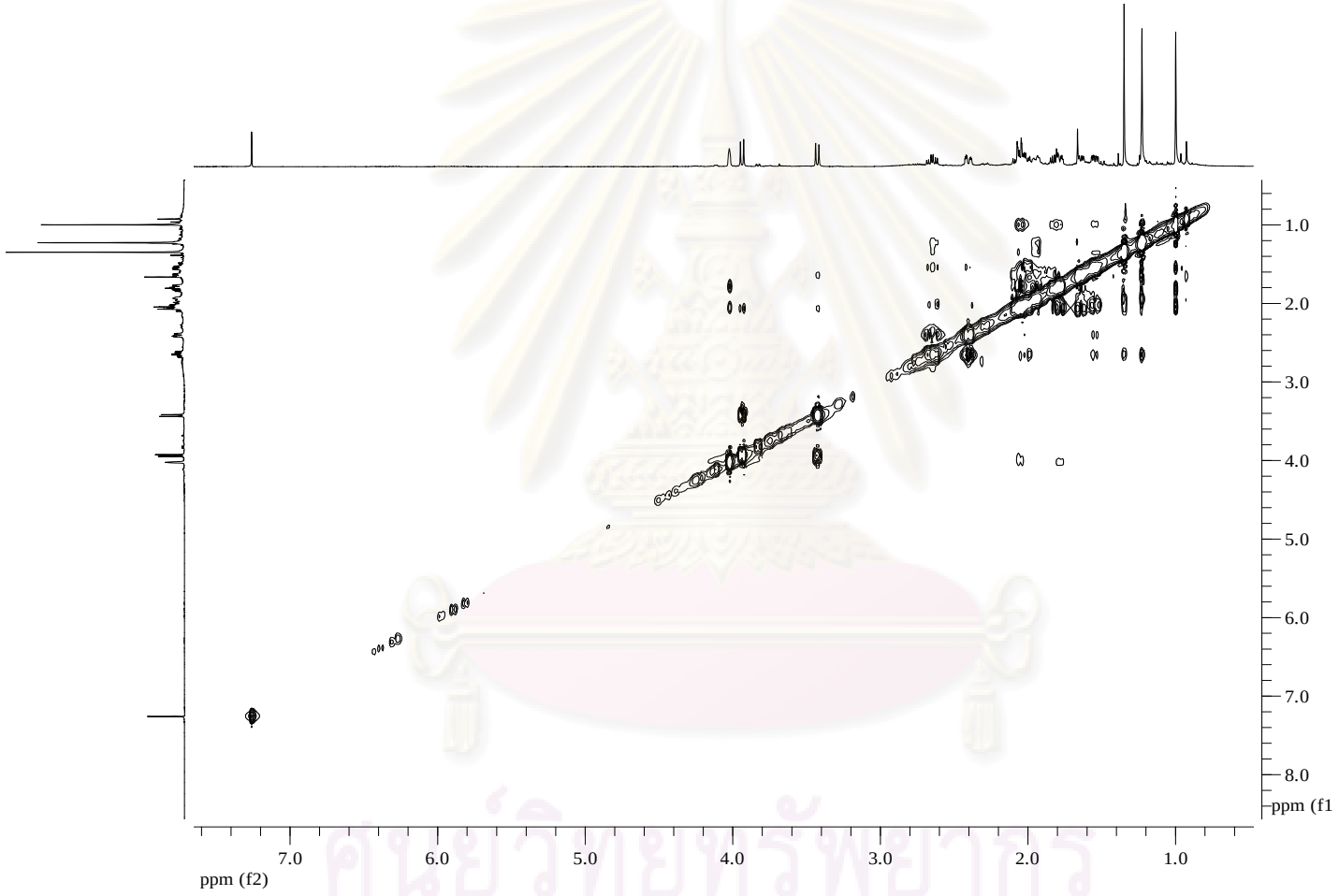

Figure B42 ^{1}H NMR spectrum of compound **7** in acetone-d_6 (Bruker DRX 400 spectrometer at 400 MHz)

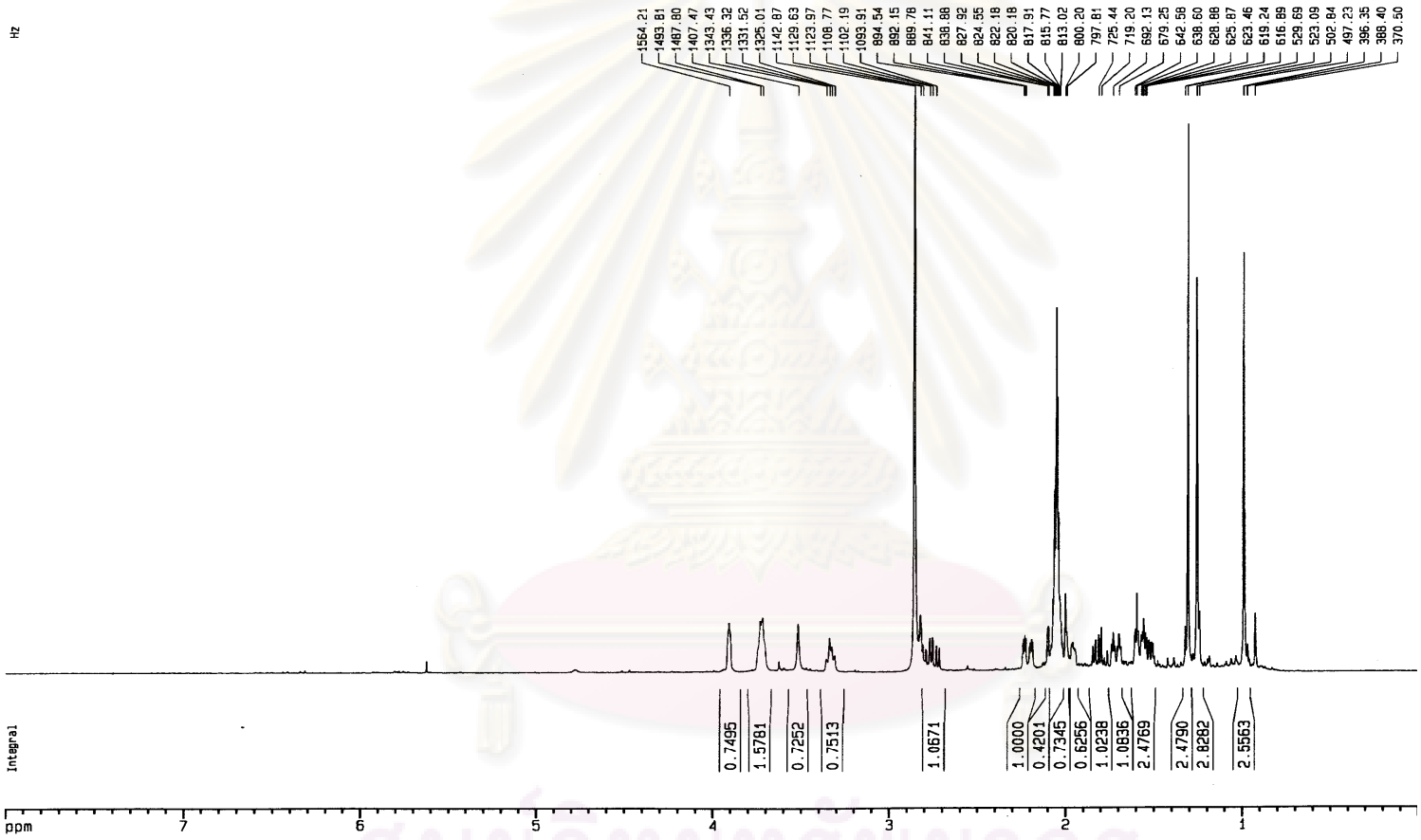

Figure B43 ^{1}H NMR spectrum of compound **7** in acetone-d_6 (Bruker DRX 400 spectrometer at 400 MHz)

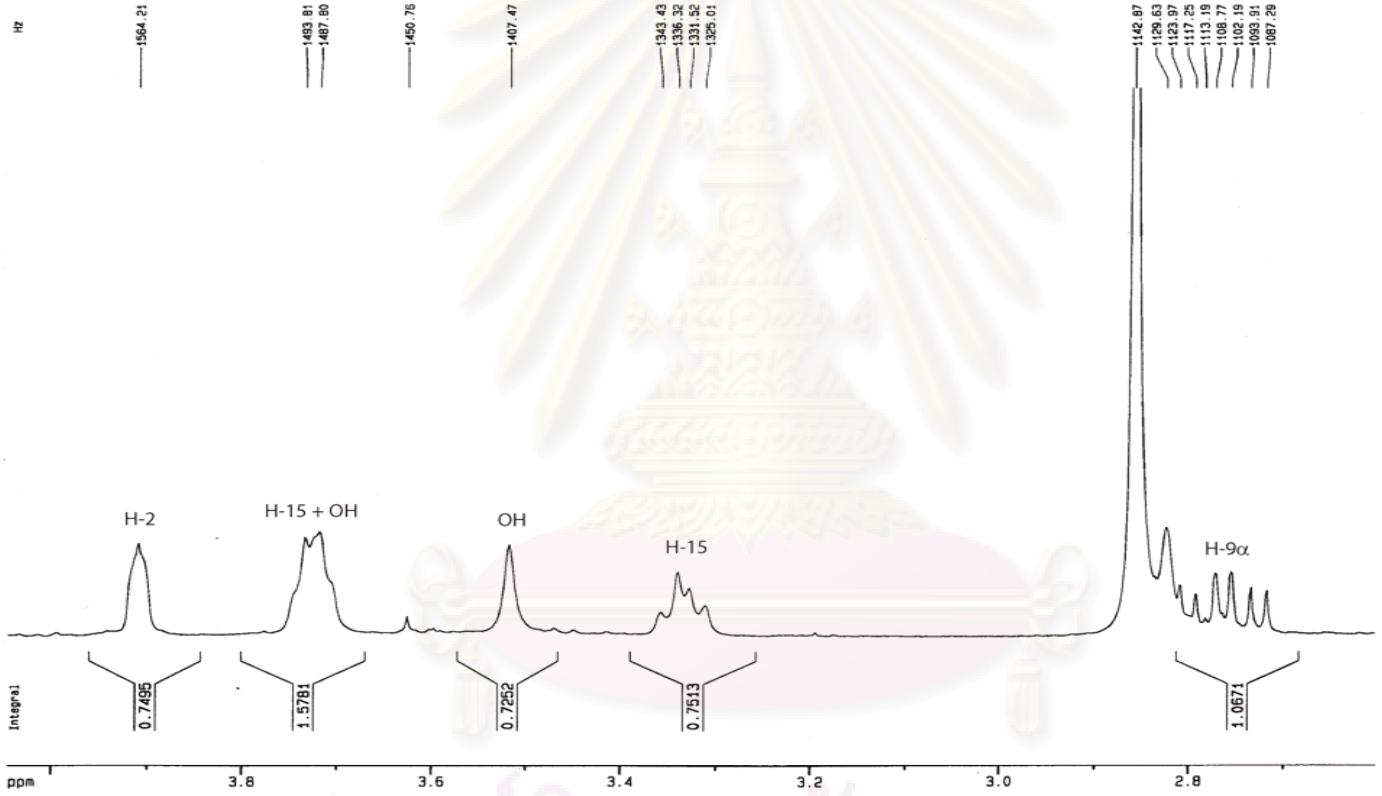

Figure B44 ^{1}H NMR spectrum of compound **7** in acetone-d_6 (Bruker DRX 400 spectrometer at 400 MHz)

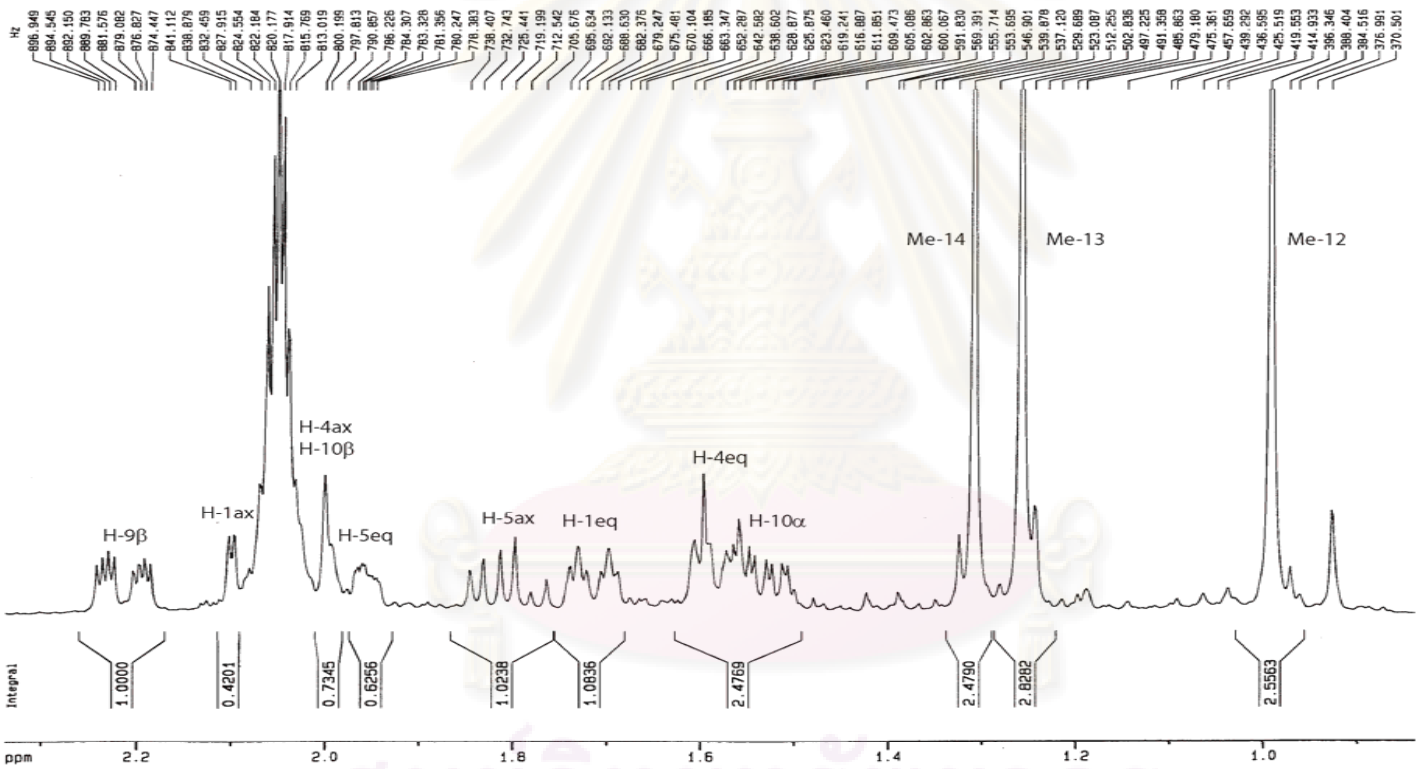

Figure B45 NOESY spectrum of compound **7** in acetone-d_6 (Bruker DRX 400 spectrometer at 400 MHz)

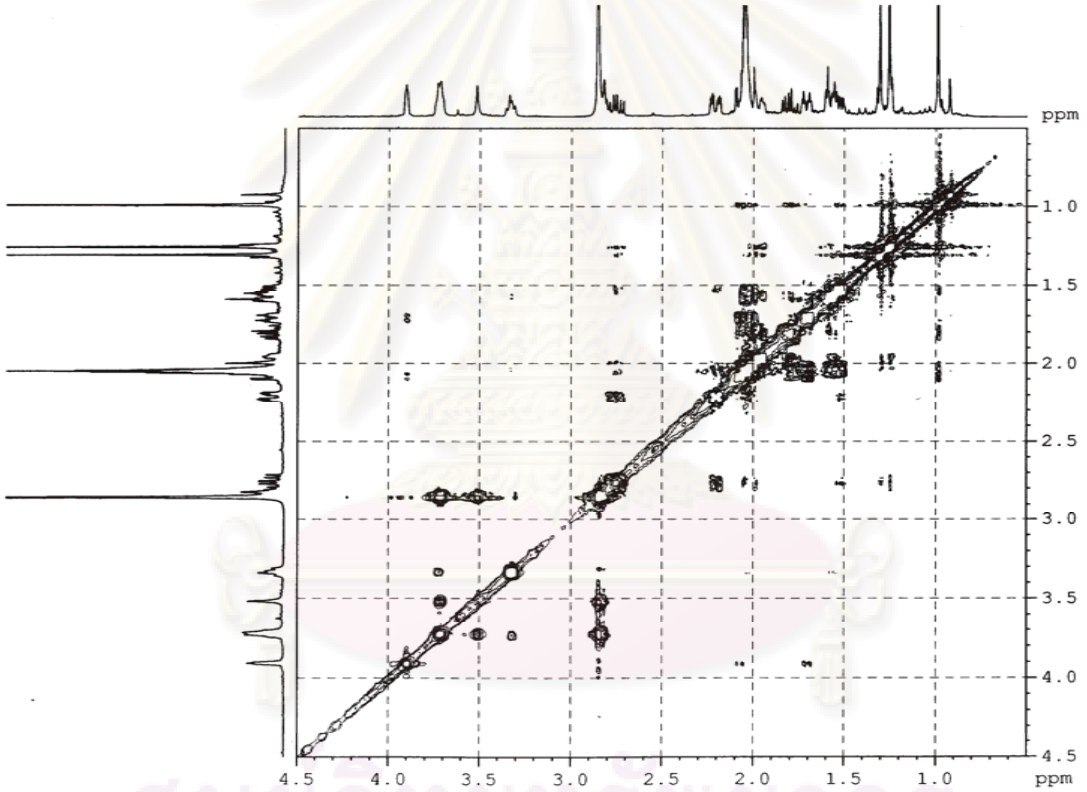

Figure B46 NOESY spectrum of compound **7** in acetone-d_6 (Bruker DRX 400 spectrometer at 400 MHz)

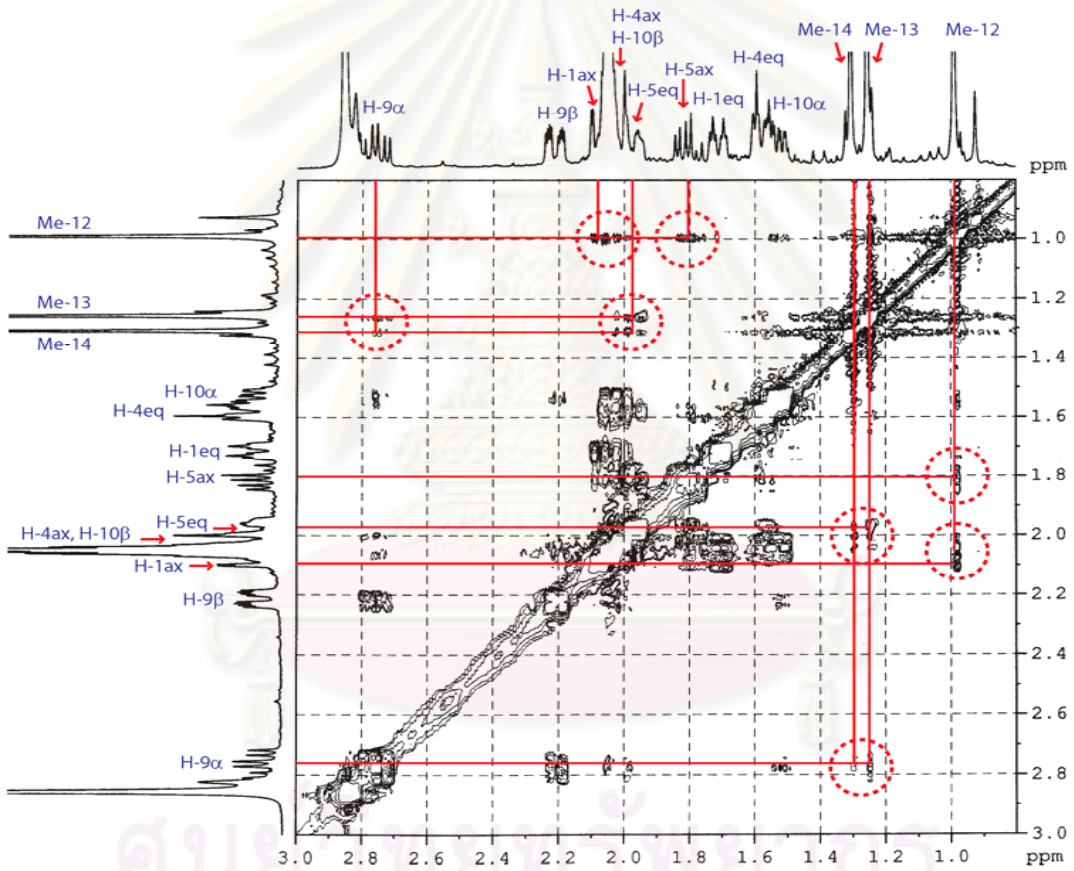

Figure B47 NOESY spectrum of compound **7** in acetone-d_6 (Bruker DRX 400 spectrometer at 400 MHz)

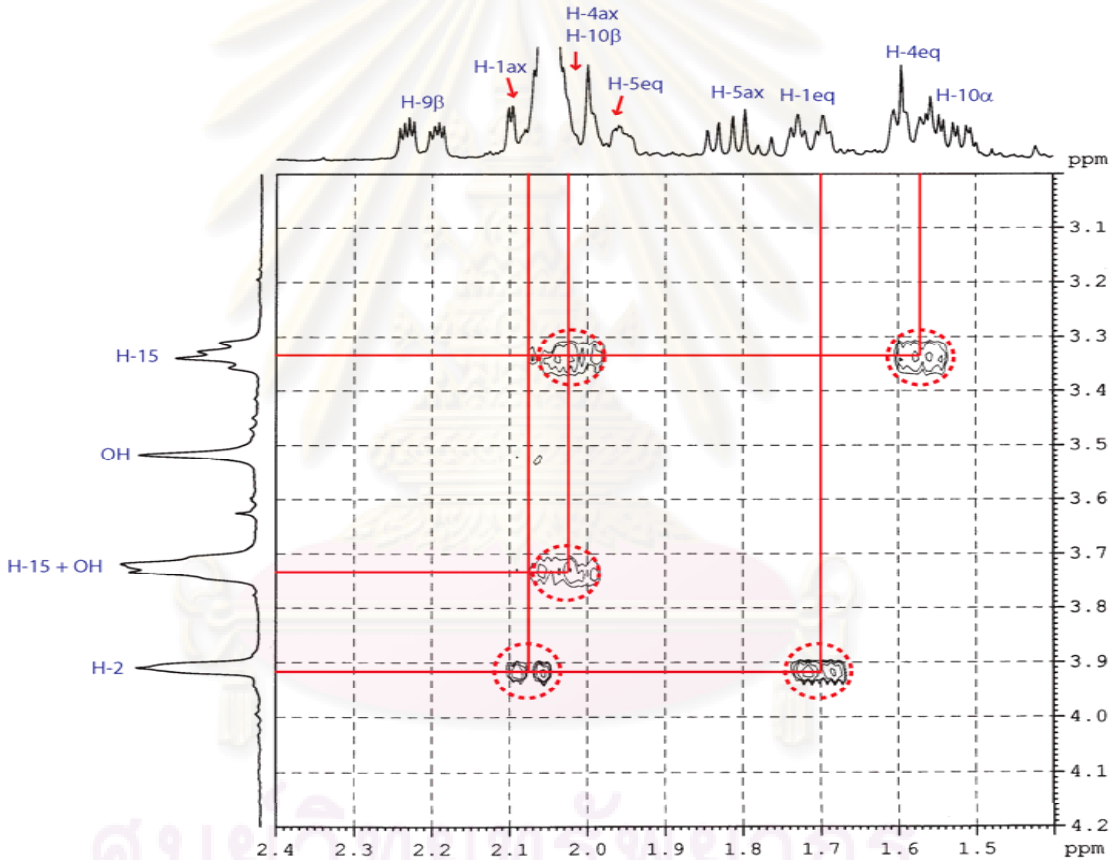

Figure B48 ^{1}H NMR spectrum of compound **8** in $CDCl_3$ (Bruker AV500D spectrometer at 500 MHz)

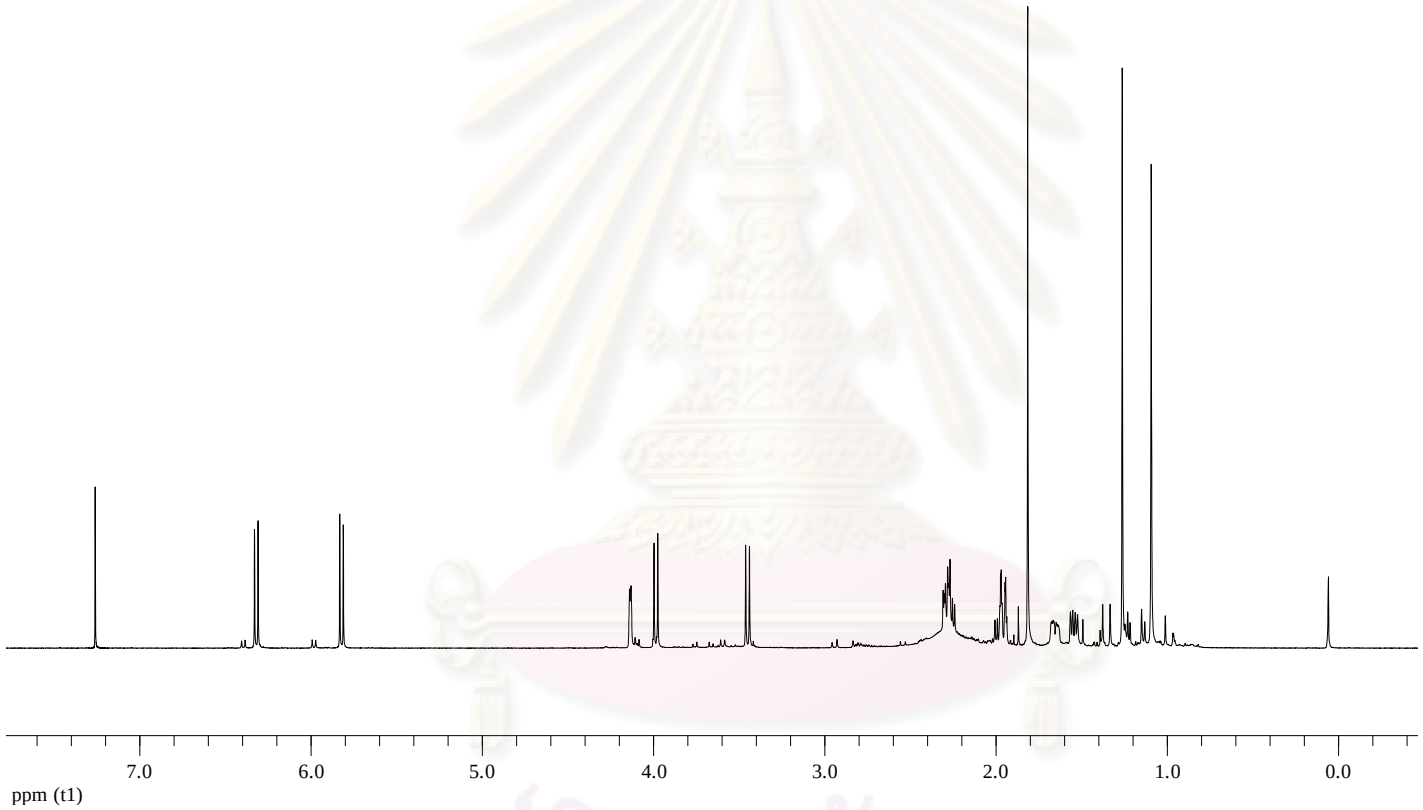

Figure B49 ^{13}C NMR spectrum of compound **8** in $CDCl_3$ (Bruker AV500D spectrometer at 500 MHz)

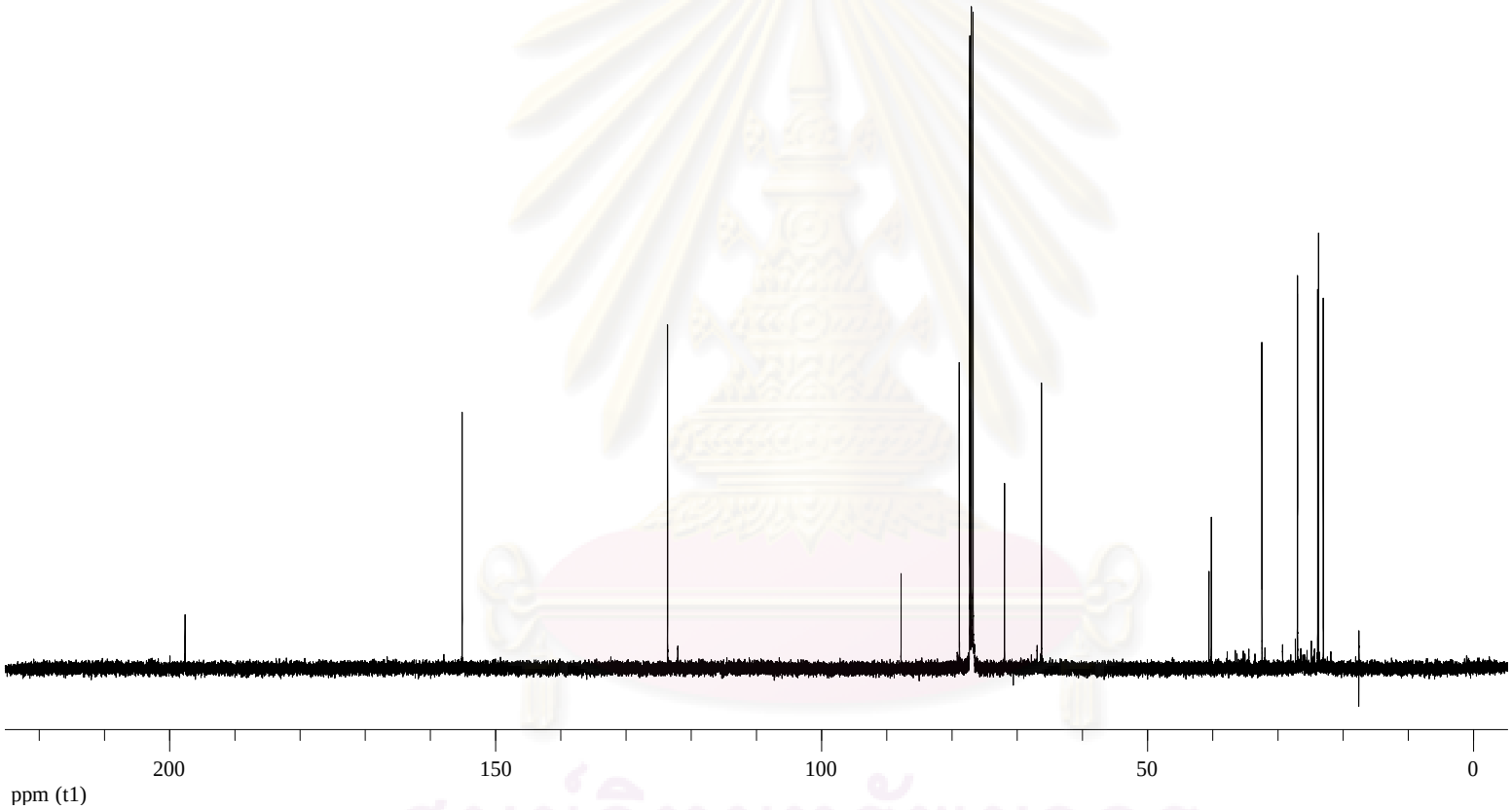

Figure B50 DEPT spectrum of compound **8** in $CDCl_3$ (Bruker AV500D spectrometer at 500 MHz)

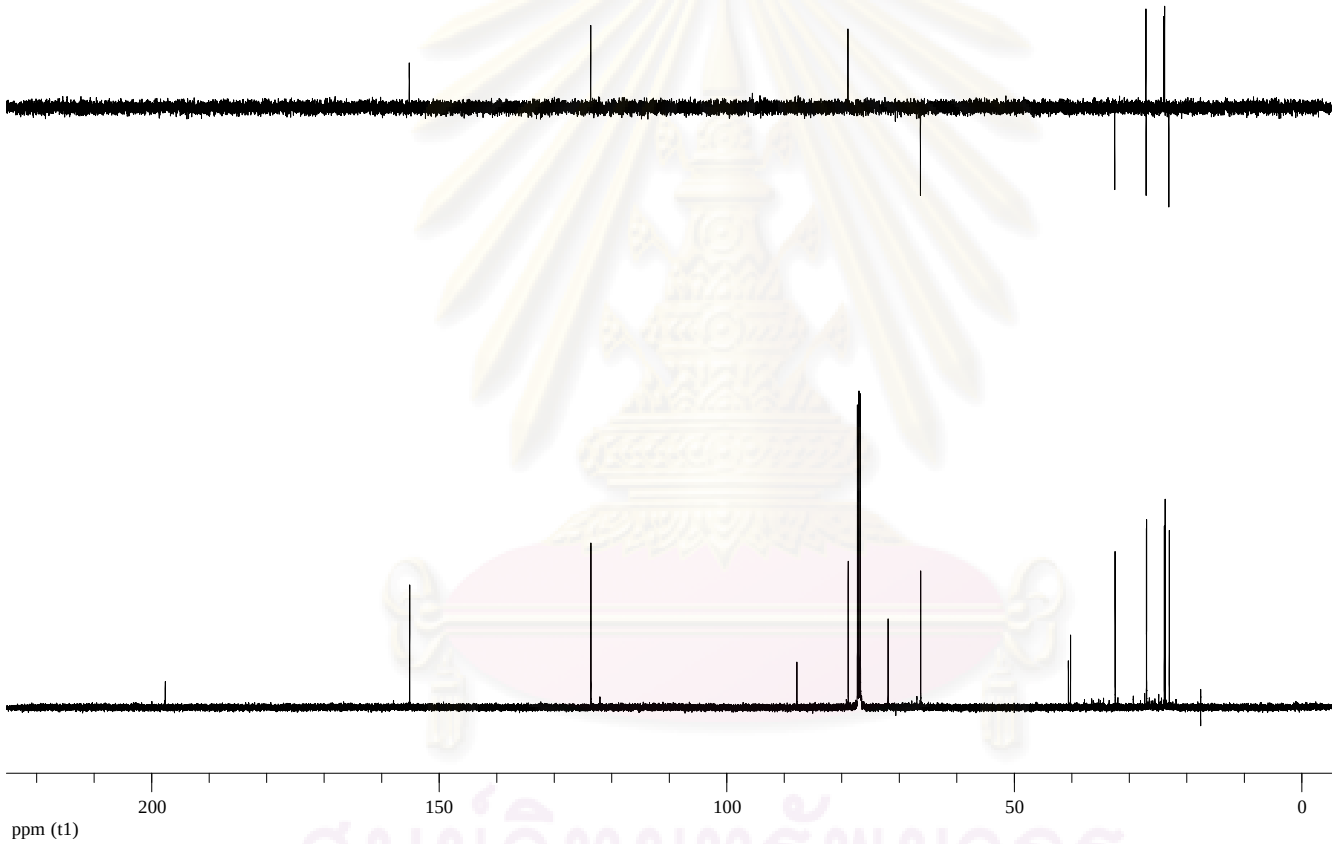

Figure B51 COSY spectrum of compound **8** in $CDCl_3$ (Bruker AV500D spectrometer at 500 MHz)

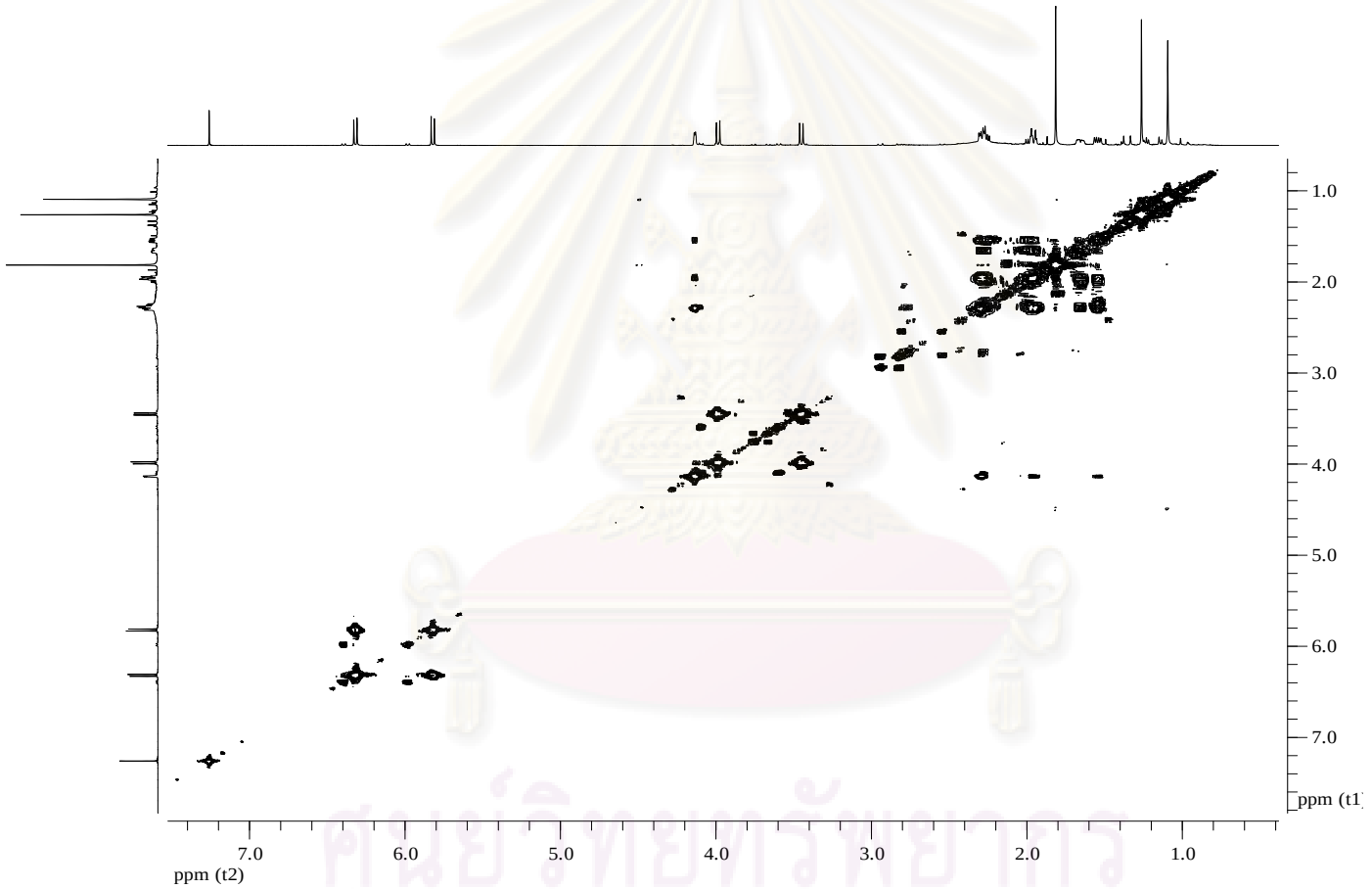

Figure B52 HMQC spectrum of compound **8** in $CDCl_3$ (Bruker AV500D spectrometer at 500 MHz)

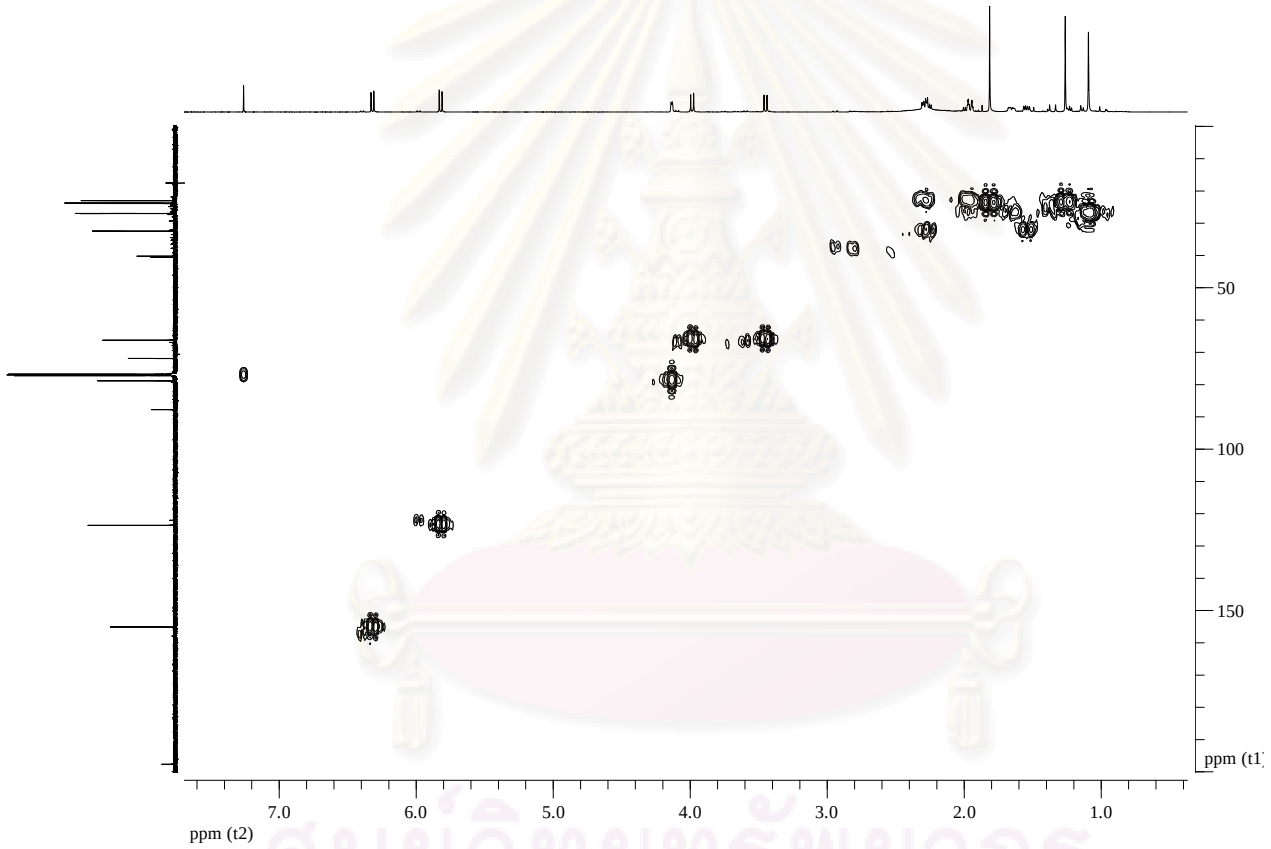

Figure B53 HMBC spectrum of compound **8** in $CDCl_3$ (Bruker AV500D spectrometer at 500 MHz)

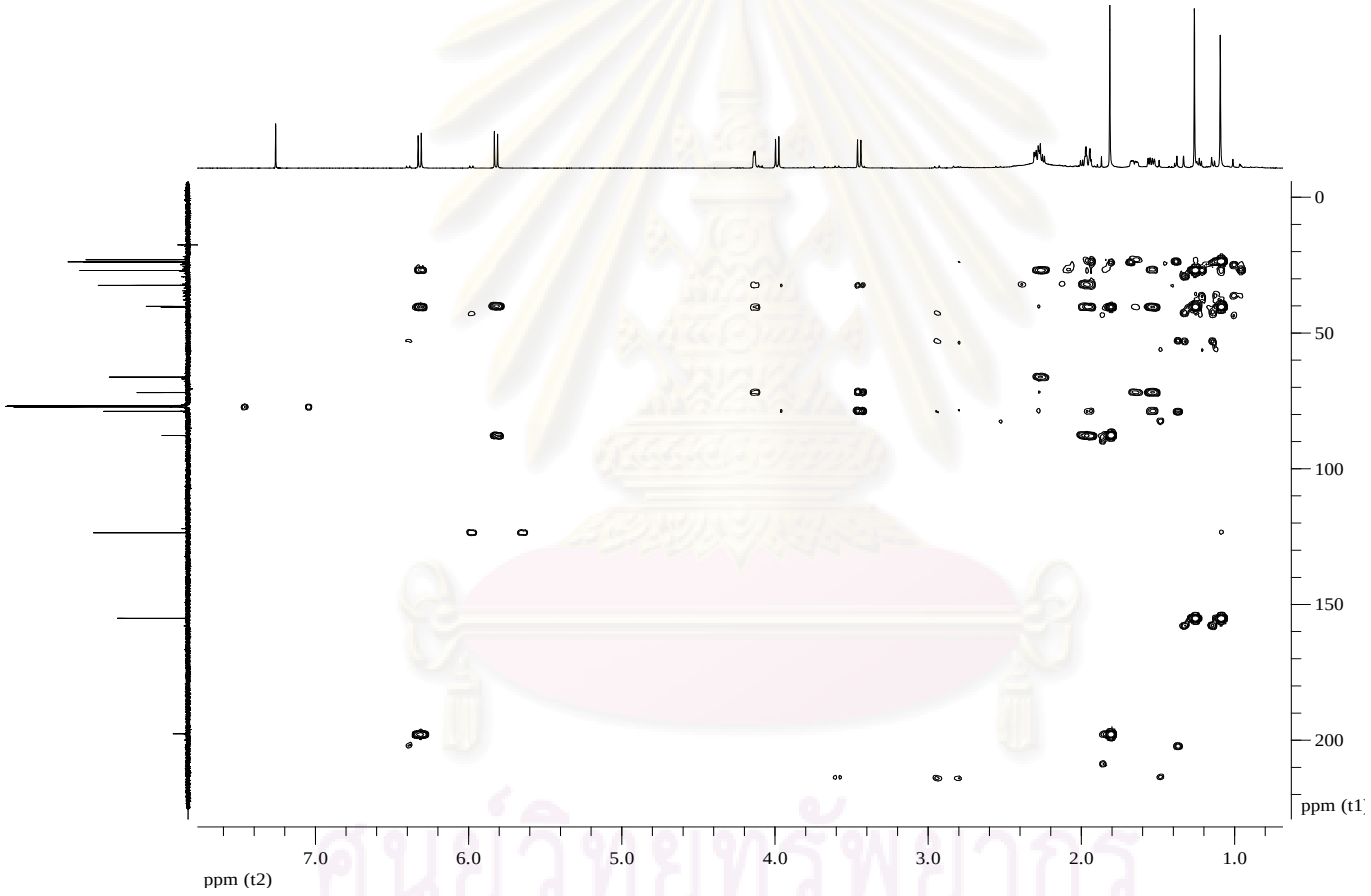

Figure B54 NOESY spectrum of compound **8** in $CDCl_3$ (Bruker AV500D spectrometer at 500 MHz)

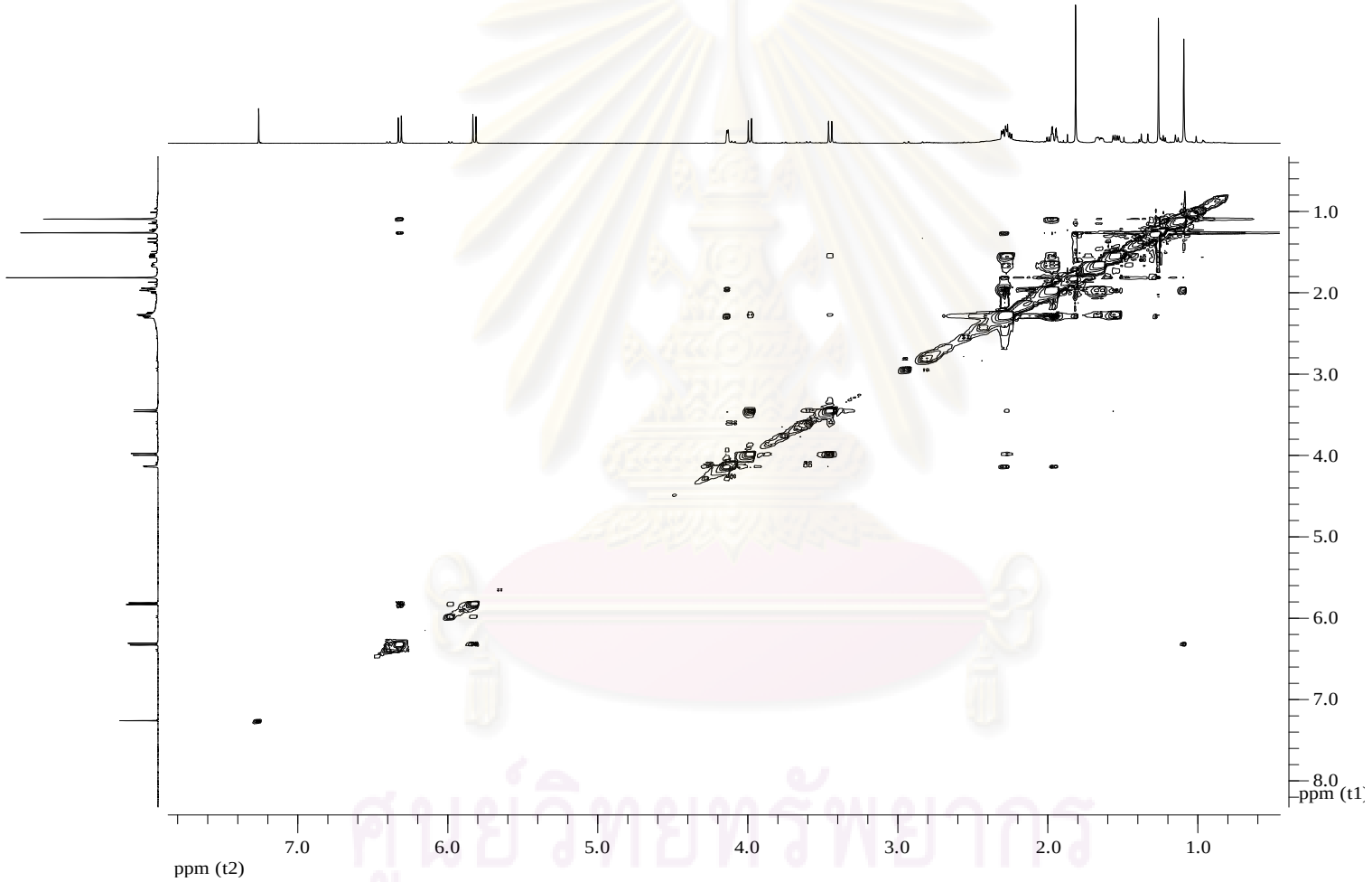

Figure B55 ^{1}H NMR spectrum of compound **8** in acetone-d_6 (Bruker DRX 400 spectrometer at 400 MHz)

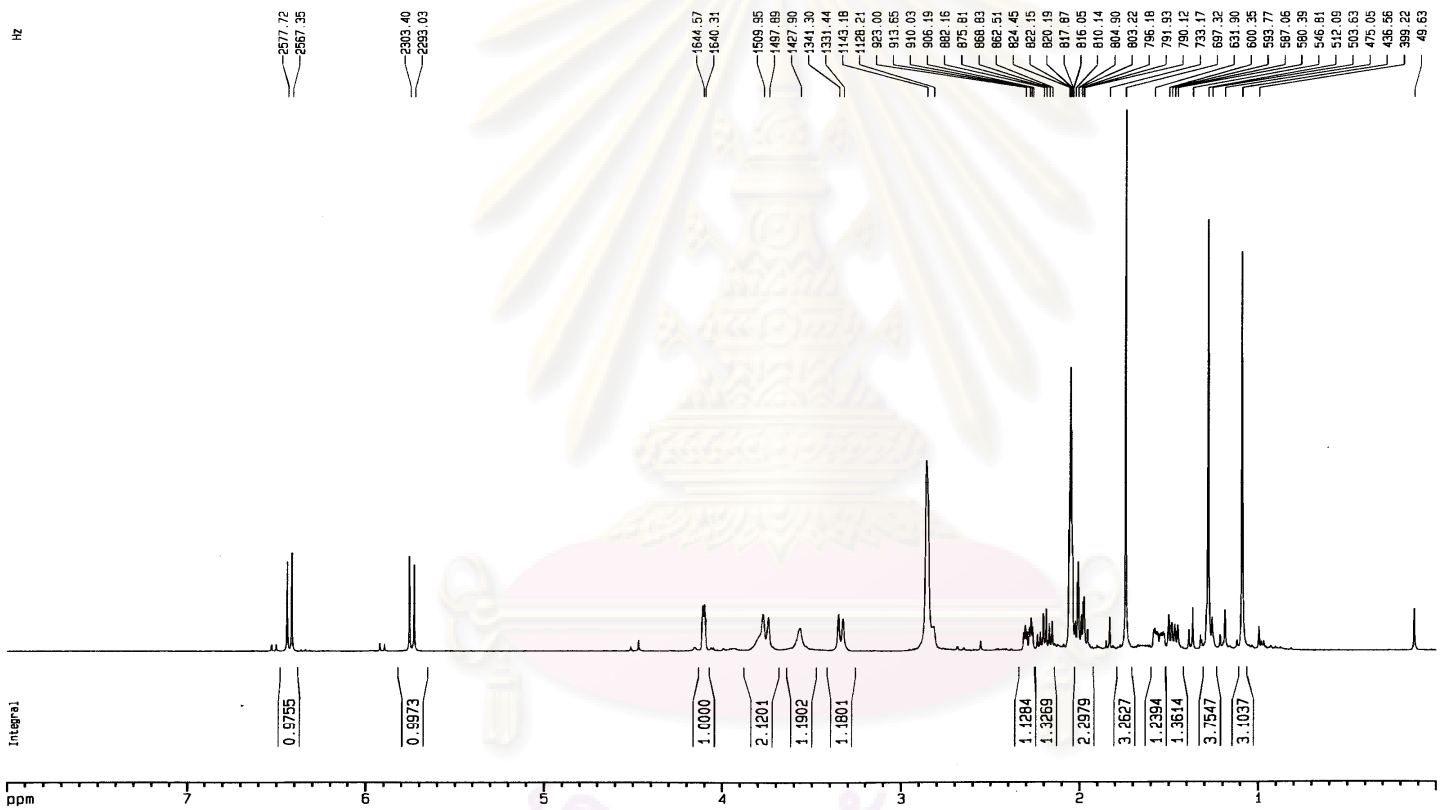

Figure B56 ^{1}H NMR spectrum of compound **8** in acetone-d_6 (Bruker DRX 400 spectrometer at 400 MHz)

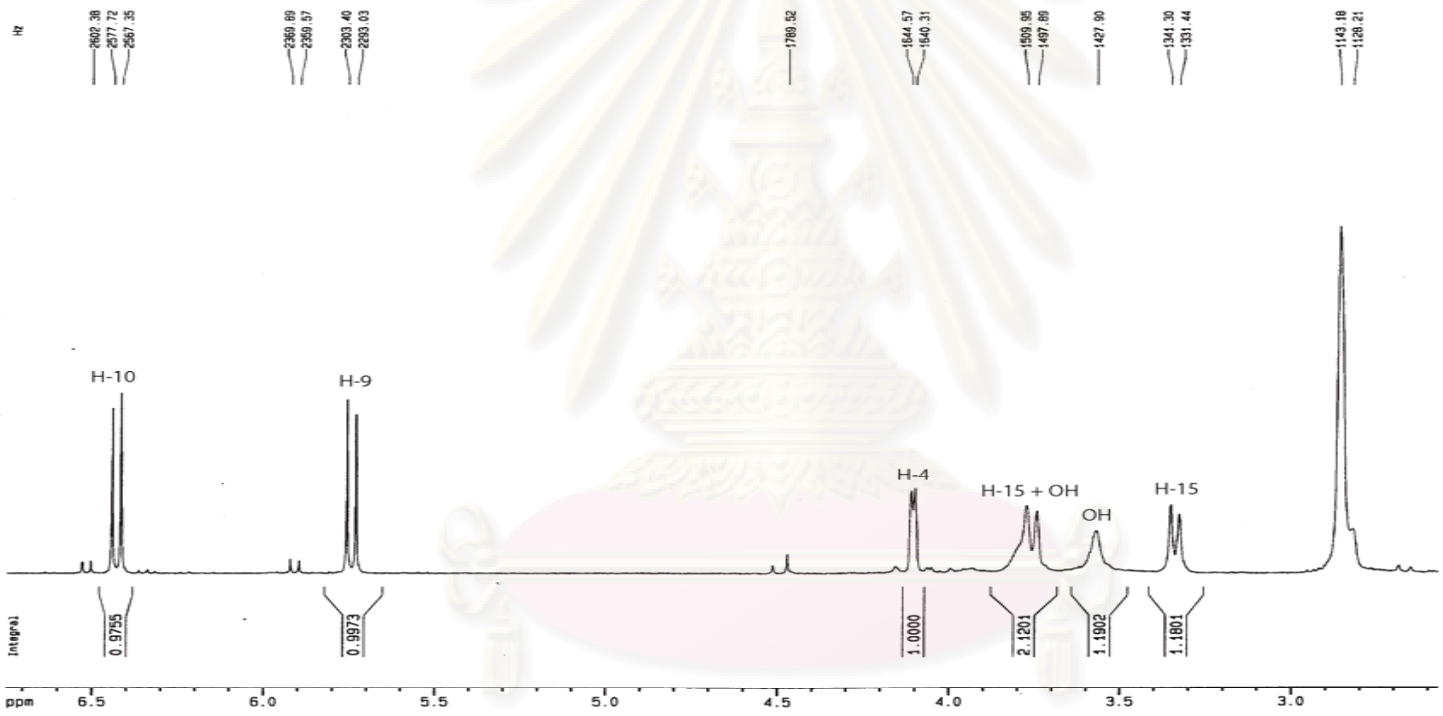

Figure B57 ^{1}H NMR spectrum of compound **8** in acetone-d_6 (Bruker DRX 400 spectrometer at 400 MHz)

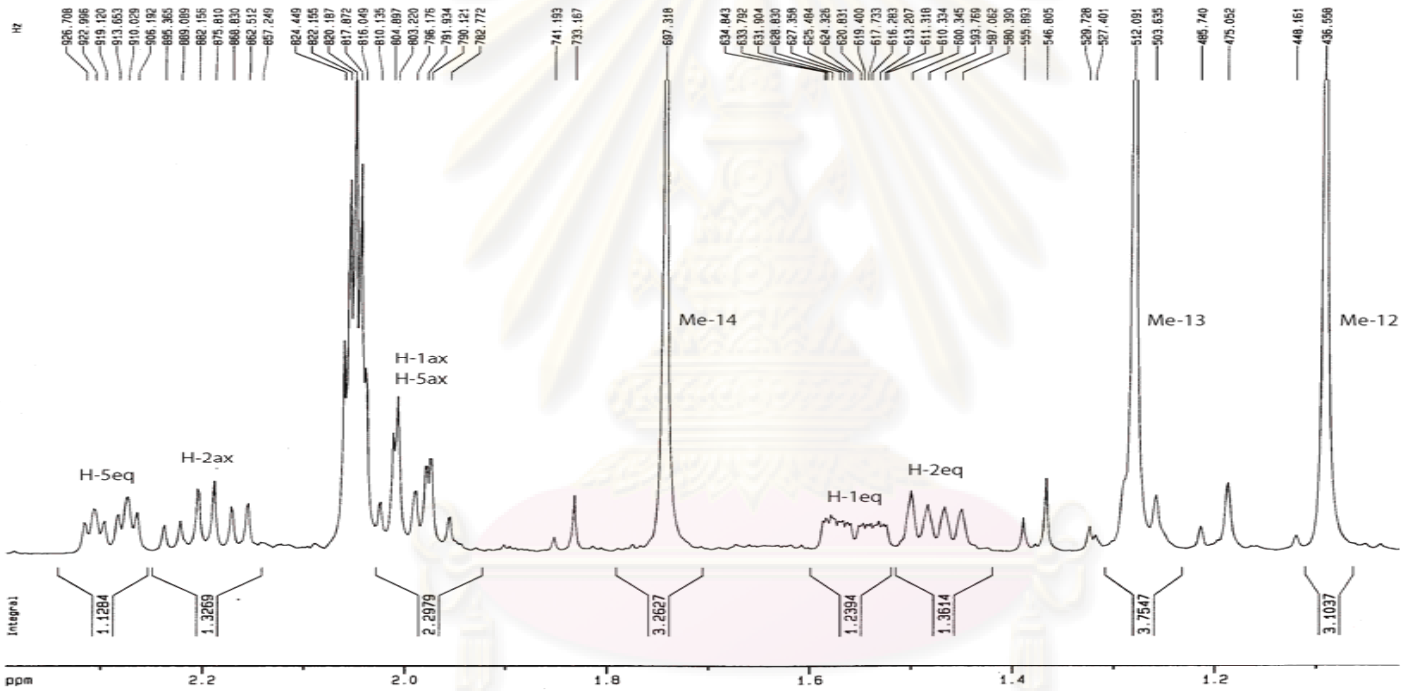

Figure B58 NOESY spectrum of compound **8** in acetone-d_6 (Bruker DRX 400 spectrometer at 400 MHz)

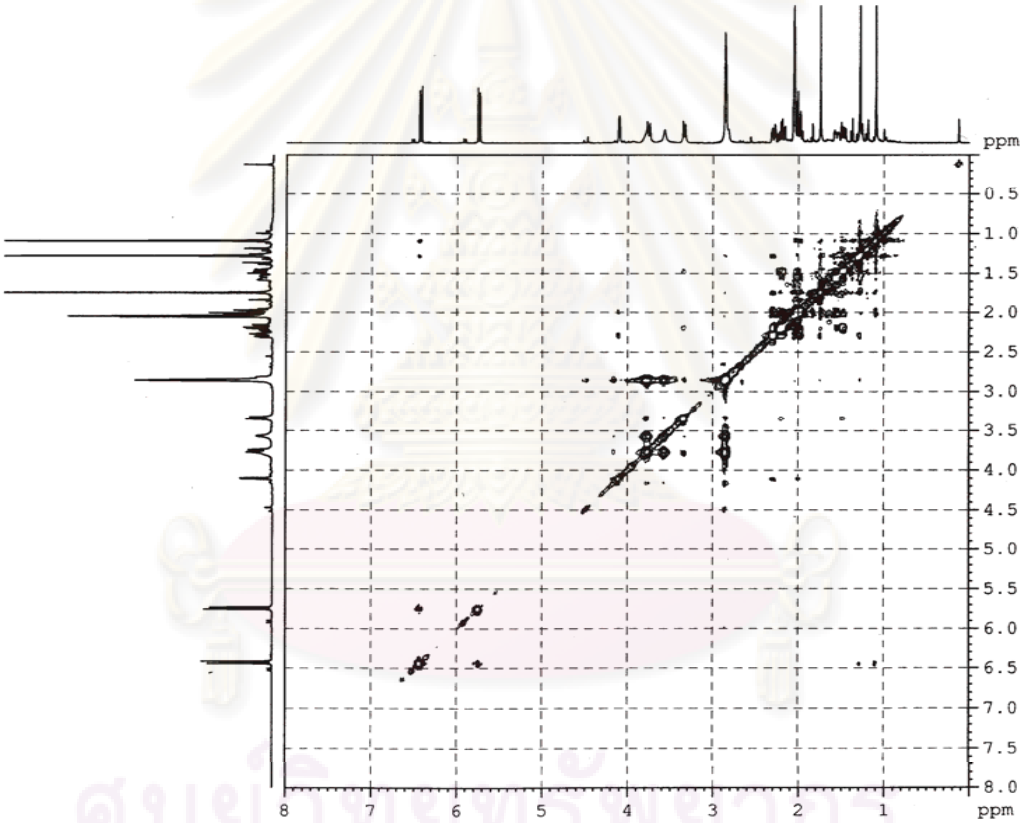

Figure B59 NOESY spectrum of compound **8** in acetone-d_6 (Bruker DRX 400 spectrometer at 400 MHz)

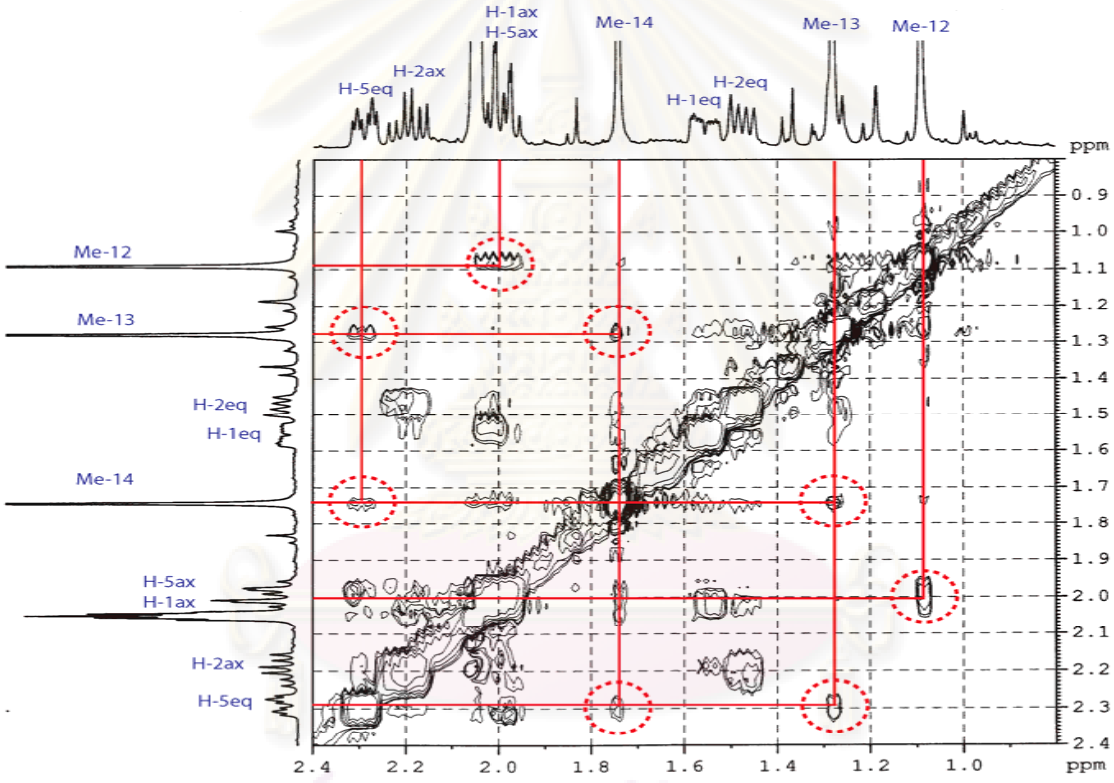

Figure B60 NOESY spectrum of compound **8** in acetone-d_6 (Bruker DRX 400 spectrometer at 400 MHz)

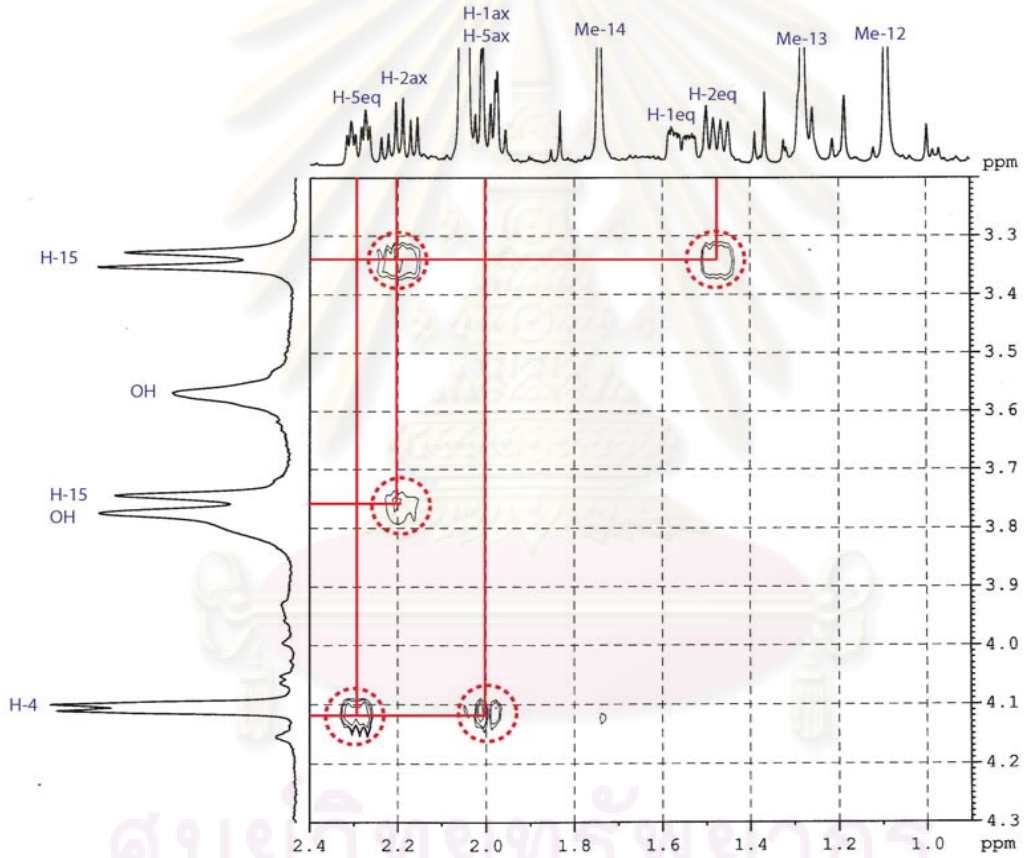

Figure B61 ^{1}H NMR spectrum of compound **9** in $CDCl_3$ (Bruker AV500D spectrometer at 500 MHz)

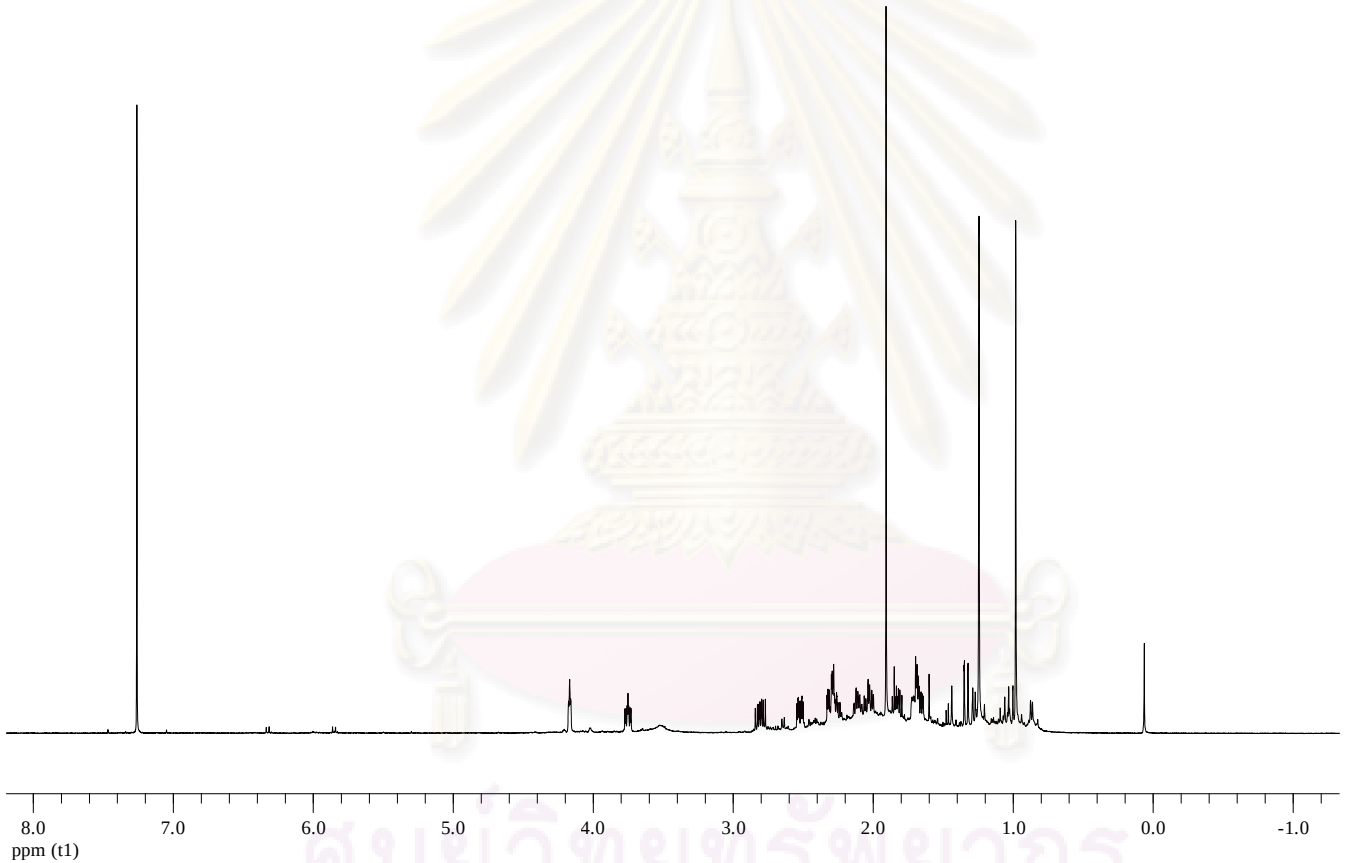

Figure B62 ^{13}C NMR spectrum of compound **9** in $CDCl_3$ (Bruker AV500D spectrometer at 500 MHz)

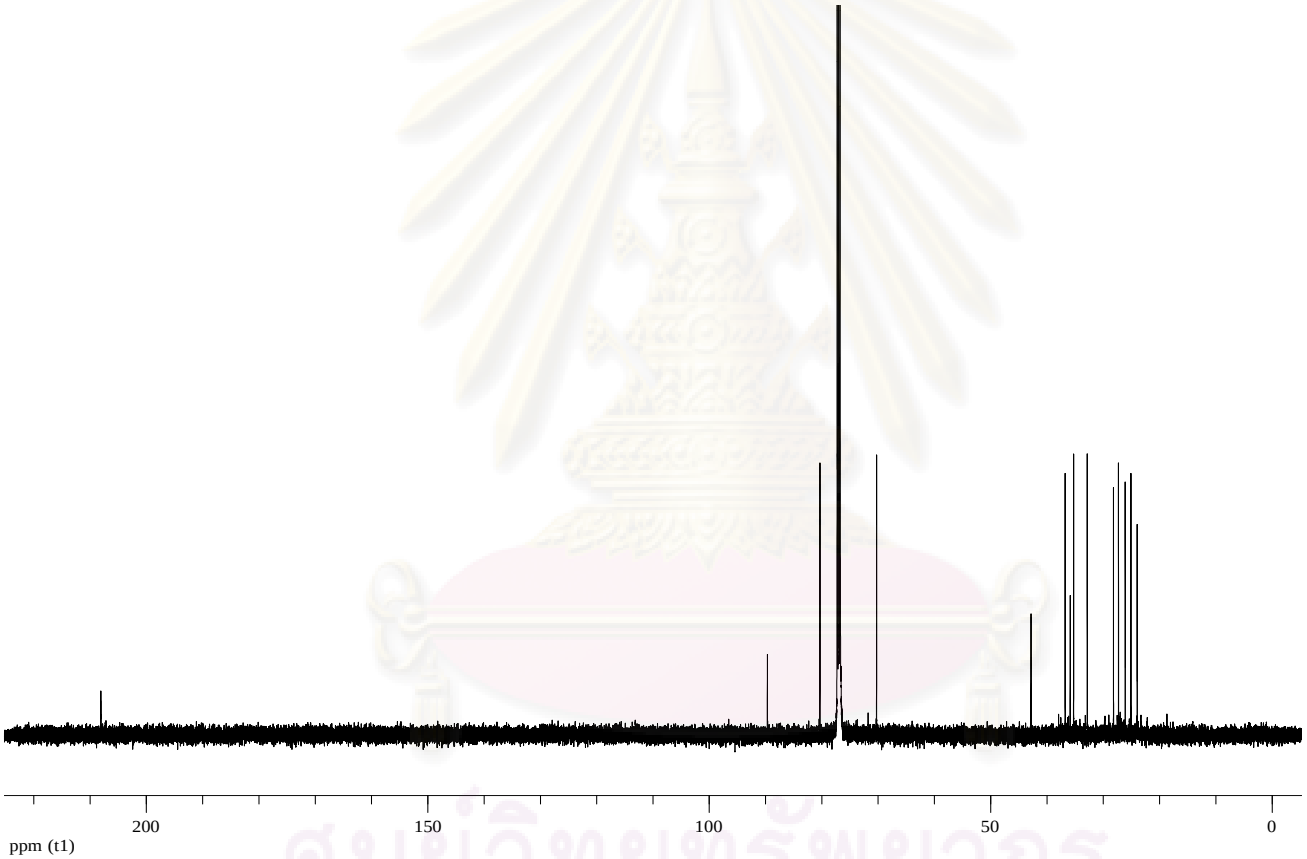

Figure B63 DEPT spectrum of compound **9** in $CDCl_3$ (Bruker AV500D spectrometer at 500 MHz)

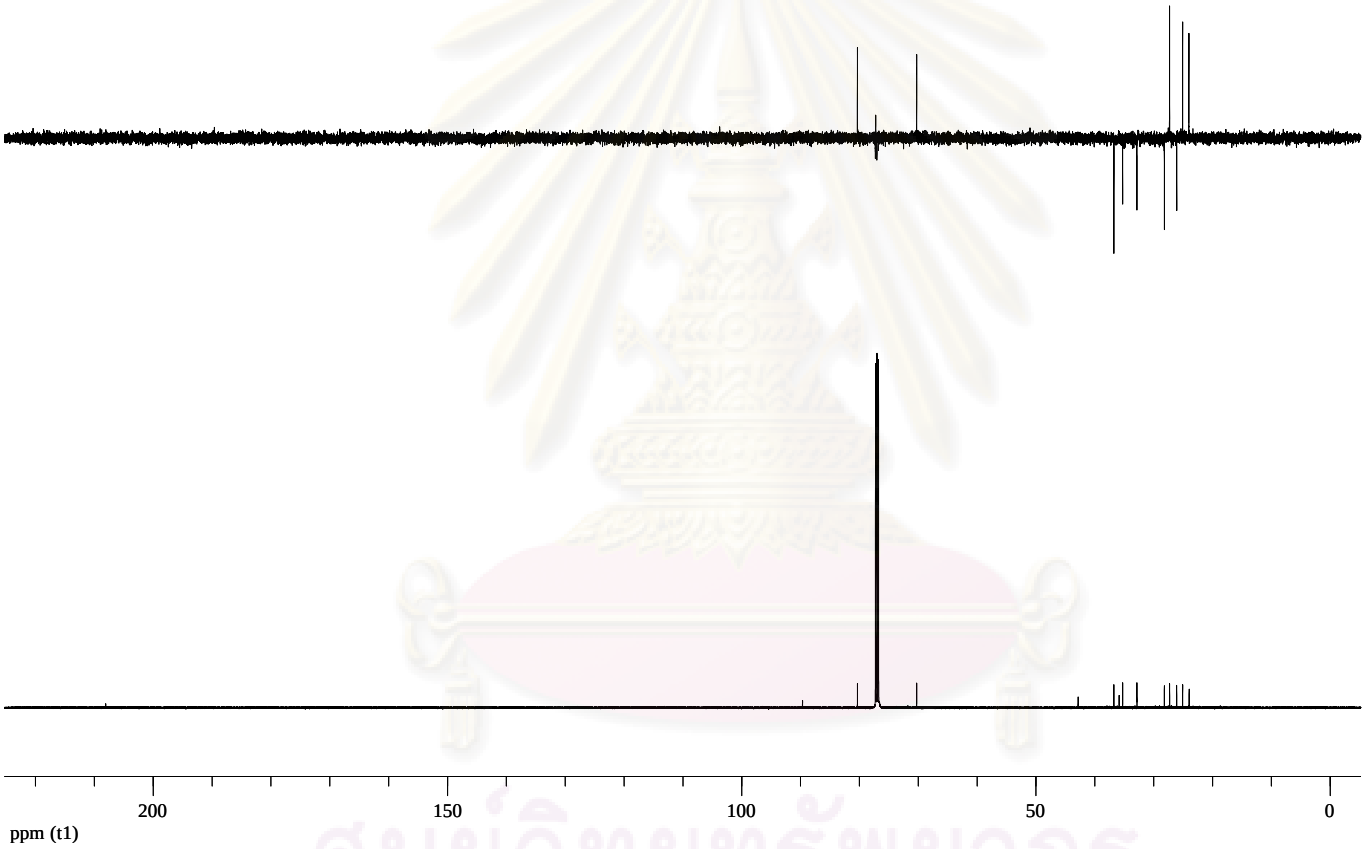

Figure B64 COSY spectrum of compound **9** in $CDCl_3$ (Bruker AV500D spectrometer at 500 MHz)

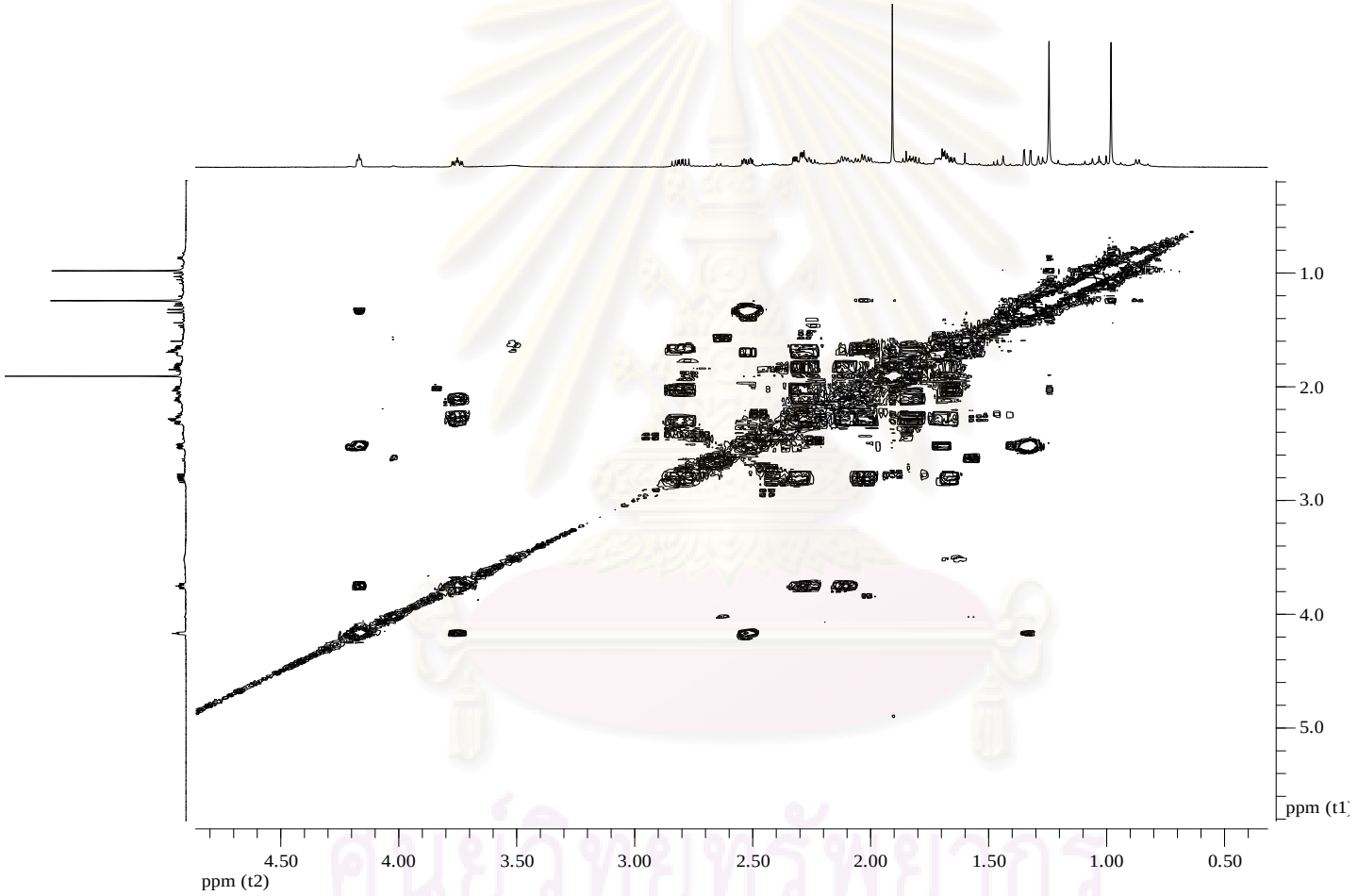

Figure B65 HMQC spectrum of compound **9** in $CDCl_3$ (Bruker AV500D spectrometer at 500 MHz)

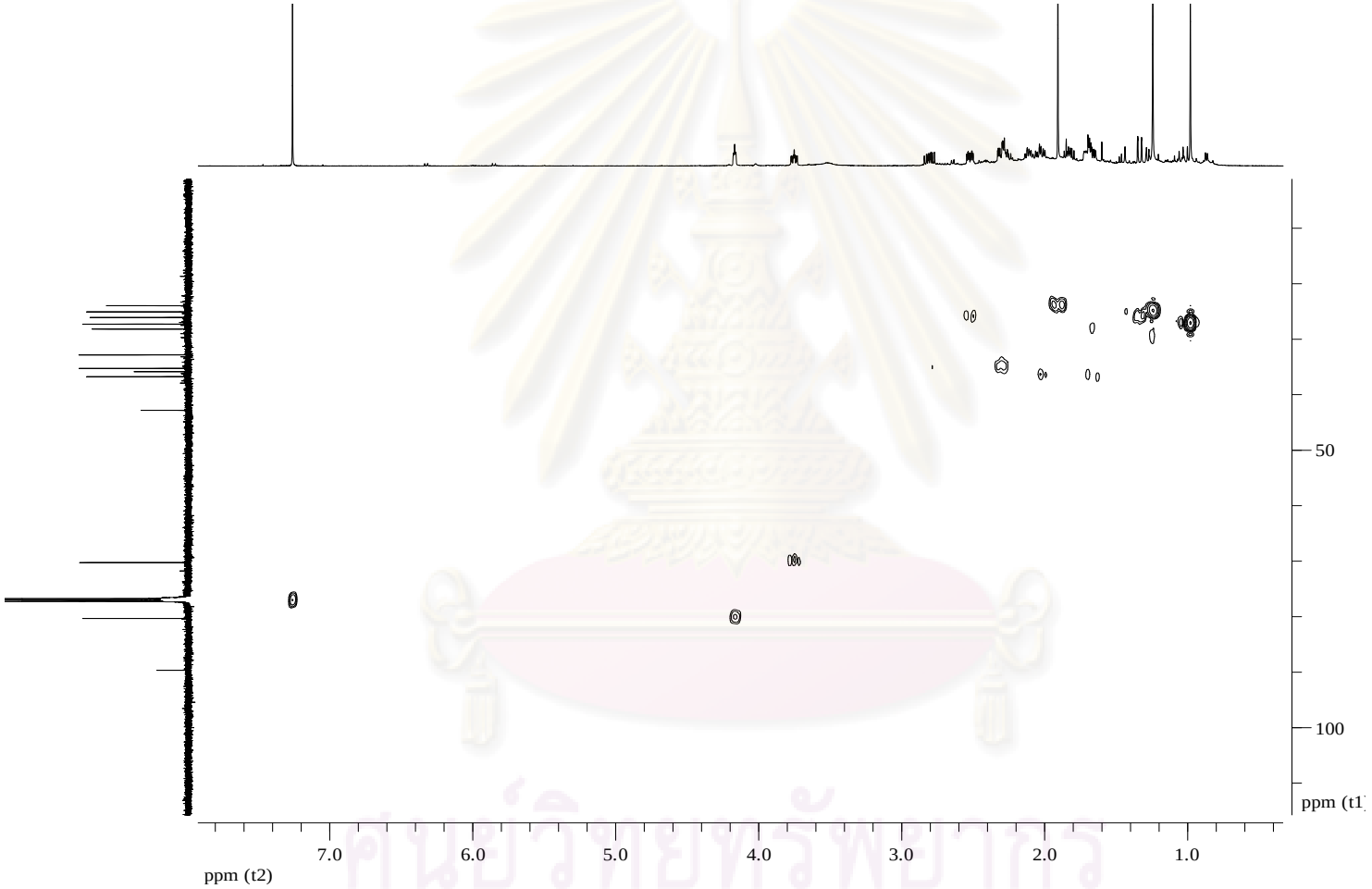

Figure B66 HMBC spectrum of compound **9** in $CDCl_3$ (Bruker AV500D spectrometer at 500 MHz)

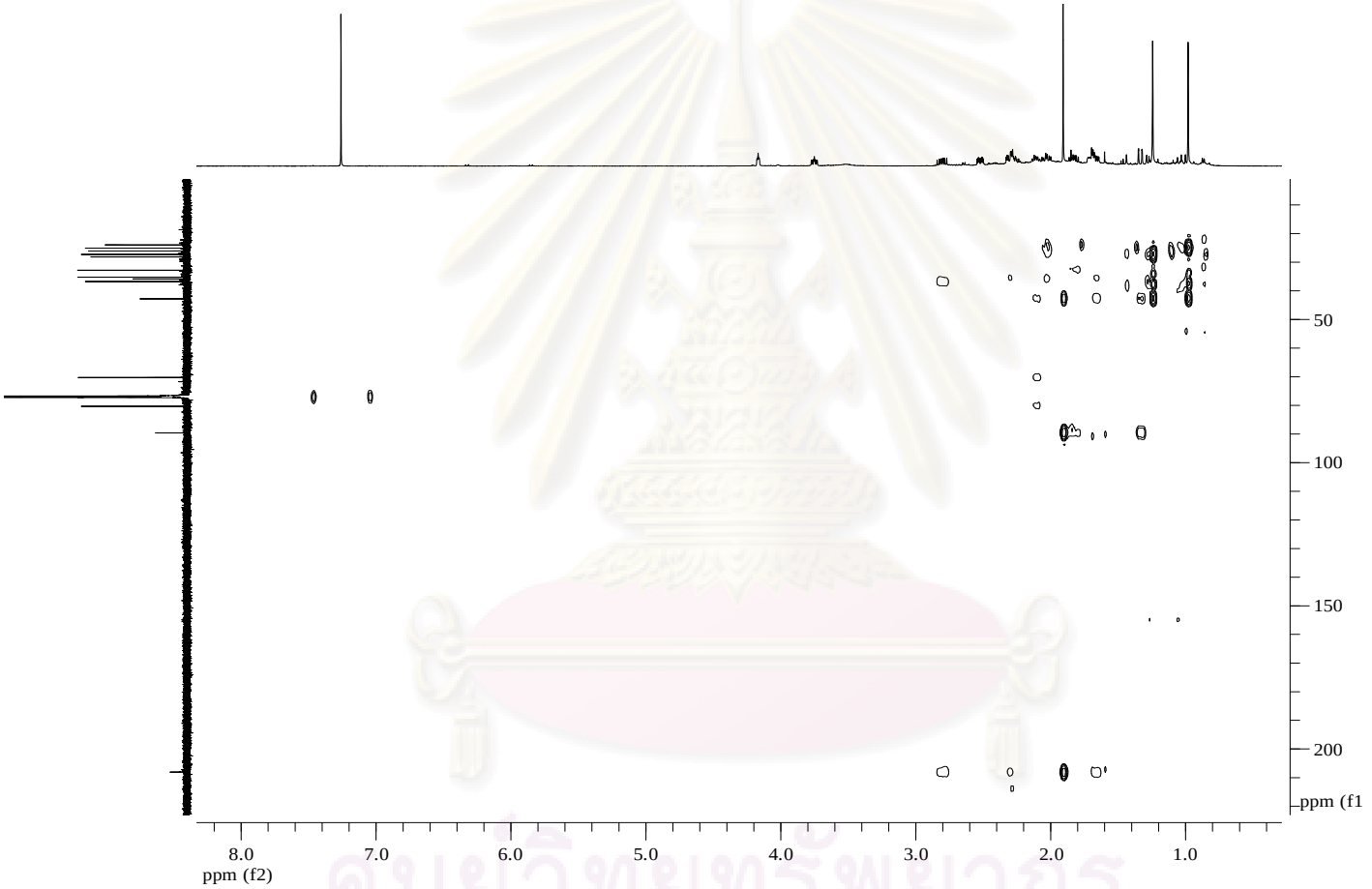

Figure B67 NOESY spectrum of compound **9** in $CDCl_3$ (Bruker AV500D spectrometer at 500 MHz)

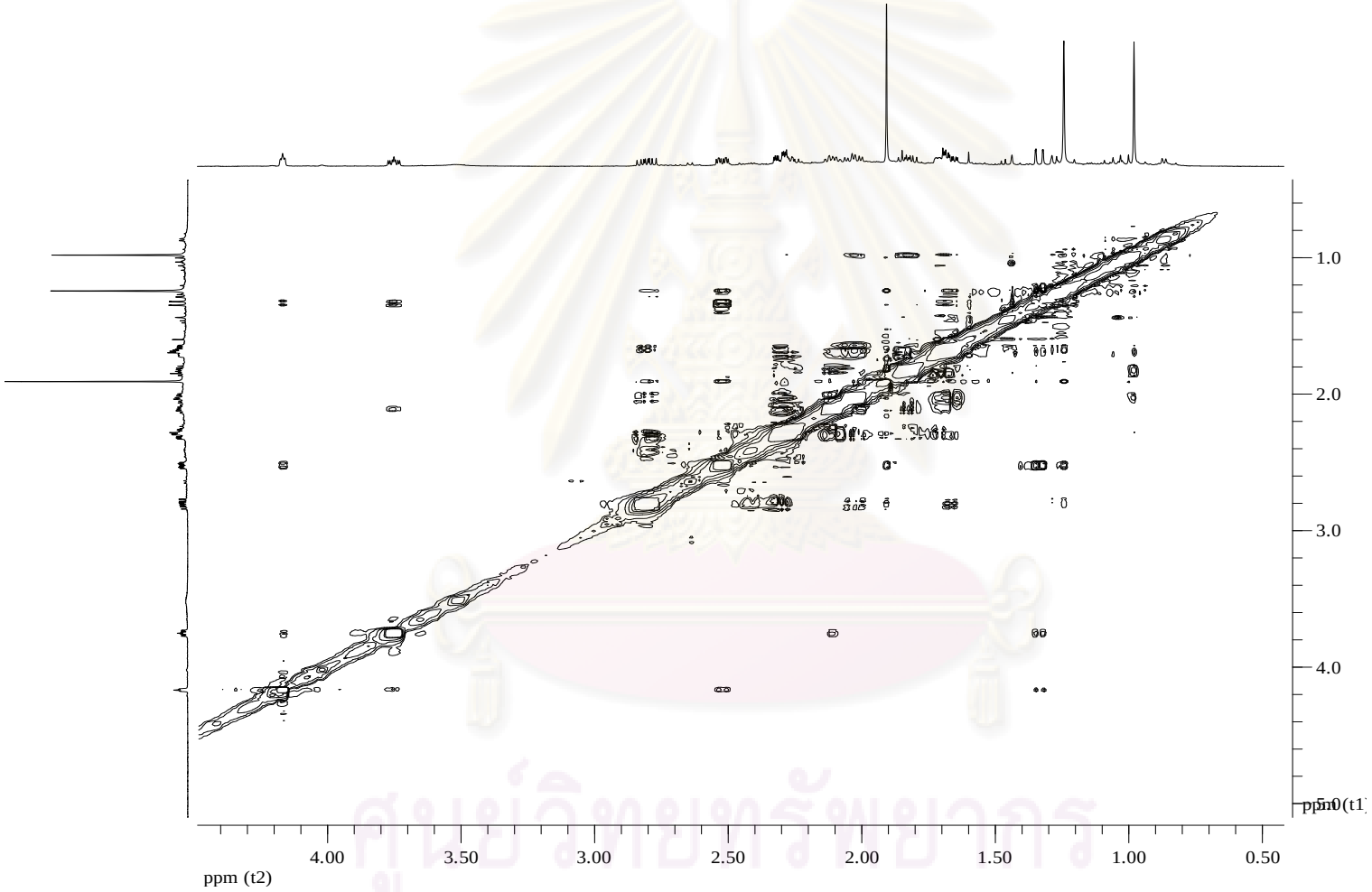

Figure B68 NOESY spectrum of compound **9** in $CDCl_3$ (Bruker AV500D spectrometer at 500 MHz)

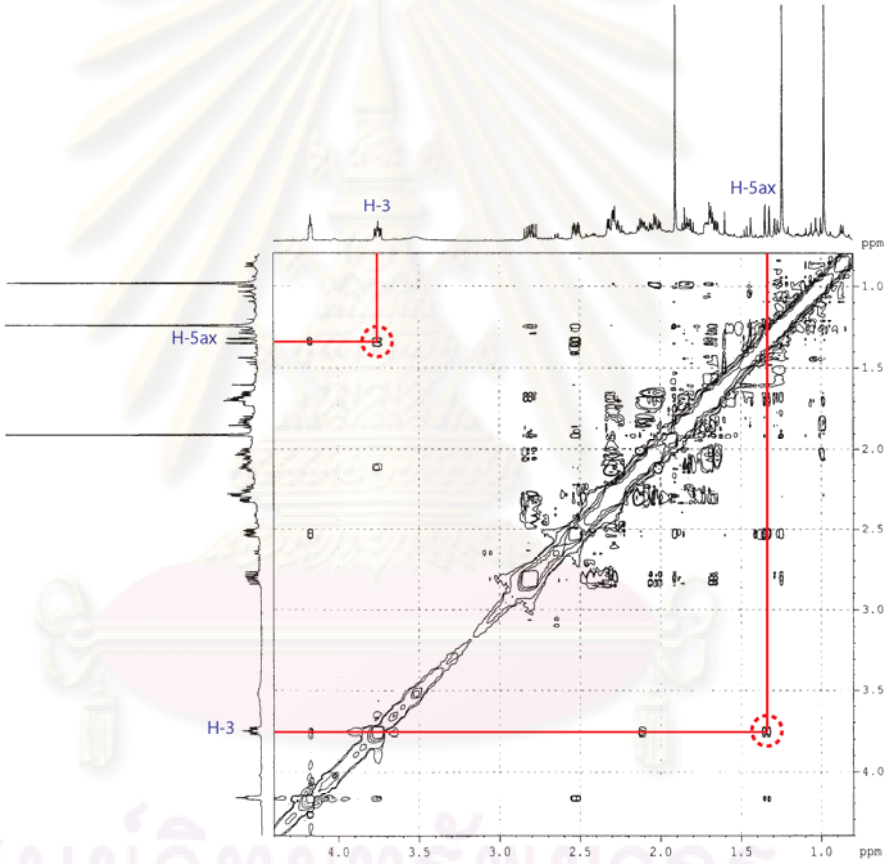

Figure B69 NOESY spectrum of compound **9** in $CDCl_3$ (Bruker AV500D spectrometer at 500 MHz)

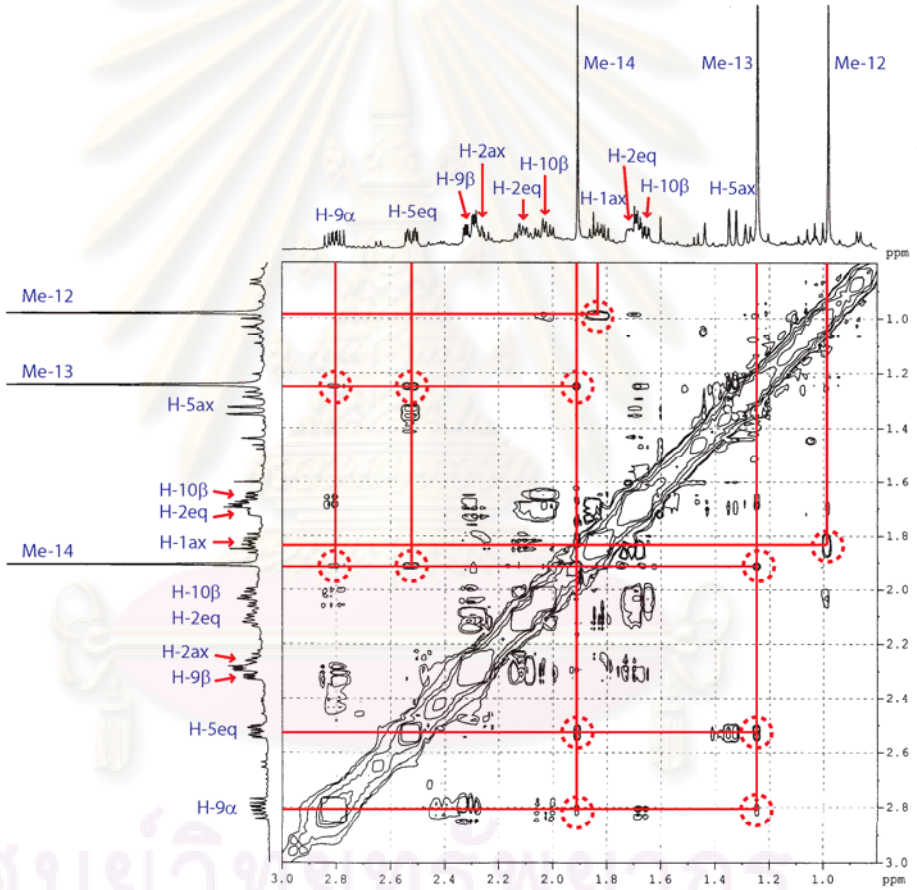

APPENDIX C

Figure C1 ESIMS of **1**

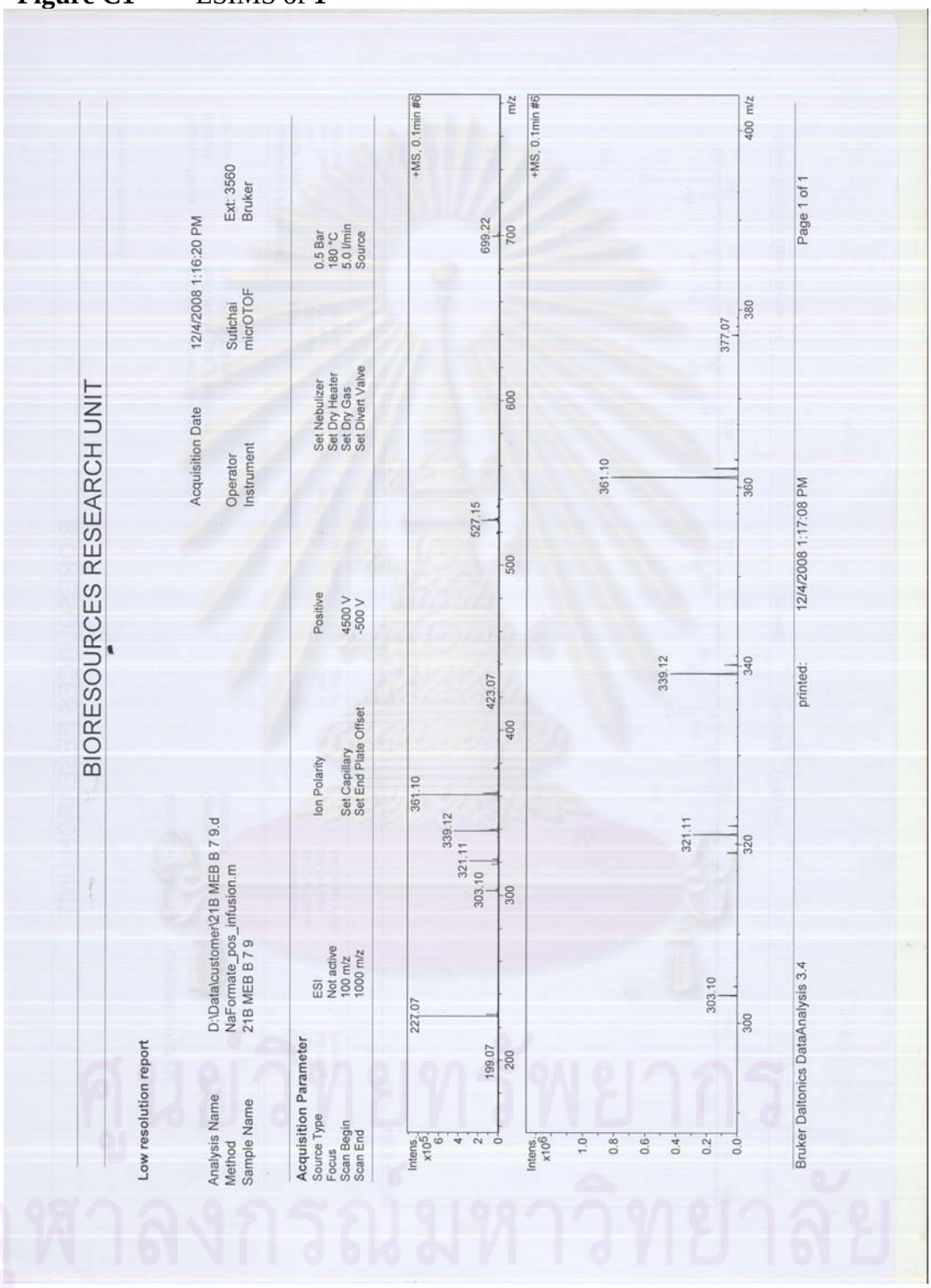

Figure C2 ESIMS of **2**

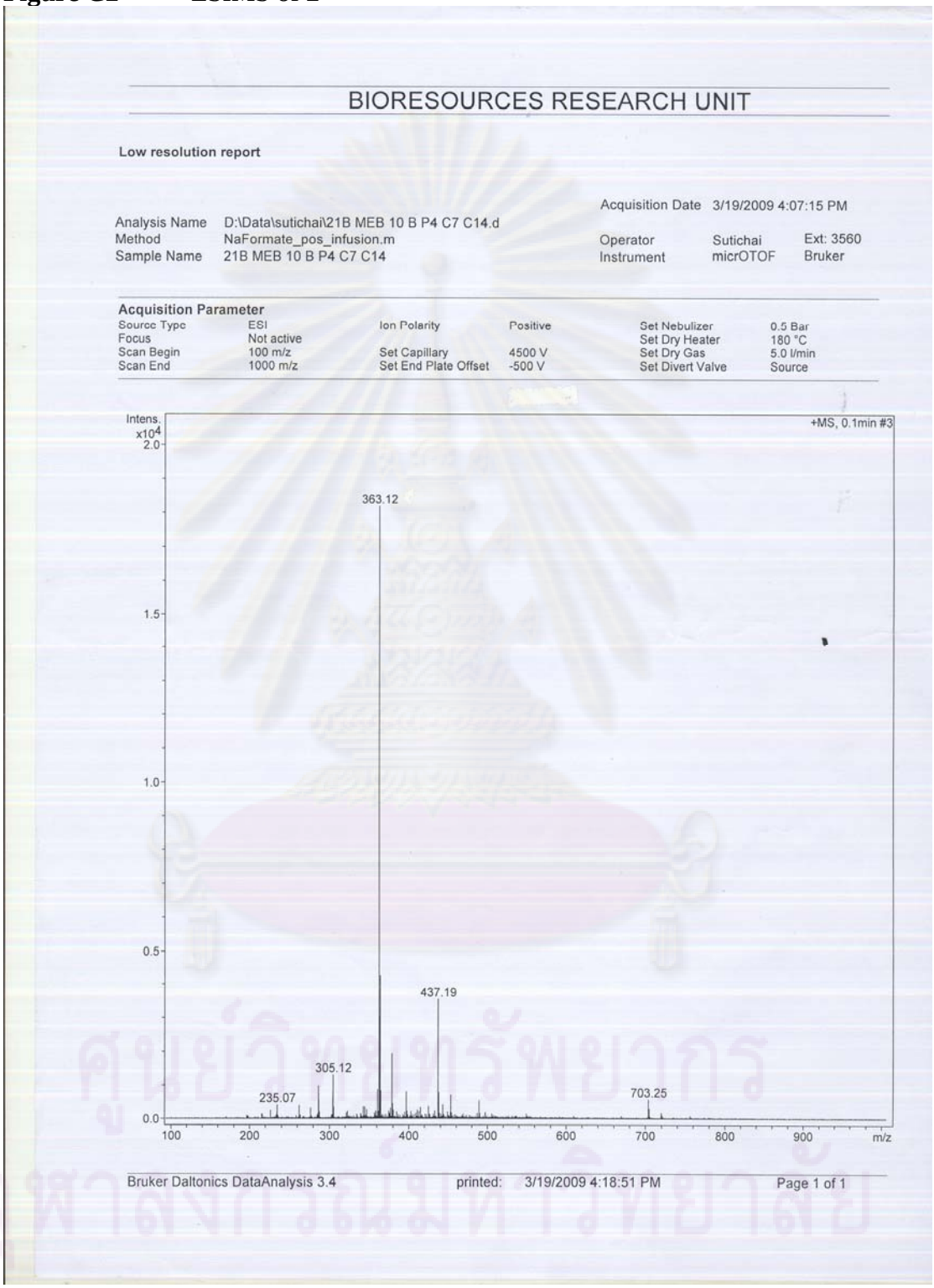

Figure C3 ESIMS of **3**

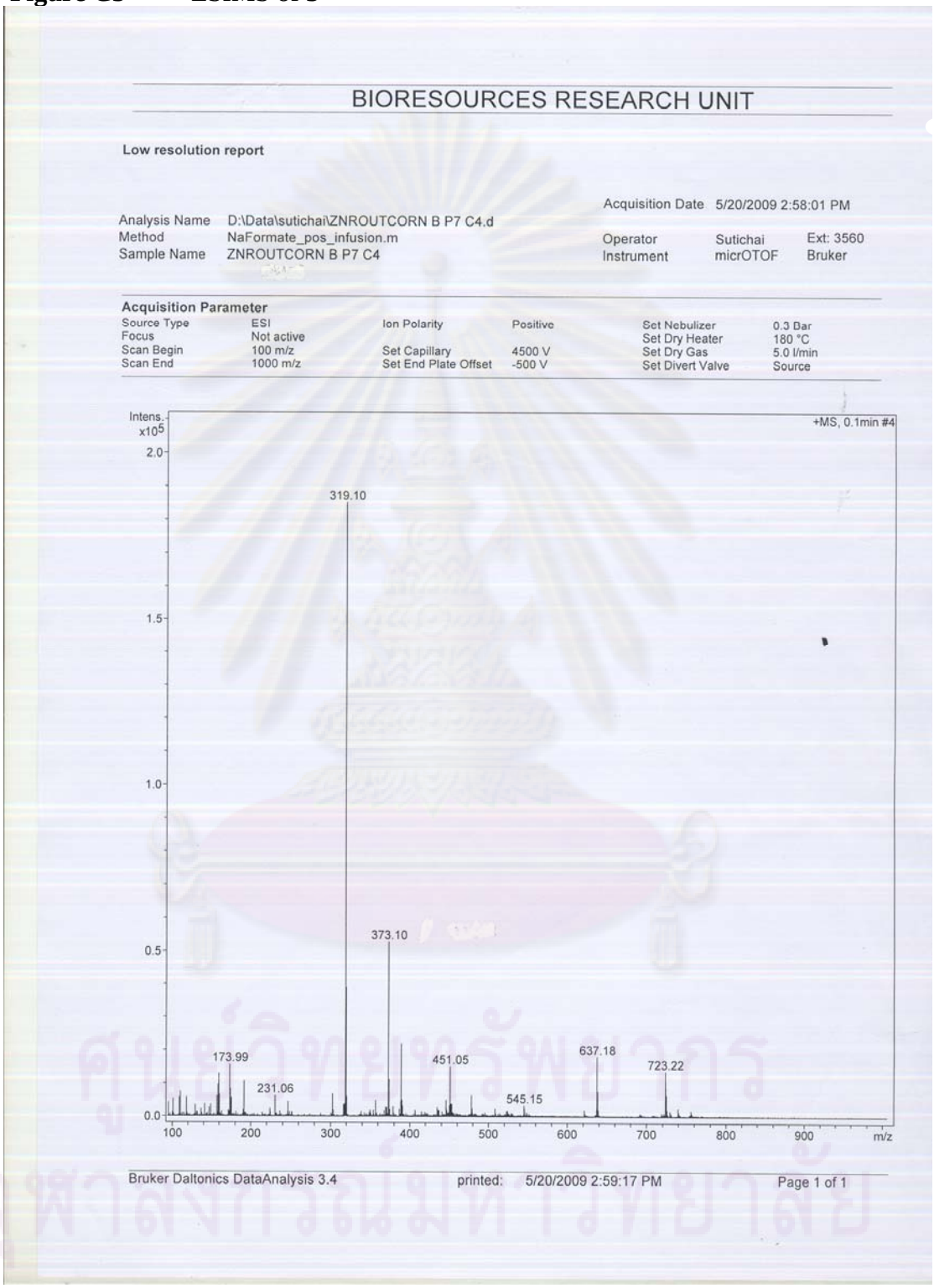

Figure C4 HRESIMS of **4**

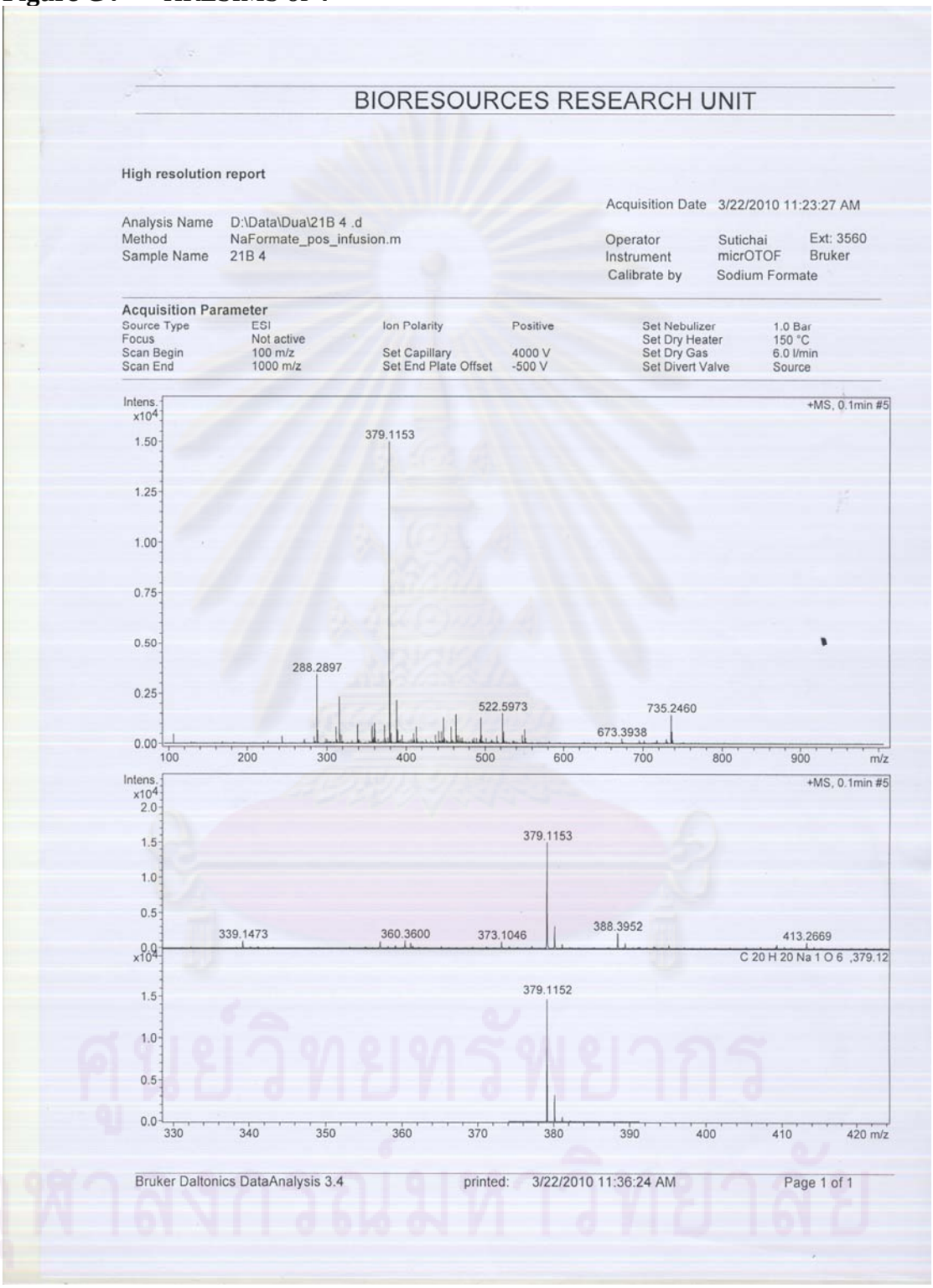

Figure C5 ESIMS of **5**

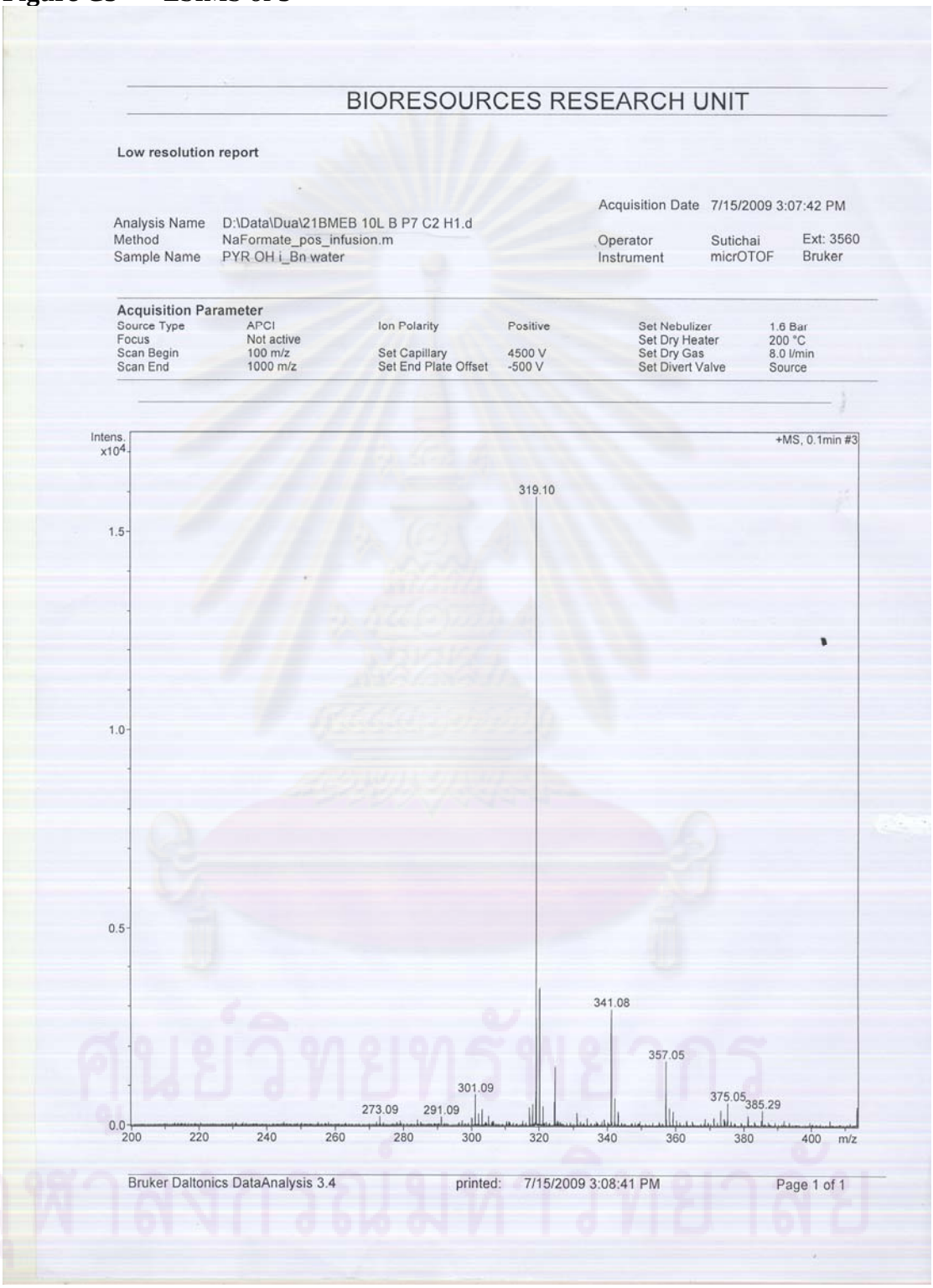

Figure C6 HRESIMS of **6**

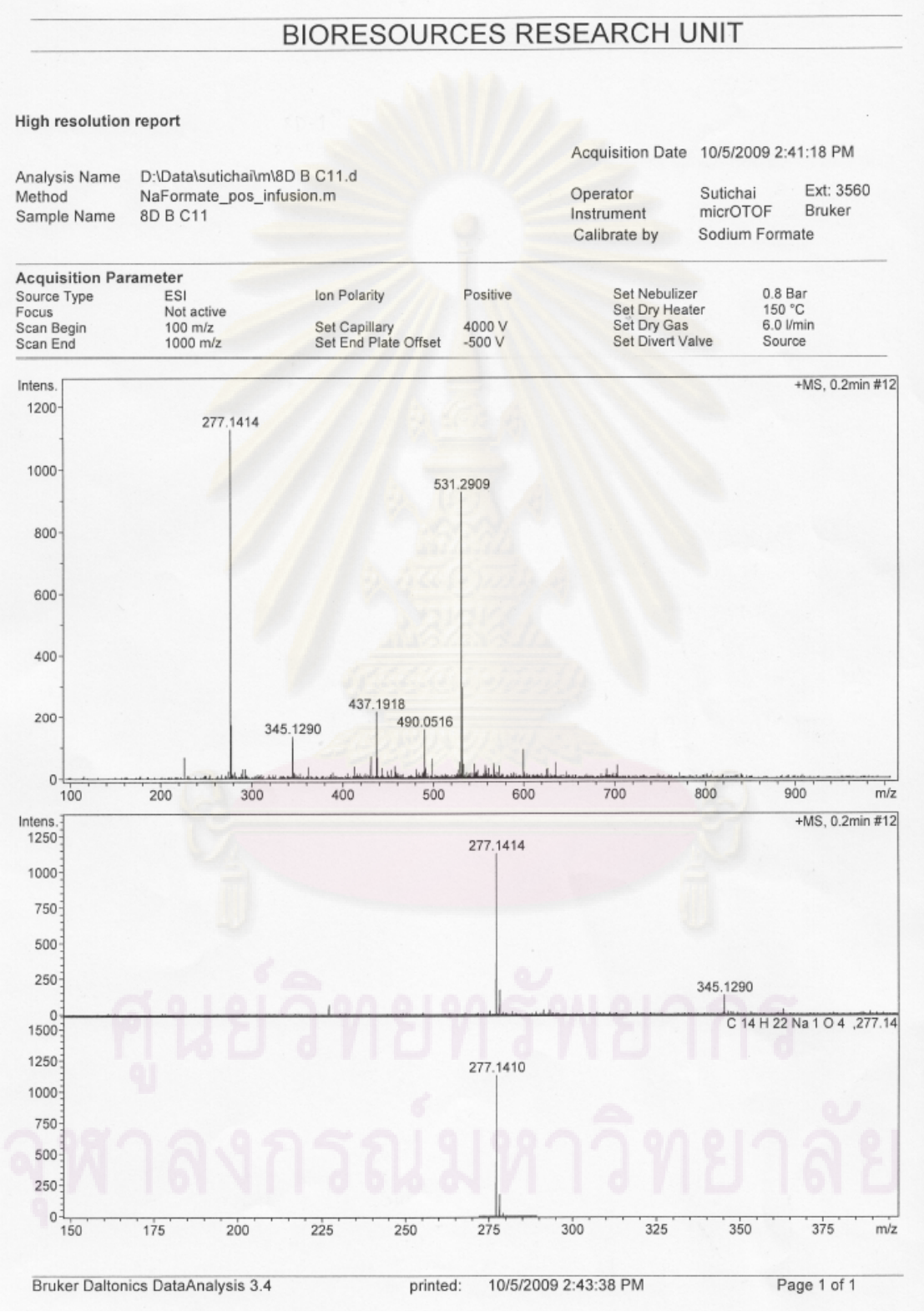

Figure C7 HRESIMS of **7**

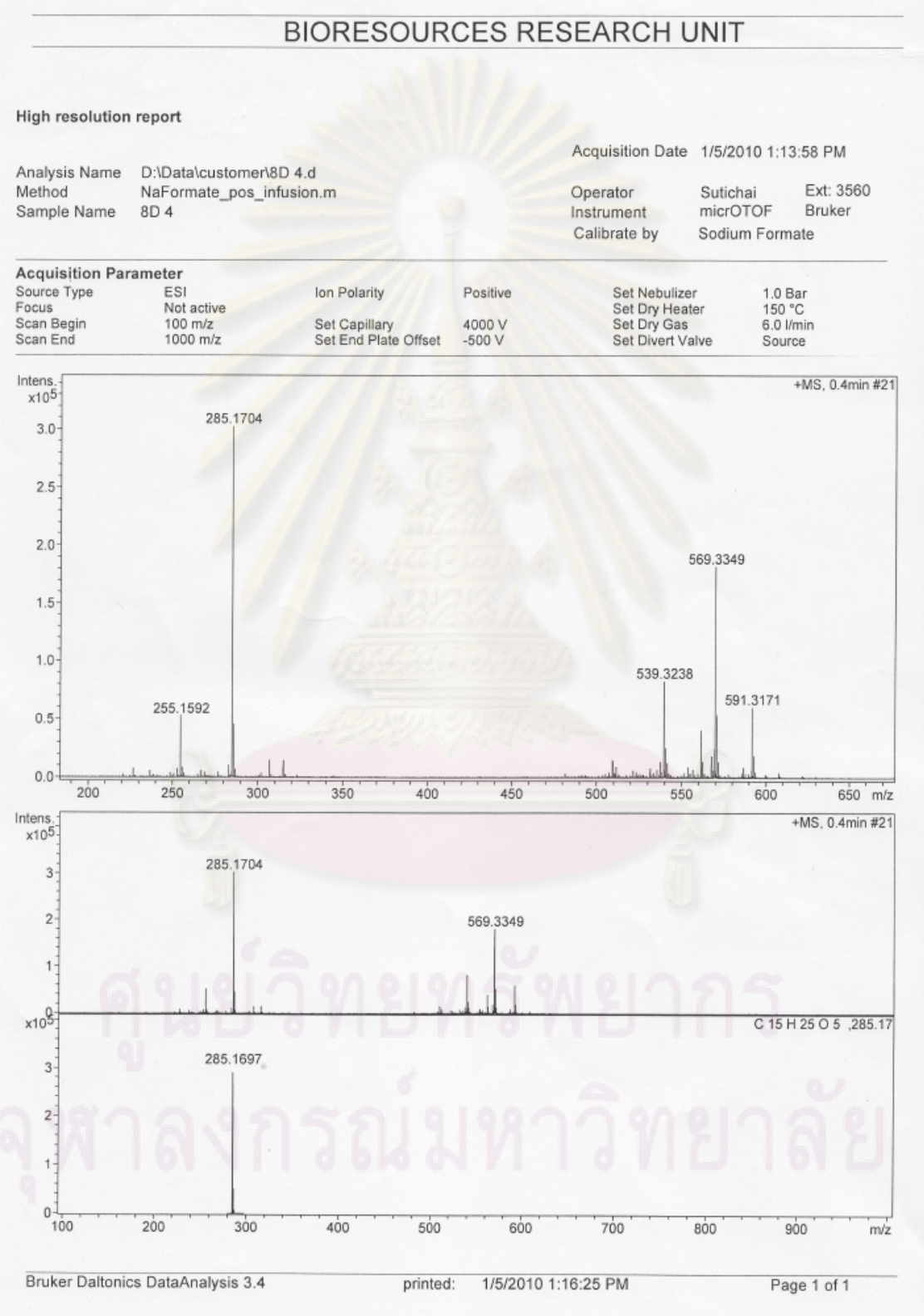

Figure C8 HRESIMS of **8**

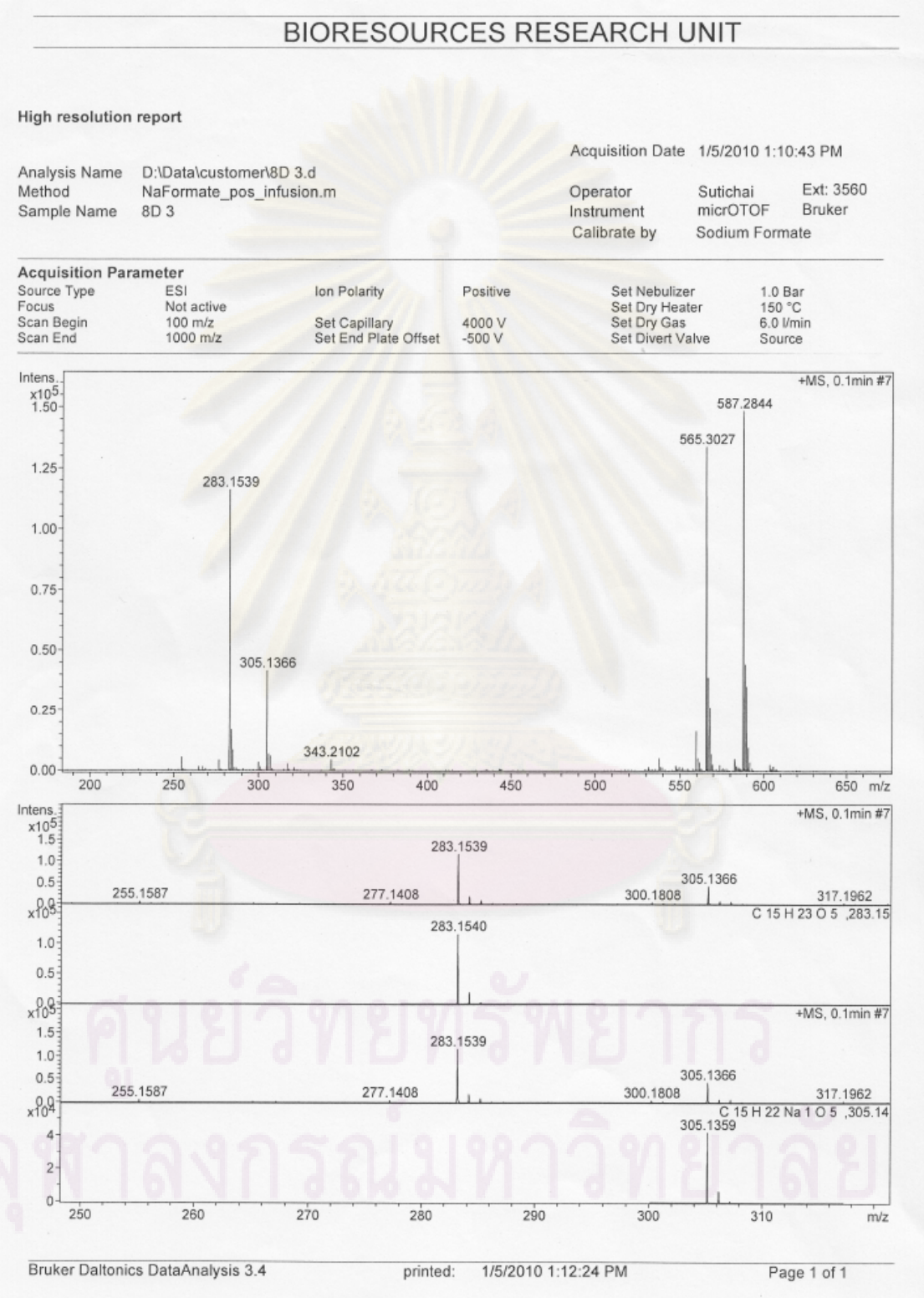

Figure C9 HRESIMS of **9**

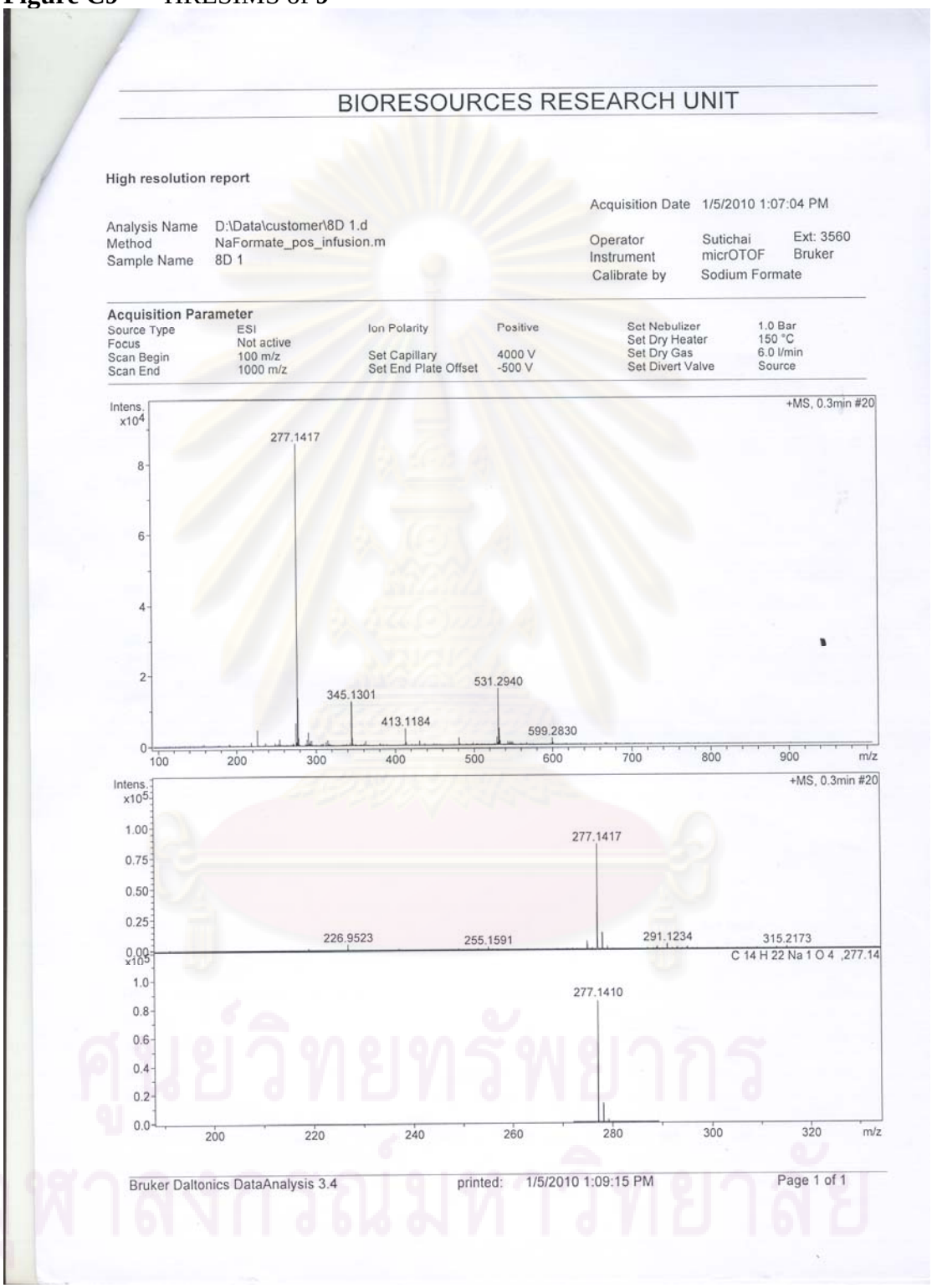

APPENDIX D

Figure D1 IR Spectrum of **1**

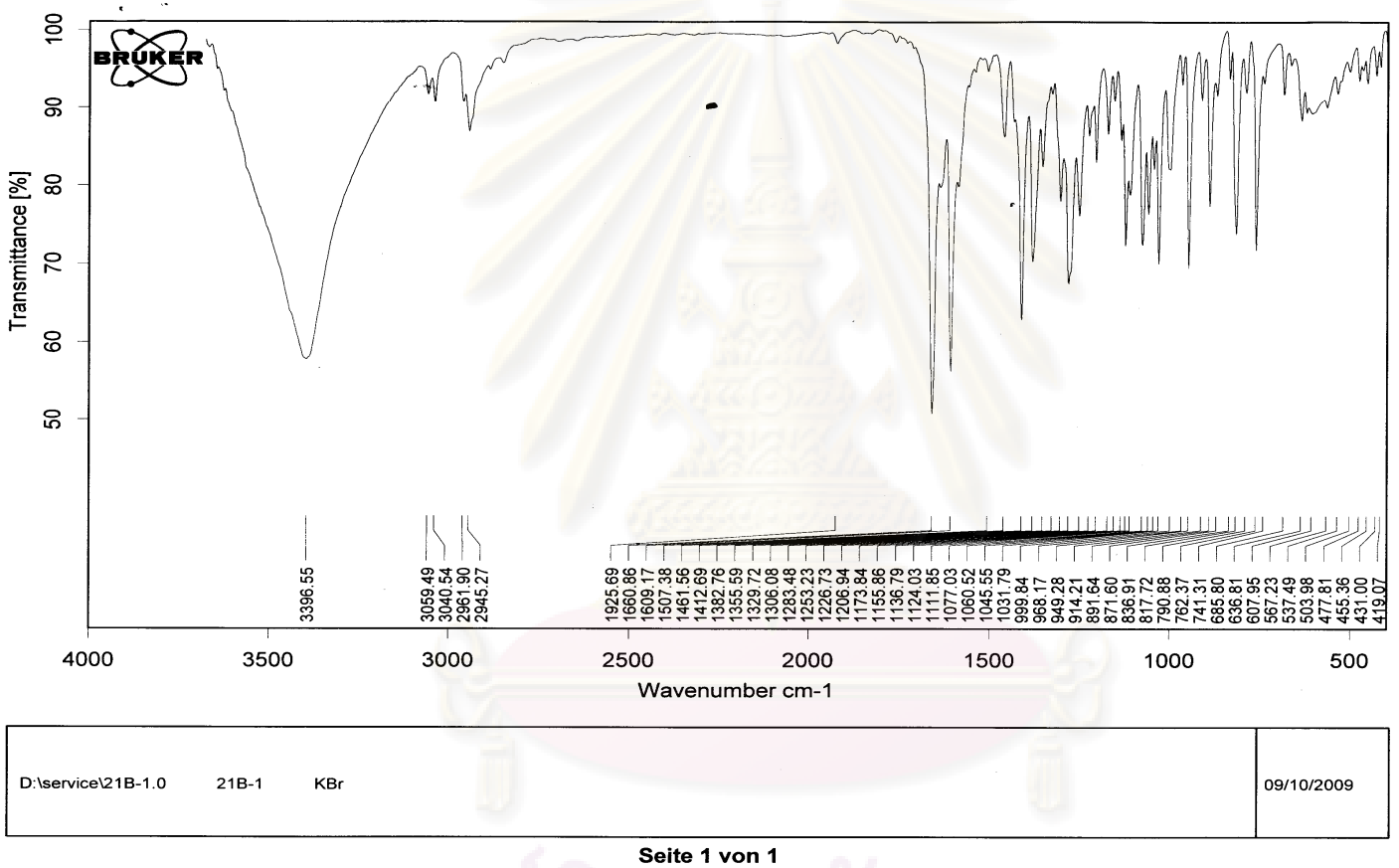

Figure D2 IR Spectrum of **2**

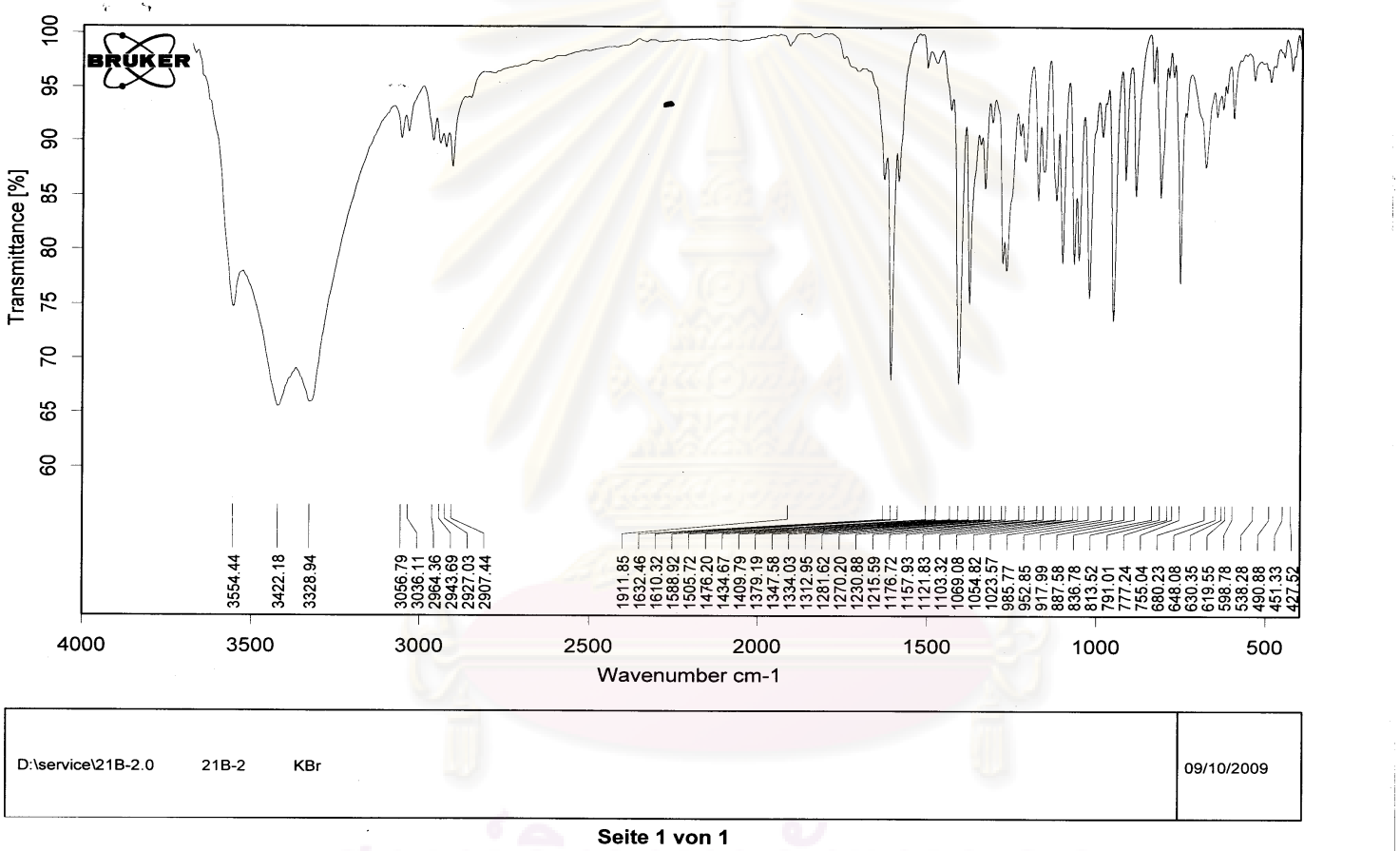

Figure D3 IR Spectrum of **3**

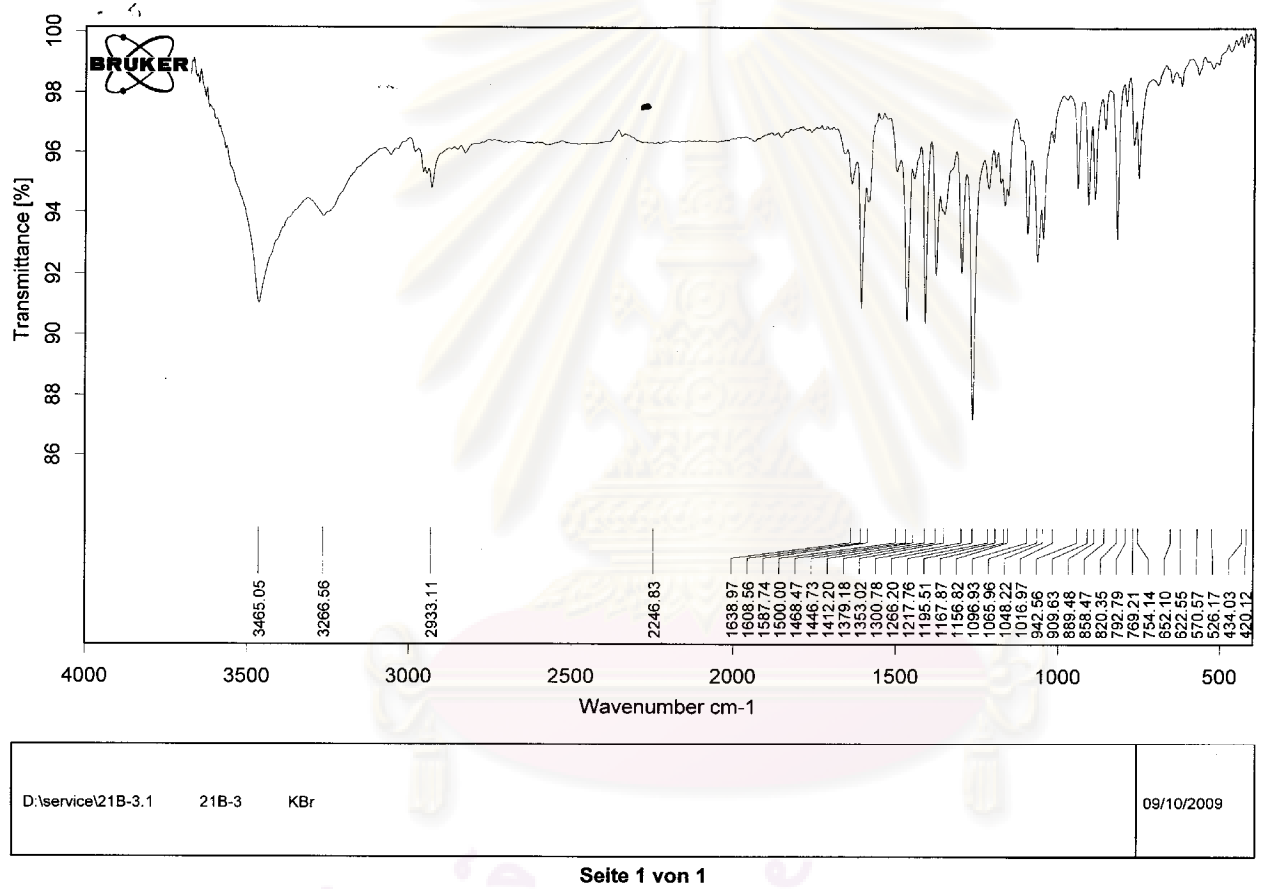

Figure D4 IR Spectrum of **4**

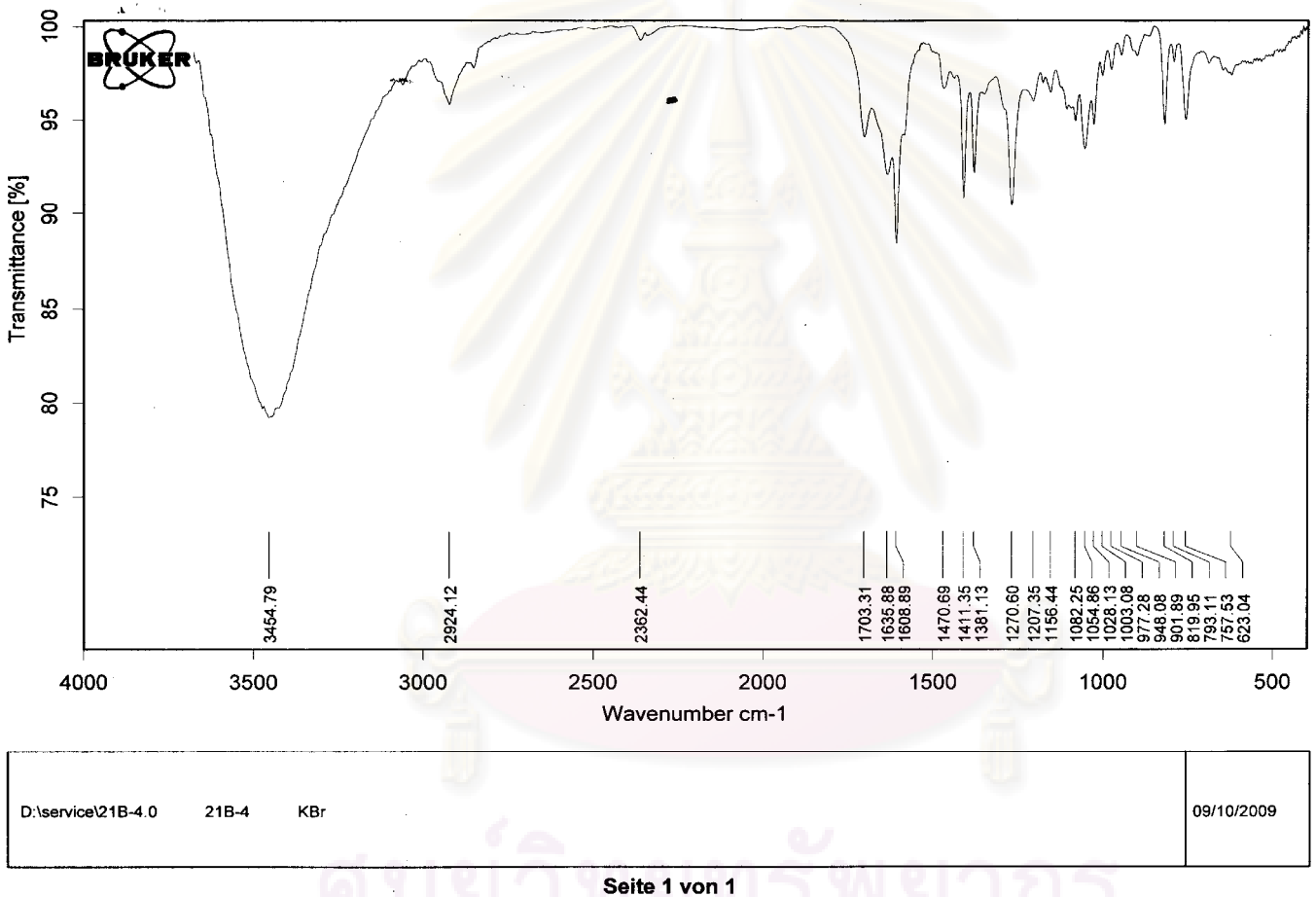

Figure D5 IR Spectrum of **5**

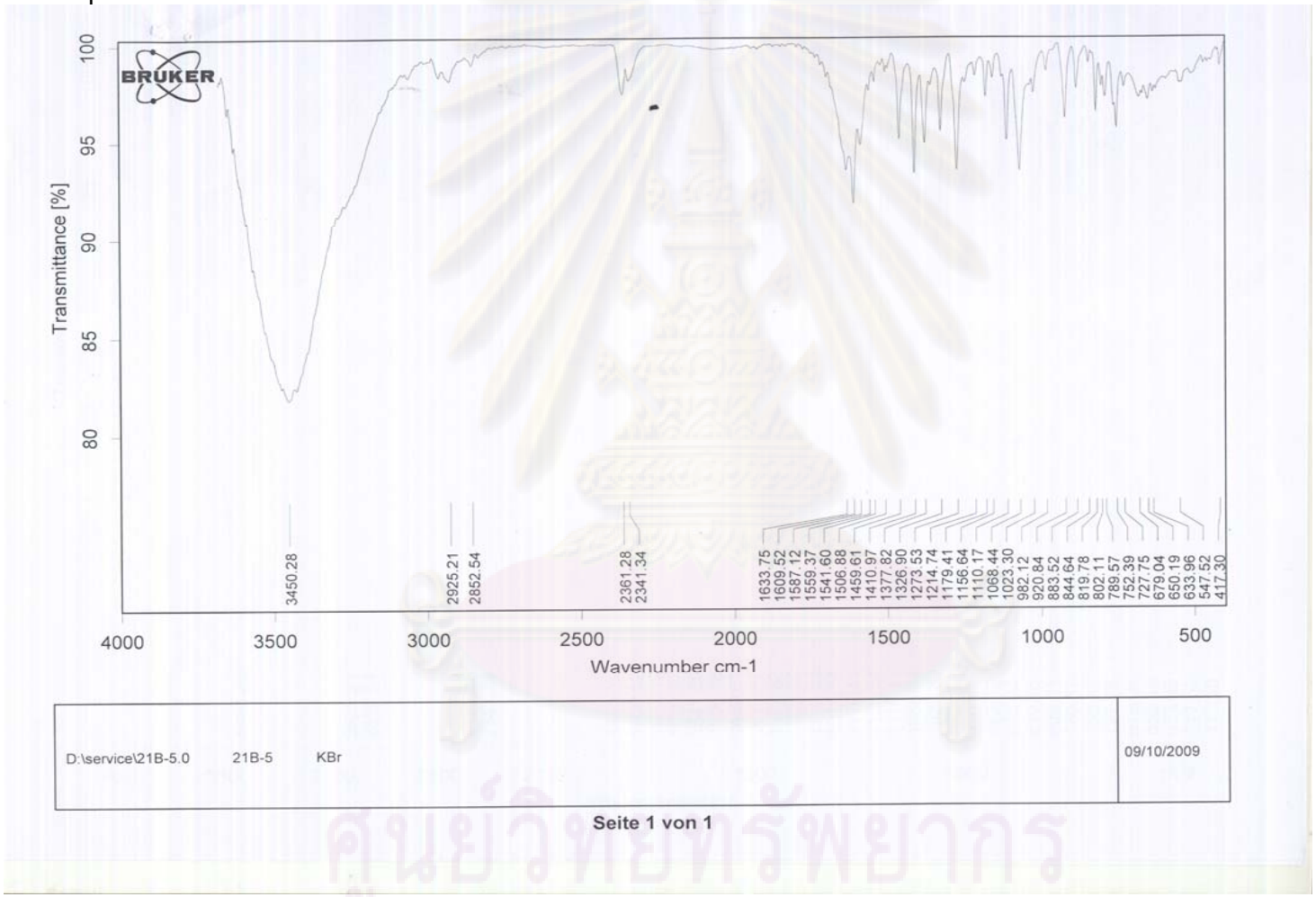

Figure D6 IR Spectrum of **6**

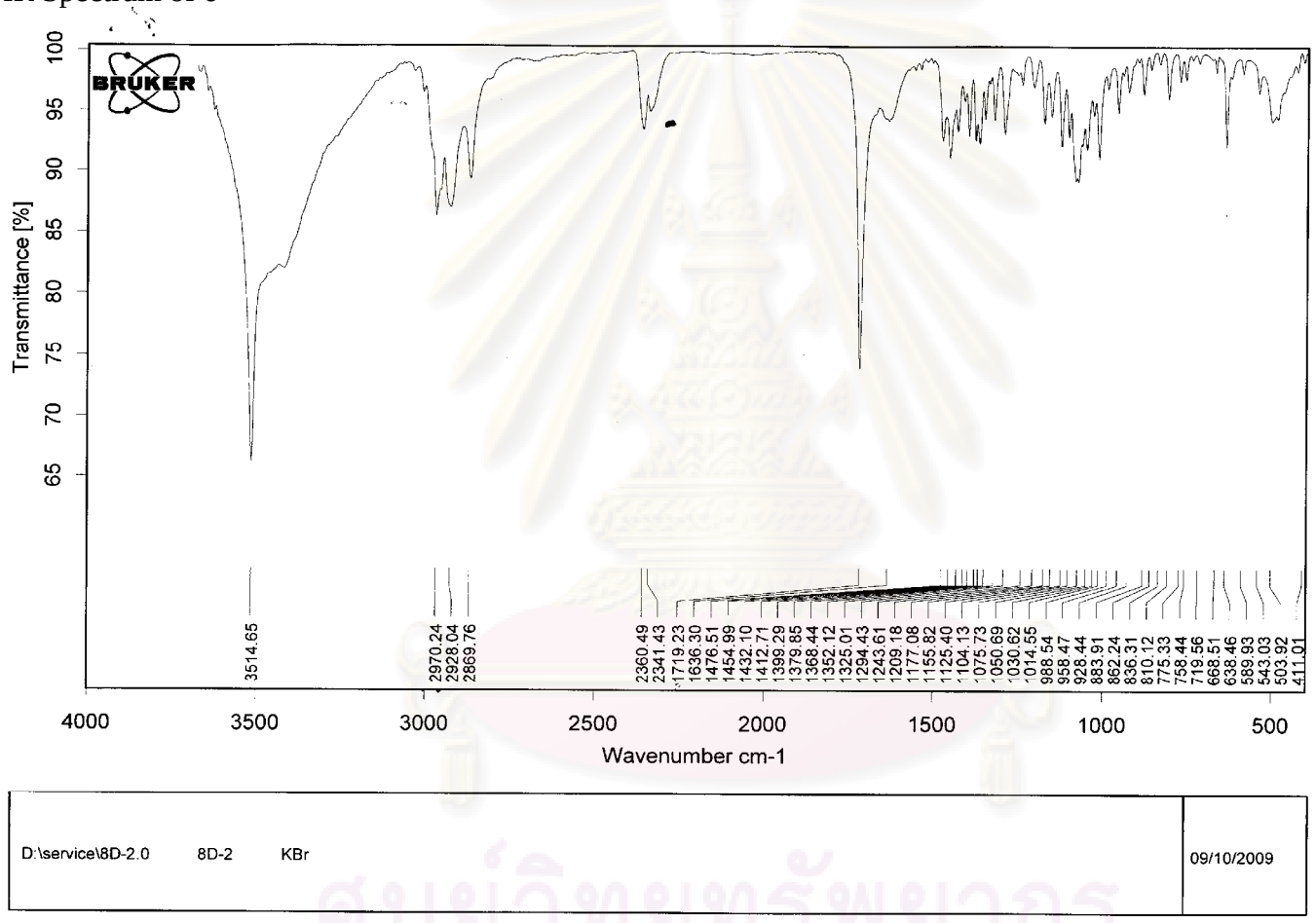

Figure D7 IR Spectrum of **7**

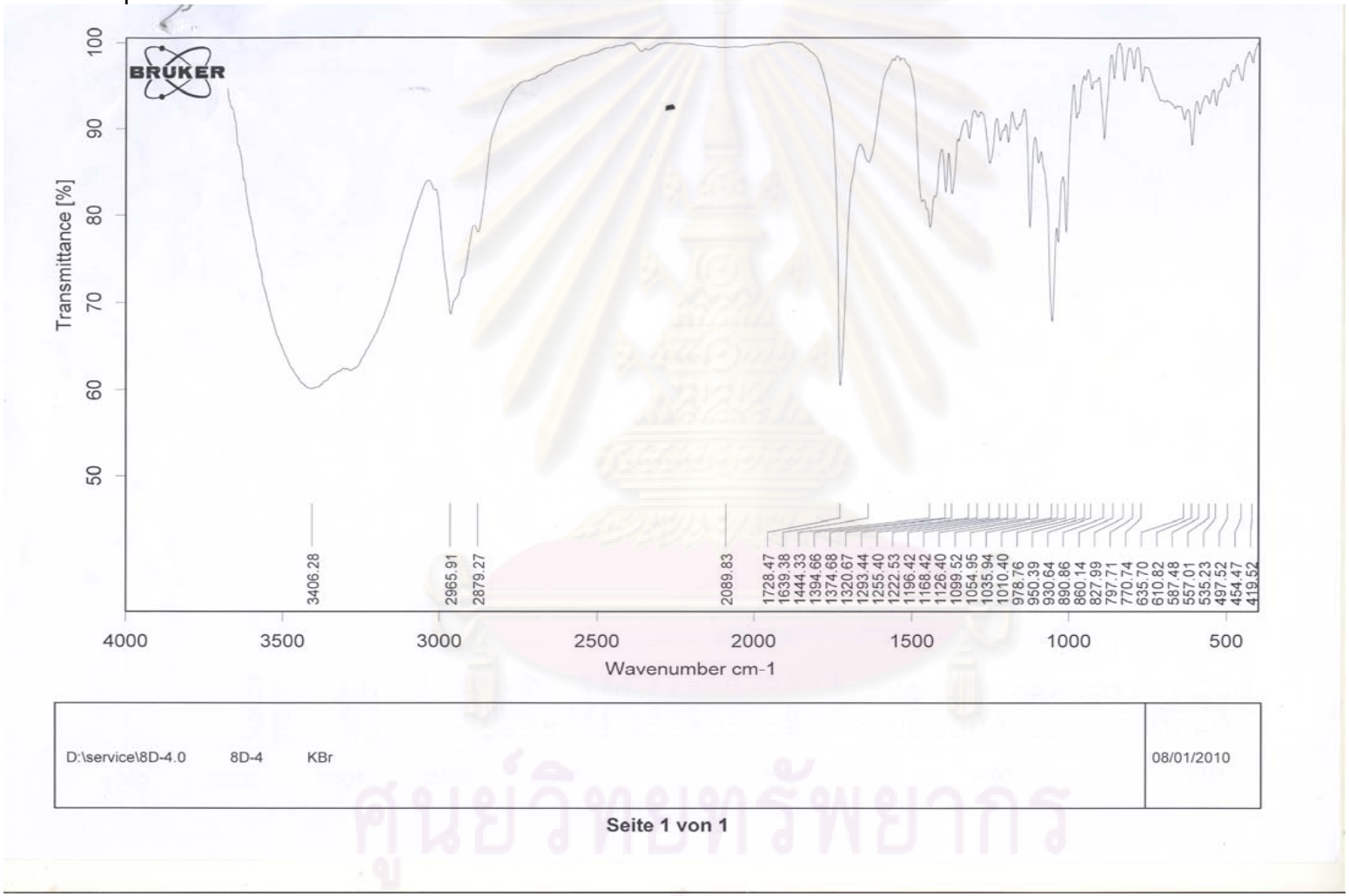

Figure D8 IR Spectrum of **8**

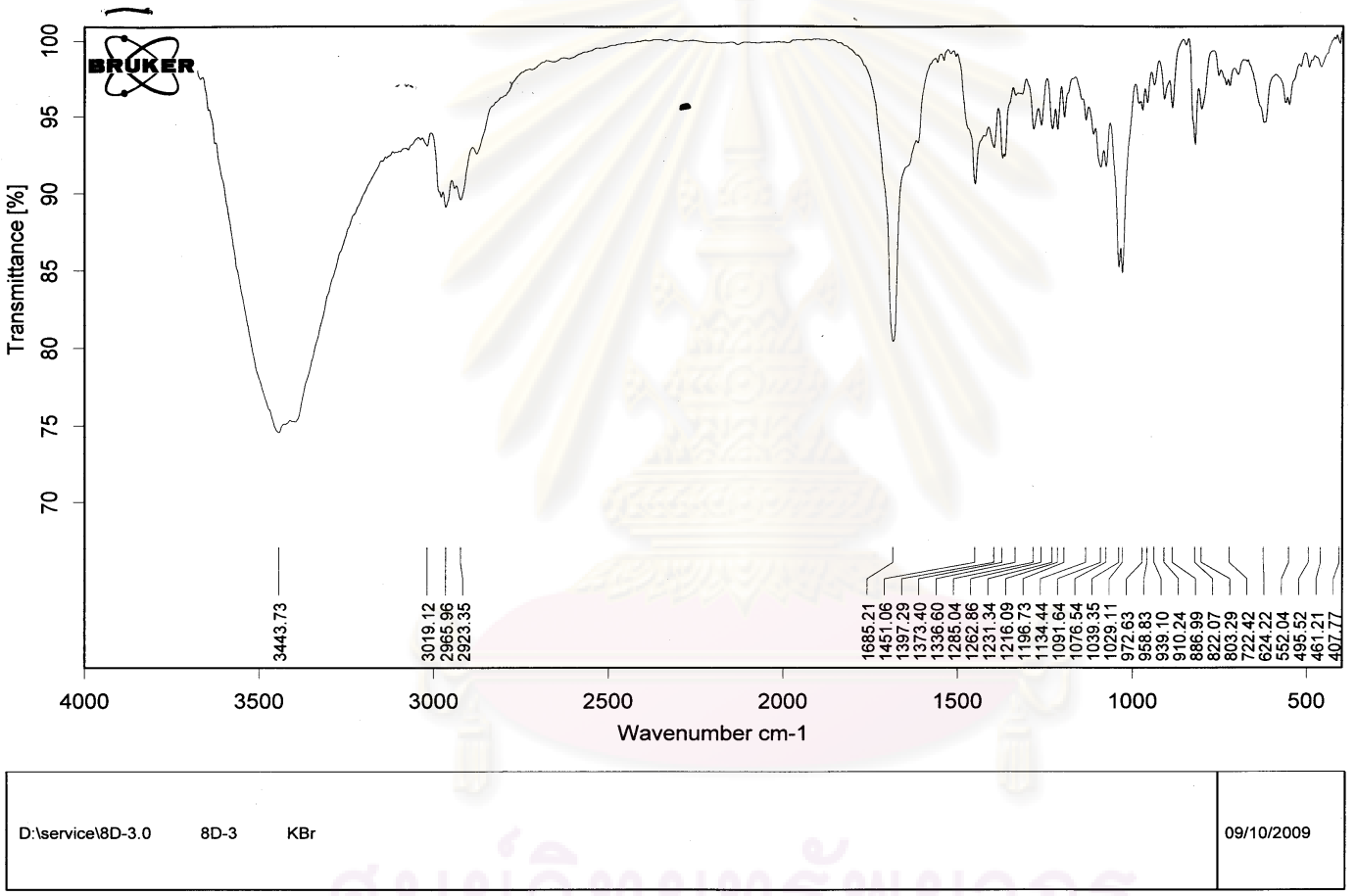

Figure D9 IR Spectrum of **9**

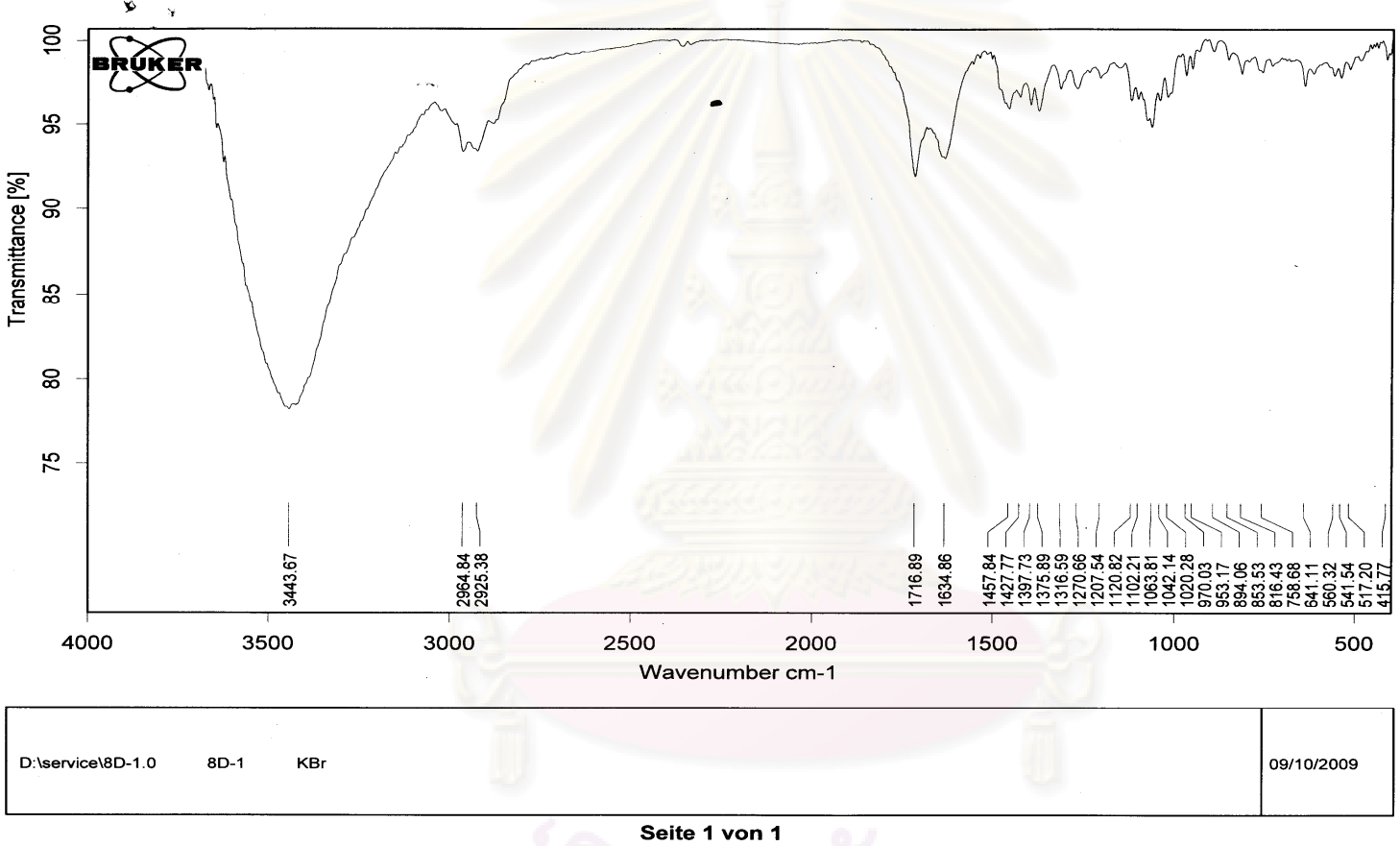

APPENDIX E

Table E1 Crystal data and structure refinement for **6**

Empirical formula	$C_{14}H_{22}O_4$
Formula weight	254.32
Crystal size	0.26 x 0.20 x 0.18 mm
Crystal system	orthorhombic
space group	$P\ 2_12_12_1$ $Z = 4$
Unit cell dimensions	a = 7.35260 Å
	b = 12.4749 Å
	c = 13.9626 Å
Temperature	293(2) K
Volume	1280.69(4) A^3
Calculated density	1.319 mg/m^3
Wavelength	0.71073 A
Absorption coefficient	0.095 mm^{-1}
F(000)	552
Limiting indices	-9<=h<=11, -19<=k<=18, -21<=l<=18
Reflections collected / unique	15534 / 4861 [R(int) = 0.0282]
Max. and min. transmission	0.9831 and 0.9757
Data / restraints / parameters	4861 / 174 / 163
Goodness-of-fit on F^2	1.059
Final R indices [I>2sigma(I)]	R1 = 0.0422, wR2 = 0.1158
R indices (all data)	R1 = 0.0534, wR2 = 0.1274
Absolute structure parameter	-0.1(8)
Largest diff. peak and hole	0.311 and -0.155 $e.A^{-3}$

Theta range for data collection	2.19 to 33.25 deg.
Completeness to theta = 33.25	99.1 %
Refinement method	Full-matrix least-squares on F^2 (SHELXL-97)

Table E2 Atomic coordinates (x 10^4) and equivalent isotropic displacement parameters (A^2 x 10^3) for **6** U (eq) is defined as one third of the trace.

Atom	x	y	z	U(eq)
C(1)	7619(1)	4104(1)	2039(1)	29(1)
C(2)	8815(2)	3261(1)	2529(1)	38(1)
C(3)	8617(2)	3210(1)	3599(1)	48(1)
C(4)	6629(2)	3051(1)	3871(1)	41(1)
C(5)	5325(1)	3896(1)	3461(1)	29(1)
C(6)	5568(1)	3979(1)	2337(1)	23(1)
C(7)	4400(2)	4899(1)	1922(1)	35(1)
C(8)	4393(2)	4982(1)	823(1)	41(1)
C(9)	4112(2)	3906(1)	333(1)	33(1)
C(10)	5210(2)	3001(1)	782(1)	30(1)
C(11)	4879(2)	2946(1)	1851(1)	29(1)
C(12)	3390(2)	3524(1)	3723(1)	51(1)
C(13)	5600(2)	4966(1)	3987(1)	45(1)
C(14)	8507(2)	5206(1)	2211(1)	49(1)
O(1)	9866(2)	2704(1)	2089(1)	63(1)

O(2)	4499(2)	4043(1)	-656(1)	48(1)
O(3)	7122(1)	3047(1)	612(1)	40(1)
O(4)	7826(1)	4047(1)	1015(1)	40(1)

Table E3 Bond lengths [Å] and angles [º] for **6**

Bond lengths

C(1)-O(4)	1.4393(12)
C(1)-C(2)	1.5318(16)
C(1)-C(14)	1.5410(16)
C(1)-C(6)	1.5718(14)
C(2)-O(1)	1.2077(16)
C(2)-C(3)	1.5021(17)
C(3)-C(4)	1.523(2)
C(4)-C(5)	1.5351(17)
C(5)-C(13)	1.5364(16)
C(5)-C(12)	1.5408(17)
C(5)-C(6)	1.5834(13)
C(6)-C(11)	1.5421(13)
C(6)-C(7)	1.5457(13)
C(7)-C(8)	1.5385(16)
C(8)-C(9)	1.5208(15)
C(9)-O(2)	1.4201(14)
C(9)-C(10)	1.5235(15)
C(10)-O(3)	1.4265(14)

C(10)-C(11)	1.5139(14)
O(3)-O(4)	1.4622(13)
Bond angles	
O(4)-C(1)-C(2)	110.44(9)
O(4)-C(1)-C(14)	98.84(9)
C(2)-C(1)-C(14)	107.44(10)
O(4)-C(1)-C(6)	111.02(8)
C(2)-C(1)-C(6)	111.41(9)
C(14)-C(1)-C(6)	116.98(10)
O(1)-C(2)-C(3)	122.96(13)
O(1)-C(2)-C(1)	122.34(12)
C(3)-C(2)-C(1)	114.68(10)
C(2)-C(3)-C(4)	110.30(11)
C(3)-C(4)-C(5)	114.63(10)
C(4)-C(5)-C(13)	109.61(10)
C(4)-C(5)-C(12)	106.33(10)
C(13)-C(5)-C(12)	105.65(10)
C(4)-C(5)-C(6)	110.16(8)
C(13)-C(5)-C(6)	113.71(9)
C(12)-C(5)-C(6)	111.04(9)
C(11)-C(6)-C(7)	105.88(8)
C(11)-C(6)-C(1)	106.35(8)
C(7)-C(6)-C(1)	111.15(9)
C(11)-C(6)-C(5)	110.11(8)
C(7)-C(6)-C(5)	110.94(8)

C(1)-C(6)-C(5)	112.12(7)
C(8)-C(7)-C(6)	115.20(9)
C(9)-C(8)-C(7)	112.92(9)
O(2)-C(9)-C(8)	107.67(10)
O(2)-C(9)-C(10)	112.55(10)
C(8)-C(9)-C(10)	113.39(9)
O(3)-C(10)-C(11)	108.92(8)
O(3)-C(10)-C(9)	115.09(10)
C(11)-C(10)-C(9)	110.78(9)
C(10)-C(11)-C(6)	110.02(8)
C(10)-O(3)-O(4)	108.61(8)
C(1)-O(4)-O(3)	112.77(8)

Symmetry transformations used to generate equivalent atoms:

Table E4 Anisotropic displacement parameters ($A^2 \times 10^2$) for **6**

The anisotropic displacement factor exponent takes the form:

$-2\ pi^2\ [\ h^2a^{*2}U11 + ... + 2\ h\ k\ a^*\ b^*\ U12\ ]$

	U11	U22	U33	U23	U13	U12
C(1)	31(1)	33(1)	23(1)	-2(1)	1(1)	-5(1)
C(2)	30(1)	49(1)	36(1)	-8(1)	-5(1)	6(1)

C(3)	44(1)	64(1)	36(1)	2(1)	-9(1)	17(1)
C(4)	52(1)	43(1)	28(1)	8(1)	-2(1)	3(1)
C(5)	32(1)	34(1)	22(1)	-3(1)	2(1)	0(1)
C(6)	27(1)	21(1)	21(1)	-3(1)	-1(1)	0(1)
C(7)	48(1)	29(1)	29(1)	-7(1)	-9(1)	12(1)
C(8)	66(1)	26(1)	32(1)	-2(1)	-15(1)	9(1)
C(9)	45(1)	32(1)	24(1)	-2(1)	-8(1)	1(1)
C(10)	40(1)	24(1)	26(1)	-5(1)	-3(1)	-1(1)
C(11)	38(1)	23(1)	26(1)	-1(1)	-2(1)	-5(1)
C(12)	41(1)	76(1)	35(1)	-5(1)	12(1)	-12(1)
C(13)	60(1)	45(1)	29(1)	-15(1)	-2(1)	2(1)
C(14)	54(1)	51(1)	43(1)	-2(1)	-1(1)	-27(1)
O(1)	48(1)	86(1)	56(1)	-25(1)	-9(1)	29(1)
O(2)	77(1)	45(1)	24(1)	0(1)	-9(1)	-5(1)
O(3)	41(1)	49(1)	31(1)	-15(1)	3(1)	5(1)
O(4)	42(1)	53(1)	25(1)	-3(1)	7(1)	-13(1)

APPENDIX F

Table F1 Minimum inhibitory concentration (μg/mL) of the following antibiotics against clinical isolated bacterial of enterococcus, staphylococcus and *P. vulgaris*.

antibiotic	EF	VEF	EFa	SA	SE	SH	PV
Ampicillin		1	64	0.125			32
Ceftriaxone	512	1024			1		2
Gentamicin	8			2			0.5
Tetracycline	8			0.125	128	32	0.25
Vancomycin		8	512				1024

* EF : *E. faecalis*, VEF : *E. faecalis* (vancomycin resistant), EFa : *E. faecium*, SA : *S. aureus*, SE : *S. epidermidis*, SH : *S. hominis*, and PV : *P. vulgaris*

** MIC presented as Geomean of 3 observations

VITAE

Ms. Supichar Chokpaiboon was born on July 24th, 1981. She was in applied-science program when she attended Satri Nakhonsawan School, where she finished her high-school level in 1999. She graduated with Bachelor's Degree of Science in Food Technology, Institute of Agricultural Technology, Suranaree University of Technology. During the time she was studying in the Master Degree in Biotechnology program, she was also scholarship the Thailand Graduate Institute of Science and Technology (TGIST) of the National Science and Technology Development Agency (NSTDA) and received the 90th Anniversary of Chulalongkorn University Fund (Ratchadaphiseksomphot Endowment Fund) for supporting her research project.

Contact address: 84/1 Rodjana Rd., Tambon Takhli, Amphur Takhli, Nakhonsawan 60140